

VTT Technical Research Centre of Finland

Review Of Assessment Methods Used In Nuclear Plant Life Management

Keim, Elisabeth; Lidbury, David

Published: 01/01/2012

Document Version
Publisher's final version

[Link to publication](#)

Please cite the original version:

Keim, E., & Lidbury, D. (2012). *Review Of Assessment Methods Used In Nuclear Plant Life Management*. European Commission EC. NULIFE No. (12)5



VTT
<http://www.vtt.fi>
P.O. box 1000FI-02044 VTT
Finland

By using VTT's Research Information Portal you are bound by the following Terms & Conditions.

I have read and I understand the following statement:

This document is protected by copyright and other intellectual property rights, and duplication or sale of all or part of any of this document is not permitted, except duplication for research use or educational purposes in electronic or print form. You must obtain permission for any other use. Electronic or print copies may not be offered for sale.



REVIEW OF ASSESSMENT METHODS USED IN NUCLEAR PLANT LIFE MANAGEMENT

Report prepared by Elisabeth Keim and David Lidbury
based on contributions by members of NULIFE Expert Groups 2 and 3

May 2012







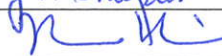
Title **Review of Assessment Methods used
in Nuclear Plant Life Management**

Report No. NULIFE (12) 5 **Issue Date** May 2012

Report Status Draft Final Revision

Deliverable(s) D-IA2.2-7, D-IA2.3-6

Dissemination Public NULIFE Only Restricted (see distribution list)

	Name & Organisation	Signature & Date
Author(s)	Elisabeth Keim, ANP-G (on behalf of EG2) David Lidbury, SERCO (on behalf of EG3)	 29.5.2012
Reviewed by	John Sharples, SERCO	 29.5.2012
Approved by	Rauno Rintamaa, VTT	 29.5.2012



Distribution List

All NULIFE Participants



Foreword

This report presents a review of assessment methods used in plant life management of nuclear power plants. The report has been produced jointly by EG2 (Integrity Assessment) and EG3 (Lifetime Evaluation) of NULIFE. Its scope is confined to the methodology and procedures used in safety analysis of nuclear pressure vessel components to provide assurance of structural integrity. The report is based on a review of information provided by organizations contributing to NULIFE EG2 and EG3, together with some additional material provided on the basis of in-kind contributions.

- The report is the result of the active collaboration of professional scientists and engineers from 16 organizations (and as such has helped facilitate the Integration Process during the initial phases of NULIFE)
- The report considers integrity assessment and lifetime management issues across the range of NPPs currently operating in EU Member States (PWR, WWER, BWR, AGR, CANDU and RBMK) (thus facilitating common understanding across a range of PLIM issues)
- The report provides numerous examples of the application of good practice / best practice methodology at national level (further facilitating common understanding)
- The report's Appendices collectively provide a valuable source of information on numerous aspects of plant life management (thereby contributing knowledge preservation and management)
- The report represents an important resource for the purpose of producing future NULIFE procedures and best practice advice.

Lastly, it should be noted that the report can be regarded as a "living document", that is to say it is foreseen that it could be usefully updated at appropriate intervals during the course of NULIFE time. It could for example be used in the road mapping process in NUGENIA.



Page intentionally left blank



CONTENTS

1	INTRODUCTION.....	9
2	OBJECTIVES & SCOPE	11
3	REFERENCES.....	12
4	DEFINITIONS AND TERMINOLOGY	12
5	SYMBOLS AND ABBREVIATIONS	13
6	REACTOR COOLANT PRESSURE BOUNDARY.....	14
6.1	REACTOR PRESSURE VESSEL.....	14
6.1.1	Vessel Belt Line	14
6.1.2	Cladding.....	18
6.1.3	Nozzles and Penetrations.....	21
6.1.4	Internals	29
6.1.5	References (RPV).....	37
6.2	OTHER VESSEL CHALLENGES (SG, PRESSURIZER).....	41
6.2.1	Stress Corrosion Cracking.....	41
6.2.2	CANDU Steam Generator Tubing	41
6.2.3	References (Other Vessels)	46
6.3	PIPING	47
6.3.1	Degradation Mechanisms	47
6.3.2	Assessment Methods.....	52
6.3.3	Lifetime Evaluation.....	56
6.3.4	References (Piping)	57
6.4	PUMPS AND VALVES.....	60
6.4.1	Pumps.....	60
6.4.2	Valves	61
6.4.3	References.....	63
6.5	PRESSURE TUBES IN CANDU AND RBMK REACTORS.....	64
6.5.1	Description of the core of pressure tube reactors.....	64
6.5.2	Degradation Mechanisms	64
6.5.3	Assessment Methods.....	66
6.5.4	Lifetime Evaluation.....	67
6.5.5	References (Pressure Tubes).....	68
6.6	HIGH TEMPERATURE COMPONENTS	70
6.6.1	Degradation Mechanisms	70
6.6.2	Assessment Methods.....	73



6.6.3	References (High Temperature Components)	81
7	INTEGRATION STATEMENT	82
8	APPENDICES	83
9	ACKNOWLEDGEMENTS	84

APPENDICES

Appendix 1	Fatigue and thermal fatigue
Appendix 2	Considerations regarding formation of corrosive films
Appendix 3	Delayed hydride cracking
Appendix 4	Erosion / corrosion
Appendix 5	Assessment on the evolution of a flaw in a class 1 Asme nuclear equipment
Appendix 6	Oxidation
Appendix 7	Thermal high cycle fatigue in piping system tees with leakage
Appendix 8	PNAEG 7 002 86 (Russian Code) / IAEA-EBP-WWER-08
Appendix 9	Delayed hydride cracking - RBMK-1500 NPP
Appendix 10	Intergranular stress corrosion cracking
Appendix 11	Irradiation induced dimensional and material property changes to the graphite
Appendix 12	Irradiation induced change of fuel channel length
Appendix 13	Guidance for application of the leak before break concept at Ignalina NPP RBMK-1500 reactors.
Appendix 14	Requirements for assessment of intergranular stress corrosion cracking damages in RBMK-1500 reactors
Appendix 15	RPV Cladding
Appendix 16	Pressurized Thermal Shock
Appendix 17	CANDU Feeder Piping

ANNEXES

ANNEX 1	RPV Cladding
---------	--------------



1 INTRODUCTION

A key objective of the Network of Excellence NULIFE (Nuclear Plant Life Prediction) is to create a European-wide platform in order to achieve scientific and technical excellence in lifetime management and prediction methodologies and to translate these into harmonized and qualified procedures as part of the Common Safety Justification Framework (CSJF).

A key element in NULIFE is the work of the four Expert Groups, which serve to cluster relevant expertise and provide a focus for activities, ranging from agreed contributions to “horizontal” WPs to internal RTD projects. Each Expert Group activity is defined as a Work Package, with a designated WP Leader. Partners in the Network normally participate in at least one Expert Group in order to promote integration. Common exercises are defined and followed for specific NPP components in order to demonstrate improvements in capabilities for lifetime evaluation. Coordination and communication between the various Expert Group activities is strengthened by the horizontal WPs and by the fact that all WP Leaders work together on the Executive Group to plan and co-ordinate the work of NULIFE.

The scope of the four Expert Groups (EG) is as follows:

- EG1 (IA-2-1) on Materials Characterization deals with the material property issues, in particular the mechanisms of materials degradation (EAC, thermal ageing, irradiation embrittlement) and characterization of the properties of aged materials, i.e. as a function of in-service conditions.
- EG2 (IA-2-2) on Integrity Assessment is concerned with establishing the state-of-the-art in methods of defect and loading assessment. EG2 deals not only with fracture mechanics methods such as those used in the assessment of PTS and LBB, but includes also a consideration of existing Codes and Procedures, NDE, failure modes, safety factors and certain special topics (effects of load history, crack arrest, secondary and residual stresses, WPS).
- EG3 (IA-2-3), on Lifetime Evaluation takes as its starting point the knowledge gaps identified by the other expert groups, and assesses these in terms of their implications for through-life structural integrity. In addition, EG3 assesses the potential for, and possible implications of, knowledge gaps outside the scope of the other expert groups. It is the purpose of EG3 to take a long-term perspective of component integrity, in particular the safety justification of components over the whole of their foreseen operational life, where the demonstration of safety margins becomes dominated by considerations of fatigue (including thermal fatigue and corrosion fatigue), irradiation embrittlement and other ageing processes (including creep and creep-fatigue).
- EG4 (IA-2-4) on Risk Assessment adds to the work of EG1, EG2 and EG3 to provide advice on the identification, characterization and management of uncertainties in lifetime evaluation, through modelling structural reliability and performing risk assessments to provide added insights into the assessment of safety margins.

The specific objectives of EG2 on Integrity Assessment are to:

- Identify components and systems that contribute significantly to plant safety and influence the total availability of both new and operating light water reactors, heavy water reactors and gas cooled reactors
- Consider potential damage mechanisms that may contribute to the degradation of components, and consider their consequences under normal operation and design basis emergency (DBE) conditions.
- Produce global recommendations and best practices reports.



- Develop the basis for a common understanding between experts from across Europe, which may lead to a harmonization of codes and standards.

The specific objectives of EG3 on Lifetime Assessment are to:

- Provide a common framework for lifetime evaluation of nuclear pressure boundary components and RPV internal structures for light water reactor, heavy water reactor and gas-cooled reactor systems.
- Provide benchmarking of specific lifetime evaluation tools (experimental and analytical procedures, evaluation criteria).
- Produce global recommendations and best practice reports.
- Develop the basis for a common understanding between experts from across Europe, which may lead to a harmonization of codes and standards.

This report has been produced jointly by EG2 and EG3. It represents a review of methodology and procedures used in safety analysis of nuclear pressure vessel components to provide assurance of structural integrity. The report is based on a review of information provided by those organizations contributing to EG2 and EG3 (see below), together with some additional information provided on the basis of in-kind contributions.

The following organizations have contributed to this document:

- | | |
|--|-------|
| • AREVA NP GmbH, Germany | ANP-G |
| • British Energy Generation Limited, UK | BE |
| • Commissariat a l'Energie Atomique, France | CEA |
| • Centre of Technology and Engineering for Nuclear Projects, Thermo-Hydraulic & Stress Analysis Department, Bucharest, Romania | CTEN |
| • E.ON Kernkraft, Germany | EKK |
| • Electricité de France, France | EDF |
| • , Helmholtz-Zentrum Dresden-Rossendorf, Germany | HZDR |
| • Institute for Nuclear Research Pitesti, Romania | INR |
| • EC JRC-IE, Petten, The Netherlands | JRC |
| • J. Stefan Institute, Slovenia | JSI |
| • Lithuanian Energy Institute, Lithuania | LEI |
| • Nuclear Research Institute Rez plc, Czech Republic | NRI |
| • Phoenix Engineering Associates Inc., USA | PEAI |
| • SERCO Energy, UK | SERCO |
| • Siempelkamp Prüf- und Gutachter Gesellschaft mbH, Germany | SPG |
| • Valtion Teknillinen Tutkimuskeskus, Finland | VTT |
| • Westinghouse Europe | WE |



2 OBJECTIVES & SCOPE

Plant Life Management comprises the technological and administrative measures which safeguard the safety requirements of relevant systems and components during the lifetime of a Nuclear Power Plant (NPP). Therefore, precautionary measures such as surveillance schemes, maintenance activities and in-service inspections are routinely applied to structures and components during plant operation to ensure maintenance of the required quality. Nevertheless, during NPP operation, degradation effects like corrosion, fatigue, and in-service degradation of fracture toughness, may significantly impact component integrity. Subsequently, the goal of each measure is to maintain component quality at the highest level, where the reference is always the appropriate quality level at the design and fabrication state, to fulfil the required tasks over the intended plant lifetime.

Suitable and applicable assessment tools are indispensable within the framework of a multidisciplinary plant life management. For providing sufficient component quality in NPPs the most important issues are:

- Knowledge and understanding of ageing-related damage mechanisms in materials and the ability to predict their through-life consequences for the performance of systems, structures or components
- Predictive models to assess the behaviour of systems, structures or components over a defined timescale
- Qualified methods for the detection and surveillance of ageing-related damage mechanisms e.g. knowledge-based recurring maintenance actions
- Qualified mitigation measures, including rectification and repairs
- Quality assured plant documentation
- Up-to-date knowledge base
- Regular evaluation of the effectiveness of all applied measures by means of a PDCA circle (Plan-Do-Check-Act)

Aspects on personal qualification and preservation of knowledge are important as well. Herein, technical services comprising suitably qualified and experienced personnel (SQEP) are one key feature for keeping the personal qualification as good as possible. Nevertheless, these personal aspects will not be considered as part of this technical document, indeed these tasks belong to aspects on management systems for instance.

The purpose of this document is to provide a preliminary summary and state-of-the-art review of assessment and lifetime evaluation methods for assessing the structural integrity of components and piping in the various types of NPPs in operation within Europe (LWR, WWER, AGR, CANDU and RBMK) from the point of view of prevention of failure by non-ductile and ductile fracture, fatigue, creep and mechanical corrosion damage under operational and postulated abnormal conditions. Priority areas for this activity within NULIFE are listed in Table 1:



Table 1 NULIFE Priority Areas

Preliminary research topics proposed by end-users	Application areas			
	Reactor pressure vessel and internals	Reactor coolant system and connected lines	Steam generators	Other components
1. Thermal fatigue	X	X	X	
2. Stress corrosion cracking	X	X	X	
3. Welds and repairs	X	X		
4. Clad properties and ageing	X			
5. Safety factors and uncertainties in damage evaluation	X	X	X	
6. Stress classification		X		
7. Other ageing issues				X

3 REFERENCES

References are listed at the end of individual Sections or Sub-sections.

4 DEFINITIONS AND TERMINOLOGY

Definitions and terminology are introduced within the context of individual Sections or Sub-sections.



5 SYMBOLS AND ABBREVIATIONS

Symbols and abbreviations are introduced within the context of individual Sections or Sub-sections. However, some more general abbreviations are listed below:

AGR	Advanced Gas-Cooled Reactor
ASME	American Society of Mechanical Engineers
BM	Base Metal
BWR	Boiling Water Reactor
CANDU	Canadian-Deuterium-Uranium
CRD	Control Rod Drive
CS	Carbon Steel
DHC	Delayed Hydride Cracking
EAC	Environmentally-Assisted Cracking
EG	Expert Group
FEM	Finite Element method
HAZ	Heat-Affected Zone
HWR	Heavy Water Reactor
IAEA	International Atomic Energy Agency
ISO	International Standards Organization
KTA	German Nuclear Safety Standards
LBB	Leak Before Break
LWR	Light Water Reactor
NPP	Nuclear Power Plant
PHWR	Pressurized Heavy Water Reactor
PTS	Pressurized Thermal Shock
PWHT	Post-Weld Heat Treatment
PWR	Pressurized Water Reactor
RBMK	Heavy Water Cooled-Graphite Moderated Pressure Tube Reactor
RCC-M	French Design and Construction Rules for Nuclear Power Plants
RPV	Reactor Pressure Vessel
SCC	Stress Corrosion Cracking
SG	Steam Generator
SS	Stainless Steel
WP	Work Package
WWER	Water Cooled-Water Moderated Energy Reactor

6 REACTOR COOLANT PRESSURE BOUNDARY

6.1 REACTOR PRESSURE VESSEL

The reactor cores of the majority of the worlds' nuclear power reactors are housed in steel reactor pressure vessels (RPVs), whose primary function is to contain both the reactor core and the primary coolant under operational conditions of temperature and pressure.

The integrity of the thick walled steel RPV is vital for safety for two main reasons. Firstly, because the RPV is the container for the reactor core, if it should develop a leak, and if the rate of coolant loss exceeds the maximum capability of the emergency cooling water system to replace it, then the reactor core could become uncovered, overheat and unless some remedial action is undertaken, ultimately melt. Secondly, a massive failure of the RPV itself could both seriously damage the reactor core and, at the same time, could damage the containment building. In this way a single postulated event could possibly outflank the various sequential barriers which prevent the escape of fission products in other postulated accident sequences, namely the fuel cladding, the primary circuit and possibly the containment building. Therefore it is necessary to demonstrate that disruptive failure of the RPV is practically excluded and has a very low probability of occurrence, bordering on the incredible, throughout its working life, since such accidents could give rise to large uncontrolled releases of radioactivity to the public.

Component integrity is considered in terms of: the vessel beltline (which receives the highest irradiation dose), cladding and nozzles / penetrations.

6.1.1 Vessel Belt Line

The methods and procedures used in the safety analysis of the RPV to ensure its structural integrity are intrinsically tied to the requirements that dangerous leakage, rapidly propagating cracks and brittle fracture of the vessel have to be eliminated. The specifications of these safety related requirements are the objective of national Nuclear Safety Standards (per example KTA, ASME, RCC-M, PNAE-G etc) to ensure that reasonable precautions are taken against the damage arising from the construction and operation of nuclear facilities. In Germany for example such safety standards contain the specifications for Materials and Product Forms, Design and Analysis, Manufacture, and In-service Inspections and Operational Monitoring [6.1.1].

6.1.1.1 Degradation Mechanisms

Irradiation Effects on the Ferritic Part (base metal, welds and HAZs)

The specific mechanisms and phenomena that are responsible for the ageing behaviour of the RPV materials in LWRs can be assessed by methods and procedures that are described as follows.

During the operation of a nuclear power plant the neutron flux affects the RPV material properties. The irradiation of ferritic steels by (fast) neutrons with sufficiently high energy causes interactions of the neutrons with the atoms of the RPV steel influencing the microstructure of the irradiated material. This leads to dynamic dislocation generation and changes in the regular atomic configuration in the crystal lattice leading to so-called displacement cascades that contribute to the formation of dislocation loops, point defect and vacancy-solute clusters. These characteristic lattice defects affect the macroscopic material properties of the irradiated material: the yield strength and tensile strength increases, the ductile-brittle transition temperature (DBTT) changes to higher temperatures and the upper shelf energy decreases. The mechanisms responsible for these irradiation induced embrittlement effects are well known in terms of matrix damage, Cu precipitation containing Ni, Mn, Si, and grain boundary segregation of P. The main influencing parameters are the

- Weld or base material
- material manufacturing processes
- chemical composition (in particular content of Cu, Ni, Mn, P, N)
- irradiation temperature
- neutron flux
- energy spectrum of the neutrons
- irradiation time
- accumulated neutron fluence (neutron flux and irradiation time).

The main investigations for understanding the irradiation embrittlement have been summarized in the FP5 project ATHENA (AMES Thematic Network on Ageing) [6.1.2] and include:

- Parametric studies with model alloys irradiated in material test reactors as a fundamental tool to investigate the neutron embrittlement. They have been performed to study the role of each element in the RPV steel (base and weld) and possible synergisms.
- Re-evaluation of surveillance data to develop trend curves.
- Use of reference materials (irradiation at different temperatures and at different fluence rates) to assess the sensitivity of specific materials to irradiation response.

To assess the real aging behaviour it is useful to investigate RPVs of decommissioned plants.

Thermal aging

Thermal aging refers to hardening caused by thermally activated diffusion of alloying elements or impurities, resulting in increased DBTT shifts with time. The potential for thermal aging embrittlement in LWR RPV steels for times of up to 40 years is considered as low, but cannot be entirely dismissed on the basis of available data. For steels with low Cu content, no significant thermal aging effects have been observed at temperatures below 300 °C. For these materials, changes in DBTT due to thermal aging need not be considered as part of the overall integrity assessment.

Hydrogen embrittlement

It is known that hydrogen may contribute to the embrittlement of RPV steels, but only under very specific conditions. The resistance of the steel for hydrogen embrittlement is dependent on the chemical composition, fluence, irradiation temperature and the type of irradiation-induced defects. Experimental investigations, including tensile testing [6.1.3], have shown that an increasing susceptibility to hydrogen embrittlement was observed at room temperature for in-situ hydrogen charged samples at slow strain rates and low irradiation temperatures. However, at temperatures higher than 250 °C hydrogen embrittlement was no longer observed. From these results it has been concluded that in-service hydrogen embrittlement will not occur in RPV materials, and that hydrogen embrittlement need not be considered as a potential degradation mechanism in aging LWR RPVs.

In the German code (KTA) hydrogen embrittlement is not considered for the RPV assessment. Research on this topic has shown that at operational temperatures ($T > 250$ °C) there is no significant influence of H on the degradation of mechanical properties of RPV steels for LWRs [6.1.4].

6.1.1.2 Assessment Methods

Irradiation behaviour

There are many trend curves and procedures in use worldwide to predict the irradiation behaviour in terms of reference temperatures for the ductile-brittle transition and their shifts induced by irradiation. These tools are mainly based on specific data bases. The most common trend curves are:

- Reg.-Guide 1.99, Rev. 2 [6.1.5]
- French FIS/FIM-Formula (RSEM Code) [6.1.6]
- French RCC-M Appendix ZG
- Eason-Model (NUREG-CR/6551) [6.1.7]
- ASTM E 900-02 [6.1.8]
- Wang-Approach [6.1.9]
- CRIEPI 2004 (Correlation describing the irradiation behaviour of Japanese RPV steels)
- Russian Assessment Code for WWER: “Guide for strength analysis of the equipment and pipelines of nuclear power units” [6.1.15]
- Guidelines on Pressurized Thermal Shock Analysis for WWER Power Plants [6.1.16]
- Advanced RPV assessment code for WWER reactors: VERLIFE “Unified Procedure for Lifetime Assessment of Components and Piping in WWER NPPs” (European Commission, Final Report, Contract N° FIKS-CT-2001-20198, September 2003) [6.1.17]

Moreover, so-called multi scale modelling of irradiation effects on material behaviour is increasingly being developed e.g. in the FP6 project PERFECT (PERFECT: Prediction of Irradiation Damage Effect in reactor Components) and continued in the FP7 project PERFORM60. Although the use of such models for real RPV materials is still not yet ready for application, essential and very promising progress has been demonstrated for some binary alloys in the Virtual Reactor simulation tools RPV-1 [6.1.10] and RPV-2 [6.1.11]. The long term irradiation behaviour (80 years of operation) of real RPV steels is investigated by means of microstructural investigations and testing in the FP7 project LONGLIFE.

Heterogeneities:

The Master Curve concept was extended to cover the brittle fracture behaviour of ferritic steels with heterogeneities. The following evaluation procedures have been developed:

- SINTAP Master Curve Extension [6.1.12]
- Master Curve extension for materials consisting of two populations [6.1.13]
- Master Curve extension for materials with random heterogeneities [6.1.13], [6.1.14]

Residual stresses:

Residual stresses are stresses that are not caused by external loadings but by heterogeneous deformations as a result of thermal stresses and phase transformations. The manufacture of the cladding on the inner RPV wall generates tensile residual stresses in the cladding and, to a lesser extent, compressive residual stresses in the ferritic part underneath the cladding. Residual stresses have to be taken into account in a proper way for structural integrity assessments in structures such as RPVs.

In some countries, residual stresses need to be considered when performing structural integrity assessments of welds. For example in the UK, methods for their treatment are included in both the EDF Energy R5 [5.6.12] and R6 [5.6.14] procedures.

The effect of residual stress on the fracture of components containing defects is considered in R6 [5.6.14]. Residual stresses contribute to the crack driving force for fracture, with interaction between primary and secondary stresses treated using the ρ or V parameters. R6 categorises short- and medium-range welding residual stresses as secondary stresses whereas long-range stresses are categorised as primary. The distinction is that secondary stresses do not affect plastic collapse.

The magnitude and distribution of the residual stress field across a section of interest in a welded component depend on a number of factors. An assumption of uniform yield stress magnitude is termed a Level 1 estimate by R6. Level 2 estimates are upper-bound profiles for particular types of as-welded joints, normalised by an appropriate yield stress; they are not necessarily self-balancing but provide conservative estimates. However, there is now a significant drive to develop more realistic Level 3 profiles from syntheses of weld modelling and measurement, using statistical approaches to quantify scatter, in order to lessen over-conservatism. R6 includes a compendium of Level 2 profiles and some limited information on Level 3 profiles for the particular case of austenitic butt welds. This is a rapidly developing research area in the UK as well as other countries.

6.1.1.3 Lifetime Evaluation

The integrity of the RPV has to be guaranteed under operation and emergency conditions for the foreseen period of operation. In this context the structural integrity analysis of the ferritic RPV belt line near the core is an essential part of the safety assessment of the RPV since the high level of neutron irradiation in this area may lead to an enhanced material embrittlement. For this reason the behaviour of the RPV beltline materials in the RPV pressure-retaining walls of LWRs is monitored under irradiation conditions by RPV irradiation surveillance programmes or dedicated irradiation programmes in other host reactors, respectively.

Irradiation surveillance

The aim of such irradiation surveillance programmes is to determine, by means of accelerated irradiated specimen capsules, the strength and toughness properties of RPV base and weld materials in the core beltline region of the RPV as a function of a defined neutron irradiation level. It is common knowledge that the heat affected zone properties are covered by the base and weld metals. The accurate determination of neutron fluences, neutron spectra and irradiation temperatures over the surveillance period and at the irradiation specimen positions is an important part of such surveillance programmes. The detailed surveillance requirements (number, orientation and location of specimens, time of insertion and withdrawal of specimen sets, testing specifications, etc) are described in special safety standards such as KTA 3203 [6.1.18], ASTM E-185 [6.1.19] and 10CFR Part 50 Appendix H, RSEM-B7213. The material behaviour characterization part of safety assessment of the RPV is based either on the RT_{NDT} concept by comparing test results (mainly from Charpy-V impact tests) obtained from advanced-irradiated specimens and unirradiated specimens, or on the fracture toughness concept by examining irradiated fracture toughness specimens (e.g. by determination of the reference temperature T_0 according to ASTM E 1921 [6.1.20]). The material curve (fracture toughness) will then be compared with the loading curve (stress intensity factor) of postulated transients resulting from PTS events.

The activities of AMES (Ageing Materials European Strategy) European network and many national and European projects like REDOS, PISA, FRAME, COBRA, ATHENA, GRETE, RADAMO, CLAD, PRIMAVERA, CUPRIVA, CARISMA have substantially improved the understanding of RPV irradiation embrittlement issues. The ageing behaviour of the RPV materials in LWRs is governed by specific mechanisms and phenomena that are well-

characterized by the research results from national and international projects supported by the European Commission.

A dedicated irradiation surveillance programme is the best method for ensuring quantification of the irradiation effects on the reactor pressure vessel materials and to predict the changes in macroscopic material behaviour of these materials by subsequent testing of the surveillance specimens. The irradiation of specimens can be performed in the specific RPV of concern itself, but nearer to the core to receive the irradiation in advance, or in a host reactor. Typically, the high energy neutron fluence or the dpa are used as damage function to define the lead factor for the determining the transfer function of the surveillance results to the RPV wall.

Micro-structural investigation techniques

The knowledge of the micro-structural material behaviour is a fundamental basis to understand and to explain the mechanisms that are responsible for the irradiation induced embrittlement effects. Micro-structural investigation techniques have emerged as sufficiently mature to be reliably applied to provide the necessary information for accurate assessment of irradiated RPV steels. The main techniques identified in the FP5 project ATHENA are [6.1.2]:

- Transmission Electron Microscopy (TEM)
- Field Emission Gun Scanning Transmission Electron Microscopy (FEGSTEM)
- Small Angle Neutron Scattering (SANS, determination of a statistically representative size distribution of clusters)
- Atom Probe Field-Ion Microscopy (AP-FIM)
- Scanning Auger Electron Spectroscopy (AES)
- Positron Annihilation Spectroscopy (PAS), using the positron lifetime and coincidence Doppler broadening for studying open-volume type atomic defects and defect impurity interactions

These methods, along with others, are able to provide information on composition and size of irradiation induced precipitations (Cu), depending on Cu, Ni, Mn content, and may give indications of any potential dose rate and late blooming effects (fast growing irradiation induced Mn-Ni precipitations in RPV steels with high Ni but low Cu content at high fluences), respectively.

Integrity assessment

The loading of postulated cracks in the RPV belt line region under emergency conditions has to be determined by fracture mechanics analysis. It has to be demonstrated that a sufficiently large safety margin exists between the loading curve and the material resistance.

For structural integrity analyses concerning RPV under PTS event, see an example in App. 16 and in [5.1.47 and 5.1.48]. For WWER reactors see also Appendix 8.

6.1.2 Cladding

Austenitic stainless steel cladding, up to a few millimetres in thickness, is applied by the weld deposition of one, or more, layers (usually two) to the inside wall of LWR RPVs. This is to inhibit general corrosive attack of the ferritic low-alloy steel base material, and to minimise any associated radioactive contamination of the reactor coolant system. Cr-Ni steel is the clad material used for most of these surfaces. As a rule, the RPV cladding should be welded in at least two passes to ensure re-crystallization of the heat affected zone in the ferritic base metal and to eliminate the potential for relaxation cracking. To neutralize dilution with the base metal, to prevent hot cracking and to induce resistance to inter-granular corrosion, a highly over alloyed clad metal is used for depositing the first pass of the austenitic cladding and a less over alloyed clad metal is used for the second pass and any subsequent passes.

The cladding is a structural feature which can be taken into account in RPV integrity assessments. A full understanding of the behaviour of clad regions under PTS conditions is essential to the development of improved methods of RPV assessment. The need for this understanding is particularly important in relation to crack front behaviour in the clad/HAZ/base metal interface region.

Comprehensive results of cladding investigations (specifically dealing with WWER claddings) are given in Annex 1.

6.1.2.1 Degradation Mechanisms

For the RPV cladding on the inside of the vessel, the following degradation mechanisms should be considered:

Irradiation embrittlement

The irradiation embrittlement is the main ageing mechanism of the RPV cladding. RPV claddings consist of welded austenitic steel with some delta ferrite. Determining the irradiation effects in RPV claddings has been the objective of more recent investigations of both WWER and western RPV claddings. As an example the Charpy-V impact tests for WWER-440 claddings did not indicate any significant shift of DBTT but a remarkable reduction of USE. Irradiation was found to increase the yield and ultimate tensile strength of the cladding slightly, see references [6.1.21] to [6.1.27] In general both the ductile initiation, fracture toughness and the tearing modulus decreases with increasing irradiation, [5.1.47]. A summary of the objectives and a list of final reports of relevant EC projects on this topic is given in Appendix A15.

Thermal aging

Thermal aging is typical ageing mechanism in cast and welded stainless steels. Some research results show that thermal ageing of RPV cladding is limited due to the applied very clean welding strips or wires and the operation temperature.

Corrosion

Because of the required water chemistry in the primary circuit of RPV-s generally no corrosion of the RPV cladding is discovered.

Thermal fatigue

No real thermal fatigue trend curves of RPV cladding are available, consequently the allowed number of thermal cycles are determined with very high safety factors. In general the cumulative usage factor is very low.

6.1.2.2 Assessment Methods (see also Reference in Appendix A15.1)

There is currently no clear consensus in Codes and Standards for assessing the influence of austenitic cladding in RPV assessments. Having said this, current nuclear safety codes for assessment of defects generally adapt simplifying assumptions for consideration of the clad region, whereby:

- the cladding is considered as a discrete region for the heat transfer analysis
- the HAZ is ignored implicitly
- only through clad flaws are considered
- flaws are allowed to initiate in the clad region

Assessment of sub-clad defects based on the above simplifying assumptions will be conservative, providing

- the sub-clad defect is modelled as an appropriate 3D surface breaking defect



- estimates of the crack driving force are made on the basis of 3D elastic-plastic finite element analyses

The presence of clad defects with sizes of depths range from 3 to 10 mm can contribute significantly to the overall probability of fast fracture from PTS loading.

The presence of residual stresses is an important factor in assessing the behaviour of under-clad cracks in RPVs. Depending on the temperature of the vessel relative to the so-called “stress free” temperature, tensile residual stresses can exist in the cladding, with a steep gradient to much lower, possibly compressive, stresses in the base metal.

Because of this gradient effect, cladding residual stresses are likely to have only a relatively small effect on the driving force for fracture at positions on a crack front below the clad-base metal interface.

During a PTS transient, the cladding is subject to significant plastic deformation, which serves to reduce the cladding stresses to a low level after the transient.

Warm pre-stressing, linked with the presence of cladding, is a factor that will tend to inhibit crack initiation in cleavage during PTS transients. WPS benefits refer here to the so-called “conservative” WPS principle, whereby cleavage fracture is predicted not to occur for that part of the transient where $dK_I/dt < 0$, even if $K_I > K_{JC}$. It is important to note that the conservative WPS principle is not applicable to the reloading phase of a PTS transient, for which $dK_I/dt > 0$.

Further details see also in Appendix A16.

Cladding defects and underclad defects can be detected by UT, eddy current and visual tests. These tests are usually included in the manufacturing program and in the periodic in-service inspections. Since the austenitic cladding is a tough material, crack propagation during service is highly unexpected.

6.1.2.3 Residual and thermal stresses

Residual stresses in RPV claddings are tensile stresses caused by the higher thermal expansion coefficient of the austenitic cladding compared to the ferritic base metal. Residual stresses occur during welding and after weld stress relieving heat treatment. During the cooling down from the heat treatment temperature this causes very high residual stresses, during the operational heat-up and cool-down cycles thermal stresses occur. The residual stresses after annealing are partially eliminated during the first hydrotest and during operation.

Numerical and experimental investigation concerning residual stresses in RPV claddings were performed in the PHARE 2.03/97 project “Qualification of new materials for replacements/repair of original materials in WWER (440/213)” and in the FP5 project ENPOWER (Management of Nuclear Plant Operation by Optimizing Weld Repairs).

6.1.2.4 Lifetime Evaluation

The cladding is a part of the RPV thus the lifetime cannot be evaluated separately. The main cladding dependent factors are:

- Residual and thermal stresses caused by the cladding manufacture
- Shielding of the base/weld material against the neutron flux

Information relevant to RPV lifetime assessments is presented in Appendix 1 (Fatigue and Thermal Fatigue), Appendix 5 (Assessment of the Evolution of a Flaw in Class 1 ASME Nuclear Equipment) Appendix 8 (Russian Code for WWERs, and VERLIFE) and Appendix 15 (Overview about the EU projects concerning cladding).

6.1.3 Nozzles and Penetrations

This section summarises the design and integrity assessment of three types of RPV nozzles of the Nordic BWR design. This is taken as an example to demonstrate the design, function and the assessment methods of nozzles and penetrations.

Nozzles and penetrations are important parts of the RPV. There are in total 279 nozzles and penetrations on the BWR 75 model of the Westinghouse (former ASEA) BWR RPVs. Oskarshamn unit 3 and Forsmark unit 3 (1200 MW) are both of BWR 75 design. In this report the three main types of nozzles for the BWR 75 are described as regarding design, material and methods for integrity assessment.

The three main nozzles are:

- large nozzles,
- internal set-on bottom nozzles,
- partially welded set-in nozzles.

Examples of the large nozzle type are the feed water inlet nozzles and the steam outlet nozzles. Nozzles for the control rods are of “internally set-on nozzles” type. Set-in nozzles are used typically for connection of small bore pipe systems to the RPV, such as system for reactor water level control (totally 13 nozzles), boron system and system for core water supply.

6.1.3.1 Design and Function of Nozzles

Feed water nozzles

The principal design of a feed water inlet nozzle is shown in Figure 1. The function of the nozzle is to lead the feed water to the RPV. The temperature of the feed water is approximately 100°C lower than that of the reactor water inside the RPV. The cold feed water must be carefully mixed with warm reactor water in order to avoid cracking of the nozzle, the RPV or the internals. Inside the feed water nozzle is a concentric pipe. The pipe conveys the feed water to the feed water sparger. The pipe and the nozzle form together an ejector that sucks up warm reactor water to the space between the pipe and the nozzle. The ejector function keeps the nozzle warm and eliminates risks for thermal fatigue. A proper design of the feed water sparger eliminates thermal fatigue cracking of the internals and RPV.

A so called “safe-end” is welded to the nozzle. A safe-end is in principle a spool-piece of a pipe made of nickel base alloy. The purposes with this design are twofold;

1. The critical weld between the nozzle and the safe-end is a shop weld that is made before the RPV is transported to site. This critical weld is made under best possible conditions in the work shop. The weld between the safe-end and the connecting stainless steel feed water pipe is a metallurgical “simpler” weld which can be made at site.
2. The nickel base alloy, Alloy 600, has a thermal expansion coefficient that is in-between those of the nozzle material, being low alloy carbon steel, and the connecting austenitic stainless steel pipe. This design will reduce the thermal stresses caused by differences in thermal expansion coefficient values.

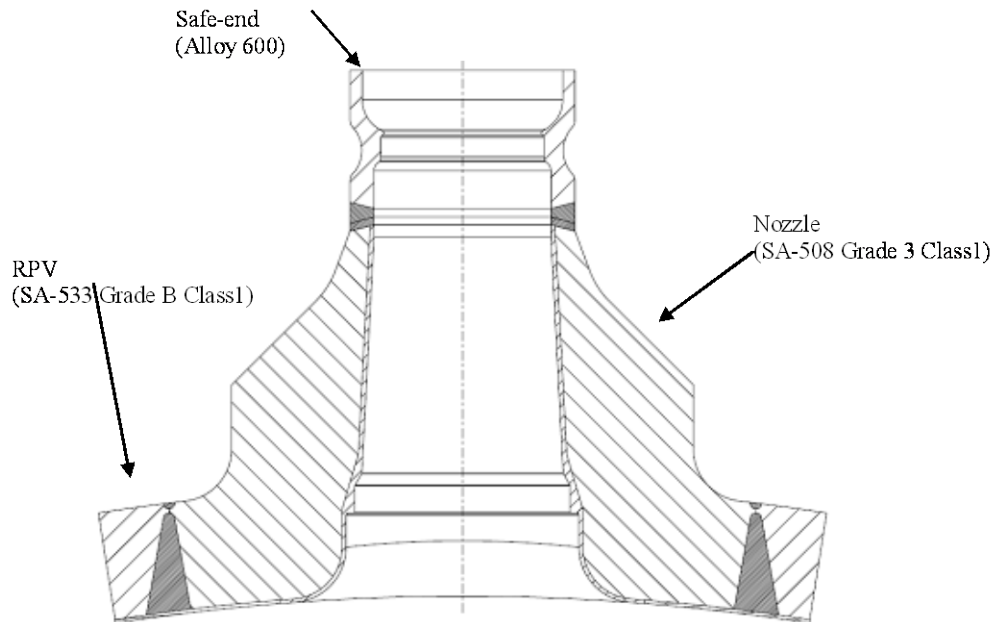


Figure 1 Feed water nozzle with safe-end.

The material of the nozzle is ASME SA-508 Grade 3 Class 1, quenched and tempered low alloy steel forgings for pressure vessels with a carbon content of max 0.25 w-percent.

The safe-end is made of Alloy 600, UNS N06600, which is a nickel-chromium-iron alloy. The weld configuration between the safe-end and the nozzle is show in Figure 2.

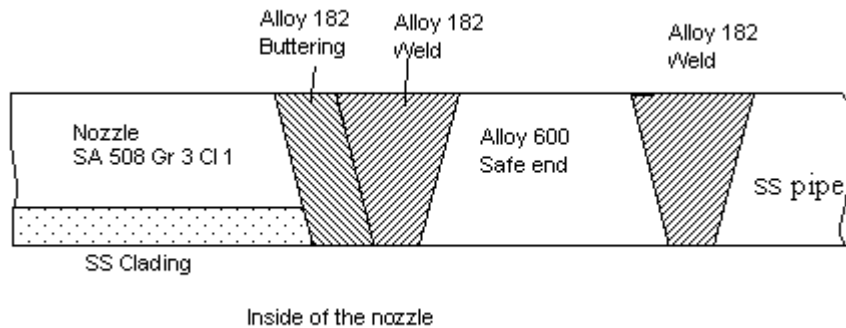


Figure 2 Principal configuration of nozzle to safe-end weld and safe-end to connecting stainless steel pipe weld.

The feed water nozzle has been manufactured in the following sequence (main steps):

- Forging-out, heat treatment and machining.
- Welding the stainless steel (SS) cladding.

- Buttering with Alloy 182
- Machining
- Welding the nozzle into the RPV
- Final heat treatment of the RPV
- Welding the safe-end to the nozzle
- Final machining
- Welding the SS pipe to the safe end (site weld).

Internal set-on nozzles

Nozzles of this type are used in the bottom part of the RPV, a typical application being nozzles for the control rods. The principal design is shown in Figure 3 below. There are totally 169 control rod nozzles for the BWR 75 design.

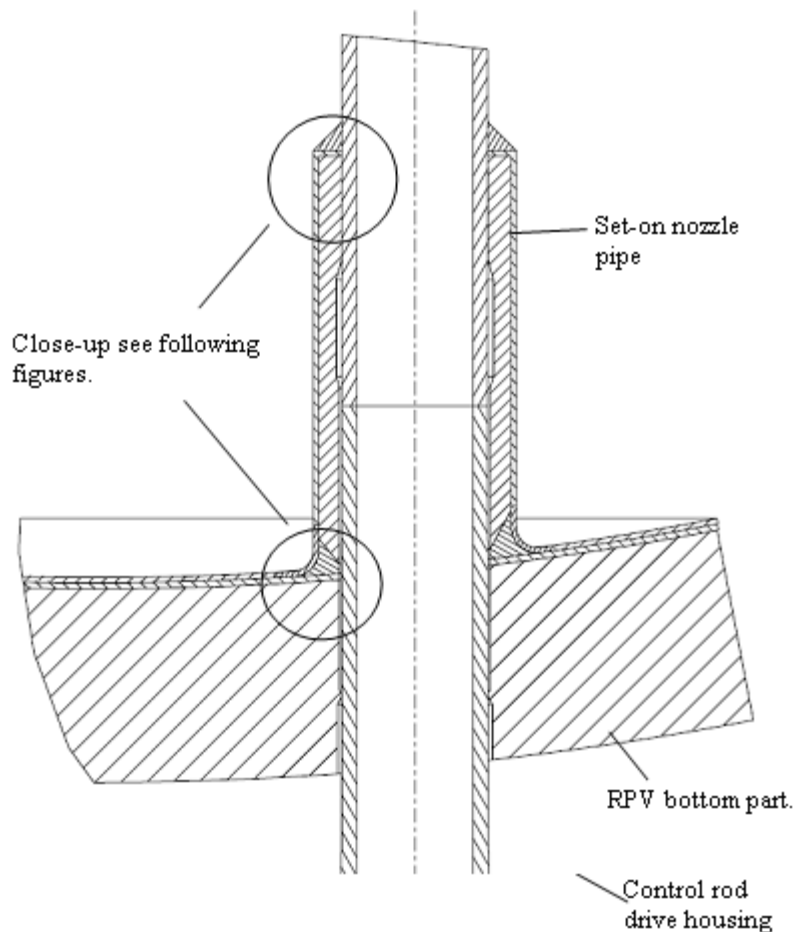


Figure 3 Control rod nozzle principle design.

The locations of the connecting weld between CRD nozzle and the CRD housing and of the weld between the CRD nozzle and the bottom part of the RPV are shown above. These locations are illustrated in detail in Figure 4 and Figure 5.

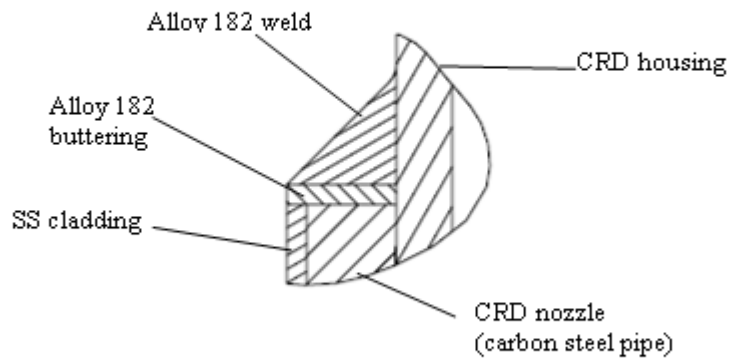


Figure 4 Detail of connecting weld between CRD nozzle & the CRD housing.

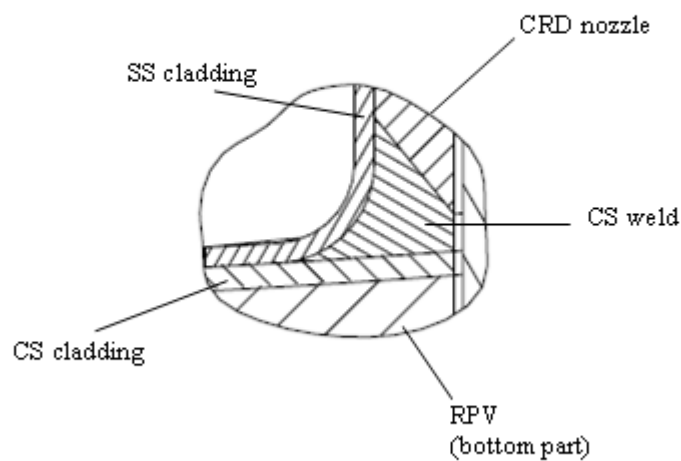


Figure 5 Details of the weld between the CRD nozzle & bottom part of RPV.



The material of the bottom part of the RPV is ASME SA-533 Type B Class 1. This material is very similar to the material for the large nozzles, ASME SA-508 Grade 3 Class 1.

The material of the CRD nozzles is Swedish Standard material SS 2103. This is a forged carbon steel with a carbon content of max C 0.16 wt-percent. The material is used in normalized condition.

The bottom part of the RPV has CS cladding and SS cladding. First are two layers of carbon steel welded to the RPV steel plate. On top of the carbon cladding are two layers of welded SS cladding. The purpose for welding the carbon steel cladding layer is to simplify the welding and heat treatment sequences and procedures. The connection weld to the RPV is made with carbon steel filler material.

The CRD nozzles have been manufactured in the following sequence (main steps):

- Welding of stainless steel cladding to the carbon steel pipe.
- Buttering with Alloy 182 to the top of the carbon steel pipe.
- Machining and weld bevel preparation.
- Welding the CRD nozzle to the RPV.
- Rough machining of the nozzle.
- Heat treatment of the complete bottom part of the RPV.
- Final machining of the nozzle.

Partially welded set-in nozzles

The principal design of a partially welded set-in nozzle, system for reactor water level control, is shown in Figure 6.

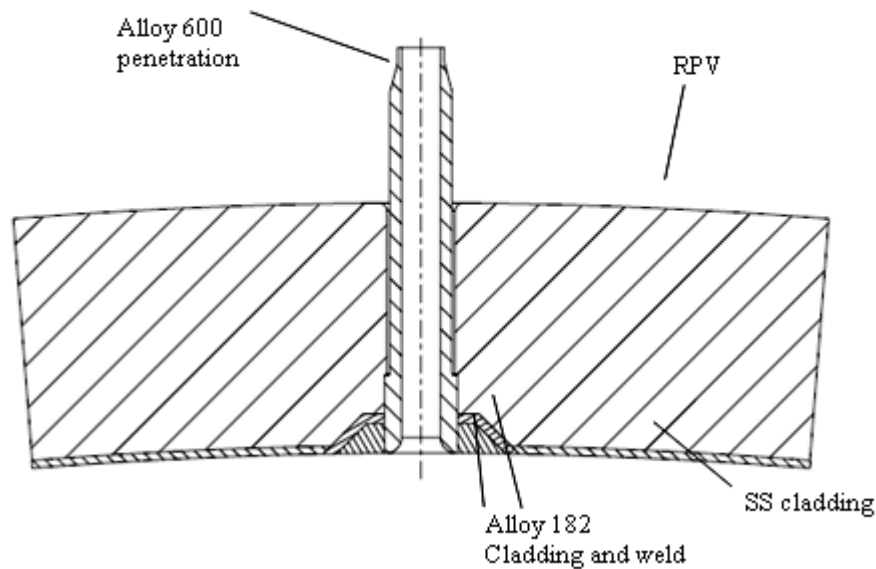


Figure 6 Principle design of a partially welded set-in nozzle.

The set-in nozzle is in principle an Alloy 600 pipe inserted from the inside of the RPV. The nozzle is welded to the RPV with Alloy 182 filler material, J-groove weld. The set-in nozzle pipe is not press fitted or shrink fitted to the RPV wall.

Note, the design of the nozzle and the through hole of the RPV wall make it impossible for the high pressure inside the RPV to push out the Alloy 600 nozzle even if the J-groove weld is completely cracked.

Alloy 600 has been chosen for the material of the partially welded set-in nozzles. The reason is that Alloy 600 has a thermal coefficient close to the low alloy steel of the RPV. Alloy 600 is also relatively easy to weld both to the RPV and to the connecting stainless steel pipe.

The set-in nozzles have been manufactured in the following sequence (main steps):

- Machining of the Alloy 600 nozzle pipe.
- Machining of the through hole and the J-groove
- Weld bevel of the RPV.
- Buttering with Alloy 182.
- Final heat treatment of the RPV upper part.
- Positioning and welding (Alloy 182) the set-in nozzle.
- Welding connecting stainless steel pipe to the nozzle (at site).

6.1.3.2 Assessment Methods

Structural verification

Structural verification, or regular stress analysis, is performed typically according to ASME code Section III, Paragraph NB-3200 [6.1.30]. Verification uses all loads and combinations in the design specification for the actual component. Loads include design, normal, upset, emergency and faulted conditions. For nozzles and penetrations, loads in the vessel and loads from attaching pipes are considered.

3D Finite Element Analysis can be done using general purpose finite element (FE) codes, such as ANSYS [6.1.31] and Abaqus [6.1.32]. Pipe loads generally come from piping analysis performed with special purpose codes, such as PIPESTRESS [6.1.33] and FPIPE [6.1.34].

In a 3D model, critical high stress sections are defined as analytical sections (ASN). As an example, the section can start on the inside of the nozzle go through the thickness of the tube and end on the outside. ASNs shall represent a probable failure path for the actual geometry. ASNs are generally not only chosen at weld positions. Examples are shown in Figure 7.

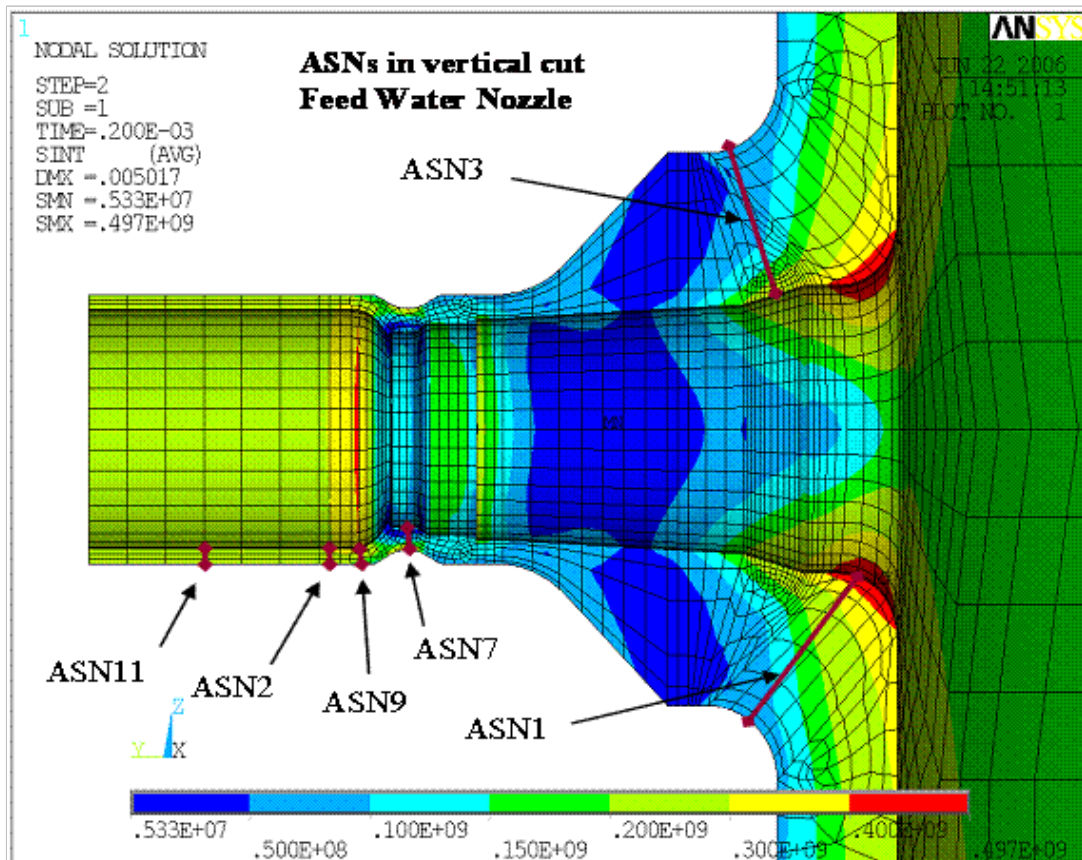


Figure 7 Typical Analytical Sections (ASNs) for stress evaluation in a feed water nozzle. Stresses [Pa] results from design pressure 84 bar including pipe load.

(Structural strength of cladding is not considered for primary loads and it is not shown here)



Stresses at the ASNs are linearised and primary and secondary stresses are checked against the corresponding allowable stresses, as given by the ASME Codes. Total stress, including peak stresses, are used in fatigue analysis using normal operation and upset loads. This includes thermal transients for an expected lifetime of 40 to 60 years. Fatigue usage is calculated for surface points (end points) on ASNs. ANSYS linearization and fatigue capabilities are modified to meet the ASME Code evaluation procedure.

Stress distributions from the structural verification may be used to provide input to subsequent fracture mechanics calculations.

Fracture mechanics

Fracture mechanics is used to determine the largest possible inspection interval in weld regions. A minimum detectable flaw is used in a crack growth calculation over time until maximum critical defect size is reached.

Additional structural calculations are often needed to define the stress state at the presumed flaw. Models from structural verification often need refinement and additional load cases must be run. Weld residual stresses are never included in the structural verification. For pipes and vessels there are standard solutions for the stress distribution in the literature. For more complex geometries weld residual stresses could be calculated using FEA.

Fracture mechanics analyses can be carried out by using the geometries and methods in handbooks/guidelines and with applicable structural integrity analysis codes, such as SACC (Safety Assessment of Components with Cracks). SACC contains routines for fracture assessment based on the R6 Method [6.1.42] and on Section XI of ASME code [6.1.35]. There are also routines for calculation of crack growth due to fatigue and stress corrosion cracking (SCC). Often, the fracture mechanics parameter driving the crack growth in the computations is the mode I stress intensity factor, K_I . Concerning surface cracks, when computing the crack growth increment by increment, one can include to the computations the K_I value from only one point along the crack front, typically crack tip/bottom, from two points, typically crack tip and surface points, or from several points. Most often the maximum K_I value along the crack front is that in crack tip. Bamford discusses this issue in ref. [6.1.43], and concludes concerning crack growth computations based on the above mentioned one or two points, that keeping the aspect ratio (crack depth divided by its length) as 1/6, leads always to conservative results. However, to include the possible changes of crack shape in the computed crack growth realisation, it is necessary to use K_I values from at least two points along the crack front. Concerning using K_I information from several points along the crack front, Cruse and Besuner [6.1.44] were the first to utilise the concept of an integrated average of the stress intensity factor. This procedure uses all available K_I values along the crack front. They achieved good matching between experimental and computed crack growth results.

For fatigue induced crack growth, Paris-Erdogan equation [6.1.36] is typically used. Whereas for SCC, the rate equation [6.1.37] is often used. Concerning these two equations, a separate task is to find applicable values for their material, temperature and environment specific parameters. Concerning metallic NPP component materials, for Paris-Erdogan equation [6.1.36] such parameter values are given e.g. in Appendix C of Section XI of ASME code [6.1.35] and SSM handbook [6.1.45]. Whereas in case of SCC, there are several sources providing more or less applicable parameter values, such as refs. [6.1.38], [6.1.39], [6.1.40], [6.1.41] and [6.1.45]. One important notion concerning loads is that in case of fatigue induced crack growth the typically high weld residual stresses can most often be excluded from the crack growth computations, whereas in case of SCC they need to be taken into account in full.

In general, the detection of a crack during inspection will lead to a repair job. Fracture mechanics can be used to show that continued operation until next outage is allowed and repairing can be postponed until then. The repaired geometry is compared to the original geometry. Any significant geometry deviation results in a new or revised structural verification for the actual component.

6.1.4 Internals

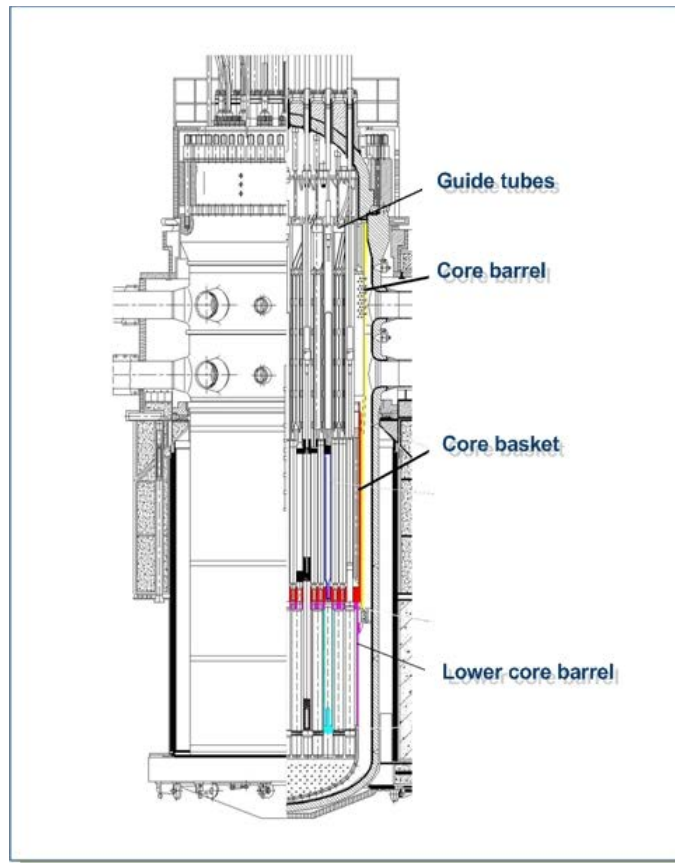
Core support structures are those structures or parts of structures which are designed to provide direct support or restraint of the core (fuel and blanket assemblies) within the reactor pressure vessel.

Internal structures are all structures within the reactor pressure vessel other than core support structures, fuel and blanket assemblies, control assemblies, and instrumentation.

These structures do not function as pressure boundaries but they play an important role as they contain the core of the reactor, channel water flow inside the vessel and both support and guide the instrumentation necessary for controlling and monitoring the reactor. Basically, the strength and fatigue analyses should be performed in accordance with the provisions of standards and procedures such as the ASME (ASME III NG) [6.1.49] for design stage. Although the operating experience has shown that high dose irradiation of stainless steel reactor internals can lead to degradations that were not taken into consideration at the design stage.

6.1.4.1 Design and Function

The reactor vessel internals, namely the guide tubes, core barrel, core basket and lower core barrel constructions (Figure 8). The internal structures of water reactors are essentially made of austenitic stainless steel since they are generally considered as having a good resistance to both water corrosion and neutron irradiation embrittlement. But after an operation for a long time, some cracking appeared.



(a)

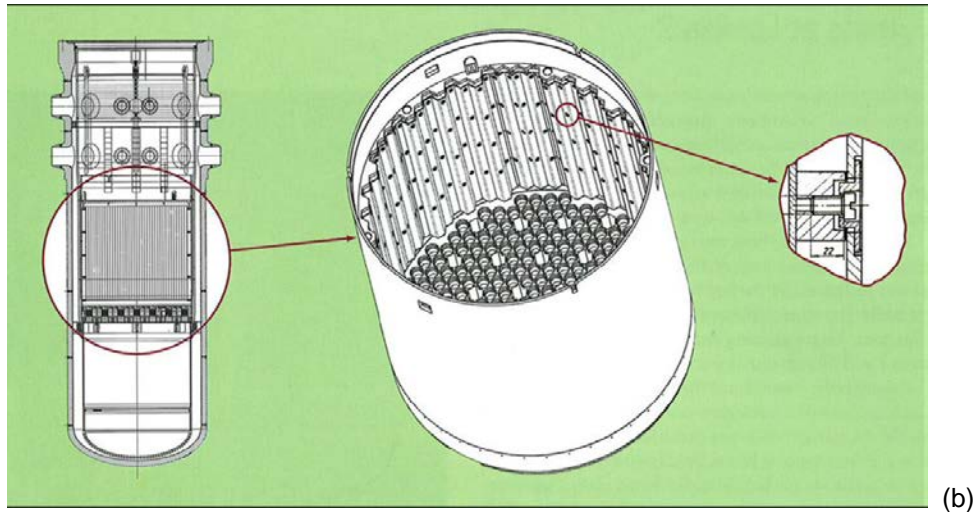


Figure 8: (a) Construction of WWER 440 RPV and internals and (b) core basket of VVER-440 [6.1.51]

The core barrel assembly of the RVI makes the transition between the polygonal core contour and the circular shape of the core barrel. The vertical baffle plates and horizontal former plates are integrated using bolted connections. The former plates to the core barrel are fixed by bolts or welds.

Loading Conditions

The loadings that shall be taken into account in designing core support structures include, but are not limited to the following [6.1.49]:

- pressure differences due to coolant flow;
- weight of the core support structure;
- superimposed loads such as those due to other structures, the reactor core, steam separating equipment, flow distributors and baffles, thermal shields, and safety equipment;
- earthquake loads or other loads which result from motion of the reactor vessel;
- reactions from supports, restraints, or both;
- loads due to temperature effects, thermal gradients and differential expansion, or both;
- loads resulting from the impingement or flow of reactor coolant, or other contained or surrounding fluids;
- transient pressure difference loads, such as those which result from rupture of the main coolant pipe;
- vibratory loads;
- loads resulting from the operation of machinery, such as snubbing of control rods;
- Handling loads experienced in preparation for or during refuelling or in-service inspection.

Functional temperature and fluence information

The nominal inlet and outlet temperature in the reactor vessel is usually around 270-300°C for the water but components can reach locally significantly higher temperatures (up to 370-380°C) due to gamma heating.

Former research results of neutron physics calculations concern the position of the wall of the reactor vessel. The fluence of the test sample estimated for 60 years practically equals with the load of the outer surface of the core barrel, and it is ~12dpa. It can be proved that the fluence value of the core boundary can be multiplied (~5-10) of the value of the core barrel, namely it can be estimated 35-60 dpa (90 dpa for bolt's head) for 60 years operation time. Table 2 shows the estimated irradiation dose on location with maximum dose.

Table 2 Estimated irradiation dose on location with maximum dose

Irradiation time [years]	Irradiation [dpa]		
	Bolt head, baffle	Shank of the bolt	Core basket
30	42	36	34
50	75	61	58
60	91	73	70

Based on the estimation, the results show 20% decrease in the bolt head and 40% decline in the shank of the bolt in radial direction. The estimated irradiation value at the bolt neck is circa 85 dpa.

6.1.4.2 POTENTIAL DEGRADATION, MATERIAL MODELS AND EVALUATIONS

Nowadays the issues concerning the RPI are a very important research area, but the available opened literature does not contain enough information of its failures and there is no a common accepted assessment method. Contrary to the reactor pressure vessel, there are few surveillance programs in place to monitor the evolution of the reactor internals materials properties. However several research projects are running such as the PERFORM 60 European project that contributes to model irradiation effects on microstructure, environment, mechanical behaviour and their interactions leading to irradiation assisted stress corrosion cracking (IASCC).

The possible ageing mechanisms of RPI is shown in Figure 9. Evaluation of these mechanisms is based on service experience, laboratory data and relevant experience from other industries.

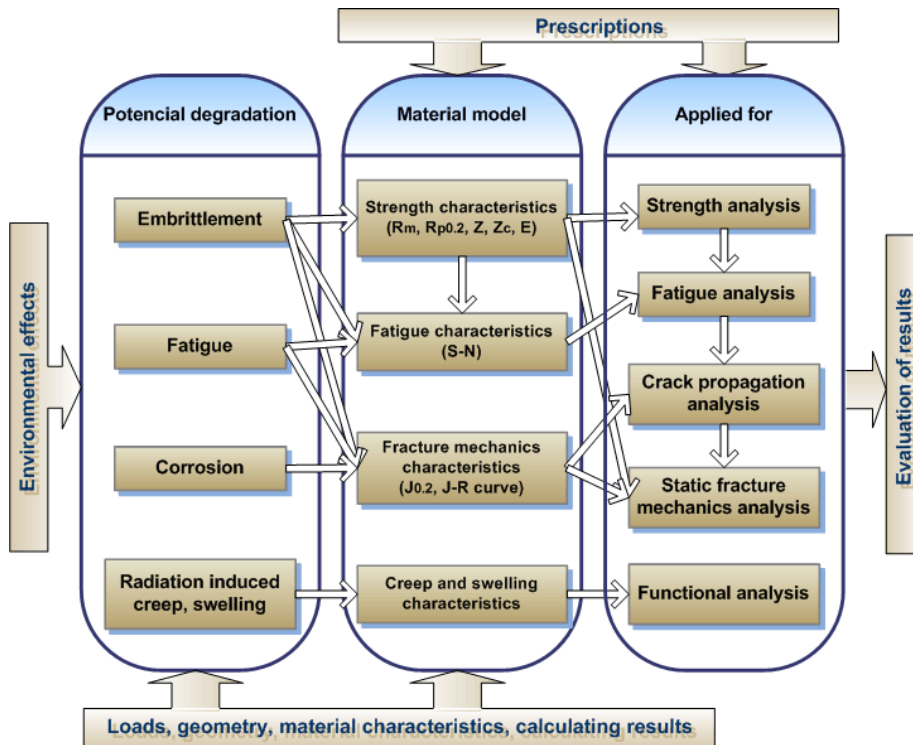


Figure 9 Evaluation methodology

During the fracture mechanical evaluation it should be examined that the changes of the material characteristics how influence the size of the allowable cracking, and the velocity of the crack propagation in RVI. Further purpose is to determine that size of crack, where in case of highest cracking exist an operating or breakdown transient, to which the examined environment loses its stability.

The austenitic steels and the base material of the reactor internals are characterized by ductile fracture mode. At the same time the effect of irradiation causes embrittlement mechanisms in the material, which can lead to decrease of the toughness of the material. These embrittlement mechanisms can decrease the Charpy test values and the J-R curve (and $J_{0.2}$). The J-R curve can be applied (beside the strength material characteristics) to the investigation of the stability of the crack or the stable crack propagation. The evaluation can be based on FAD or J-R curve, for instance according to Appendix K of ASME BVPC, Volume XI.

The main stream of the researches concentrates on the baffle bolt cracking. Up to now this operating experience is mostly limited to the baffle bolt cracking issue in PWRs.

6.1.4.3 Material Characteristics

The main structural material used for Western type reactors are A304, A304L, A316, A316L, for WWER it is titanium stabilized austenitic stainless steel 08Ch18N10T (equivalent to A-321); minor parts were made from nickel alloy ChN35VT-VD (this material is used for studs and is tungsten alloyed) and the steel 14Ch17N2.

Static strength material characteristics

The evolution of the defect microstructure during LWR irradiation strongly affects the strength and mechanical properties of the alloy. With increasing dose, the yield strength increases, and ductility and fracture toughness decrease. Relative to the unirradiated value for an annealed

material, the yield strength can increase by a factor of 4 at moderate dose. The increase in yield strength can be seen to follow a square root dose dependence reaching saturation by ~10-20 dpa. Radiation-induced hardness increases consistently with the dislocation loop microstructure.

The RVI suffer by several degradation mechanisms in course of reactor operation, from among these the most serious problem is the change of material properties and J-R curve due to neutron irradiation. The requested data to characterize the operational change of material properties means the material changes due to irradiation. To perform the calculations the material characteristics and J-R curve should be determined concerning 50 and 60 years relevant to the expected maximum fluence.

The J_c static crack growth resistance and the K_{Jc} stress intensity factor as a function of the size of irradiation also can be determined. For example for 30 dpa $J_c = 15 \text{ kJm}^{-2}$ and $K_{Jc} = 51 \text{ MPa}\sqrt{\text{m}}$ (for the base metal), and both material characteristics turn into saturation over 30-35 dpa (in case of the base metal and the weld material too).

Material characteristics concerning resistance of the fatigue and fatigue crack propagation

Fatigue curves applied in the design stage are quite conservative and can be valid after long time operation. For instance fatigue curves for WWER can be calculated based on strength characteristics. Investigations show that the calculated fatigue curves run above the fatigue curve according to PNAE. In this manner the earlier fatigue analyses will be valid for the 50-60 years operation time, as illustrated in Figure 10.

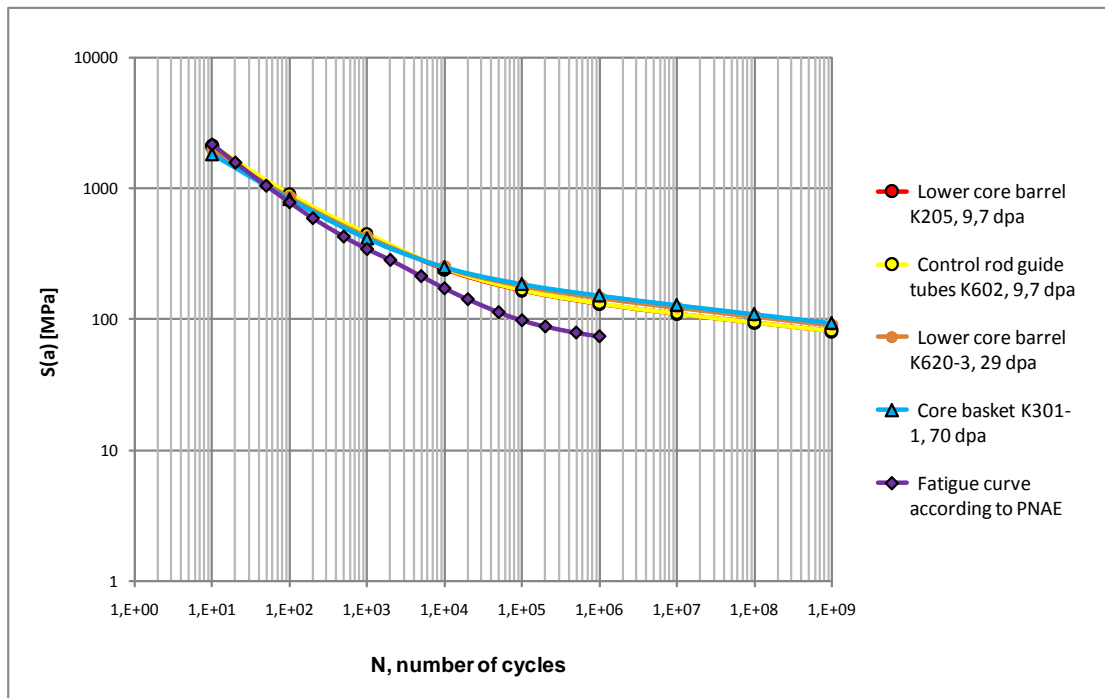


Figure 10 Fatigue curves concerning 60 years operation time, r=0

Since the operating load cycles do not cause neither significant load, neither large number of cycles and the CUF value is usually much smaller than 0.2, thus these do not cause fatigue crack propagation. The crack propagation can result only from the vibration of the reactor internals, if the stress intensity factor due to vibration load effects larger than the threshold SIF of the fatigue crack propagation (ΔK_{th}). The vibration caused numbers of cycles are as big that the small crack propagation velocity can cause promptly a larger crack size. Therefore the allowable crack size has to be as small that the vibration load cannot cause crack propagation.

The currently known examinations did not reveal cracks in the dangerous cross-section of the control rod guide tubes and lower core barrel.

Material characteristics concerning the resistance of the stress corrosion crack propagation

After longer operation, the appearance of stress corrosion cracking cannot be excluded in the reactor vessel internals. This crack propagation is function of the temperature, the media and other outer effects, like the neutron irradiation. To investigate the possibility of the crack propagation the threshold of the KISCC stress intensity factor is needed. Although the initiation decreases with increasing fluence up to a dose, unfortunately there is no consensus on the exact level of this threshold, nor the dose of the saturation. Some available experimental results are summarized in [6.1.53].

Stable crack propagation analysis for the crack appearing in fastener bolts can be performed. The ASME standard does not contain information regarding calculation of the crack appearing in bolt, thus the calculations can be performed according to the FITNET procedure [6.1.52] (based on BS 7910).

From the point of view of the irradiation induced stress corrosion crack the critical environment are the fastener bolts of basket, which can be characterized with fast irradiated neutron fluence and the stagnant environments.

Swelling

The irradiation swelling of austenitic stainless steels is well known in fast reactors, where the operating temperatures and neutron fluxes are higher than in PWRs. Until recently, it was considered that irradiation swelling did not occur at temperatures below 365°C and that PWR internal structures would not be affected. According to [6.1.55], after long-term operation and high neutron doses (mainly baffle bolts and flux thimble tubes) have shown the presence of bubbles or voids. The resulting swelling remains however very limited.

Test results about the creep and swelling of the materials of the VVER internal structures due to irradiation are only available in limited quantity. There are abundant data available about the swelling of the steels 304 and 306 in literature, which steels have similar chemical composition to the Russian steels marked with Ch18N9, 08Ch18N10T and Ch16N11MZ, and it is likely to happen that the changes in the physical-mechanical attributes due to irradiation will be alike.

It was established in the CIR program that almost all of the austenitic steels damage at the same level due to swelling caused by radiation, in the range of determined temperature and irradiation dosage.

It was also stated that at the same integrated dosage, the temperature dependency of the swelling with the increase of the speed of the irradiation dosage will move to higher temperature range, i.e. at lower temperature the slower rate of irradiation can cause the same damage as the fast irradiation at higher temperature. There are only limited quantities of data available about the relation of the swelling of the austenitic stainless steel and the flux in point of neutron radiation. The decrease of the swelling at the increase of the irradiation flux can also be seen at the 08Ch18N10T and AISI 304L steels.

The mechanical stress also greatly affects the swelling of the austenitic steels. The testing of pipes under pressure, showed at the AISI 316 austenitic steel [6.1.56] that the irradiation at the stress level not greater than the yield strength of the material, in non-irradiated status (~138 MPa) will cause the increase of swelling. At the same time the decrease of swelling can be experienced with the given irradiation conditions at the stress level greater than the yield strength of the material. Practically the effect of the algebraic sign of the stress to the swelling due to irradiation in the austenitic steels is unknown.

In the research program of the Prometey Institute, they've irradiated specimens consisting of 08Ch18N10T steel as base material and its welds in BOR-60 reactor at the temperature of 330÷350°C and at the damaging dosage of 30-46 dpa. They've noticed that in the case of the irradiation of the 08Ch18N10T base material and weld at lower temperature (330÷350°C), the swelling is almost non-existent (less than 0,1%) (see also Fig. 15), i.e. if the components of the internal equipment are made from 08Ch18N10T base material and weld and their maximum operating temperature is 350 °C the swelling can be neglected. The swelling of the 08Ch18N10T steel with the conservative estimation relative to the small damaging flux is ~2,6 %, at the conditions stated above at the increase of the length of the irradiation to 60 dpa. The Prometey Institute has used plenty of research results analyzed and generalized in [6.1.57] to create a database concerning the swelling of the 08Ch18N10T steel.

The data and the experimental results published by H. M. Chung [6.1.55] confirm that while the materials irradiated in fast reactor at the temperature typical in our case, don't swell notably, at the irradiation intensity according to a polygon cope swelling can be expected on larger scale. So the swelling of the PWR internal structures operating for 50-60 years should be reckoned with even at a relatively lower temperature. So during the analysis the connections verified for the fast irradiated specimens have to be adapted to the measuring results of the specimens exposed to lower irradiation intensity.

Up to now the highest swelling measured in PWR components remains limited (below 0.25%) [6.1.57], but there is an uncertainty on the long term effects, especially considering 60 years of operation.

Effect of swelling

The swelling will appear primarily in the component exposed to high gamma irradiation. The changes of the swelling appearing in the wall of the basket should be determined in order to demonstrate the distribution of the swelling of the wall. In the wall of the basket (at the half of the height of the zone) can be described the swelling along the wall with the help of the swelling relation given by Prometey Institute [6.1.58], assuming that the value of the irradiation can be decreased with 40 % in the wall.

The examination results show that the swelling and the irradiation induced stress corrosion crack are the most significant degradation mechanisms (among the degradation mechanisms) in the course of prolongation of the operation time of the RVI.

From the point of view of the swelling the critical environments are the follows: basket component at the middle part of the zone, baffle, fastener bolts and cylinder of the core basket.

Based on measurement results and the presumable irradiated and temperature data, with complete certainty cannot be excluded that 0.5-1.0 % swelling will cause deformation, tightening in the fasteners bolts after 30 years operation time. The deformation of the baffle can influence the installation, assemblage and the joints too. The appearance of abrasion places on the matt surfaces will be the first sign of this deformation.

The swelling caused hindered expansion of the bolt and the possible stress corrosion cracking of the bolts can lead to fracture.

Stress relaxation

Under irradiation the initial prestress applied in the baffle bolts is reduced by irradiation-enhanced creep, at least in a first phase. In a later phase the irradiation swelling of the baffle plates could induce an increase of the stresses. This is shown when baffle bolts are replaced, by a decrease of the unbolting torque as a function of the dose received by the bolt. Up to now the potential increase due to swelling is not seen in the plants



6.1.4.4 Conclusions

The examination results show that the swelling and the irradiation induced stress corrosion crack are the most significant degradation mechanisms (among the degradation mechanisms) in the course of prolongation of the operation time of the RVI.

From the point of view of the swelling the critical environments are the follows: basket component at the middle part of the zone, baffle, fastener bolts and cylinder of the core basket.

Based on measurement results and the presumable irradiated and temperature data, with complete certainty cannot be excluded that 0.5-1.0 % swelling will cause deformation, tightening in the fasteners bolts after 30 years operation time. The deformation of the baffle can influence the installation, assemblage and the joints too. The appearance of abrasion places on the matt surfaces will be the first sign of this deformation.

From the point of view of the irradiation induced stress corrosion crack the critical environment are the fastener bolts of basket, which can be characterized with fast irradiated neutron fluence and the stagnant environments. The swelling caused hindered expansion of the bolt and the possible stress corrosion cracking of the bolts can lead to fracture.

It is necessary to perform more accurate estimation in order to examine the expected actual damage of the components under the influence of swelling. The point of these estimation is to accurate the present conservative determination of the life expectancy considering the actual flow and irradiation conditions. To make these examinations it is necessary to determinate the actual irradiation temperature of the bolts, polygon skirt and the basket skirt considering the real gamma heating and local flow conditions. Based on the actual irradiation temperatures the estimated swelling values of the given components and hereby the extent of the examinations probably significantly can be reduced.

Using the accurate swelling value, FEM analyses are needed in order to determine the presumable deformation of the basket components. With these FEM analyses we get previous information relating to limited assembling and manageability, permissibility of hindered expansion.

6.1.5 References (RPV)

- [6.1.1] KTA 3201 "Components of the Reactor Coolant Pressure Boundary of Light Water Reactors". Part 1: Materials and Product Forms, June 1998; Part 2: Design and Analysis, June 1996; Part 3: Manufacture, June 1998; Part 4: In-Service Inspections and Operational Monitoring, June 1999.
- [6.1.2] R. Gerard. "ATHENA Thematic Network - Final report", February 2005.
- [6.1.3] M. Uhlemann, G. Müller, A. Ulbricht, J. Böhmert. "Effect of Hydrogen on Toughness of Irradiated Reactor Pressure Vessel Steels", Reactor Safety Research Project No. 1501267, Final Report, December 2004.
- [6.1.4] Mueller, G.; Uhlemann, M.; Ulbricht, A.; Boehmert, J.: Influence of hydrogen on the toughness of irradiated reactor pressure vessel steels. *Journal of Nuclear Materials* (2006)359, 114-121
- [6.1.5] US NRC Regulatory Guide 1.99 Revision 2 "Radiation Embrittlement of Reactor Vessels Materials", May 1988.
- [6.1.6] RSEM Code, Article B7212. "In-service Inspection Rules for Mechanical Equipment of PWR Nuclear Islands", (RSEM) (July 1990).
- [6.1.7] NUREG CR-6551. "Improved Embrittlement Correlations for Reactor Pressure Vessel Steels", Prepared by E.D. Eason, J.E. Wright, and G.R. Odette, September 1998.
- [6.1.8] ASTM E 900-02. "Guide for Predicting Radiation-Induced Transition Temperature Shift in Reactor Vessel Materials, E706 (IIF)" Annual Book of ASTM Standards, Vol. 12.02, American Society for Testing and Materials, West Conshohocken, PA., 2002.
- [6.1.9] J.A. Wang, N.S.V. Rao, S. Konduri. "The development of radiation embrittlement models for US power reactor pressure vessel steels", *Journal of Nuclear Materials*, 362 (2007) 116-127.
- [6.1.10] S. Jumel, J.C. Van-Duysen. "RPV-1: A Virtual Test Reactor to simulate irradiation effects in light water reactor pressure vessel steels", *Journal of Nuclear Materials*, 340 (2005) 125-148
- [6.1.11] EURATOM FP6 Integrated Project PERFECT ("Prediction of the Effects of Irradiation on Reactor Components", 2004-2008.
- [6.1.12] Structural Integrity Assessment Procedures for European Industry. SINTAP Procedure Final Version: November 1999.
- [6.1.13] K. Wallin, P. Nevasmaa, A. Laukkanen, T. Planman, "Master Curve analysis of heterogeneous ferritic steels", *Engineering Fracture Mechanics*, Volume 71, Issues 16-17, November 2004, Pages 2329-2346.
- [6.1.14] H.-W. Viehrig, M. Scibetta, K. Wallin, Application of advanced Master Curve approaches on WWER-440 reactor pressure vessel steels, *International Journal Pressure Vessel and Piping* 83(2006), pp. 584-592.
- [6.1.15] Guide for strength analysis of the equipment and piping of nuclear power units, PNAE G 7 002 86, Energomashizdat, Moscow, 1989, in Russian.
- [6.1.16] Guidelines on Pressurized Thermal Shock Analysis for WWER Power Plants: A Publication of the Extra budgetary Programme on Safety of WWER and RBMK Nuclear Power Plants, IAEA Publication IAEA-EBP-WWER-08, Rev. 1, January 2006

- [6.1.17] Unified Procedure for Lifetime Assessment of Components and Piping in WWER NPPs – VERLIFE, European Commission, Final Report, Contract N° FIKS-CT-2001-20198, September 2003.
- [6.1.18] Safety Standard of the Safety Standards Commission (KTA). “Surveillance of the Irradiation Behaviour of Reactor Pressure Vessel Materials of LWR Facilities”, KTA 3203 (6/01)
- [6.1.19] American Society for Testing and Materials. “Conducting Surveillance Tests for Light Water Cooled Nuclear Power Reactor Vessels”, ASTM E 185 (1994).
- [6.1.20] Standard Test Method for Determination of Reference Temperature, T_0 for Ferritic Steels in the Transition Range, ASTM E 1921-03, Annual Book of ASTM Standards, Vol. 03.01, American Society for Testing and Materials, West Conshohocken, PA, 2003.
- [6.1.21] Guidelines on Pressurized Thermal Shock Analysis for WWER Nuclear Power Plants (Rev. 1) IAEA-EBP-WWER No. 8 (Rev.1)2006, English, (File Size: 1447 KB). Date of Issue: 23 May 2006.
- [6.1.22] VERLIFE. Unified Procedure for Lifetime Evaluation of Components and Piping in WWER NPPs
- [6.1.23] F. Gillemot, M. Horvath, G. Uri, T. Fekete, E. Houndeffo, B. Acosta, Debarberis, H.-W. Viehrig: “Radiation stability of WWER RPV cladding materials”, International Journal of Pressure Vessels and Piping 84 (2007) 469–474
- [6.1.24] N.Alekseenko et al, “Radiation Damage of Nuclear Power Plant Pressure Vessel Steels” American Society of Nuclear Engineers ANS, Yearly meeting USA, 1997
- [6.1.25] V. A. Nikolaev, I. P. Kursevich, E. V. Nesterova, O.Yu. Prokoshev, V. V. Rybin: “Brittle fracture tendency of anticorrosive cladding metal on pressure vessels of water-cooled reactors” UDK 621.791.92:539.56:621.039.536.2
- [6.1.26] M. Bethmont (EDF) – P. Soulat (CEA) – B. Houssin (FRA): “Mechanical properties of reactor pressure vessel cladding. Effect of thermal ageing and irradiation” 1995.
- [6.1.27] F. Gillemot, M. Horváth, G. F. Gillemot, M. Horváth, G. Úri, H-W. Viehrig, L. Debarberis, T. Fekete, E. Houndeffo. “Behaviour of irradiated RPV: Behaviour of irradiated RPV cladding”, Paper presented for AMES workshop, 6-8 February 2006, Hévíz (Hungary).
- [6.1.28] J.S. Lee, I.S. Kim, R. Kasada, A. Kimura. “Microstructural characteristics and embrittlement phenomena in neutron irradiated 309L stainless steel RPV clad”, Journal of Nuclear Materials, 326 (2004) 38-46.
- [6.1.29] Payraudeau, K., K. Zamoum, T. Pasquiar. “Reactor Pressure Vessel of Tricastin Unit 1 Core Zone Inspection - Comparison of Non-Destructive Examination Results Among Two Core Areas Inspections Performed in 1999 and in 2003”, ASME Pressure Vessels and Piping Conference, Vol. 487, July 2004, San Diego, California USA.
- [6.1.30] ASME Boiler and Pressure Vessel Code Section III, Division 1, Article NB-3200. 2010 Edition.
- [6.1.31] ANSYS Release 11.0 Documentation. Ansys Inc, 2008, Canonsburg, USA.
- [6.1.32] Abaqus, Analysis User’s Manual, Version 6.11-1. Dassault Systèmes, 2011, Providence, RI, USA.
- [6.1.33] PIPESTRESS 3.6.2, User's Manual. DST Computer Services SA, 2009, Switzerland.
- [6.1.34] ASME – FPIPE –Ohjelman ASME NB Jälkikäsittelijä – Referenssimanuaali. Engineering Office FEMdata Oyj, 5.5.2011, Espoo, Finland. (in Finnish)

- [6.1.35] ASME Boiler and Pressure Vessel Code, Section XI. 2010 Edition.
- [6.1.36] Paris, P., C., Erdogan, F. A Critical Analysis of Crack Propagation Laws. Journal of Basic Engineering, Vol. 85, 1960, pp. 528-534.
- [6.1.37] Congleton, J., Craig, I., H. Corrosion Fatigue. In: Corrosion Processes, Editor Parkins, R., N. Applied Science Publishers, 1982.
- [6.1.38] U. Morin, C. Jansson, B. Bengtsson, Crack growth rates for Ni-base alloys with the application to an operating BWR, Proceedings of the 6th International Conference on Environmental Degradation of Materials in Nuclear Power System, 1993.
- [6.1.39] BWRVIP-130: BWR Vessel and Internals Project, BWR Water Chemistry Guidelines – 2004, Revision, EPRI, Palo Alto, CA: 2004. 1008192.
- [6.1.40] Codes for Nuclear Power Generation Facilities-Rules on Fitness-for Service for Nuclear Power Plants, JSME S NA1-2004.
- [6.1.41] M. Ozawa, Y. Yamamoto, K. Nakata, M. Itow, N. Tanaka, M. Kikuchi, M. Koshiishi, J. Kuniya, Evaluation of SCC crack growth rate in alloy 600 and its weld metals in simulated BWR environments, Proceedings of the 12th International Conference on Environmental Degradation of Materials in Nuclear Power System – Water Reactors – Edited by T.R. Allen, P.J. King, and L. Nelson TMS (The Minerals, Metals & Materials Society), 2005.
- [6.1.42] R6 Method - Assessment of the Integrity of Structures containing Defects, Revision 4. British Energy (BE). 2004 update of 2001 edition.
- [6.1.43] Companion Guide to the ASME Boiler & Pressure Vessel Code - Criteria and Commentary on Select Aspects of the Boiler & Pressure Vessel and Piping Codes, Third Edition. Editor: Rao, K., R. American Society of Mechanical Engineers (ASME), 2009, New York, USA.
- [6.1.44] Cruse, T., A., Besuner, P., M. Residual life prediction for surface cracks in complex structural details. J. of Aircraft 1975;12(4).
- [6.1.45] Dillström, P. et al. 2008. A Combined Deterministic and Probabilistic Procedure for Safety Assessment of Components with Cracks – Handbook. SSM Research Report 2008:01, Swedish Radiation Safety Authority (Strålsäkerhetsmyndigheten, SSM). Stockholm, Sweden, 2008. 27+196 p.
- [6.1.46] Guidelines for Prediction of Irradiation Embrittlement of Operating WWER-440 Reactor Pressure Vessels. IAEA TECDOC 1442. 2005. [\(ISBN:92-0-105605-2\)](#).
- [6.1.47] Elisabeth Keim, Roland Hertlein, Ulf Ilg, Günter König, Norbert Schlüter, Martin Widera, Brittle Fracture Safety Analysis of GERMAN RPVS Based on Advanced Thermal Hydraulic Analysis, Proceedings of PVP 2008, 2008 ASME Pressure Vessels and Piping Conference, July 17-20, 2008, Chicago, Illinois, USA
- [6.1.48] .E. Keim, C. Schmidt, A. Schöpfer, R. Hertlein, Life Management of reactor pressure vessels under pressurized thermal shock loading: Deterministic procedure and application to Western and Eastern type of reactors, IAEA INTERNATIONAL WORKING GROUP on LIFE MANAGEMENT OF NUCLEAR POWER PLANTS, SPECIALISTS MEETING on Methodology and Supporting Research for the Pressurized Thermal Shock Evaluation Rockville, Maryland, United States of America, 18-20 July, 2000
- [6.1.49] ASME Boiler and Pressure Vessel Code, ASME, New York (2003).
- [6.1.50] Regulations for strength analysis of equipment and piping of nuclear power plants, PNAE G-7-002-87, Energoatomizdat, Moscow, 1989.

- [6.1.51] J.J. Regidor, A. Ballesteros, Tecnatom S.A., Spain; K. Heid, P. Luostarinen, „Inspection and Replacement of Baffle Former Bolts in VVER-440 Reactor Type”, 6th International Conference on NDE in Relation to Structural Integrity for Nuclear and Pressurized Components, October 2007, Budapest, Hungary
- [6.1.52] FITNET Procedure, Annex A: Stress Intensity Factor (SIF) Solutions, 2008 January
- [6.1.53] PERFORM 60 D3.2-1: “Review of existing methods of predicting the effect of irradiation on internals materials in the context of 60 years of operation”, December 2010
- [6.1.54] PERFORM 60 D3.2-1: “Review of existing methods of predicting the effect of irradiation on internals materials in the context of 60 years of operation”
- [6.1.55] Chung HM, “Assesment of void swelling in austenitic stainless steel core internals” (NUREG/CR-6897), Argonne National laboratory, 2006.
- [6.1.56] Prediction of Fatigue Crack Growth Rate of Austenitic Steels Taking into Account Effect of Irradiation and Environment. V.A. Fedorova, B.Z. Margolin (CRISM “Prometey, St. Petersburg, Russia), X. National Conference, Saint Petersburg.
- [6.1.57] Vaszina N.K., Margolin B.Z., Gulenko A.G., Kurszevics I.P., Ausztenites acélok sugárzás okozta duzzadása: különböző tényezők hatása. Kísérleti adatok feldolgozása és az alapvető egyenletek kialakítása, Anyagismeret kérdései, №4 (48), 2006. - 69-89. oldalak.
- [6.1.58] Generalization of experimental data and development of methods for prediction of physical –mechanical properties of irradiated material for pressure vessel internals concerning to the blocks 1-4 of the Paks Nuclear Power Plant, Final Connon Report Rev01, Margolin B.Z., Kursevich I.P., Gulenko A.G., Vasina N.K., Minkin A.J., Buchatsky A.A., Saint-Petersburg, 2008.

6.2 OTHER VESSEL CHALLENGES (SG, PRESSURIZER)

6.2.1 Stress Corrosion Cracking

The CEA/Corrosion Service chairs the TC 156/WG 9 and the CEA best practice guidelines have been formalized, modified and adopted gradually since 1987 as ISO standards. They are updated frequently. The following standards are generally applied for Stress Corrosion Cracking experiments and can be used as reference guidelines:

- **ISO 8044** **Corrosion of metals and alloys** **Basic terms and definitions**
- **ISO 11845** **Corrosion of metals and alloys** **General principles for corrosion testing**
- **ISO 7539** **Corrosion of metals and alloys** **Stress corrosion testing**
 - ISO 7539-1 Part 1 General guidance on testing procedures
 - ISO 7539-2 Part 2 Preparation & use of bent-beam specimens
 - ISO 7539-3 Part 3 Preparation & use of U-bend specimens
 - ISO 7539-4 Part 4 Preparation & use of uniaxially loaded tension specimens
 - ISO 7539-5 Part 5 Preparation & use of C-ring specimens
 - ISO 7539-6 Part 6 Preparation & use of pre-cracked specimens for tests under constant load or constant displacement
 - ISO 7539-7 Part 7 Method for slow strain rate testing
 - ISO 7539-8 Part 8 Preparation & use of specimens to evaluate weldments
 - ISO 7539-9 Part 9 Preparation & use of pre-cracked specimens for tests under rising load or rising displacement

6.2.2 CANDU Steam Generator Tubing

A detailed and comprehensive life assessment of the steam generating equipment will include the pressure boundary, the external support structure, the tubing, and all the key internal sub-components. Tubing is a key sub-component. For CANDU-6 NPPs, the steam generator (SGs) tubing is made from alloy 800. These have experienced relatively little SG tube corrosion to date. For instance, at the Wolsong NPP Unit 1 plant (having 21 years of in-service experience), there are only nine SG tubes that are plugged, none as a consequence of corrosion. Seven of these exhibited plugging before in-service operation, out of the total population of over 14,000 tubes. For other CANDU-6 SGs and Indian PHWRs the situation is similar. Elsewhere, the record with Alloy 800 SG tubing is similar after more than 30 years' in-service experience, [6.2.1].

Based on the detailed plant SG studies performed to date, the overall SG condition at several CANDU 6 plants appears to be good with no obvious compromise to attaining the design life. However, there is sufficient uncertainty over the condition of SG secondary side internals that the life extension assessment requires additional inspection and analysis. The conclusions and recommendations are focused on water chemistry control, proactive inspections/monitoring program, and periodic cleaning on both primary and secondary sides of the steam generators.

6.2.2.1 Degradation Mechanisms

The operation and maintenance of steam generators is one of the most crucial and complex element in the success of pressurized water reactor operations. For many nuclear utilities steam generators remain the leading cause of plant outage hours, high maintenance costs and reduced



generating capacity. As a result, more and more utilities are faced with the reality that steam generators will not endure for the life of the plant, and will require either expensive repairs or complete replacement. Therefore, the effective management of steam generators requires more than solving the problems as they arise; it requires anticipation of issues so that effective planning can be performed in advance. Consequently, it is necessary to set-up a comprehensive Steam Generator Degradation Program in order to support implementation of an operating, maintenance and replacement strategy. All these actions will support power production, safely, reliably and a competitive cost of the nuclear energy. A steam generator strategy must specify a balance between the objectives of reducing short and long term capital, and operation and maintenance budgets. To extend steam generator life, most of the remedial measures must address operational effects on steam generator degradation, [6.2.2].

Maintenance activities intended to extend steam generator life and reduce the potential for costly forced shutdowns must be implemented at the NPP. A comprehensive inspection program is able to detect problems at an early stage so that necessary actions can be implemented. The flexibility of several tube repair options can reduce the effect of reduced thermal performance due to plugging of tubes. Defective steam generator tubes can be sleeved at the location of the defect to permit the tube to remain in service. Understanding the impacts and benefits of the different mitigation strategies is important so that implementation can occur at the optimal time.

Decisions which affect the conditions in the steam generator must consider the impact of any mitigation strategies on the steam generator degradation and life. These decisions may include operating temperature versus production efficiency, water chemistry strategies, controls impurities and the performance improvement of related equipment (e.g. condensers).

Water chemistry is not the main damaging factor of the steam generator. Although water chemistry can contribute to, or in extreme cases, cause steam generator degradation, materials and associated failure mode susceptibility can be more correlated to long-term steam generator degradation.

The main types of CANDU 6 steam generator tubing degradations are shown in Table 3. Figure 11 shows the main types of damage occurring in the steam generator.

Table 3 : Main types of CANDU 6 steam generator-tubing degradations

Region	Importance to SG Life Management
Tubing-boiling zone Secondary side	Crevice corrosion in this area (under deposits) has contributed mostly SG incapability
Tubing-boiling zone Primary side	Circumferential stress corrosion cracking at the tube sheet rolled joint area has been a significant concern for SG
U-Bends	The U-Bend area is affected by damages because of stresses, vibration and fouling
Support-boiling zone	Design influences fouling susceptibility, which affects corrosion and thermal hydraulic performance
Tube sheet area	In the tube sheet area the corrosion cause problems consisting in tubes degradation near the tube sheet at the contact with the sludge pile

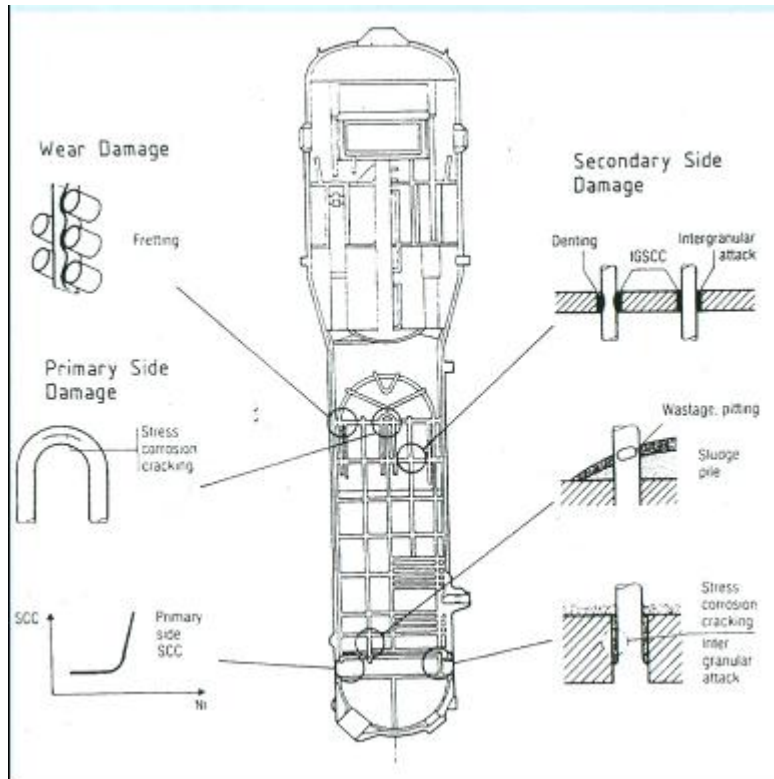


Figure 11 Main types of damage occurring in the steam generator [6.2.3]

6.2.2.2 Assessment Methods

The main goals of the experimental program, developed at INR Pitesti on the important steam generator materials (1y-800 and carbon steel SA508cl.2) are: assessment of the corrosion kinetics, development of corrosion testing simulation devices for tube-tube sheet joints with and without deposits in normal and abnormal steam generator operation conditions, chemical cleaning of deposits. Other issues of the Program were focused on: concentration of impurities and corrosion products on simulated defects, the influence on the corrosion of tubes and tube sheet materials, the achievement of correlation between the presence of deposits and the intensity of crevice corrosion at tube-tube sheet joints.

6.2.2.3 Lifetime Evaluation

The main aspects of the material ageing management of steam generator tubing are the described below [6.2.4], [6.2.5], and [6.2.6]:

Material ageing management of steam generator tubing

The operation and maintenance of steam generators is one of the most crucial and complex elements in the success of pressurized water reactor operations. For many nuclear utilities steam generators remain the leading cause of plant outage hours, high maintenance costs and reduced generating capacity. As a result, more and more utilities are faced with the reality that steam generators will not endure for the life of the plant, and will require either expensive repairs or complete replacement. Therefore, the effective management of steam generators requires more than solving the problems as they arise; it requires anticipation of issues so that effective planning can be performed in advance. Consequently, it is necessary that a comprehensive Steam Generator Degradation Programme exists to support implementation of an operating,



maintenance and if required, a replacement strategy that supports power production, safely, reliably and a competitive cost. A steam generator strategy must specify a balance between the objectives of reducing short and long term capital, and operation and maintenance budgets, with the risk of unscheduled or extended outage and a reduced plant availability factor. To extend steam generator life, most of the remedial measures taken must address operational effects on steam generator degradation.

Maintenance activities intended to extend steam generator life and reduce the potential for costly forced shutdowns must be implemented at the NPP. A comprehensive inspection programme is able to detect problems at an early stage so that necessary actions can be implemented. The flexibility of several tube repair options can reduce the effect of reduced thermal performance due to plugging of tubes. Defective steam generator tubes can be sleeved at the location of the defect to permit the tube to remain in service. Understanding the impacts and benefits of the different mitigation strategies is important so that implementation can occur at the optimal time.

Having in view the experimental results and the INR Pitesti experience in the field of steam generator degradation we consider that the main aspects of the material ageing management of steam generator tubing are as follows:

Design criteria for corrosion prevention and control:

- Minimizing number of crevices;
- Reducing excessive dry out regions;
- Optimizing recirculation ratio;
- Modifying flow distribution to improved the sludge management ;
- Increasing blow down capacity;
- Improvement of accessibility for inspection and maintenance;
- Improvement of stress distribution in the tube – tubesheet area .

Specific actions for corrosion prevention and control:

- Condensate polishing systems (full flow or side arm);
- Magnetic filter systems for feed water;
- Systems for detecting and locating condenser leaks;
- Balance of plant systems;
- Materials selection for condensers feed water heaters, and moisture separator reheaters;
- Drain routing for heaters and MSR;
- Optimization of turbine plant chemistry;
- Analytical systems for continuous monitoring of feed water;
- Low-down heat recovery systems;
- Improved make-up water systems.

Water chemistry control and treatment measures for corrosion prevention and control:

- All Volatile Treatment (AVT): specification for impurity limits;
- Amines for condensate pH control: morph line, cyclohexilamine;
- Oxygen scavengers: hydrazine, catalyzed hydrazine;



- Inhibitors for denting: crevice neutralizers, boric acid;
- Chelating treatments: continuous, intermittent;
- Lay-up treatment.

Operating practice and maintenance measures for corrosion prevention and control

These measures consist of:

- condenser maintenance,
- air in leakage control practices,
- sludge removal by water jet lancing,
- chemical cleaning, intermittent high blow down rate,
- periodic tube inspections,
- inspections of internals,
- tube removal and examination;
- preventive plugging,
- lay-up procedures.

6.2.3 References (Other Vessels)

- [6.2.1] INTERNATIONAL ATOMIC ENERGY AGENCY, "Nuclear power plant life management processes: Guidelines and practices for heavy water reactors", IAEA-TECDOC-1503, IAEA, Vienna (2006), ISSN 1011-4289.
- [6.2.2] D. Lucan, M. Fulger, L. Velciu, "Experimental Research Concerning CANDU Steam Generator Components", International Congress on Advanced Nuclear Power Plants CD-ROM Proceeding, Seoul, KOREA, May 15-19, 2005.
- [6.2.3] Cojan, M., Radu, V., Parvan, I., Lucan, D., Florescu, Gh., "Application and importance of ageing management in CANDU 6 PLIM / PLEX programmes", paper presented at the CNE 2004 – The 7th Regional Energy Forum – FOREN 2004 "Sustainable Energy Development and European Integration", Neptun, Romania, 13÷17 June 2004.
- [6.2.4] D. Lucan, M. Fulger, L. Velciu, Gh. Jinescu, "Corrosion Processes Specific of the CANDU Steam Generator and Mitigation Methods", Proceedings 4-th International Conference of the Chemical Societies of the South-East European Countries, Belgrade, Serbia and Montenegro, July 18-21, 2004.
- [6.2.5] D. Lucan, M. Fulger, Gh. Savu, "Concentration Processes on Simulated Defects of the CANDU Steam Generator Materials", International Congress on Advances in Nuclear Power Plants CD-ROM Proceeding, Cordoba, Spain, May 4-7, 2003.
- [6.2.6] D. Lucan, M. Fulger, Gh. Ionescu, "The Study of the Impurities Concentration Processes into CANDU Steam Generator Crevices", Proceedings 4-th CNS International Steam Generator Conference, Toronto, Ontario, Canada, May 5-8, 2002.

6.3 PIPING

Piping systems are an integral part of nuclear power plants and require different levels of structural integrity justification depending on their safety significance. Examples of piping systems include PWR primary loops, feed water and main steam lines, BWR main feed water lines and AGR boiler feed and steam lines. Piping materials are predominantly ferritic and austenitic stainless steels. Welds in particular are an important feature from a structural integrity point of view. Welds to be considered may include those joining similar material pipes together or to other components and dissimilar metal welds connecting pipes to other components.

Piping systems exhibit degradation mechanisms due to different types of mechanical and thermal loading in combination with environmental effects and susceptible material. For design basis conditions, such mechanical and thermal loadings include:

- Loadings caused by the fluid, e.g. by its pressure, temperature, pressure transients, temperature transients, thermal stratification, stripping, mixing, fluid forces and vibrations,
- Loadings arising due to the pipe itself, e.g. dead weight, pre-stressing and residual stresses (due to fabrication),
- Loadings imposed by adjacent components, caused e.g. by restraint to thermal expansion or pump oscillations, and
- Ambient loadings transferred by component support structures and imposed e.g. by anchor displacement, vibrations or due to earthquake.

If of sufficient magnitude, these loads can result in the following failure modes/degradation mechanisms:

- fracture,
- fatigue failure,
- inadmissible deformations,
- at higher temperatures creep failure (not at service temperatures of LWR) and
- corrosion-assisted cracking.

Thermal aging may degrade material properties resulting in an increase of susceptibility to cracking. Water chemistry, flow behaviour and susceptible material contribute to erosive wear on piping inner walls, localized and general corrosion and increase susceptibility to corrosion-assisted cracking and fatigue. All of these issues result in a complex array of degradation mechanisms that must be accounted for within any piping system management program.

6.3.1 Degradation Mechanisms

Piping systems exhibit degradation mechanisms due to various types of loading mentioned above, susceptible material and environment. Thermal aging degrades material properties, resulting in increased susceptibility to cracking under load and environmental conditions. Susceptible material, water chemistry and flow behaviour contribute to erosive wear on piping inner walls, localized and general corrosion and increases susceptibility to corrosion-assisted cracking and fatigue. All of these issues result in a complex array of degradation mechanisms that must be accounted for within any piping system management programme.

Knowledge of pipework aging is the key to effective life management. This means coordinating aging management activities within a systematic management programme, managing aging mechanisms through prudent operating procedures and practices; detecting and assessing aging



effects through effective inspection, monitoring, and assessment methods; managing aging effects using proven maintenance methods and effective control of water chemistry.

In parallel, this requires profound understanding of piping materials and material properties; stressors and operating conditions; likely degradation sites and aging mechanisms; and effects of aging on safety margins.

For example in LWRs, the primary piping ageing knowledge is derived from the primary piping baseline data, the operating and maintenance histories, and external experiences. Numerous reviews are available on the issues involved and approaches used in different countries; examples include the IAEA reports [6.3.1], [6.3.2]. A systematic approach to piping aging is also prominent in the sophisticated in-house component/ageing damage matrices used by most operators. A prominent example at national level is the GALL (generic ageing lessons learned) report [6.3.3], in which the US-NRC brought together relevant US experience of both aging mechanisms and the associated TLAA (time-limited aging assessment) methods. The IAEA is currently exploring an analogous approach at international level. In view of this, the following subsections highlight issues raised by the EG2/EG3 participants where such scope exists for developing further guidance on dealing with the relevant age related degradation mechanisms. These descriptions are not intended to be comprehensive.

6.3.1.1 Fatigue

Thermal fatigue

Generally both stainless and carbon steels should be considered susceptible to thermal fatigue when subjected to cyclic loading. Degradation caused by thermal fatigue may be found in either weld or base metal locations, but it is restricted to non-main coolant loop piping in PWRs, except for high cycle fatigue in high temperature difference mixing nozzles. The specific design of the piping system is also a critical factor in determining its susceptibility to thermal fatigue. Thermal fatigue can be caused by thermal transients, thermal stratification, thermal striping, and/or turbulent penetration. The requirements on maintaining fatigue cumulative usage factors below 1.0 should be examined when the impact of thermal fatigue is assessed. In-service inspection requirements should be followed and augmented if necessary. The in-service inspection, monitoring, and assessment element can in some cases be supported by qualified inspection techniques (e.g. those qualified to the requirements of European Network for Inspection and Qualification [6.3.4], Appendix VIII of Section XI of the ASME Code [6.3.31] or French RSE-M Code [6.3.32]) and German KTA 3201.4 [6.3.45] and 3211.4 [6.3.46] codes for primary and secondary piping respectively, since the detection of fatigue cracking is difficult. Effective local leakage detection techniques and thermal fatigue monitoring systems (e.g. local thermocouple matrices arranged azimuthally on the piping OD) should be considered. If thermal fatigue degradation is discovered, the user needs to analyze the flaw or flaws, including the root cause, in order to determine if the flawed component is fit for continued operation.

Vibration fatigue

Vibration fatigue is a high cycle mechanical fatigue mechanism which may affect any piping system. Small diameter piping and socket weld locations particularly have been shown to be susceptible to high cycle fatigue. For these cases, vibratory fatigue cracking is often caused by pump- or cavitations-induced pressure pulsations if an excitation frequency coincides with the structural (natural) frequency of the piping. Cracking often initiates at the toe of the weld and may be detected by inspection techniques or leak monitoring.

When justification for continued operation cannot satisfactorily be made, management of fatigue degradation may require repair or replacement. Operating experience may provide insight regarding locations susceptible to vibratory fatigue degradation.

Environmentally Assisted Fatigue (EAF)

In recent years, the influence of LWR coolant environment to the fatigue behaviour of components has been discussed internationally. In 2007 the U.S. Nuclear Regulatory Commission provided a "Guideline for evaluating fatigue analyses incorporating the life reduction of metal components due to effects of the light-water reactor environment for new reactors" [6.3.43]. The publication is mainly based on NUREG/CR-6909 [6.3.44] which provides relevant fatigue data for carbon steels, low-alloy steels, Ni-Cr-Fe alloys and austenitic stainless steel grades (e.g. 304, 316, 316NG). NUREG/CR-6909 has indicated that current design curves may be non-conservative for piping in LWR environments. The US-NRC Regulatory Guide endorses the design curves developed in [6.3.43] for the incorporation in design of new reactors while stating that "the design of the current fleet of reactors is satisfactory" because of "significant conservatism in quantifying other plant-related variables (such as cyclic behaviour, including stress and loading rates) involved in cumulative fatigue life calculations". The ASME Boiler and Pressure Vessel code is currently being updated by the development of code cases that follow a similar approach to that established in NUREG/CR-6909. The Japanese JSEM code has similarly been updated. The German KTA 3201.2 code contains environmental fatigue attention levels (0.2 for stainless steels and 0.4 for ferritic steels).

The extent of environmental influence on fatigue initiation is still a matter of ongoing international debate. Whilst the small specimen data underpinning the model developed in NUREG/CR-6909 indicate a significant environmental effect, this is not necessarily reflected in operating experience or the results of component-like specimen testing. NUREG/CR-6909 introduces an environmental penalty factor (F_{en}) to describe the relation between admissible load cycle in air in comparison to admissible load cycles in LWR environment. Various numerical procedures were developed. All of these methods have in common that they numerically "fit" admissible load cycles obtained in air environment to admissible load cycles obtained in LWR coolant environment. The relation is defined by the scalar variable " F_{en} " which varies e.g. depending on material batches under consideration as well as testing techniques and conditions like the definition of failure criterion.

Existing approaches like NUREG/CR-6909 [6.3.44] can be seen as a first approach for assessment of EAF, but is widely regarded as excessively conservative. Concerted international effort is currently focussed on development of assessment procedures that account for environmental effects in a way that is more representative of LWR plant.

Thermal Stratification and Striping (Mixing Problems)

Thermal stratification in horizontal sections of piping systems due to hot and cold portions of the fluid may occur when the fluid is stagnant or flowing very slowly. This causes global bending ("banana" effect) and local deformation ("pear" effect), see Figure 12.

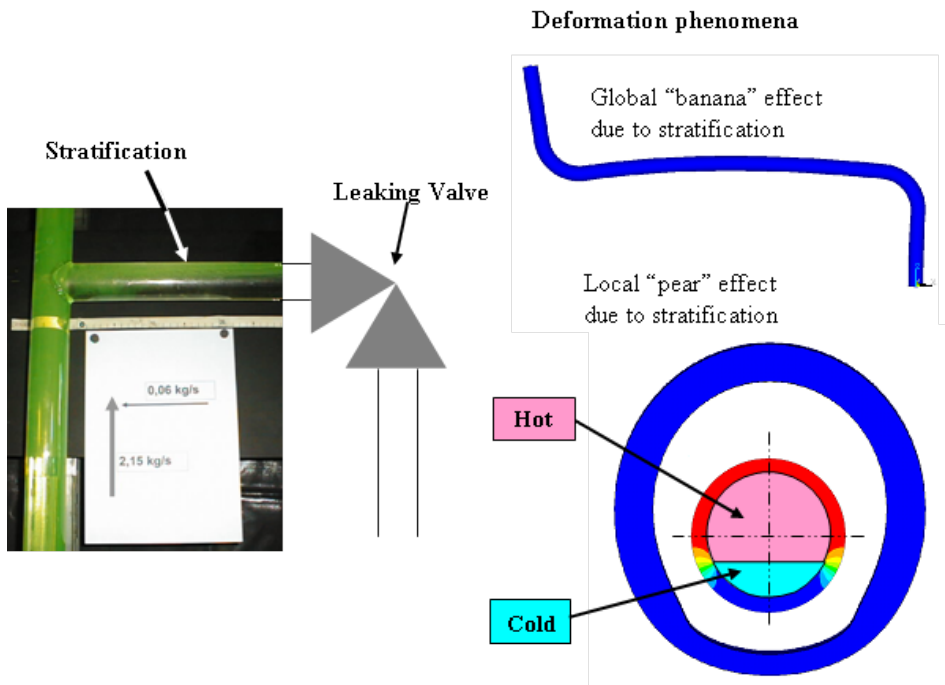


Figure 12 Thermal Stratification Phenomena.

In case of changes in time in the interface between the hot and cold portions of the fluid, this load becomes cyclic and causes fatigue as well. Thermal stripping (rapid oscillation of the thermal boundary interface along the piping inside surface) causes, on the whole, cyclic local thermal stresses at the inner surface of the pipe wall, see Figure 13.

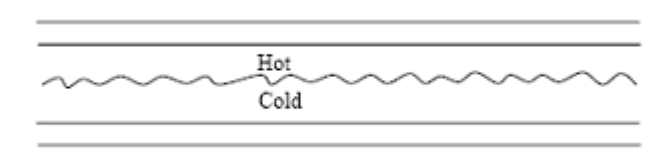


Figure 13 Thermal stripping due to fluctuation of the interface in a stratified flow.

Plant experience of turbulent mixing has shown that crack initiation under conditions of high cycle fatigue can occur in a relatively short time (i.e. several hundred operational hours in relation to a typical design lifetime of 40 years or more). A key development in the understanding of high cycle fatigue came about with publication of USNRC Bulletin 88-08 [6.3.1]-[6.3.8] in response to three thermal fatigue failures in un-isolable portions of piping systems attached to the reactor coolant loop piping. This was followed by bulletin 88-11 [6.3.9] specifically addressing pressurizer surge line thermal stratification. PWR plants have subsequently developed a range of measures for the management of high cycle fatigue, including inspection of susceptible locations, instrumented piping to measure thermal stratification and made permanent modifications to preclude thermal fatigue failures.

Whilst assessment tools are in place for addressing high-cycle thermal fatigue in the U.S. [6.3.16] and Japan [6.3.26] and to an extent in Europe with the publication of the NESCF thermal fatigue report [6.3.24], no full international consensus on assessment approach has yet been reached. This, to an extent, reflects the fact that national development programs are geared towards specific national integrity issues, e.g. small bore non-isolable pipework in the U.S. and mixing tees in Europe. Significantly, IAEA Guidelines [6.3.27] claim that pressure and temperature monitoring of piping susceptible to thermal cycling is the most reliable method to ensure structural

integrity. This would imply that further application and validation of available assessment methods is required to confirm applicability in actual plant applications. Assessment methods for fatigue initiation and growth are discussed in more detail in Section 6.3.2. Appendix 1 provides additional information relating to fatigue and thermal fatigue.

6.3.1.2 Thermal Ageing

Thermal ageing degradation is primarily of interest for cast stainless steel materials and welds made from stainless steel filler material. Cast stainless steels and stainless steel weld materials have a duplex structure consisting of austenite and (delta)-ferrite phases. This (delta)-ferrite decomposition results in a reduction in the material's fracture toughness and Charpy-impact energy. The effect of thermal ageing should be taken into account for any location where cast or weld stainless steel materials are used. This is especially true if a leak-before-break (LBB) analysis is to be justified for an affected piping component (e.g. sections of the main coolant loops in PWRs). Thermal ageing of primary coolant piping can be a safety issue if a material develops a very low level of fracture toughness which reduces the defect tolerance of the component. Ideally, piping materials should be chosen that are not susceptible to thermal ageing. Where degradation does occur in piping, it may be necessary to consider repair or displacement. Where components are replaced, a comprehensive analysis of the removed component would be recommended.

6.3.1.3 Corrosion

Stress corrosion cracking (SCC)

In general, SCC is a concern for instrument penetrations made from Alloy 600 and welded to the piping via Alloy 182 filler material. The most susceptible degradation site is the inside surface of the penetration where some Alloy 182 can be directly in contact with primary water in which case the degradation mechanism is known as Primary Water Stress Corrosion Cracking (PWSCC). Degradation of PWR stainless steel piping can also occur due to SCC, typically as trans-granular SCC from the outside surface due to contamination by chloride residues in combination with water condensation. Augmented in-service inspection programmes may be required for susceptible components (e.g. Alloy 600 penetrations and Alloy 182 dissimilar metal welds).

Intergranular SCC (IGSCC)

is associated with sensitised material. For example, sensitised austenitic stainless steels are susceptible to IGSCC in an oxidising environment. Sensitisation of unstabilised austenitic stainless steels is characterised by a precipitation of a network of chromium carbides with depletion of chromium at the grain boundaries, making these boundaries vulnerable to corrosive attack. Heat Affected Zones (HAZs) may become sensitised as a consequence of manufacture, and therefore control of heat input needs to be carefully considered.

Transgranular SCC

is caused by aggressive chemical species, especially if coupled with oxygen and combined with high stresses [6.3.33], [6.3.34]. Degradation generally occurs at a slow rate in terms of both crack initiation and propagation. (10^{-9} to 10^{-6} m/s). The sequence of events involved in the SCC process is usually divided into three stages [6.3.35]:

1. crack initiation,
2. steady state crack propagation, and
3. final failure.

Boric acid corrosion (BAC)

BAC may cause degradation of PWR primary components due to leakage of boronated coolant. A reduction in PH levels leads to enhanced corrosion rates. Evaporation of boronated water at high temperatures results in concentration of the boric acid and corrosion rates are increased. Field experience and test results indicate that the corrosion rates for carbon steels and low-alloy steels exposed to PWR primary coolant leakage are greater than previously estimated and could be unacceptably high. PWR plants now typically have augmented inspection programmes that effectively control BAC. These have been developed based on plant experience, particularly the Davis-Besse plant in the USA where significant degradation was revealed by inspection of the RPV head.

Flow accelerated corrosion (FAC)

FAC is associated with the combined action of corrosion and erosion (i.e. the mechanical action of a fluid on a metal surface) [6.3.36], [6.3.37]. The corrosion resistance of unalloyed or low alloyed ferritic steels in water and steam depends on the formation of protective oxide layers. If these layers are removed, the corrosion attack on the metal surface can occur in the form of metal dissolution. The flow conditions shift the equilibrium between protection layer removal and formation which determines the material consumption. The severity of erosion varies with the material type, the fluid temperature, the fluid velocity, the oxygen content in the fluid and the component geometry. As previously noted, carbon and low-alloy steels are susceptible to FAC [6.3.33], [6.3.34]. FAC takes place at low flow velocities and the corrosion rate is constant. The difference between generalised corrosion and FAC is the effect of water flow at the oxide-feed water interface [6.3.36]. Consequences of the corrosion/erosion mechanism are the thinning of component walls, which if undetected may result in leakage or rupture. The severity of the degradation depends on the total stress as well as on the deposition of the eroded particles at locations where there is a low flow velocity (wastage) [6.3.34].

6.3.2 Assessment Methods

To prevent ductile fracture, all nuclear design codes provide rules to calculate sufficient wall thickness of pipes in order to limit the primary stresses. Furthermore, by means of a stress analysis along with a classification of stresses and limitation of stress intensities it has to be proved, in conjunction with the material properties, that neither primary stresses nor the range of primary and secondary stresses cause relevant plastic deformations or progressive distortions (ratchetting). The design codes commonly used within Europe include ASME III, the German KTA code and the French RCC-M code.

To design against fatigue failure, analyses are performed limiting the equivalent stress range derived from primary, secondary and peak stresses in conjunction with the number of cycles on the basis of strain range based fatigue curves. Fatigue usage factors are commonly calculated to justify component lifetimes at the design stage. Design code assessments are often updated throughout plant life (e.g. following repair or replacement activities) and also via periodic safety reviews that are scheduled at intervals throughout plant life. Design codes include defect tolerance assessment procedures to provide continued justification of component integrity throughout plant lifetime. These defect tolerance assessments provide assurance against through-life failure by comparison with either postulated defect sizes, manufacturing inspection results or defects revealed by in-service inspection. Codes and procedures also exist to provide supporting analyses throughout plant life. Examples include R5 and R6 in the UK, ASME XI, RSE-M (France) and KTA (Germany). Throughout plant life, assessments/analyses are often referred to as Engineering Assessment Methods (EAMs). These generally include fracture mechanics based procedures for assessing the significance of real or postulated defects in structures. Several of the key EAMs used in the European nuclear industry are described in the following paragraphs.



The ASME code is widely used in Europe, together with other locally developed EAMs for nuclear engineering assessments, some examples of which are shown below:

France – RCC-M (App. ZG), RCC-MRx (App. A16), RSE-M (App. 5.4 – 5.6)

UK – R6, R5 (High temperature creep), BS7910

Germany – KTA (KTA 3201, KTA 3206, KTA 3211, KTA 1403)

Czech Republic – NTD AME (App. X – XIV), VERLIFE (App. X - XIV)

Finland – YVL Guides

Sweden – SSM Guides and SSM Handbooks

EAMs provide assurance of component integrity that form an important constituent of nuclear safety justifications throughout Europe. The philosophy of demonstrating nuclear safety varies according to the regulatory requirements of individual countries and also according to the nuclear safety significance of the component. For example, EAMs are one strand of the Break Preclusion Concept (BPC) in Germany and also provide one part of a multi-legged safety argument for the more safety significant components in the UK.

6.3.2.1 LBB

For justifying the structural integrity of piping systems in nuclear power plants, the leak-before-break (LBB) concept is considered in many European countries. LBB is aimed at demonstrating that forewarning of defect growth will be provided by detectable leakage well in advance of catastrophic failure.

There are basically four distinct approaches used within Europe that are available for undertaking LBB assessments. It must be emphasized however, that all approaches have some similarities to each other. Of the four approaches, the UK and French are country specific and not generally adopted elsewhere. Both the German Basis Safety Concept (BSC), which is now being called the Integrity Concept (IC), and the American Standard Review Plan (SRP) 3.6.3, form the basic foundation for most countries. An overview of the four different approaches is provided below:

BSC / IC

This method originated in Germany, and is used in other countries such as Spain and the Netherlands. The BSC / IC provides the overriding safety procedure for the assessment and structural integrity maintenance of nuclear power plants and includes the Break Preclusion Concept (BPC) as one of the arguments. The BPC provides a means by which the complete cleavage of a pipe should be avoided. One of the legs of the BPC includes LBB so that, even if a crack forms, the leakage of fluid will be detected with significant margin to pipe failure. As such, the LBB section of the BPC forms a “defence in depth” argument for the prevention of pipe failure; which will be accompanied by preclusion of other failure mechanisms and other detection and prevention measures.

The LBB assessment itself is applied only to the most probable locations, such as welds, sections of increased load or material degradation and geometric features. The assessment applied uses the detectable leak rate to determine the crack size required for confident LBB detection and compares this to the critical crack size. In these calculations, only deterministic calculations are used. This deterministic approach and defence in depth argument within the BSC / IC renders probabilistic approaches unnecessary.

SRP-3.6.3

This method originated in the USA, and is used in other countries such as Czech Republic, Lithuania, Spain and Finland. SRP-3.6.3 is a detectable leakage procedure for LBB. The procedure was initially developed to remove the need for multiple pipe-whip restraints. These can be removed where it can be shown that a crack will be detectable prior to pipe failure, thus

allowing intervening action before a pipe-whip occurrence. The procedure is only applicable to an entire section of piping, not individual components or welded joints. The procedure also excludes the use of LBB when water-hammer, corrosion, creep, erosion, fatigue or environmental condition can lead to component failure within the lifetime of the NPP.

The LBB argument in SPR-3.6.3 can only be applied once the reliability of the detection system can be demonstrated. As with other LBB procedures the basic principle is to use the detectable leak rate to determine the crack size required for confident LBB detection and compares this to the critical crack size to ensure suitable margins exist. One difference with the SPR-3.6.3 procedure is the allowance for additional margins to be applied. For example, in the Czech Republic, factors of 1.4 and 2 are required by the Czech regulator on the loads applied and crack sizes respectively.

R6

The R6 procedure for LBB originates and is primarily applied in the UK. The approach is based on two methods: 1) the “detectable leakage method” where it is required to demonstrate that there is a sufficient margin between detectable leakage crack length and limiting crack length assuming a through-wall defect from the onset (in line with SRP-3.6.3 referred to above), and 2) the “full LBB procedure” whereby a known or postulated defect is initially considered which has not yet penetrated through the wall. The second of these is more complex and involves crack growth calculations through life for the initially part-penetrating defect. The R6 approach is heavily based on sensitivity analyses within deterministic calculations and does not apply specific safety margins.

The LBB argument in R6 can usually only be used as part of a defence in depth argument and can not usually be applied when there are multiple defects (consistent with most of the other approaches). Allowances for some more complex situations, i.e. to allow for high temperature creep and/or complex geometries, are provided.

RCC-MRX Appendix 16

The RCC-MRX procedure for LBB originates and is primarily applied in France. Appendix 16 of RCC-MRX includes details of how to implement a LBB analysis. As with the other methods, LBB estimates are made by comparing the crack size that allows for the leak to be detected and that which causes component failure. This comparison is quantified by a reserve factor of 2 in the two crack sizes and a factor of 10 on the detection capability (i.e. detectable leak rate). Some account for the crack dimensions are provided by accounting for different internal and external crack lengths.

6.3.2.2 Fracture Mechanics Methods

Simplified fracture mechanics concepts are used for the demonstration of LBB. The corresponding conservative calculation of the critical through-wall crack length (TWC) is necessary. The methods usually used by AREVA NP GmbH for the evaluation of ductile failure of components are the Flow Stress Concept (FSC) and the Plastic Limit Load (PLL) for circumferential cracks. For axial cracks, the formula developed by the Battelle Memorial Institute (BMI) and the RUIZ formula are applied to correlate the material parameters (yield strength, ultimate tensile strength, and Charpy toughness), defect data (through-wall crack length), geometry data (pipe diameter, wall thickness) and loading conditions (internal pressure, external bending moment) for a theoretical prediction of ductile failure. The prerequisites for the applicability of simplified fracture mechanics methods for circumferential cracks (FSC, PLL) and for axial cracks (RUIZ-, BMI- formula) are; first, the fulfilment of a ductility criterion (i.e. impact energies of the material of more than 45 Joule at the relevant temperatures), and second, the use of material properties of the base material (instead of weld material or HAZ properties).

Fracture mechanics based structural integrity analyses are also needed when assumed/identified degradation mechanism(s) can locally drive crack growth. For NPP piping systems, these mechanisms are mainly SCC and fatigue.

Fracture mechanics analyses can be carried out by using the geometries and methods in handbooks/guidelines, such as SINTAP procedure [6.3.38], R6 Method [6.3.39] and SSM handbook [6.3.40], and with applicable structural integrity analysis codes. Often, the fracture mechanics parameter driving the crack growth in the computations is the mode I stress intensity factor, K_I . Concerning surface cracks propagated by SCC or fatigue, the K_I or K_I range based crack growth is usually computed increment by increment, until a case specific maximum allowable crack size is reached. For fatigue induced crack growth, Paris-Erdogan equation [6.3.41] is typically used. Whereas for SCC, the rate equation [6.3.42] is often used. These analysis issues are discussed in more detail in earlier section concerning "nozzles and penetrations", and therein in section "assessment tools".

Definitions for maximum allowable crack sizes concerning NPP piping components are given e.g. in Section XI of ASME code [6.3.31]. When having detected a crack, the purpose in this approach is to assess with fracture mechanics procedures whether the crack can grow to reach/exceed the maximum allowable size before the next inspection or not. In the former case, a repair or component replacement has to be carried out right away, whereas in the latter case the remedial actions can be postponed at least until the next inspection, allowing thus more time to plan and prepare these actions.

6.3.2.3 German Safety Standard KTA

Integrity assessment of these effects is performed in German NPPs as part of the integrity concept according to German Safety Standard KTA [6.3.28], e.g. described in the final report of the NESC Thermal Fatigue Project [6.3.29]. Temperature monitoring (stratification, plug-type transients, etc.) is a key issue in this concept.

The analytical integrity evaluation may be performed as piping code analysis or alternatively as a detailed finite element (FE) calculation to provide more realistic data instead of conservative assumptions. As load input for these integrity analyses, either specified conservative loads or temperature measurement results may be used. The basis for the analysis procedures is given in technical codes and standards as amongst others the ASME-Code Section III [6.3.30] or the German Safety Standard KTA [6.3.28]. Based on these analyses, it has to be shown that no repeated plasticity occurs and that the fatigue usage factor doesn't exceed the cyclic load bearing capability of the material.

Appendix 7 provides additional information regarding thermal high-cycle fatigue in piping system tees with leakage.

6.3.2.4 Fatigue crack initiation and growth

In Japan, the U.S and Europe, separate but similar initiatives are being undertaken with a view to providing guidance on significance and assessment of high-cycle fatigue. A distinction can be made between the efforts being made in Japan and the U.S, and those in Europe, with respect to environmental effects. Both Japan [6.3.26], [6.3.17] and the U.S [6.3.43], [6.3.16] have produced similar guidelines to allow for the influence of primary water chemistry on fatigue endurance in terms of fatigue strength reduction factors. It is emphasized that the issue of environmental fatigue is a general concern in relation to cyclic loading and is not necessarily specific to high-cycle thermal fatigue as considered here. In Europe, in the context of high-cycle thermal fatigue, this concept (environmental fatigue) has not yet been generally accepted. Whilst it is accepted that environment may play a role in fatigue endurance in general, the uncertainty in many other parameters associated with high-cycle thermal fatigue (e.g. local heat transfer and loading frequency to name but two) suggests these need to be investigated further if consistent safety factors are to be proposed and accepted.

In other respects, the methodologies being followed to assess high-cycle thermal fatigue in the U.S., Japan and Europe, appear similar in strategy. They all recognize the difficulty in generalizing an evaluation method given that mixing conditions will be dependent upon local pipework geometry and the flow pattern and have all made use of operational experience to date in defining screening criteria to determine the potential significance of thermal fatigue. In the U.S, a survey of fatigue related plant integrity issues, identified non-isolable small-bore branch lines ($\leq 4"$) as a potential area for further investigation. Testing and evaluation has lead to models being developed for determining the fatigue susceptibility of non-isolable, normally stagnant branch lines [6.3.13]-[6.3.15]. For swirl flow in particular, the models allow the location of cyclic interaction to be predicted and an estimate of the cyclic frequency [6.3.16].

In contrast, work being undertaken in Japan [6.3.17] and Europe [6.3.18]-[6.3.24] addresses larger diameter pipework and specifically addresses turbulent mixing at tee intersections. Assessment guidelines include a phased assessment approach with phases of screening, simplified analysis and lastly detailed analysis.

A key issue of the simplified (sinusoidal) assessment method proposed in Europe is that it has been developed taking plant experience into account. In ref. [6.3.22] examples are provided of predicted fatigue usage factors related to observed crack depths. On the basis of the correlations, it is concluded that:

- A usage factor of 1 corresponds to a crack less than 1 mm in base metal areas
- A usage factor of 4 corresponds to a crack less than 1 mm in weld areas.

As a general observation, the method is considered significantly conservative is the case of weld assessment.

In Germany, a practical monitoring-based approach to managing high cycle-thermal fatigue is being applied [6.3.25]. Supporting sensitivity analysis to key issues and variables associated with predicting crack initiation, in terms of usage factor, show a variation of a factor of one hundred in terms of predicted crack initiation depending on the choice of variables and values taken into account during the assessment.

6.3.3 Lifetime Evaluation

Information on aspects of lifetime evaluation of piping is detailed in the following appendices: Appendix 1 (Fatigue and Thermal Fatigue), Appendix 7 (Thermal High Cycle Fatigue) and Appendix 17 (CANDU piping).

6.3.4 References (Piping)

- [6.3.1] Safety Aspects of Long-Term Operation of Water Moderated Reactors: Final Report, IAEA, Vienna, 2007
- [6.3.2] IAEA-TECDOC-1361, Assessment and management of ageing of major nuclear power plant components important to safety-primary piping in PWRs, IAEA, July 2003.
- [6.3.3] Generic Ageing Lesson Learned (GALL) Report, NUREG-1801 Vols 1&2, US NRC, September 2005
- [6.3.4] European Methodology for Qualification, Issue 2. ENIQ report no. 2. European Commission report EUR 17299 EN, 1997
- [6.3.5] NRC Bulletin No. 88-08, 'Thermal stresses in piping connected to reactor coolant systems', U.S. Nuclear Regulatory Commission, June 22, 1988.
- [6.3.6] NRC Bulletin No. 88-08 Supplement 1: 'Thermal stresses in piping connected to reactor coolant systems', U.S. Nuclear Regulatory Commission, June 24, 1988.
- [6.3.7] NRC Bulletin No. 88-08 Supplement 2: 'Thermal stresses in piping connected to reactor coolant systems', U.S. Nuclear Regulatory Commission, August 4 1988.
- [6.3.8] NRC Bulletin No. 88-08 Supplement 3: 'Thermal stresses in piping connected to reactor coolant systems', U.S. Nuclear Regulatory Commission, April 9, 1989.
- [6.3.9] NRC Bulletin No. 88-11: 'Pressurizer Surge Line Thermal Stratification', U.S. Nuclear Regulatory Commission, June 24, 1988.
- [6.3.10] Roos E., Heter K.H., Otremba F., Metzner K.J., 'Effects of Thermal Loads to Stress Analysis and Fatigue Behaviour', Trans. SMiRT 16 Washington DC, Paper #1726, August 2001.
- [6.3.11] Hu L.W., 'Numerical simulation study of high cycle thermal fatigue caused by thermal striping', Proc. 3rd Int. Conf. on Fatigue of reactor components, Seville, Spain 3-6 October 2004.
- [6.3.12] Nakamura A., 'Investigation of flow structure and temperature fluctuation in a closed branch pipe connected to main pipe', Proc. 3rd Int. Conf. on Fatigue of reactor components, Seville, Spain 3-6 October 2004.
- [6.3.13] Spain, L., Carey J., Deardorff A.F., 'Overview of Material Reliability Project Fatigue Activities', Proc. 3rd Int. Conf. on Fatigue of reactor components, Seville, Spain 3-6 October 2004.
- [6.3.14] Deardorff A.F., Keller J.D., Davis J.M., Carey J., 'Thermal Fatigue Management Guidelines For Normally Stagnant Non-Isolable RCS Branch Lines', Proc. 3rd Int. Conf. on Fatigue of reactor components, Seville, Spain 3-6 October 2004.
- [6.3.15] Keller J.D., Bilanin A.J., Kaufman A.E., Carey J., 'Thermal Cycling Screening and Evaluation Methodology and Application to Pressurized Water Reactor Branch Line Piping', Proc. 3rd Int. Conf. on Fatigue of reactor components, Seville, Spain 3-6 October 2004.
- [6.3.16] EPRI MRP-146, 'Management of Thermal Fatigue in Normally Stagnant Non-Isolable Reactor Coolant System Branch Lines, Report No. 1011955, June 2005.
- [6.3.17] Nakamura T., Madarame H., 'Current Status of Development on Codes for Fatigue Evaluation in JSME', Proc. 3rd Int. Conf. on Fatigue of reactor components, Seville, Spain 3-6 October 2004.

- [6.3.18] Beaud F., Musi S., Faidy C., 'Industrial models for thermal fatigue crack initiation and propagation in mixing zones of piping systems', Transaction of the 17th SMiRT conference, 2003.
- [6.3.19] Chapuliot S., Gourdin C., Payen T., Magnaud J.P., Monavon A., 'Hydro-Thermal-Mechanical Analysis of Thermal Fatigue in a Mixing Tee', Nuclear Eng. Design 235(2005) 575-596.
- [6.3.20] Amiable S., Chapuliot S., Constantinescu A., Fissolo A., 'A Comparison of Lifetime Prediction Methods for a Thermal Fatigue Experiment', Int. J. Fatigue 28 (2006) 692-706.
- [6.3.21] Odile G., Escaravage C., Simoneau J.P., Faidy C., 'High Cycle Thermal Fatigue: Experience and State of the Art in French LMFRs', Trans. SMiRT 16 Washington DC August 2001, Paper #1311.
- [6.3.22] Faidy C., 'Thermal Fatigue in Nuclear Power Plants: French Experience and On-going Program', Proc. 3rd Int. Conf. on Fatigue of reactor components, Seville, Spain 3-6 October 2004.
- [6.3.23] Faidy C., 'Thermal Fatigue in Mixing Areas: Status and Justification of French Assessment Method', Proc. 3rd Int. Conf. on Fatigue of reactor components, Seville, Spain 3-6 October 2004.
- [6.3.24] Dahlberg M., Nilsson K.F., Taylor N., Faidy C., Wilke U., Chapuliot S., Kalkhof D., Bretherton I., Church J.M., Solin J., Catalano J., 'Development of a European Procedure for Assessment of High Cycle Thermal Fatigue in Light Water Reactors: Final Report of the NESC-Thermal Fatigue Project', EUR 22763 EN, ISSN 1018-5593, 2007.
- [6.3.25] Dittmar S., Huttner C., 'Fatigue Analyses as Aid for the In-Service Monitoring, Possibilities and Limitations', Proc. 3rd Int. Conf. on Fatigue of reactor components, Seville, Spain 3-6 October 2004.
- [6.3.26] JSME, 'Guideline for Evaluation of High-Cycle Thermal Fatigue of a Pipe', JSME S017-2003, 2003.
- [6.3.27] IAEA, 'Assessment and Management of Ageing of Major Nuclear Power Plant Components Important to Safety: Primary Piping in PWRs', TECDOC-1361, July 2003.
- [6.3.28] KTA 3201 "Components of the Reactor Coolant Pressure Boundary of Light Water Reactors", Part 2: Design and Analysis, June 1996. Part 4: In-Service Inspections and Operational Monitoring, June 1999
- [6.3.29] Development of a European Procedure for Assessment of High Cycle Thermal Fatigue in Light Water Reactors: Final Report of the NESC-Thermal Fatigue Project European Commission, DG-JRC/IE Petten, 2007
- [6.3.30] ASME – Nuclear Boiler and Pressure vessel Code – Section III – ASME 2004
- [6.3.31] ASME Boiler and Pressure Vessel Code, Section XI. 2010 Edition.
- [6.3.32] RSE-M, In Service Inspection Rules for the Mechanical Components of PWR Nuclear Power Islands. AFCEN, France, 1997 Edition.
- [6.3.33] Safety aspects of nuclear power plant ageing. IAEA-TECDOC-540, International Atomic Energy Agency (IAEA), Vienna, Austria, 1990. 200 p.
- [6.3.34] Uhlig's Corrosion Handbook, 2nd Edition (Editor Revie, R., W.), John Wiley & Sons, Inc., Ottawa, Ontario, Canada, 2000. 1391 p.
- [6.3.35] Jones, R., H. (Editor). Stress-Corrosion Cracking. ASM International, Ohio, 1992. 448 p.



- [6.3.36] Smith, C., L., Shah, V., N., Kao, T., Apostolakis, G. Incorporating Aging effects into Probabilistic Risk Assessment - A Feasibility Study Utilizing Reliability Physics Models. Report NUREG/CR-5632, U.S. Nuclear Regulatory Commission (USNRC), 2001.131+112 p.
- [6.3.37] Safe Management of NPP Ageing in the European Union, Final Report. European Commission, Nuclear Safety and Environment, 2001. 363 p.
- [6.3.38] SINTAP - Structural Integrity Assessment Procedures for European Industry; Final Procedure: November 1999. Project funded by the European Union (EU) under the Brite-Euram Programme: Project No. BE95-1426, Contract No. BRPR-CT95-0024.
- [6.3.39] R6 Method - Assessment of the Integrity of Structures containing Defects, Revision 4. 2004 update of 2001 edition. British Energy (BE).
- [6.3.40] Dillström, P. et al. 2008. A Combined Deterministic and Probabilistic Procedure for Safety Assessment of Components with Cracks – Handbook. SSM Research Report 2008:01, Swedish Radiation Safety Authority (Strålsäkerhetsmyndigheten, SSM). Stockholm, Sweden, 2008. 27+196 p.
- [6.3.41] Paris, P., C., Erdogan, F. A Critical Analysis of Crack Propagation Laws. Journal of Basic Engineering, Vol. 85, 1960, pp. 528-534.
- [6.3.42] Congleton, J., Craig, I., H. Corrosion Fatigue. In: Corrosion Processes, Editor Parkins, R., N. Applied Science Publishers, 1982.
- [6.3.43] U.S. Nuclear Regulatory Commission Regulatory Guide 1.207, 2007, “Guidelines for evaluating fatigue analyses incorporating the life reduction of metal components due to effects of the light-water reactor environment for new reactors”
- [6.3.44] O. K. Chopra, W. J. Shack, Effect of LWR Coolant Environments on the Fatigue Life of Reactor Materials, NUREG/CR-6909, ANL-06/08, February 2007
- [6.3.45] KTA 3201.4
- [6.3.46] KTA 3211.4

6.4 PUMPS AND VALVES

The design and construction of pumps and valves should fulfil the functional requirements and not lead to an increase of loads or stresses. In order to achieve this, the following aspects need to be considered:

- Favourable conditions for component service loadings taking system loads into account (e.g. actuating, closing and fluid forces)
- Favourable distribution of stresses, especially in areas of structural discontinuity
- Avoidance of sharp corners (significant stress raisers) at wall thickness transitions, especially for components subjected to transient temperature loadings
- Avoidance of welds in areas of high local stresses

Selection of materials appropriate to operational conditions (e.g. medium, temperature, loadings, functional requirements)

- Qualified manufacturing process

6.4.1 Pumps

Pump casings may be of forged, cast or welded design. The pump casings should be so designed that the required functional capability is maintained in the event of pipe forces and moments as well as loadings from external events occurring in addition to the operational hydraulic and thermal loads [6.4.1] and [6.4.2].

The design of the pump casing and the pertinent systems should permit adequate accessibility for maintenance, replacement of wear parts and repair purposes.

6.4.1.1 Pump Design

The adequacy of the design of the pump casing shall be demonstrated either:

- by an investigation through experimental stress analysis,
- by detailing satisfactory service performance of other comparable pumps under similar operating conditions, or
- by finite element (FE) stress analysis, or
- by an analytical stress analysis (e.g. analysis of cylindrical or spherical shells, torispherical, ellipsoidal or flat heads and branch connections, for instance according to refs. [6.4.1] and [6.4.3]).

In any case, the design of the pump needs to meet the stress limits for the different loading levels, as defined e.g. in refs. [6.4.1] and [6.4.2].

An example of the design of a main coolant pump, relevant to a German PWR 1300 MW system, is illustrated in Figure 14.

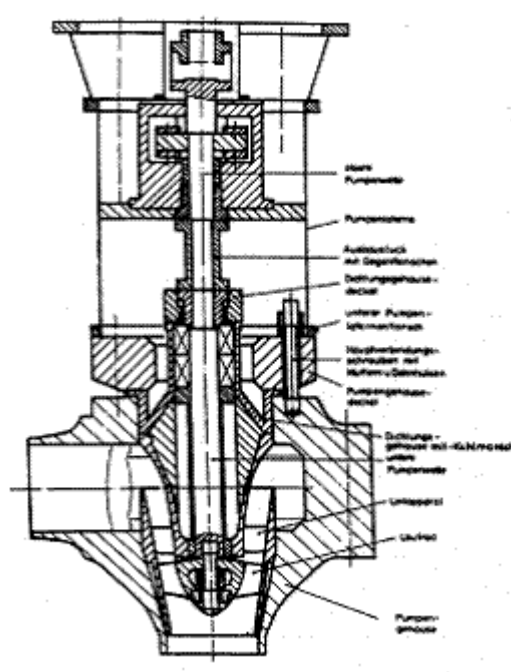


Figure 14 Design of a main coolant pump of a German PWR 1300 MW.

6.4.2 Valves

Valves serve to open the flow, close the flow or regulate flow through piping sections. Valve bodies may be of forged, cast or welded design. The valve bodies should be designed to be so stiff that the required stability is maintained in the event of excessive pipe forces and moments as well as loads from external events occurring in addition to the operational thermal loads. The design of the valve bodies and the pertinent systems should permit adequate accessibility for maintenance, replacement of worn parts and repair purposes. The design should particularly provide smooth tapers and cross sectional transitions.

Valves can be safety important components and, as a minimum, continued functionality must be ensured during emergency and fault conditions. The pressure boundary of safety important valves should be designed so that at emergency loads no inadmissible deformations occur.

The adequacy of the design of the valve bodies can typically be demonstrated by appropriate design codes such as KTA[6.4.1] and ASME [6.4.2]. For valves designed to these codes an example calculation is given below.

6.4.2.1 Calculation Example

The most highly stressed region of the body under internal pressure is at the neck to flow passage junction and is characterized by circumferential tension stress normal to the plane of the centre line, with the maximum value at the inside surface. The following rules are intended to control the general primary membrane stresses and secondary stresses in this crotch region.

Primary Membrane Stress due to Internal Pressure

In the crotch region the maximum primary stress is to be determined by the pressure area method (see Figure 15). From an accurately drawn layout of the valve body, depicting the finished section of the crotch region in the mutual plane of the bonnet and flow passage centre lines, determine the fluid (load bearing) area A_p and the effective cross-sectional (metal) area

A_p and A_G are based on the internal surface of the body after complete loss of metal assigned to corrosion allowance.

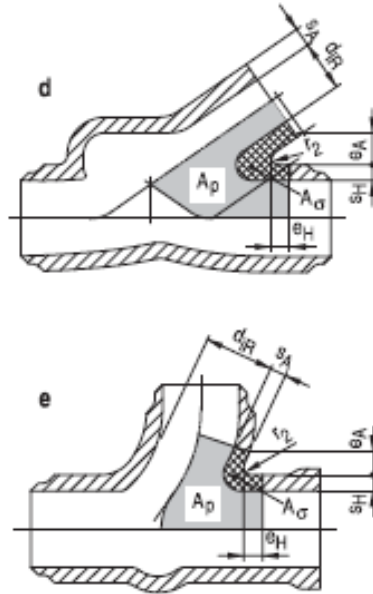


Figure 15 Pressure Area Method.

General stress analyses

For valve bodies meeting the geometric requirements of ASME III, NB 3500 [6.4.2] or KTA 3201.2, Chapter 8.3 [6.4.1], it should be checked based on the critical section A-A at the crotch, whether the range of allowable primary membrane plus bending stresses in loading level 0, A and B is not exceeded:

$$P_{lp} + P_{eb} \leq 1,5 \cdot S_m \quad [6.4.1]$$

where:

P_{lp} : local membrane stress due to internal pressure,

P_{eb} : secondary stresses due to pipe reaction.

Due to the design of the valve body, it should also be satisfied that the range of primary plus secondary stresses due to internal pressure, pipe reaction and thermal effects does not exceed 3 times the value of S_m :

$$Q_p + P_{eb} + 2 \cdot Q_{T3} \leq S_n = 3S_m,$$

where Q_p is the sum of primary plus secondary stresses at crotch resulting from internal pressure and Q_{T3} is the maximum thermal secondary membrane plus bending stress resulting from structural discontinuity and fluid temperature change rate. Figure 16 illustrates the critical cross section A-A for valve bodies.

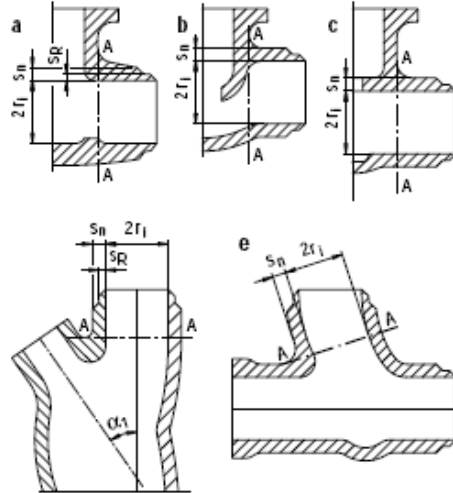


Figure 16 Critical cross section A-A for valve bodies.

Fatigue analysis

A fatigue analysis should be performed for all valves with the specified number of load cycles according to ASME III, NB 3545.3 [6.4.2] or KTA 3201, chapter 8.3.6 [6.4.1], respectively.

The maximum total stresses, S_{p1} , on the body inside and, S_{p2} , on the body outside is determined by assuming a fluid temperature change rate not exceeding 55 K/hr.

With the larger value of S_{p1} and S_{p2} taken as, S_a , the allowable number of load cycles is obtained from the fatigue curves for ferritic or austenitic materials.

6.4.3 References

- [6.4.1] KTA Safety Standards KTA 3201.2 Components of the Reactor Coolant Pressure Boundary of Light Water Reactors; Part 2: design and Analysis, 06/1996
- [6.4.2] ASME Pressure Vessel and Piping Code 2007, ASME III, Division 1, NB
- [6.4.3] ASME Pressure Vessel and Piping Code 2007, ASME III, Division 1, Appendices

6.5 PRESSURE TUBES IN CANDU AND RBMK REACTORS

Two types of pressure tube reactors are or have recently been under operation in Europe: the CANDU6 reactor (CANada Deuterium Uranium–Pressurized Heavy Water Reactor) in Romania, with heavy water as coolant and moderator, equipped with horizontal pressure tubes and the RBMK-1500 (Reaktor Bolchoj Mochnosti Kanalnij (in Russian) – Channelized Large Power Reactor) in Lithuania water cooled, graphite moderated vertical pressure tube reactor. As opposed to the single pressure vessel PWR concept, these reactor types are based on a number of individual pressure vessels, called pressure tubes (PTs).

6.5.1 Description of the core of pressure tube reactors

The CANDU-PHWR design uses natural uranium, as UO_2 pellets and heavy water as both coolant and moderator. The reactor core is contained in a cylindrical austenitic stainless steel tank (calandria), which holds the heavy water moderator at low temperatures ($< 80^\circ C$) and low pressure (~ 0.1 MPa). The ends of the cylinder are closed with two parallel end shields which are perforated with holes for the fuel channels, the holes are arranged in a square lattice pattern. Thin walled Zircalloy 2 tubes are fastened to each inner tube sheet and act as stays for the end shields in order to form a leak tight tank. The holes in each end shield are connected with stainless steel tubes (lattice tubes).

Each fuel channel consists of a Zr–2.5%Nb pressure tube of 103 mm diameter joined to martensitic stainless steel end fittings, and occupies the tubular holes or lattice sites formed by each combined lattice tube and calandria tube. In the reactor, there are 380 channels. The fuel channel end fittings are supported on a pair of sliding bearings at each end, and the pressure tube is supported and separated from the calandria tube by annular spacers.

The RBMK-1500 is a graphite moderated, boiling water, multi-channel reactor [6.5.4]. The RBMK reactor is designed to use a graphite moderator in the graphite brick form, surrounded by zirconium-niobium pressure tubes containing the nuclear fuel and coolant. The graphite structure consists of 2488 channels, made up of columns of bricks each with an axial hole for the channel tube. There are 2052 PTs in total. These are used for fuel (1661 PTs), control rods and instruments (391 in total). The remaining 436 channels around the edge of the core are filled with graphite rods to act as the reflector. The central segment pressure tubes are an 88 mm outside diameter (4 mm thick wall) tube, made from zirconium-niobium alloy (Zr + 2.5% Nb). The primary ageing mechanisms for Zirconium Pressure Tubes operating in both CANDU and RBMK reactors are:

- Delayed Hydride Cracking;
- Irradiation and thermal creep resulting in the diameter to increase;
- Material property changes due to embrittlement of zirconium alloy under irradiation and hydrogen absorption.

6.5.2 Degradation Mechanisms

6.5.2.1 Delayed Hydride Cracking (DHC)

Zirconium and its alloys have a low absorption of heat neutrons and maintain good mechanical properties at temperatures up to $390-400^\circ C$. However, zirconium alloys can absorb hydrogen during operation as a consequence of corrosion reaction with water. Hydrogen redistributes easily at elevated temperatures. At high temperature the hydrogen migrates under concentration and stress gradients. Hydrogen has very limited solubility in zirconium alloys, this being less than 1 ppm at room temperature and about 80 ppm at $300^\circ C$. Whenever the solubility is exceeded a

zirconium hydride phase will be precipitated and as this phase is brittle it can have an impact on the mechanical properties of the alloy. The worst embrittlement in PTs occurs when hydrides are oriented normal to the principal stress. When the terminal solid solubility is exceeded in a component such as a pressure tube that is highly stressed for long periods of time, delayed hydride cracking (DHC) failures may occur. DHC is a phenomenon where a crack can propagate in stepwise fashion as a result of hydrogen redistribution ahead of the crack tip under a stress level below the yield stress [6.5.10]. The high mobility of hydrogen enables hydrides to redistribute. If stress levels are sufficiently high the local hydrogen concentration can exceed the terminal solid solubility, and the hydride platelets precipitate in the primary cracking direction.

Delayed hydride cracking has been recognized as the potential cause of failure of pressure tubes in both CANDU and RBMK reactors. The DHC velocity in the pressure tubes in both types of reactor was evaluated experimentally. The results of the evaluation with thermomechanical treatment are presented in [6.5.15], [6.5.23]. Applicable testing standards and assessment procedures for characterising DHC are described in Appendixes 3 and 9.

6.5.2.2 Creep

The hexagonal close packed crystal structure of zirconium alloys and the operating conditions (temperature and neutron field) are responsible for thermal creep, irradiation growth and irradiation creep of the material. Four types of pressure tube deformation are taken into account [6.5.16]:

- Axial Elongation
- Diametral Expansion
- Wall Thinning
- Fuel Channel Sag

Axial Elongation

The pressure tube elongation is a linear function of time, the maximum elongation rate being 5 mm/year for the first CANDU reactors. This fact has required a modification of the bearing length at both ends of the tubes, feeder pipe spacing and fuel machine offsets. Due to the large variation of the elongation rate from one tube to the other, this parameter is monitored for each tube. This offers information on the lead time planning for corrective action.

In respect of the linear elongation of the RBMK pressure tubes, the maximum-recorded elongation value after 8 years of operation was 8.45 mm [6.5.17]. The design allowance for PT bellows extension from PT tube elongation in the reactor is 50 mm. For the Ignalina NPP, the PT tube elongation was not a limiting feature for the PTs.

Diametral Expansion

Diametral expansion increases the amount of the primary coolant to flow around the fuel bundles, slightly reduces the critical channel power at constant flow but could be the cause of an unacceptable fuel cooling. Although the diametral expansion rate is about 0.1 mm/year, in the CANDU type reactor, the design requirement of pressure tube diametral expansion is limited to 5% of the initial diameter to avoid creep rupture and squeezing of the garter spring spacers between the pressure and the calandria tubes.

Regarding RBMK PTs, the tube diameter increases with time is of high importance; such changes can become a critical factor in determining whether or not a gap exists between the tube and the surrounding graphite stack. A systematic inspection of tube diameters during operation is implemented to develop a reliable prediction of tube diameter increase. The operation temperature and irradiation dose in the RBMK reactors pressure tube radial expansion will be linear for the lifetime of the reactor with the intercept at 111.60 mm and the slope coefficient being 6.94×10^{-5} mm/MWd [6.5.17].

Wall thinning

The periodic inspection of this parameter has proved that the wall thickness of the pressure tubes during the operation is within the value assumed in the design analysis.

Fuel channel sag

The horizontally-oriented pressure tube sags between the spacers, separating each pressure tube from the surrounding calandria. Increasing the number of spacers (from two to four) ensures that the pressure tubes do not contact the calandria tubes during the 30 year design life.

6.5.2.3 Irradiation Effect on Mechanical Properties

Irradiation increases yield and tensile strength, tube hardness and reduces ductility and fracture toughness. In addition, the susceptibility to DHC increases slightly and the DHC crack velocity increases particularly at the inlet end of the CANDU PT due to the lower irradiation temperature, [6.5.19]. An effect of irradiation on the material properties of Zr-2.5Nb pressure tubes occurs after the first few years of operation. It is expected that the mechanical properties will be adequate to achieve the 30 years design life.

In Romania, INR initiated an irradiation programme to study the influence of neutron irradiation on cold-worked Zr-2.5Nb, used as structural pressure tube material in the CANDU Unit-1 in the Cernavoda NPP. Irradiation has been performed for more than six years in the INR TRIGA Steady State and Testing Materials Reactor. The testing conditions (inert helium atmosphere, high temperature and neutron flux) have been assured in a Capsule-type device, placed in the TRIGA reactor active zone. After 11400 hours of irradiation, the fluence attained a value of about $3.5 \times 10^{24} \text{ n/m}^2$ ($E > 1 \text{ MeV}$), which is characteristic for mechanical properties saturation. Post-irradiation examination has been conducted to characterize the pressure tube samples from the mechanical point of view, as a function of the testing temperature, direction of loading (longitudinal or transversal) and type of material (cut from the rolled joint area or from tube). The experimental results and the structural integrity evaluation have been presented at the E-MRS Conference, [6.5.19].

During the operation of RBMK reactors, the irradiation dose causes material property changes of the zirconium alloy pressure tubes. Compared with initial properties, it has been observed that the yield limit is increased by 32-57%, ultimate strength by 26-49%, and the relative elongation is decreased 1.5-3 times. Studies have shown that the stabilization of short-term mechanical properties of PT tube material occurs approximately after the fluence $(1-1.5) \times 10^{24} \text{ n/m}^2$ ($E > 1 \text{ MeV}$).

6.5.3 Assessment Methods

Leak-before-break based on DHC

It is important to determine the life of the pressure tubes due to both crack initiation and the subsequent DHC propagation before the crack penetrates the pressure tubes and catastrophic failure occurs. It is also important to predict the Critical Crack Length (CCL) - condition for which crack initiation and DHC propagation can be prevented before the crack can grow to instability. The ability to shut down the reactor before the pressure tube ruptures is the basis for the leak before break (LBB) criteria.

To ensure LBB in a pressure tube it is required that:

- The crack length at the wall penetration is less than the CCL for unstable propagation;
- The leak from the through wall crack is detectable;
- The reactor can be put into a depressurized condition before the crack exceeds the critical crack length - CCL



The acceptance criteria for a deterministic assessment is $t > T$, where t is the time available to detect the leak and to take action and T is the time required to detect the leak and to take action. The information required to support LBB are: crack length at leakage, critical crack length and the DHC crack velocity.

The new CANDU pressure tubes have a large margin between leak and break. In spite of this advantage, efforts are made to improve the performance of PTs under operation, to extend the service-life time.

Fracture toughness plays a major role in critical crack length determination and is thus important from a LBB perspective. For this reason improvements have been made to minimize the concentration of the trace elements, like chlorine and phosphorous, and to control the carbon concentration, [6.5.6] so as to minimise embrittlement.

6.5.4 Lifetime Evaluation

Further information on lifetime evaluation of pressure tubes is presented in Appendices to this document. Appendix 3 and Appendix 9 cover aspects of delayed hydride cracking (DHC); Appendices 13 and 14 respectively cover leak before break (LBB) and intergranular stress corrosion cracking (IGSCC) of RBMK-1500 reactor austenitic cooling system piping..

6.5.5 References (Pressure Tubes)

- [6.5.1] Cheadle, B.A., Coleman, C.E., Price, E.G., Bajaj, V.K., Clending, W.R., "Advanced in Fuel Channel Technology for CANDU Reactors", AECL – 11059, May 1994
- [6.5.2] Coleman, C.E., Cheadle, B.A., " CANDU Fuel Channels", AECL – 11755, January 1979
- [6.5.3] IAEA-TECDOC-1037 – "Assessment and management of ageing of major nuclear power plant components important to safety", August 1998
- [6.5.4] Almenas, K., Kaliatka, A. and Uspuras, E., Ignalina RBMK-1500. A source Book, extended and updated version, Ignalina Safety Analysis Group, Lithuanian Energy Institute, 1998.
- [6.5.5] Levinskas R, Grybenas A., Makarevicius V. Influence of Temperature on the Axial Hydride Cracking Rate of the Fuel Channel Pressure Tube // Materials Science ISSN 1392-1320, 2002. - Nr. 2. - p. 388-391.
- [6.5.6] Price, E.G., Moan, G.D., Coleman, C.E., "Leak-before-break experience in CANDU reactors", presented at ANS-ASME Topical Mtg, Myrtle Beach, USA, 1988
- [6.5.7] Moan, G.D., Coleman, C.E., Proce, E.G., Rodgers, D.K., Sagat, S., "Leak-before-break in the pressure tubes of CANDU reactors", Int.
- [6.5.8] Perryman, E.C.W., Pickering Pressure Tube Cracking Experience, Nucl. Energy, 17 (1978), pp.95-105
- [6.5.9] Platanov P.A., Ryazantseva, A.V., Saenko, G.P, Knizhnikov, Y.N., Viktorof, V.F., The study of the cause of cracking in zirconium alloy fuel channel tubes, Poster paper at ASTM Zirconium in the Nuclear Industry-8th International Symposium
- [6.5.10] IAEA-TECDOC-1410, Delayed hydride cracking in zirconium alloys in pressure tube nuclear reactors, October 2004
- [6.5.11] Coleman, C.E., Cheadle, B.A., Ambler, J.F.R., Lichtenberg, P.C., Eadie, R.L., "Minimizing hydride cracking in zirconium alloys", Can. Met. Quarterly 24 No.3 , 1985, (also AECL – 9126)
- [6.5.12] Cheadle, B.A., Coleman, C.E., Ambler, J.F.R., "Prevention of delayed hydride cracking in zirconium alloys" ASTM Spec. Tech. Publ. 939(1987), (also AECL-9415)
- [6.5.13] Cheadle B.A., Coleman, C.E., Price, E.G., Bajaj, V.K., Cladening, W.R., "Advances in fuel channel technology for CANDU reactors" presented at IAEA Techn. Comm. Mtg on Advances in Heavy Water Reactor, Toronto, Canada, 1993 (also AECL-11059)
- [6.5.14] Causey, A.R., Cheadle, B.A., Coleman, C.E., Price, E.G., Improving the service life and performance of CANDU Fuel Channels, presented at the IEAE Technical Committee Meeting on "Advances in fuel channel technology for CANDU reactors", Bombay, India, January, 1996 (also AECL – 11543)
- [6.5.15] Roth, M., Choubey, R., Coleman. C.E., Ritchie, I., Measurement of DHC in CANDU Pressure Tubes, 17th Int. Conf. Struct. Mechanics in Reactor Technology, (SMiRT 17) Prague, 2003, Paper G350.
- [6.5.16] Safety Analysis Report for Ignalina NPP, Task group 7 Report "Prediction of Fuel Channel Lifetime at Ignalina NPP" July, 1995.
- [6.5.17] Hopkinson K.I., Marsden B.J., Dundulis G., Kopustinskas V., Liaukonis M., Augutis J., Uspuras E., Prediction of fuel channel-graphite gas-gap behaviour in RBMK reactors. Nuclear Engineering and Design, ISSN 0029-5493. - 2003. - Vol. 223. - P. 117-132.

- [6.5.18] Sagat, S., Coleman, C.E., Griffiths, M., Wilkins, B., ASTM Conference on Zirconium in Nuclear Industry, 1993
- [6.5.19] Negut, Gh., Ancuta, M., Radu, V., Ionescu, S., Stefan, V, Uta, O., Prisecaru, I, Danila, N., The irradiation effects on zirconium alloys, The European Materials Conference, E-MRS SPRING 2006 Nice France, May 29-June 2, 2006
- [6.5.20] Mechanical test data for Ignalina irradiated TMO-2 pressure tube material. V. Grigoriev, R. Jakobsson.-Studsvik Nuclear AB, 2001.
- [6.5.21] G. Dundulis, A. Grybenas, R. Janulionis, V. Makarevicius Ageing Assessment of RBMK–1500 Fuel Channel in Case of Delayed Hydride Cracking // Proceed. of Second International Symposium on Nuclear Power Plant Life Management, Book of Extended Synopses, 15-18 October 2007. Shanghai, China, 2007. P. 224-225.
- [6.5.22] Theaker J.R., Choubey, R., Moan, G.D., Aldridge S.A., Davis, L., Graham, R.A., Coleman, C.E., "Fabrication of Zr-2.5Nb Pressure Tubes to Minimize the Harmful Effects of Trace Elements", Zirconium in the Nuclear Industry, STP 1245
- [6.5.23] Investigation of RBMK fuel channel aging process and determination of safe operation criteria. Final report, LEI, 2006, Kaunas. This project was supported by Lithuanian Science Foundation.

6.6 HIGH TEMPERATURE COMPONENTS

High temperature reactors in Europe have mainly been the Advanced Gas Cooled Reactors (AGRs), which are still operating in the UK and Fast Breeder Reactors (FBRs) that have operated in the UK and France. These reactors operate at temperatures up to approximately 600°C and many components manufactured from austenitic stainless steel are susceptible to creep and creep-fatigue degradation mechanisms. Such components include piping associated with the steam generation systems in AGRs and various components in the primary circuit in FBRs .

6.6.1 Degradation Mechanisms

6.6.1.1 Thermal Ageing

Since diffusion rates are higher in body-centred cubic (B.C.C.) structures (ferritic steels) than in face-centred cubic (F.C.C.) structures (austenitic steels), the former are more susceptible to thermal aging degradation. The important parameters for these mechanisms are the operating time and temperature, as well as the chemical composition and more generally the manufacturing conditions (existence of heterogeneities).

When assessing the consequences of thermal aging, the main problem lies in the fact that the long-term evolution of the microstructure and of the mechanical properties must be precisely known. General models are available, which predict the kinetics of phase transformation; however they must be used very carefully since the studied systems are very complex.

The term of “thermal aging” covers many diffusion-based mechanisms that enable metallurgical systems to revert to stable thermodynamic equilibrium states. This reversion to equilibrium occurs through a micro-structural evolution that results in an evolution of the material properties. Since the formed microstructures contain obstacles to dislocation motion – precipitates, etc. - , thermal aging often induce hardening and embrittlement characterized by a decrease in ductility and/or increase in ductile brittle transition temperature (DBTT).

The main thermal aging mechanisms that may occur in PWR components are the following:

Spinodal decomposition

This is the de-mixing of the initial phase into two new phases occurring instantaneously in a progressive and very slow way. This mechanism is encountered in the chromium-rich ferritic phase of cast duplex stainless steels that are used for some primary circuit components (elbows, pipes, pump casings, valve casing, etc.). It results in an important hardening and embrittlement.

Segregation

When affecting grain boundaries, the segregation of chemical elements can reduce either the interfacial cohesion (thus promoting inter-granular fracture) or the corrosion resistance of boundaries (in case of their chromium depletion). For instance the segregation of phosphorus at grain boundaries may result in the detrimental embrittlement of bainitic steels used for PWR pressurizers that operate at about 350°C.

Precipitation

This consists in the nucleation, growth and possible coarsening of a second phase, up to thermodynamic equilibrium. When the precipitation is very fine and homogeneously distributed within grains, this mechanism can be highly hardening. Precipitations seldom occur at low operating temperatures as encountered in PWRs (around 300°C). However, the precipitation of a hardening Cr-rich phase in martensitic stainless steels (Type 13-4 PH, 17-4 PH) used for valve stems exemplifies this mechanism.



Dynamic strain aging

DSA consists in a coupling between deformation (dislocations mobility) and diffusion of solute atoms such as nitrogen and carbon. These atoms pin dislocations, which results in material hardening. This may occur for carbon steels used in secondary piping.

Ordering

Finally, ordering may occur. It is a regular arrangement of atoms of different chemical species which are initially randomly distributed. This highly hardening mechanism takes place in alloys containing nickel and chromium, where Ni₂Cr compound is formed. However, for temperatures lower than 400°C, this phenomenon has never been found in nickel alloys (type 600) in the absence of neutron irradiation.

6.6.1.2 Creep

Creep may be defined as a time-dependent deformation at elevated temperature and constant stress. It follows, then, that a failure from such a condition is referred to as a creep failure or, occasionally, a stress rupture. The temperature at which creep begins to be an active mechanism depends on the alloy composition, and the actual operating stress will, in part, dictate or determine the temperature at which creep begins.

The end of useful service life of the high-temperature components in a boiler (the superheater and reheater tubes and headers, for example) is usually a failure by a creep or stress-rupture mechanism. The root cause may not be elevated temperature, as fuel-ash corrosion or erosion may reduce the wall thickness so that the onset of creep and creep failures occur sooner than expected.

However, regardless of the cause, the failure will exhibit the characteristics of a creep or stress rupture. Indeed, the ASME Boiler and Pressure Vessel Code recognizes creep and creep deformation as high-temperature design limitations and provides allowable stresses for all alloys used in the creep range. One of the criteria used in the determination of these allowable stresses is 1% creep expansion, or deformation, in 100,000 hours of service. Thus, the code recognizes that over the operating life, some creep deformation is likely. Indeed creep failures do display some deformation or tube swelling in the immediate region of the rupture.

At elevated temperatures and stresses, much lower than the high-temperature yield stress, metals undergo permanent plastic deformation called creep. Figure 17 shows a schematic creep curve for a constant load; a plot of the change in length versus time. The weight or load on the specimen is held constant for the duration of the test.

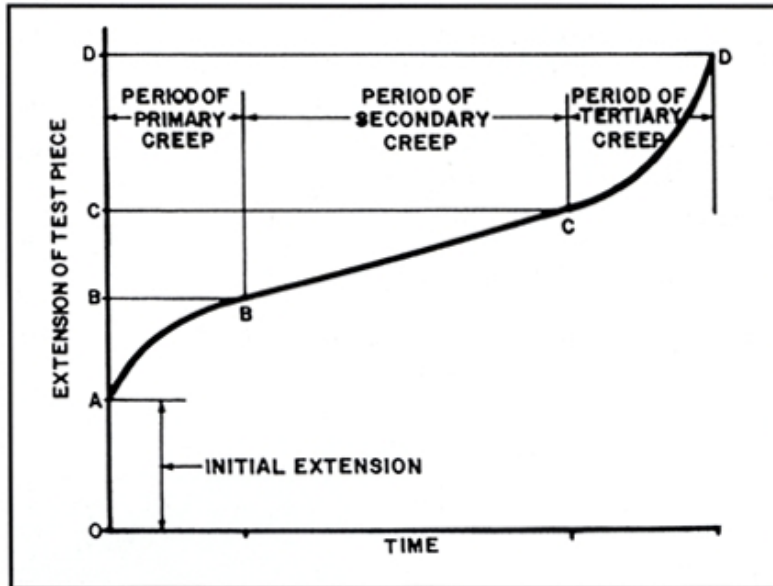


Figure 17 Schematic creep curve.

There are four portions of the curve that are of interest:

An initial steep rate that is at least partly of elastic origin, from point "0" to point "A" in Figure 17.

This is followed by a region in which the elongation or deformation rate decreases with time, the so-called transient or primary creep, from region "A" to "B" of Figure 17. The portion from point "0" to point "B" occurs fairly quickly.

The next portion of the creep curve is the area of engineering interest, where the creep rate is almost constant. The portion from "B" to "C" is nearly linear and predictable. Depending on the load or stress, the time can be very long; two years in an experiment and several decades in service.

The fourth portion of the creep curve, beyond the constant-creep-rate or linear region, shows a rapidly increasing creep rate which culminates in failure. Even under constant-load test conditions, the effective stress may actually increase due to the damage that forms within the microstructure.

Without going into a detailed discussion of the atom movements involved in creep deformation, suffice it to say that creep deformation occurs by grain-boundary sliding. That is, adjacent grains or crystals move as a unit relative to each other. Thus, one of the microstructural features of a creep failure is little or no obvious deformation to individual grains along the fracture edge.

The first two stages will not leave any microstructural evidence of creep damage. Somewhere along the linear portion of Figure 17, the first microstructural evidence of damage appears as individual voids or pores. The location of these first voids or holes varies, often noted at the junction of three or more grains, occasionally at nonmetallic inclusions. These individual voids grow and link to form cracks several grains long, and finally failure occurs. The ultimate rupture is by a tensile overload when effective wall thickness is too thin to contain the steam pressure.

Since creep deformation occurs by grain-boundary sliding, the more grain boundary area, the easier creep deformation will be. Creep deformation and creep strength are a grain-size sensitive property. Thus a larger grain size improves creep strength. For austenitic stainless steels, SA213 TP321H for example, the ASME Code requires a grain size of #7 or coarser, to assure adequate creep strength. The elevated temperatures where creep occurs lead to other microstructural



changes. Creep damage and microstructural degradation occur simultaneously. For carbon steels and carbon-1/2 molybdenum steels, iron carbide will decompose into graphite. For the low-alloy steels of T-11 and T-22, the carbide phase spheroidizes. Thus, creep failures will include the degraded microstructures of graphite or spheroidized carbides along with the grain-boundary voids and cracks characteristic of these high-temperature, long-time failures.

While creep failures are expected for superheaters and reheaters operating at design conditions, deviations from these parameters will promote early failures. The steam temperature always varies somewhat from individual tube to tube, and the design allows for this variability. However, when the range of temperatures is larger than accounted for, the hottest tubes fail sooner than expected. A more likely cause of premature failure is the slow increase in tube-metal temperatures due to the formation of the steam-side scale.

Steam reacts with steel to form iron oxide along the inner surface of the tube. The microstructures themselves will show the grain-boundary sliding and the resultant creep cracks or voids. For stainless steels, the microstructures are similar in that the failure is by grain-boundary-sliding and crack formation.

In a superheater or reheater tube, often the first indication of creep damage is longitudinal cracks in the steam-side scale. As creep deformation expands the tube diameter, the brittle ID scale cannot follow the expansion. Cracks develop in an axial or longitudinal direction which is perpendicular to the principle hoop stress. With time, the tube continues to expand, and these cracks widen. This wide crack shortens the path from steam to steel; iron oxide forms preferentially at the tip of the crack, as there is less oxide thickness to protect the steel; and a cusp forms within the steel tube. The cusp acts as a notch or a stress raiser, reducing the local wall thickness. Creep voids form here, often before any other obvious grain-boundary damage appears elsewhere within the microstructure. With continued high-temperature operation, creep cracks grow from the cusp and ultimately weaken the cross section to the point where failure occurs. Creep failures are characterized by the following:

- bulging or blisters in the tube
- thick-edged fractures often with very little obvious ductility
- longitudinal "stress cracks" in either or both ID and OD oxide scales
- external or internal oxide-scale thicknesses that suggest higher-than-expected temperatures
- intergranular voids and cracks in the microstructure

In components which operate at high temperatures, changes in conditions at the beginning and end end of operation, or during operation, result in transient temperature gradients. If these transients are repeated, the differential thermal expansion during each transient results in thermally induced cyclic stress. The extent of the resulting fatigue damage is dependent of the nature and frequency of the transient, the thermal gradient in the component, and the material properties. Components which are subject to thermally induced stresses generally operate within the creep range so that damage due to both fatigue and creep have to be taken into account; methods for such assessments are described in the following section.

6.6.2 Creep/Fatigue Assessment Methods

6.6.2.1 The RCC-MR Code

The RCC-MR code [6.6.1] "Design and Construction rules for mechanical components of FBR nuclear islands and high temperature applications" was developed to support the design of Sodium Fast Breeder Reactors in France. The rules and requirements provided by this Code are,

however, not limited to fast reactors and RCC-MR is therefore applicable to other types of high temperature reactors.

The rules for piping systems deal in particular with :

- Plastic instability
- Creep
- Ratchetting
- Fatigue

Table 4 illustrates the general presentation of the RCC-MR code. The RCC-MR is split into five sections defined as follows:

- Section I provides sets of design rules for various types of components,
- Section II contains procurement specifications for parts and products which can be used for components designed and manufactured according to RCC-MR,
- Section III is devoted to rules for applying the various destructive and non destructive examination methods,
- Section IV gives the rules relating to the various qualifications for welding operations and welding procedures,
- Section V provides rules relating to manufacturing operations other than welding.

Table 4 Contents of the RCC-MR code [6.6.1]

	Title	Reference symbol
SECTION I	NUCLEAR ISLAND EQUIPMENT	
	Subsection "A": General	RA
	Subsection "B": Class 1 components	RB
	Subsection "C": Class 2 components	RC
	Subsection "D": Class 3 components	RD
	Subsection "H": Supports	RH
	Subsection "K": Examination and handling mechanisms	RK
	Subsection "Z": Technical appendices	RZ
SECTION II	MATERIALS	RM
SECTION III	EXAMINATION METHODS	RMC
SECTION IV	WELDING	RS
SECTION V	FABRICATION	RF

Subsection Z contains a number of appendices referenced in the other subsections of Section I. Table 5 lists the content of Subsection Z.

Table 5 Contents of subsection Z – Appendices

Appendix	Title
A3	Characteristics of materials
A6	Design of bolted assemblies
A7	Analyses taking account of buckling
A9	Characteristics of welded joints
A10	Elastoplastic analysis of a structure subjected to cyclic loading
A11	Elasto-visco-plastic analysis of a structure subjected to cyclic loading
A12	Design rules for shells of revolution subject to external pressure and cylinders under axial compression
A14	Design rules for linear type supports
A15	Design rules for dished heads subject to internal pressure
A16	Guide for Leak Before Break analysis and defect assessment
A17	Design of flat tubeplates

The A16 Appendix – LBB analysis and defect assessment

The RCC-MR proposes, in its appendix A16, all tools required to evaluate the defect parameters in the frame of the Leak Before Break (LBB) procedure:

- Appendix A16.2000 : defect used in the analysis
- Appendix A16.3000 : defect assessment (general rules)
- Appendix A16.4000 : Leak Before Break
- Appendix A16.7000 : methods (detailed procedure for flaw analysis) – parameters
- Appendix A16.8000 : compendium
- Appendix A16.9000 : material properties

All of these nuclear type rules can be easily adapted for non-nuclear components. The more specific nuclear aspects are the safety factors associated with the rules.

An important effort in development of the analytical methods for the calculation of fracture parameters (K_I , J ,...) has been made in the last 10 years within the framework of collaboration between CEA, EDF and AREVA-NP, and of R&D actions involving CEA and IRSN. These activities led to a unified presentation of the common methods of the RCC-MR code and the RSE-M code ("Rules for In-service Inspection of Nuclear Power Plant Components" which defines the requirements for in-service inspection of French Pressurized Water Reactors). The calculation of fracture mechanics parameters, and in particular the stress intensity factor K_I and the J integral, has been widely developed for industrial configurations. These improvements have been made using an important three-dimensional Finite Element (F.E.) calculation data base of cracked piping components. Concerning the J parameter, the accuracy of the method has been presented to the French Safety Authority: each year, a meeting is organized to present new developments and discuss the accuracy of the predictions. This has led to a systematically conservative method but still sufficiently accurate. All the developments have been integrated into the 2005 edition of RSE-M [6.6.2] and in the 2007 edition of RCC-MR [6.6.1].

The analytical methods proposed in the RCC-MR code [6.6.1] to calculate the stress intensity factor and J are provided in [6.6.3], [6.6.4], [6.6.5], [6.6.6], and [6.6.7]. These methods are the basic tools of the proposed defect assessment procedures. The following sub-sections give an overview of these procedures.

The Leak Before Break procedure

The Leak Before Break (LBB) procedure can be applied for safety demonstration of a nuclear power plant. The aim is to check that a postulated or a detected defect will not lead to the component failure, even when it grows to full penetration, which would lead to a leakage large enough to be detected. This procedure is mainly developed for Sodium Fast Breeder Reactors. This LBB procedure is based on a series of analyses (defect assessment, flow rate evaluation, etc.), each needing specific tools. Important work at CEA focused on checking and improvement of these tools [6.6.8] and some modifications will be included in the 2006 addendum of RCC-MR [6.6.1]:

- Influence of the initial size of the defect
- Consideration of the defect straightening after penetration

Fatigue analysis

Fatigue crack initiation

The time of the initiation phase that takes place before growth of a crack-like fabrication defect can be handled through an initiation usage factor, roughly evaluated with a similar methodology to that for an uncracked body fatigue usage factor, replacing the stress range by a relevant parameter

calculated at a material characteristic distance from the defect.

The method is based on conventional material properties used for the design: for each cycle, the elastic singular stress is first calculated using the Creager field at a distance *d* from the crack tip (this distance is supposed as a material property), and the Neuber rule is applied to account for plasticity. The obtained elastic-plastic strain is then used to determine the number of cycles to failure through the fatigue curve, and allows the definition of the fatigue usage factor for the considered cycle. The summation of the usage factors for all the load history gives an estimation of the remaining life before fatigue initiation. A specific treatment is performed if creep loading is not negligible. Reference [6.6.9] gives the detail of this approach.

Fatigue crack growth

Crack growth rate evaluation is then based on the Paris law criteria (*da/dN* – ΔK), eventually taking into account a crack closure effect, and has to be determined for one, two or three crack tips depending on the crack shape (three crack tips for the embedded flaw for example).

In A16 appendix, the possibility to take into account larger plasticity is given:

$$\Delta K_{\text{eff}} = \sqrt{\frac{E \cdot \Delta J}{1 - \nu^2}} \tag{Eq. 14}$$

where ΔJ is the J parameter variation, calculated for the complete loading variation and assuming a material cyclic behaviour. This formulation is more appropriate for high level of cyclic loading [6.6.10] and thermal loading (dominant at high temperature).

Critical crack size evaluation

In the A16 appendix [6.6.1], modifications were performed to improve the determination of the critical defects in terms of stability: the knowledge of this defect is an important input into the LBB procedure. Different parts of the RSE-M procedure are codified:

- Numerical algorithms for 1-D (through wall crack) or 2-D (surface crack) crack propagation analysis (i.e. direct determination of the maximum endurable load and the associated crack growth).
- Crack growth rate evaluation with the classical $JR-\Delta a$ criteria or with the alternative G_{II} criteria [6.6.11].

Creep analysis

For creep crack initiation, an adaptation of the fatigue rule is proposed: at the same distance d , the elastic stress is calculated from the Creager field, and used to determine the elastic-plastic stress through the Neuber rule. This stress is related to the corresponding failure time on the creep design curve. This failure time allows the creep usage factor calculation. The stress relaxation could also be taken into account. If a creep-fatigue combination is considered, for each cycle, the fatigue and creep usage factors are determined independently and used in an interaction diagram to determine the margin to crack initiation.

In the frame of crack propagation analyses under creep conditions, Appendix A16 provides an analytical method for the C^* calculation [6.6.1], [6.6.9], similar to the method for the J calculation.

This C^* parameter (essentially time dependent J) is used to determine the creep crack growth rate through the creep crack growth curve relating in general da/dt to C^* with a power law. When a creep-fatigue loading is considered, the crack extension is determined cycle by cycle: the fatigue and creep loadings are treated independently and leads to a fatigue and creep crack extensions which are summed to the previous crack length to update the defect geometry. Specific decomposition of the cycle has to be performed to determine the part of the cycle which effectively contribute to the creep loading (in particular in presence of a cyclic thermal loading).

6.6.2.2 R5 Procedure for Lifetime Assessment of High Temperature Components

UK procedures for assessing the lifetime of high temperature components were developed in the 1970s and 1980s within the former Central Electricity Generating Board (CEGB). These enabled assessments of the integrity of both fossil-fired and nuclear power generating plants. Although there were design codes for high temperature plants at that time, more accurate life assessment methods were needed to address, for example, weldments and defect tolerance, which were not covered in the design codes. The procedures developed within the CEGB became known as the R5 Procedures and were based on reference stress and shakedown methods in order to lessen the conservatism in design code routes based on elastic analysis. R5 is now maintained by EDF Energy Nuclear Generation Ltd (formerly known as British Energy Generation Ltd) in collaboration with Serco, Rolls-Royce and ANSTO. A continuing R5 development programme ensures that advances in R5 address the key issues relevant to UK high temperature nuclear plants. The R5 development programme runs in parallel with materials data test programmes covering the principal materials of interest, e.g. austenitic 300 series and Essete 1250 stainless steels and ferritic steels such as 0.5CrMoV, 2.25Cr and 9Cr. These materials test programmes reflect the increasing interest in long term material properties, of austenitic steels in particular, due to the safety case requirements for PLEX justifications for the UK Advanced Gas-Cooled Reactor (AGR) fleet, and also thermal aging effects on materials properties.

The R5 procedures [6.6.12] are a UK nuclear power industry standard, regularly used in safety cases for structural integrity assessments of AGR components operating in the creep range. The procedures are also relevant to high temperature plants outside the nuclear power generation industry. Although R5 does not have the status of a national code or standard, similar approaches to those in R5 for defect assessments are now included in BS 7910 [6.6.13], for example. Confidence in the application of R5 has been obtained by programmes of experimental validation and numerical research. In individual assessments, further confidence is obtained by the use of appropriately conservative materials data and by sensitivity analyses. Such analyses



are an important element of an R5 assessment and are used to demonstrate that the result of the assessment is not sensitive to realistic variations in the input parameters.

Assessment of the safe operating life of components, operating at temperatures that are sufficiently high for creep to be a potential failure mechanism, may be divided into two types. The first is assessment of the time for cracking to occur in an initially defect-free component as a result of combined creep and fatigue damage, which can be performed using the R5 Volume 2/3 procedure. The time to initiate a defect of a defined size can be calculated using Volume 2/3. The second type is assessment of the time for an existing crack in a component to grow to a limiting size as a result of creep and fatigue mechanisms, which can be performed using the R5 Volume 4/5 procedure. This latter defect may have been detected in service, be postulated to occur in a component based on inspection limitations for example, or result from a Volume 2/3 assessment. The limiting size of the defect is determined using the R6 defect assessment procedure [6.6.14], also maintained by EDF Energy Nuclear Generation Ltd in association with Serco, Roll-Royce, TWI, Frazer-Nash Consultancy and NRG (R6 is also used for assessing defect tolerance of the UK PWR reactor).

The R5 procedures provide an assessment of the continuing integrity of a component, where the operating lifetime might be limited by one of the following mechanisms:

- excessive plastic deformation due to a single application of a loading system,
- creep rupture,
- ratchetting or incremental plastic collapse due to a loading sequence,
- creep deformation enhanced by cyclic load,
- initiation of cracks in initially defect-free material by creep and creep-fatigue mechanisms,
- the growth of flaws by creep and creep-fatigue mechanisms.

R5 is now at Issue 3. The former Volumes 2 and 3 of R5 have been combined into a single procedure for assessing defect-free structures and the former Volumes 4 and 5 were combined into a single procedure for assessing defects in structures. Thus, in R5 Issue 3 there are now 5 volumes in total:

Volume 1	The overview
Volume 2/3	Creep-fatigue crack initiation procedure for defect-free structures
Volume 4/5	Procedure for assessing defects under creep and creep-fatigue loading
Volume 6	Assessment procedure for dissimilar metal welds
Volume 7	Behaviour of similar weldments: guidance for steady creep loading of ferritic pipework components

Volume 1 provides an overview, which indicates the overall scope and restrictions of R5 by reference to the other volumes, provides a route for following the detailed procedures given elsewhere in R5, and compares R5 with other approaches. Materials data requirements for performing an R5 assessment are also described. Volumes 6 and 7 are essentially specialized applications of the creep-fatigue damage calculations of Volume 2/3 and the creep and creep-fatigue crack growth calculations of Volume 4/5, respectively, to particular weldments and operating conditions found in AGRs.

The creep-fatigue methods of Volume 2/3 address components that operate within creep-modified shakedown limits. These cover both strict shakedown and global shakedown conditions, where the latter allows zones of cyclic plasticity in the steady cyclic state in the component

provided these are restricted to at most 20% of the component cross-section. Outside this limitation, more detailed assessment is required, and R5 gives some advice on the use of cyclic inelastic analysis. An important difference between R5 Volume 2/3 and some other high temperature assessment procedures is the use of ductility exhaustion rather than life fraction rules to assess creep-fatigue damage accumulation. Damage accumulation prior to the steady state is also quantified in R5 Volume 2/3 and is of particular relevance to components containing high initial residual stresses (see Section 5.6.2.4).

Volume 4/5 covers the growth of defects. Rules are set down for determining whether creep and fatigue are significant or insignificant and creep-fatigue interaction effects are addressed. The defect tip can lie either within or outside any region of surface cyclic plasticity. For short defects, where the tip is within the surface cyclic plastic zone, the creep-fatigue crack growth law is based on a creep-modified high strain fatigue law. For defects outside a cyclic region, and for cases of strict shakedown, crack growth is based on adding creep crack growth characterised by C^* or $C(t)$ and fatigue extension obtained from a Paris fatigue law. Appendices to Volume 4/5 provide advice on treating defects in weldments, the calculation of an incubation time for crack growth based on sigma-d or failure assessment diagram methods, probabilistic fracture mechanics calculations and advice on crack growth under combined primary and secondary stresses. This last area, in particular, has undergone significant recent development, driven by the needs to assess austenitic welds where the component may operate within the transient creep regime (see Section 5.6.2.4).

High temperature leak-before-break assessment is not included in R5 but is addressed within the R6 procedure. A procedure for performing a high temperature LBB assessment is set out based on detection prior to the defect growing to a limiting size or failing by creep rupture. Reference stress methods are described for calculating the time-dependent change in crack opening area and hence the leak rate.

R5 is routinely used within EDF Energy Nuclear Generation Ltd for justification of continued operation of high temperature components, both inside and outside the containment. Table 6 gives a summary of some of the areas of application. Assessments may consider either damage or crack-like flaws detected during service or, particularly for areas which are difficult to inspect, flaws postulated for the purposes of safety case arguments.

During high temperature service, welding residual stresses relax and redistribute due to the accumulation of creep strain. The AGR reactors have tended to operate at temperatures lower than original design. Hence the times for relaxation of the welding residual stresses can be a significant proportion of planned plant life. These relaxation creep strains, additional to those occurring due to primary stress, can lead to accelerated creep damage and possible reheat crack initiation, particularly at locations with high stress triaxiality and in materials with low creep ductility. For example, repair welds are a potential location of reheat crack initiation due to the high levels of tensile residual stress that can exist over the length of the repair. An important parameter in assessing the rate of stress relaxation of the secondary stress, and hence the additional creep strain accumulation, is the elastic follow-up factor, quantified by the scalar Z in R5 [5.6.12], where Z approaches infinity in the limit of primary, load-controlled stress. Methods for evaluating Z at the point of interest, for example based on simple bounding estimates or elastic-creep analysis, are given in R5.

Welding residual stress also affects crack growth rates. The driving force for creep crack growth is quantified by $C(t)$, the transient equivalent of the steady-state parameter, C^* . $C(t)$ reduces with increasing time, approaching the value of C^* for the primary loads as the secondary stresses relax, at a rate dependent on a value of the elastic follow-up factor Z . The magnitude of $C(t)$ can also reduce with increase in crack size for cases where the stress intensity factor due to the residual stress is falling as the crack grows. Creep crack growth is then calculated in R5 by integrating a crack growth law of the form $da/dt=A(C(t))^q$, where q is a material constant, so that

increased crack growth rates are predicted in the presence of tensile residual stress, where $C(t) > C^*$.

Table 6 Typical Applications of R5 on UK Nuclear Plant

R5 Volume	Material	Component	Comments
Volume 2/3	Austenitic Stainless Steels; Alloy 600 and 800	Boiler components also reactor internals; e.g. insulation, superheater and reheater headers	Hot end, mostly thinner sections
Volume 2/3	Ferritic	E.g. superheater pipework	Thermal transients, e.g. bore thermal fatigue cracking
Volumes 4/5, 7	Ferritic	Pipework	
Volumes 4/5, 7	Austenitic Stainless Steels	Headers and pipework	E.g. reheat cracking, mainly thick-walled but also some thin-wall components
Volume 6	316:2.25Cr; 316:9Cr; 316:C-Steel	E.g. Upper transition joints	Crack initiation; but also some consideration of crack growth using Volume 4/5. Fatigue only for C-Steel Joints

6.6.3 References (High Temperature Components)

- [6.6.1] RCC-MR Code, 2002 edition (addendum 2006 in preparation), "Design and Construction Rules for Mechanical Components of FBR Nuclear Islands and high temperature applications" appendix A16, Tome I, vol. Z, Paris, AFCEN, Paris.
- [6.6.2] RSE-M Code, "Rules for In-service Inspection of Nuclear Power Plant Components", 1997 Edition + 1998, 2000 and 2005 addenda, AFCEN, Paris.
- [6.6.3] Marie, S., Chapuliot, S., Kayser, Y., Lacire, M.H., Drubay, B., Barthelet, B., Le Delliou, P., Rougier, V., Naudin, C., Gilles, P. and Triay, M., 2006, "French RSE-M and RCC-MR code appendixes for flaw analysis: Presentation of the fracture parameters calculation – Part I : General overview", accepted in International Journal of Pressure Vessel and Piping.
- [6.6.4] Marie, S., Chapuliot, S., Kayser, Y., Lacire, M.H., Drubay, B., Barthelet, B., Le Delliou, P., Rougier, V., Naudin, C., Gilles, P. and Triay, M., 2006, "French RSE-M and RCC-MR code appendixes for flaw analysis: Presentation of the fracture parameters calculation – Part II : Cracked plates", accepted in International Journal of Pressure Vessel and Piping.
- [6.6.5] Marie, S., Chapuliot, S., Kayser, Y., Lacire, M.H., Drubay, B., Barthelet, B., Le Delliou, P., Rougier, V., Naudin, C., Gilles, P. and Triay, M., 2006, "French RSE-M and RCC-MR code appendixes for flaw analysis: Presentation of the fracture parameters calculation – Part III : Cracked pipes", accepted in International Journal of Pressure Vessel and Piping.
- [6.6.6] Marie, S., Chapuliot, S., Kayser, Y., Lacire, M.H., Drubay, B., Barthelet, B., Le Delliou, P., Rougier, V., Naudin, C., Gilles, P. and Triay, M., 2006, "French RSE-M and RCC-MR code appendixes for flaw analysis: Presentation of the fracture parameters calculation – Part IV : Cracked elbows", accepted in International Journal of Pressure Vessel and Piping.
- [6.6.7] Marie, S., Chapuliot, S., Kayser, Y., Lacire, M.H., Drubay, B., Barthelet, B., Le Delliou, P., Rougier, V., Naudin, C., Gilles, P. and Triay, M., 2006, "French RSE-M and RCC-MR code appendixes for flaw analysis: Presentation of the fracture parameters calculation – Part V : Elements of validation" accepted in International Journal of Pressure Vessel and Piping.
- [6.6.8] Y. Kayser, S. Marie, C. Poussard and C. Delaval, 2006, "Leak before break procedure: Recent modification of RCC-MR A-16 appendix and proposed improvements", submitted to International Journal of Pressure Vessel and Piping.
- [6.6.9] Moulin, D. Drubay, B., and Laiarinandrasana, L., 1999, "A synthesis of the Fracture Assessment Methods Proposed in the French RCC-MR Code for High Temperature", WRC Bulletin N°440.
- [6.6.10] Chapuliot, S, Lacire, M.H. and Marie, S., 1999, "Stress intensity factors of through wall cracks in plates and tubes with circumferential cracks", ASME Pressure Vessel and Piping Conference, Boston (USA), Vol. 388, pp. 13-21.
- [6.6.11] Marie, S. and Chapuliot, S., 2002, '2D crack growth simulation with an energetic approach', Nuclear Engineering & Design, Vol. 212, , pp. 31-40.
- [6.6.12] R5, Assessment Procedure for the High Temperature Response of Structures, Issue 3, British Energy Generation, Gloucester, UK (2003).
- [6.6.13] BS7910:2005, Guide to Methods for Assessing the Acceptability of Flaws in Metallic Structures, British Standards Institution, London (2005).
- [6.6.14] R6, Assessment of the Integrity of Structures Containing Defects, Revision 4, with amendments to May 2006, British Energy Generation, Gloucester, UK (2006).



7 INTEGRATION STATEMENT

The ability of NULIFE to deliver procedures and best practice advice is a key integration driver, one that is critical to the Network's success.

The overall policy is to target the production of advanced technological approaches compatible with available higher level harmonized guidance e.g. IAEA TEC DOCs. Well established standards in specific areas such as the ASTM materials testing standards and the ASME code section for boilers and pressure vessels have to be considered as part of this process. Additionally, national standards and procedures such as the German KTA Rules, the French RCC-M code, and the UK R6 and R5 procedures, have also to be considered, along with examples of the way in which they are applied to different reactor systems in different countries.

The knowledge base so obtained will form the basis for the development of good-practice / best-practice and guidance documents on integrity assessment, component qualification and plant life time management. Procedures and best practice documents are considered important in facilitating the following activities within NULIFE:

- Integration
- Education and training of new generations of engineers urgently needed for the life extension of Generation II, deployment of Generation III and development of Generation IV reactors
- Future harmonisation of safety standards and safety requirements within the EU Member States, and wider

The four Expert Groups (materials, integrity, lifetime and risk) provide a framework for ensuring consensus and peer review within the NULIFE community, i.e. beyond that of the organizations/experts directly involved in the development of specific procedures.

At its highest level, the Network actively supports the development of a Common Safety Justification Framework. This report represents a first step towards creation of such a Framework on the following counts:

- The report is the result of the active collaboration of professional scientists and engineers from 16 organizations (and as such has helped facilitate the Integration Process during the lifetime of NULIFE)
- The report considers integrity assessment and lifetime management issues across the range of NPPs in EU Member States (PWR, WWER, BWR, AGR, CANDU, RBMK and FBR) (thus facilitating common understanding across a range of PLIM issues)
- The report provides numerous examples of the application of good practice / best practice methodology at national level (further facilitating common understanding)
- The report's Appendices collectively provide a valuable source of information on numerous aspects of plant life management (thereby contributing knowledge preservation and management)
- The report represents an important resource for the purpose of producing future procedures and best practice advice within the EC.

Lastly, it should be noted that the report can be regarded as a "living document", that is to say it is foreseen that it could be usefully updated at appropriate intervals during the course of time. It could for example be used in the road mapping process in NUGENIA.



8 APPENDICES

Appendices 1-17 provide further details regarding degradation mechanisms and lifetime evaluation, as summarised in Table 7.



9 ACKNOWLEDGEMENTS

This report represents the work of many people. In particular, contributions due to the following persons are gratefully acknowledged:

Eberhard Altstadt	FZD
Milan Brumovsky	NRI
Peter Budden	BE
Stephane Chapuliot	CEA
Leon Cizelj	JSI
Marjorie Erickson	PEAI
Ferenc Gillemot	AEKI
Gintautas Dundulis	LEI
Börje Gustafsson	WE
Dana Lauerova	NRI
Jean-Paul Massoud	EDF
Dominique Moinereau	EDF
Gerhard Nagel	EKK
Tomas Nicak	ANP-G
Elena Parfumì	JRC
Vasile Radu	INR
Sven Reese	EKK
Maria Roth	INR
Johannes Seichter	SPG
Frederic Blom	NRG
John Sharples	SERCO
Adam Toft	SERCO
Arja Saarenheimo	VTT



Table 7 Summary of Appendices

Appendix No.	Title	Contributor(s)	Applicable Systems	Topics
Appendix 1	Fatigue and thermal fatigue	JRC ANP-G	<ul style="list-style-type: none"> • LWR (PWR, WWER) • PHWR (CANDU) • AGR (steam pipe work) 	<ul style="list-style-type: none"> • Introduction, materials, service conditions • Physical Description of the Mechanism • Applicable Testing & Standards For Characterisation of Mechanisms • Governing Codes & Specification For Application In Power Plants • Research Possibilities To Improve Code & Standard and Gaps
Appendix 2	Considerations regarding formation of corrosive films			<ul style="list-style-type: none"> • Carbon and martensitic steels • Nickel alloys
Appendix 3	Delayed Hydride Cracking (DHC)	INR	CANDU, RMBK Pressure tubes PWR, BWR, CANDU Zircaloy-4 fuel claddings	<ul style="list-style-type: none"> • Physical description of mechanism • Service conditions/environment • Materials • Susceptible components • Applicable testing standard(s) for characterising mechanism • Governing Codes and Assessment Procedures for NPP integrity and lifetime assessment • Current research programmes • Knowledge gaps • Future research requirements



Table 7 Summary of Appendices

Appendix No.	Title	Contributor(s)	Applicable Systems	Topics
Appendix 4	Erosion / Corrosion	INR	<p>High Pressure feedwater heaters, Steam Generator inlets, feedwater pumps, and CANDU feeders.</p> <p>Steam extraction piping, cross-over piping (High Pressure turbine to moisture separator), steam side of feedwater heaters, and CANDU feeders.</p>	<p>Flow-Assisted or Flow-Accelerated Corrosion (FAC)</p> <ul style="list-style-type: none"> • Physical description of mechanism • Service conditions/environment • Materials • Susceptible components • Applicable testing standard(s) for characterising mechanism • Current research programmes • Knowledge gaps
Appendix 5	Assessment On The Evolution of A Flaw In A Class 1 ASME Nuclear Equipment	CTEN	Cernavoda NPP#2 Pressurizer	<p>Presents an evaluation of the flaws (weld indication) at PZX found during the inaugural inspection for the Cernavoda NPP #2 pressurizer.</p> <p>All the indications have been evaluated based on the procedure in ASME Code Section XI.</p>

Table 7 Summary of Appendices

Appendix No.	Title	Contributor(s)	Applicable Systems	Topics
Appendix 6	Oxidation	INR	Piping; SG Tubesheet; SG tubing.	<p>Study focus on CANDU plant. Topics include:</p> <ul style="list-style-type: none"> • Physical description of mechanism • Service conditions/environment • Materials • Susceptible components • Applicable testing standard(s) for characterising mechanism • Governing Codes and Assessment Procedures for NPP integrity and lifetime assessment • Current research programmes • Knowledge gaps • Future research requirements



Table 7 Summary of Appendices

Appendix No.	Title	Contributor(s)	Applicable Systems	Topics
Appendix 7	Thermal High Cycle Fatigue in Piping System Tees with Leakage	SPG	Piping Tees with relevant temperature differences between run and branch fluid, especially with a “dead end” and possibly valve leakage.	<ul style="list-style-type: none"> • Physical Description of Mechanism • Service conditions/environment • Materials • Susceptible components • Applicable testing standard(s) for characterising mechanism • Governing Codes and Assessment Procedures for NPP integrity and lifetime assessment • Current research programmes • Knowledge gaps • Future research requirements • Useful Resource Documents



Table 7 Summary of Appendices

Appendix No.	Title	Contributor(s)	Applicable Systems	Topics
Appendix 8	PNAE G 7 002 86 (Russian Code) / IAEA-EBP-WWER-08	FZD	Fracture mechanical evaluation of the RPV of WWER type reactors during a pressurised thermal shock.	<ul style="list-style-type: none"> • Introduction • Scope • Methodology <ul style="list-style-type: none"> <i>Sequences To Be Considered</i> <i>Acceptance Criteria</i> <i>Assumptions For Pts Analysis</i> <i>Thermal Hydraulic Analysis</i> <i>Structural Analysis</i> <i>Integrity Assessment</i> <i>Material Properties</i> <i>Corrective Actions</i> <i>Computer Codes</i> <i>Quality Assurance</i> • Details of the PTS analysis <ul style="list-style-type: none"> <i>Irradiation effects to material properties</i> <i>PTS Analysis for WWER reactors</i> • Current R&D activity • Knowledge gaps • Future research requirements • References



Table 7 Summary of Appendices

Appendix No.	Title	Contributor(s)	Applicable Systems	Topics
Appendix 9	Delayed Hydride Cracking RBMK-1500 NPP	LEI	RBMK-1500 nuclear power plant reactor fuel channels	<ul style="list-style-type: none"> • Physical Description of Mechanism • Service conditions/environment • Materials • Susceptible components • Applicable testing standard(s) for characterising mechanism • Governing Codes and Assessment Procedures for NPP integrity and lifetime assessment • Current research programmes • Knowledge gaps • Future research requirements
Appendix 10	Inter-granular Stress Corrosion Cracking	LEI	RBMK-1500 nuclear power plant reactor cooling system piping components	<ul style="list-style-type: none"> • Physical Description of Mechanism • Service conditions/environment • Materials • Susceptible components • Applicable testing standard(s) for characterising mechanism • Governing Codes and Assessment Procedures for NPP integrity and lifetime assessment • Future research requirements • References



Table 7 Summary of Appendices

Appendix No.	Title	Contributor(s)	Applicable Systems	Topics
Appendix 11	Irradiation Induced Dimensional and Material Property Changes To The Graphite	LEI	RBMK-1500 nuclear power plant reactor fuel channels and the graphite moderator bricks	<ul style="list-style-type: none"> • Physical description of mechanism • Service conditions/environment • Materials • Susceptible components • Applicable testing standard(s) for characterising mechanism • Governing Codes and Assessment Procedures for NPP integrity and lifetime assessment • Knowledge gaps • Future research requirements
Appendix 12	Irradiation induced change of fuel channel length	LEI	RBMK-1500 nuclear power plant reactor fuel channels	<ul style="list-style-type: none"> • Physical description of mechanism • Service conditions/environment • Materials • Susceptible components • Applicable testing standard(s) for characterising mechanism • Governing Codes and Assessment Procedures for NPP integrity and lifetime assessment



Table 7 Summary of Appendices

Appendix No.	Title	Contributor(s)	Applicable Systems	Topics
Appendix 13	Guidance for application of the leak before break concept at Ignalina NPP RBMK-1500 reactors.	LEI	RBMK-1500 reactors	<ul style="list-style-type: none"> • Introduction • Scope • Methodology • Applications to lifetime assessment of degraded materials & components • Associated material test standards
Appendix 14	Requirements for Assessment of Intergranular Stress Corrosion Cracking Damages in RBMK-1500 Reactors	LEI	RBMK-1500 reactors	<ul style="list-style-type: none"> • Introduction • Scope • Methodology • Applications to lifetime assessment of degraded materials & components • Associated material test standards



Table 7 Summary of Appendices

Appendix No.	Title	Contributor(s)	Applicable Systems	Topics
Appendix 15	RPV Cladding	various	LWR, WWER & western RPV claddings	(N.b. the following are contained within Annex 1) <ul style="list-style-type: none"> • Introduction, materials • Chemistry of RPV Claddings • Defects in the Cladding • Microstructure of the cladding • Mechanical properties • Properties and Assessment Tools for Characterizing PWR Cladding Crack Susceptibility • Characterization of Residual Stresses Under Cladding • Properties and Assessment Tools for Characterizing WWER Cladding Crack Susceptibility • Lifetime Evaluation considering cladding properties • Summary and suggestions for further study
Appendix 16	Pressurized thermal shock	VTT	LWR, WWER & western RPV	<ul style="list-style-type: none"> • RPV • Cladding • Thermal stresses • Fracture mechanics • Brittle fracture • Finite element method



Table 7 **Summary of Appendices**

Appendix No.	Title	Contributor(s)	Applicable Systems	Topics
Appendix 17	CANDU Feeder Piping	Various	CANDU	<ul style="list-style-type: none">• Degradation Mechanisms• Lifetime Evaluation





APPENDICES

Appendix 1	Fatigue and thermal fatigue
Appendix 2	Considerations regarding formation of corrosive films
Appendix 3	Delayed hydride cracking (dhc)
Appendix 4	Erosion / corrosion
Appendix 5	Assessment on the evolution of a flaw in a class 1 Asme nuclear equipment
Appendix 6	Oxidation
Appendix 7	Thermal high cycle fatigue in piping system tees with leakage
Appendix 8	PNAEG 7 002 86 (Russian Code) / IAEA-EBP-WWER-08
Appendix 9	Delayed hydride cracking - RBMK-1500 NPP
Appendix 10	Intergranular stress corrosion cracking
Appendix 11	Irradiation induced dimensional and material property changes to the graphite
Appendix 12	Irradiation induced change of fuel channel length
Appendix 13	Guidance for application of the leak before break concept at Ignalina NPP RBMK-1500 reactors.
Appendix 14	Requirements for assessment of intergranular stress corrosion cracking damages in RBMK-1500 reactors
Appendix 15	RPV Cladding
Appendix 16	Pressurized Thermal Shock
Appendix 17	CANDU Feeder Piping



ANNEXES

ANNEX 1

RPV CLADDING (details)



APPENDIX 1 FATIGUE AND THERMAL FATIGUE

CONTENTS

- A1.1 Introduction, materials, service conditions**
- A1.2 Physical Description of the Mechanism**
- A1.3 Applicable Testing & Standards For Characterisation of Mechanisms**
- A1.4 Governing Codes & Specification For Application In Power Plants**
- A1.5 Research Possibilities To Improve Code & Standard and Gaps**
- A1.6 References**



Page intentionally left blank

A1.1 Introduction, Materials, Service Conditions

Fatigue is present as an active damage mechanism on structural components in all reactor types. It is considered in the design codes for different operational transients (ASME A and B levels (normal and upset conditions). Separate assessments may be made for local phenomena such as vibration loads. Table A1.1 provides a general overview of the affected components and materials.

Table A1.1 Overview of Fatigue-Affected Components and Materials

Reactor type	Component class	Materials	Fatigue phenomena
LWR (PWR, WWER)	Primary piping	Stainless steels Carbon steels	Thermal fatigue (LCF, HCF) Vibration fatigue (HCF)
	Vessel, flanges and penetrations	Carbon steels, Ni-based alloys	Thermal fatigue (LCF) Vibration fatigue (HCF)
	Internals	Stainless steel Ni-based alloys	
	Steam generator	Stainless steels Carbon steels	Thermal fatigue (LCF, HCF) Vibration fatigue (HCF)
PHWR (CANDU)	Steam piping	Stainless steels Carbon steels	Thermal fatigue (HCF) Vibration fatigue (HCF)
	Steam generator	Stainless steels Carbon steels	Thermal fatigue (HCF) Vibration fatigue (HCF)
AGR (steam pipe work)	Main steam piping	Stainless steel	Creep-thermal fatigue
	Reheat outlet	CrMoV	Creep-thermal fatigue
	Reheat inlet	Carbon steel	Thermal fatigue

A1.2 Physical Description of the Mechanism

Fatigue is the progressive structural change that occurs in materials subjected to cyclic stresses and strains that may result in cracks or fracture after a sufficient number of cycles. Fatigue damage is caused by the simultaneous action of cyclic stress, tensile stress and plastic strain. The cyclic stress starts the crack and the tensile stress produces crack growth. The process consists of three stages:

- initial fatigue damage leading to crack nucleation and crack initiation;
- progressive cyclic growth of a crack until the remaining un-cracked cross section of a part becomes too weak to sustain the loads imposed
- final fracture or collapse of the remaining cross section.

Fatigue cracks initiate and propagate from regions of strain concentration. Since components contain local strain concentration at welds, geometric discontinuities or flaws, these provide natural locations from which cracks can initiate and grow. The driving forces for fatigue include operational transients, but also vibration or localized cyclic thermal gradients. It is noted that the environment often plays a role in the initiation and growth process.

Reactor coolant components are subject to several different aging mechanisms, and the fatigue is one of the most significant [A1.1]. Locations known to experience fatigue on LWRs include:

- the surge and spray lines and several branch lines and nozzles (charging line, safety injection lines) experience significant low thermal fatigue caused by thermal stratification and cycling, and high cycle fatigue caused by striping;
- the bimetallic welds made with stainless steel filler metal experience low cycle fatigue damage caused by thermal expansion mismatch during heat-up and cool down transients, combined with corrosion sensitivity;
- the cast stainless steel piping experiences a low fatigue in the inclined nozzle of the safety injection line;
- the socket welds between instrument penetration lines and piping experience cracking caused by vibration fatigue;
- thermal sleeves experience cracking caused by vibration and thermal fatigue.

LWR primary system piping has not experienced ruptures in operation, except some small diameter piping that failed by vibration fatigue. The potential failure consequences are small, intermediate or large break loss of coolant accident, which can lead to severe accidents.

Assessment of fatigue damage is typically performed in accordance with procedures given in structural design and operation assessment codes. There are three main options:

- 1) exclusion of fatigue damage by demonstrating that cyclic loads are below a threshold
- 2) evaluation of the cumulative usage factor in relation to fatigue design curves
- 3) flaw evaluation, i.e. assessment of fatigue crack growth and demonstration of LBB.

A1.3 Applicable Testing & Standards for Characterisation of Mechanisms

Laboratory fatigue tests can be classified as crack initiation or crack propagation. In crack initiation testing, specimens are subjected to the number of controlled loading cycles required for a fatigue crack to initiate and grow to a critical size or fracture.

In crack propagation testing, fracture mechanics methods are used to determine the crack growth rates of pre-existing cracks under cyclic loading. Fatigue crack propagation test can be performed in environment (corrosion fatigue).

Some standard testing methods are available [A1.2]. ASTM E606 is the standard practice for strain-controlled fatigue test. This practice covers the determination of fatigue properties of nominally homogenous materials by the use of test specimen subjected to uniaxial forces. No restrictions are placed on environmental factors such as temperature, pressure, humidity, medium and others provided they are controlled throughout the test and are detailed in the data report.

ASTM E 466 is the standard practice for conducting force controlled constant amplitude axial fatigue tests. The axial force fatigue test is used to determine the effect of variations in material, geometry, surface condition and stress on the fatigue resistance of metallic materials subjected to direct stress for relatively large number of cycles. For thermo-mechanical fatigue, a code of practice has been developed in the form of CEN Workshop Agreement.

ASTM E647 is the standard test method for measuring of fatigue crack growth rates. This method covers the determination of fatigue crack growth rates from near-threshold to K_{max} controlled instability. Results are expressed in term of the crack tip stress intensity factor range, defined by the theory of linear elasticity. This test method is divided into two main parts. The first

part gives general information concerning the recommendations and requirements for fatigue crack growth rate testing. The second part is composed of annexes that describe the special requirements for various specimen configurations, special requirements for testing in environments and procedures for non visual crack size determination. In addition, there are appendices that cover techniques for calculating da/dN , determining fatigue crack opening force and guidelines for measuring the growth of small fatigue cracks.

Feature tests i.e. tests involving simulated fatigue performed under laboratory conditions, have an important role to play for verification of assessment procedures and for establishing transferability of standard fatigue curves to component-life situations. In case of NESC-Thermal Fatigue project five cases have been brought together for thermal fatigue, including digital records of the induced temperature distributions, as well as calculated thermal stresses from reference finite element calculations, where available. Detailed information from each test has been collected in a dedicated report [A1.3].

It is noted that AREVA and CEA have the FATHER program on a large scale metallic tee (data is restricted) and that further feature testing is on-going at CEA, EDF, JRC and Serco. The OECD IAGE group has also proposed to develop a database of component fatigue tests.

A1.4 Governing Codes & Specification for Application in Power Plants

Design of the reactor coolant system piping components is based on the expected number of transients during the plant operation. The fatigue analyses serve as a basis for verification of adequate margin of safety against the initiation of a fatigue crack.

The kinetics of fatigue damage experienced by components of nuclear power facilities with light water reactors is governed by a number of simultaneous processes:

- unsteady mechanical and thermal stresses loading in transients, alternating in a general case with steady-state conditions and giving rise to a series of loading half-cycles with various amplitudes and maximum stresses, which are separated by steady-state loading conditions with possible coincident vibrations;
- variations of metal condition for in-service conditions (loss of ductility due to aging, coolant effects and irradiation, hardening or softening under cyclic elastic-plastic loading, radiation hardening, formation of oxide films with properties dissimilar to those of the metal);
- corrosive and mechanical interaction between coolant and metal.

For all the above processes is difficult to produce integrated models based on empirical data for the accumulation of fatigue and corrosion fatigue damage in the component metal, with allowance, operational factors and their interaction. The equations employed to assess the condition of components in terms of cumulative fatigue damage are modified fatigue curve equations of Manson-Coffin-Langer type, in which the essential data on the metal are confined to mechanical characteristics under static tension. These equations determine the durability at the time of crack initiation and make allowance for operating conditions.

The fatigue analyses methods from the ASME codes section III and XI [A1.4], [A1.5] are widely used in the US and internationally, and have formed a basis for several other codes. Recent proposed developments (revision of the fatigue strength curves and margins, explicit inclusion of environment effects and possibility to use apply an "initiation + crack growth approach") can have wide implications in the industry.

The German practice is described in the KTA Standard [A1.6]. The procedure is principally equivalent to the ASME Code. The fatigue design curves in this standard are identical those presently in the ASME Code up to 10^6 cycles.

The French design rules presented in the RCC-M [A1.7] and RCC-MR [A1.8] (for high temperature) were originally derived from ASME fatigue analysis methods, but have added different aspects, some directly concern fatigue analysis of piping systems:

- crack like defect fatigue analysis method (RCC-M appendix ZD);
- Ke optimization for stainless steel piping (RCC-M B3650);
- combination of finite element approaches and piping rules (RCC-M appendix ZE).

In Japan some dedicated standards have been developed for low and high cycle fatigue [A1.9] and also for thermal fatigue [A1.10], [A1.11].

In the case of WWER NPPs the design for most of Class 1 components followed the Soviet norms [A1.12]. Recently the Soviet norms and ASME III were used.

In Europe, there is now EU directive on pressure equipment safety (PED = Pressure Equipment Directive). Components subject to ionizing radiation i.e. on NPPs are not formally subject to the PED. However in some cases compliance with its requirements and those of the related harmonized standards such as EN13445 are being requested by safety authorities.

The thermal fatigue is not a major aging mechanism for the main coolant piping but could be for surge, spray and branch lines. The surge and spray lines and branch lines are made of austenitic stainless steel in all PWRs. Licensees were informed [A1.13] of unexpected surge line movements in the plant in an NRC Information Notice 88-80, followed by Bulletin 88-11 [A1.14], [A1.15]. The welds joining the austenitic stainless steel piping and ferritic piping are called dissimilar metal welds. These welds experience thermal fatigue damage. A principal source of fatigue damage in the pressurized surge line and nozzles is the thermal stresses associated with design-basis thermal transients and the thermal stratification. No specific standard are dedicated to thermal fatigue, and the evaluation are performed in the general fatigue framework of already mentioned standards by means of cumulative usage factors.

Two French nuclear codes include flaw assessment procedures: the RSE-M code [A1.16] and RCC-MR [A1.17]. An important effort of development of these analytical methods has been made for the last 10 years in the frame of collaboration between CEA, EDF and AREVA-NP, and in the frame of R&D actions involving CEA and IRSN. The calculation of fracture mechanics parameters and in particular the stress intensity factor K_I and the J integral has been widely developed for industrial configuration. In the R6/rev.4 British procedure [A1.18] the limiting condition of a structure is evaluated by reference to two criteria, fracture and plastic collapse. Structural integrity relative to the limiting condition is evaluated by means of a Failure Assessment Diagrams (FADs). These procedures require assessment points to be plotted on the FAD, the location of each assessment point depending upon the applied load, flaw size, material properties, etc. Another Fitness-for-Service procedure [A1.19] defines fitness-for-service as the ability to demonstrate the structural integrity of an in-service component containing a flaw or damage. It is a result of a need for standardization of the fitness-for-service assessment techniques for pressurized equipment.

A1.5 Research Possibilities to Improve Code & Standard and Gaps

The following areas have been identified:

Load evaluation (particularly for thermal and vibration fatigue)

- Development of more reliable methods for determining thermal fatigue loading spectra for fast, turbulent mixing time: a) transfer functions from mock-ups; b) CFD and LES simulation codes;
- Methods to define areas concerned by fluctuations for establishing ISI requirements;

- Optimization of load monitoring procedures for vibration fatigue.

Strain evaluation and fatigue crack initiation

- Strain evaluation through elastic and plastic correction for stainless steels on account of the very complex cyclic stress-strain curve;
- High cycle fatigue curve from 10^5 to 10^9 cycles, and the question of endurance limit existence for stainless steel under constant or random loads;
- Mock-up tests confirm all the methodologies;
- Improved understanding of the effect of potentially detrimental factors on fatigue resistance (crack initiation): un-flushed weld, counter-bore surface finished, mean strain or stress, etc.;
- More fundamental work on surface behaviour under high cycle fatigue loads: crack initiation criteria and corresponding key parameters, fatigue crack growth of small cracks (0.1 to 3mm), effects of detrimental parameters, etc.
- Develop multiscale approaches to predict strain localisations. These shall include multiscale features, such as for example grains, inclusions, grain boundaries, dislocations etc.

Crack growth analysis

- Fatigue crack growth procedure for thermal cycling with one crack;
- Determining the consequences of periodic under/over loads; of networks of small cracks and of mean stress or strains.

Others

- Procedures for non-cylindrical component and nozzle corners in particular: local loads, strain evaluation, mean stress or strain definition, critical crack size in forged stainless steel nozzle;
- Improved ISI performance requirements, mainly for thick stainless steel with welds or cast pipe;
- Integration of advanced fatigue assessment approaches in probabilistic codes;
- Assessment method and safety factor differences between class 1, 2 and 3 components;
- Comparison nuclear and non-nuclear codes for fatigue assessment.



A1.6 References

- [A1.1] IAEA-TECDOC_1361 Assessment and management of aging major nuclear power plant components important to safety –Primary piping in PWRs, IAEA , July 2003
- [A1.2] Annual book of ASTM standards, Section three, Metals test methods and analytical procedures, Vol. 03.01, ASTM international, 2007
- [A1.3] NESCF Report “Database of Component Mock-Up Experiments”, NESCF (04) 08 Rev.1, June 2005
- [A1.4] ASME ASME Boiler and Pressure Vessel Code, Section III Components – Rules for Construction of Nuclear Power plant, American Society of Mechanical Engineers, New York (2004)
- [A1.5] ASME ASME Boiler and Pressure Vessel Code, Section XI – Rules for In -service Inspection, (2004)
- [A1.6] KTA 3201 Part2 Components of the Reactor Coolant Pressure Boundary of Light Water reactors, Design and Analysis, June 1996
- [A1.7] RCC-M French Design and Construction Rules for Mechanical Components of PWR Nuclear Islands
- [A1.8] AFCEN RCC-MR Design and Construction Rules for Mechanical Components of FBR Nuclear Islands and High Temperature Applications, Tour Framatome, F92084 Paris La Defense Cedex, Edition 2002
- [A1.9] JSME Technical Standard for Construction of NPP Components, The Japan Society of Mechanical Engineers, 2003
- [A1.10] JSME Guidelines for evaluation of High Thermal Fatigue of Pipe, The Japan Society of Mechanical Engineers, 2003, S017
- [A1.11] JSME Guidelines for Practising Technical Standard for High Cycle Thermal Fatigue, The Japan Society of Mechanical Engineers, 2003
- [A1.12] PNAE Rules for strength analysis of components and pipelines of nuclear power installations, PNAE G-7-002-86, M., Energoatomizdat; 1989.
- [A1.13] EA/CSI/R(2005)8 Thermal Cycling in LWR Components in OECD-NEA member Countries, CSNI Integrity and aging group, JT00187965, 2005
- [A1.14] USNRC Safety Injection Piping Failure, USNRC Bulletin 88-01 (1988)
- [A1.15] USNRC Pressurizer Surge Line thermal Stratification, USNRC Bulletin 88-11 (1988)
- [A1.16] AFCEN RSE-M code. Rules for In-service Inspection of Nuclear power Plant components. Paris 1997, Edition +1998, 200 and 2005
- [A1.17] RCC-MR Design and Construction Rules for Mechanical Components of FBR Nuclear Islands and High Temperature Applications, Tour Framatome, Appendix A16, Tome I, vol.Z 2007 Edition
- [A1.18] R6-Revision 4 Assessment of the integrity of structures containing defects. Barnwood, Gloucester: British Energy Generation Ltd; 2001.
- [A1.19] API 579 Recommended Practice for Fitness-for Service, American Petroleum Institute, January 2000



APPENDIX 2 CONSIDERATIONS REGARDING FORMATION OF CORROSIVE FILMS

CONTENTS

- A2.1 Introduction**
- A2.2 Carbon and martensitic steels**
- A2.3 Nickel alloys**
- A2.4 References**



Page intentionally left blank

A2.1 Introduction

The films formed by corrosion of the structural materials contain a variety of oxides and hydroxides as a function of chemical composition of the materials, having different thicknesses and porosities depending on coolant oxidation conditions.

In formation process of the corrosive layers on surface two mechanisms exists: one as result of physic-chemical reaction between fluid and metallic ions and other of the corrosion products deposition, the both depending on alloys nature and chemical composition of the environment.

A2.2 Carbon and Martensitic Steels

Under highly reducing ($O_2 < 0,1 \text{ ppm}$) and alkaline ($\text{pH} = 10.2 \times 10^8$) conditions and at temperatures more than 180°C , the magnetite film (Fe_3O_4) is the major corrosion product formed on carbon and martensitic steel, by Schikorr's reaction [A2.1]



and



The magnetite solubility has an important role in formation mechanism of the oxide layers. It depends on electrochemical potential of the solution, which depends on the solution pH, the concentration of H_2 (D_2), O_2 , Cl^- and temperature [A2.2].

By analysis complementary methods was evidenced that the magnetite, formed into composition very close by stoichiometric report, ensures from beginning an adherent and protective oxide film.

The protective oxide film confers the metallic interface with resistance to oxidation and hydratation, phenomena, which appear at fluid/metal, interface and generate corrosion products as different oxides, hydroxides and oxi-hydroxides of iron and alloying elements from steels.

Magnetite evolution by iron reaction with aqueous environment conducts to thinness of the component walls and to an excessive transport of the crud in system.

The corrosion mechanism of these materials in alkaline environment at high temperature consists in the formation of two overlapped layers of iron oxide compounds and was assume to conform to the Potter and Mann model [A2.3].

Initially, an amorphous oxide film forms, but magnetite nuclei develop on this film and increase without a preferential orientation, conducting after certain time to formation of thin film with fine granulation.

This interior oxide layer is a compact, continuous, adherent and fine-grained (granule dimension being $0.05 \div 2 \mu\text{m}$) oxide. He grows into the metal at the metal-oxide interface and occupies the volume of the corroded metal.

In the second stage, over this internal film, which is in direct contact with the metal, the magnetite crystals develop at oxide/metal interface, simultaneous with his development at oxide/solution interface, forming a film with a bigger granulation. Thus the corroded iron that cannot precipitate as the inner layer diffuses through it as Fe^{2+} ions to the oxide-coolant interface. There, if the coolant already is saturated in dissolved iron, the emerging Fe^{2+} will tend to supersaturate the fluid boundary layer and provoke the precipitation of the outer oxide layer.

The magnetite of the outer layer forms coarser crystals, usually octahedral or tetrahedral habit with sizes of the order of a few micrometers ($0.05 \div 2 \mu\text{m}$).

Therefore, the exterior oxide layer is formed by re-deposition of iron ions from solution. He is no continuous, no uniform and no adherent, but his growth is controlled by iron solubility and concentration in solution.

The interior oxide layer being microcrystalline and containing alloying elements as Cr, from the ground metal, can form complex oxides with low solubility, but the exterior oxide layer from big magnetite crystals (about 1µm) can contain Mn or Ni.

The proportions of internal and exterior layers are roughly 50-50 [A2.4].

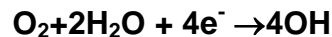
The kinetics of the formation and the growth of the magnetite protective oxide layer was considered initially as a parabolic law, followed by a cubic or logarithmic law. But, because the fortuitous character of the second magnetite layer, the steel corrosion in aqueous environment can be under a mixed control, thus that the kinetics of oxide film growth is of parabolic form ($y=kx^n$) and logarithmic form ($y=k \ln x-C$) in the first period, after that it is considered probable that a linear growth law ($y=Ax+B$) follows.

The corrosion rate decreases with the growth of the oxide thickness, being in correlation with the magnetite solubility, which depends strongly on water chemistry.

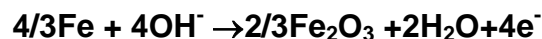
Thus, the isothermal laboratory corrosion experiments have shown that, in contaminated environment with Cl⁻ (>0.5ppm) and high concentration of O₂ (100÷500ppm), the corrosion rate increases and duplex, porous and no adherent magnetite films are formed.

When the concentration of these anions exceeds the permissible limits the magnetite (Fe₃O₄) will transform into hematite (Fe₂O₃) that, being easily detachable, will allow the exposure of metallic under layer at very high subsequent corrosion.

In water with oxygen, the corrosion potential of carbon and martensitic steel is controlled by cathodic reaction of oxygen reduction, and it is in the range of stability of Fe₂O₃:



and



The morphology and the protective properties of the oxide film depends on the oxygen and Cl⁻ concentration, but the parameter, which controls the corrosion, is oxygen diffusion.

The corrosion process is characterized by the formation of some inhomogeneous corrosion product layers at the corroding surface, presenting active pits.

A2.3 Nickel Alloys

In the case of nickel alloys (Incoloy-800) besides Fe oxides are formed Cr and Ni oxides, as well as complex oxides of Fe, Cr or Ni (FeCr₂O₄ and NiFe₂O₄).

The exterior side of the corrosive films, formed on Incoloy-800 alloy, consists from magnetite particles deposits and of iron oxides with a tendency for increasing in the first time of nickel content and then of the chromium content.

Thus, in the beginning, an exterior layer enriched in iron and nickel oxides (FeO, FeOOH, Fe₂O₃, Fe₃O₄, NiO and NiFe₂O₄) forms.

Formation takes place progressively. Oxidation of the chromium, due to oxygen diffusion in the alloy bulk, occurs preferentially and a thin, nonporous and homogenous oxide film is uniformly distributed on the surface, forming a barrier to transport of other ion species at the oxide/oxidizing surface. This internal oxide layer contains Cr₂O₃ and Fe Cr₂O₄.

The increase of the barrier oxide film takes place by oxygen diffusion to interior and chromium diffusion to exterior, and the increasing rate can be described by parabolic rate law:

$$\frac{dw_p}{dt} = \frac{k_p}{w_p} \quad \text{Eq. A2.1}$$

where

w_p is the metal weight used in barrier oxide film formation in mg/dm^2

k_p is the parabolic rate constant in $\text{mg}/\text{dm}^2 \cdot \text{month}$

The growth of the barrier non porous oxide film, described by above equation, decreases with the increase of the exposure time and will begin to be prevalent the increase of the exterior oxide film richly in Ni-Fe, which contains also, quantities relatively small of Cr, Mn and Mo. While the exposure time increases, the oxidation rate depends linear of this and takes place after equation:

$$\frac{dw_1}{dt} = k_1 \quad \text{Eq. A2.2}$$

where

w_1 = metal weight implicated in non-barrier oxide film in mg/dm^2 ,

k_1 = linear rate constant in $\text{mg}/\text{dm}^2 \cdot \text{month}$.

The stability of the barrier oxide film decreases with the increase of its thickness, caused either of mechanical tensions generated in oxide during of its thickening or due to transformation reaction at barrier/no barrier interface.

The oxidation varies linearly with the exposure time but after long exposure times. Because of the thickening of the oxide film, equilibrium is established between the increase of the interior nonporous oxide layer and its transformation rate in exterior porous oxide layer.

The corrosion process is dependent on a lot of material parameters (surface state, metallurgical structure due to some thermal treatments, as well as existence of some mechanical tensions), and depends by the water chemistry (pH, chemical impurities concentration).

In normal conditions of water chemistry ($\text{pH}=10.2 \div 10^8$ and chemical impurities concentration under maximum permissible values), Incoloy-800 alloy corrosion is uniformly and the double-layers oxide films are protective and adherent.

EIS determinations showed that these films correspond to a homogeneous model with two adherent oxide layers, the internal oxide layer being thinner ($C_{\text{int.}} > C_{\text{ext.}}$) and more protective ($R_{\text{int.}} > R_{\text{ext.}}$).

A2.3 References

- [A2.1] S.Velmurugan, A.L. Rufus, V.S. Sathyaseelan T.V. Padma Kumari, Nuclear Energy, 34(2), (1992).
- [A2.2] F.H. Sweeton, C.F.Jr.Baes, „ The Solubility of Magnetite and Hydrolysis of Ferrous Iron in Aqueous Solutions at Elevated Temperatures”, J. Chem. Thermodynamic, vol.2, (1995).
- [A2.3] E.C.Potter, G.M.W.Mann, “Oxidation of Mild Steel in High Temperature Aqueous Systems”, Proc.1st.Int.Cong.Metallic-Corrosion, London.
- [A2.4] N.Arbeau, H.Allsop, „Kinetics of Corrosion Product Release from Carbon Steel Corroding in High Temperature, Lithiated Water”, Corrosion NACE 54, no.6 (1998).



APPENDIX 3 DELAYED HYDRIDE CRACKING (DHC)

CONTENTS

- A3.1 Physical Description of Mechanism**
- A3.2 Service Conditions / Environment**
- A3.3 Materials**
- A3.4 Susceptible Components**
- A3.5 Applicable testing standard(s) for characterising mechanism**
- A3.6 Governing Codes and Assessment Procedures for NPP integrity and lifetime assessment**
- A3.7 Current research programmes**
- A3.8 Knowledge gaps**
- A3.9 Future research requirements**
- A3.10 References**



Page intentionally left blank

A3.1 Physical Description of Mechanism

The time dependent mechanism, called Delayed Hydride Cracking (DHC) is a sub-critical crack growth mechanism occurring in zirconium alloys as well as other hydride-forming materials that requires the formation of brittle hydride phases at the crack tip and the sequent failure of that hydride resulting in a crack extension. When a tensile stress is applied, hydrogen accumulates by diffusing up the stress gradient at the flaw tip where a hydride forms. The hydride grows as more hydrogen accumulates and, if the critical conditions of hydride size, maximum stress and critical strain are reached, the hydride cracks, and the flaw extends by the length of the hydride. The process is then repeated, Figure A3.1.

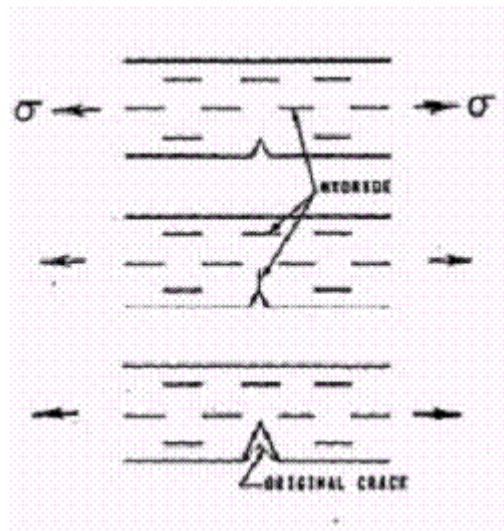


Figure A3.1 A schematic illustration of a single step in DHC starting with a notch under stress, (top), hydride precipitation at the notch (middle) and fracture of hydride and crack extension from the notch (bottom).

A3.2 Service Conditions / Environment

The conditions responsible of DHC involve: mechanical state of stress, temperature, hydrogen concentration exceeding the limit of solubility.

The phenomenon of cracking can be generally described by the dependence of the crack growth rate or crack velocity on the applied stress intensity factor. The general shape of such a relationship has been shown to be similar to that demonstrated in many forms of environmentally assisted cracking [A3.1], [A3.2].

At stress intensities below a threshold, K_{IH} , cracks do not grow even though a quantity of hydride may accumulate at a crack tip under stress. In DHC, the transition to the plateau velocity portion of the velocity vs. K_I curve is quite abrupt [A3.3] and then the velocity does not change significantly increasing K_I until the applied K_I approaches the fracture toughness corresponding to the initiation of unstable fracture for the material under test, Figure A3.2.

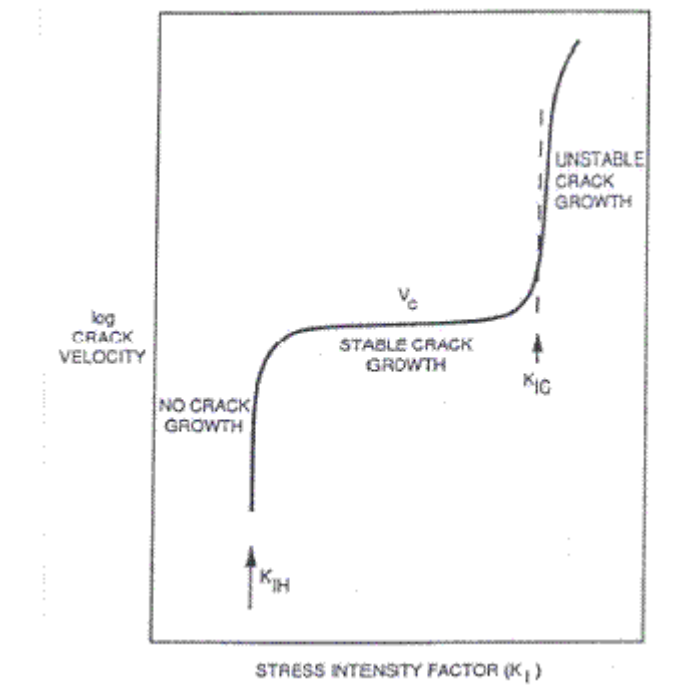


Figure A3.2 A schematic representation of the relationship between crack velocity and stress intensity factor exhibited by the DHC phenomenon.

A3.3 Materials

Zirconium Alloys (Zy-4, Zr-2.5%Nb)

A3.4 Susceptible Components

- CANDU, RMBK Pressure tubes
- PWR, BWR, CANDU Zircaloy-4 fuel claddings

DHC was the cause of leakage of twenty tubes out of 780 Zr-2.5Nb pressure tubes of CANDU plants at Pickering Unit 3 and 4, [A3.4], the main cause being the high residual stresses (up to 700MPa) in the rolled-joint areas. The cracks initiated on the inner surface and grew radially and axially in a series of bands.

The Zr-2.5Nb partly re-crystallized pressure tube of a RMBK reactor cracked in a similar way, but DHC initiated on the outside surface. Twenty tubes out of 20000 tubes leaked due to DHC phenomenon in the first years of operation at Kursk and Chernobyl reactors, [A3.5].

This step-wise progression may leave striations on the fracture surface corresponding to each step of crack propagation that can often be observed with a low power light microscope, Figure A3.3.

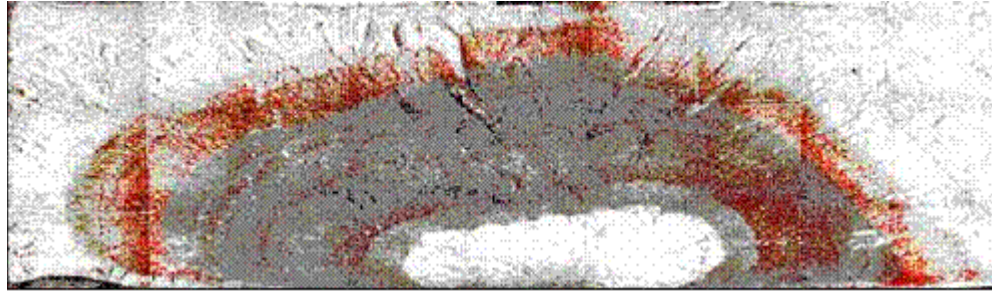


Figure A3.3 Through-wall crack in a CANDU Zr-2.5 Nb pressure tube, showing oxidized crack growth bands. The crack initiated at the inside surface just inboard of the rolled joint.

In some Zircalloy nuclear fuel cladding used in BWR reactors, hydride cracking is strongly implicated in long splits that allowed substantial leakage of fission products [A3.6]. The cracks grow through-wall and may be over 1 m long. The fractures are characterized by brittle regions in “striations” or “chevrons”, with the crack front often leading towards the outside surface of the cladding [A3.7].

A3.5 Applicable Testing Standard(s) for Characterising Mechanism

ASTM E 399-90–“Standard Test Method for Plane-Strain Fracture Toughness of Metallic Materials” (for CT specimen preparation)

A3.6 Governing Codes and Assessment Procedures for NPP Integrity and Lifetime Assessment

- R.Choubey – DHC Axial Velocity Test Procedure for IAEA Round-Robin Test Program, AECL, Report No. FC-IAEA-02, T1.20.13-CAN-27363-20, Nov. 1998;
- V.Grigoriev, R.Jakobsson – DHC Axial Crack Velocity Measurements in Zirconium alloy Fuel Cladding. Pin-Loading Tension (PLT) Test Procedure for IEAEA Round Robin Test Program, Studsvik/N-05/281, 2005

A3.7 Current Research Programmes

- AIEA Vienna CRP - on “Hydrogen and Hydride Induced Degradation of the Mechanical and Physical Properties of Zirconium-based Alloys” [A3.8]
- IAEA-CRP on “Delayed Hydride Cracking (DHC) of Zirconium Alloy Fuel Cladding”;
- Romanian National Fuel Channel R-D Programme

A3.8 Knowledge Gaps

- establishment of DHC temperature limit

A3.9 Future Research Requirements

- DHC temperature limit measurements on Zircaloy-4 claddings

A3.10 References

- [A3.1] DUTTON, R., NUTTALL, K., PULS, M.P., SIMPSON, L.A., "Mechanism of Hydrogen-Induced Delayed Hydride Cracking in Hydride Forming Materials", Metall. Trans.A, 8A, (1977), 1553–1562.
- [A3.2] COLEMAN, C.E., "Cracking of Hydride-forming Metals and Alloys", Comprehensive Structural Integrity, Elsevier, Eds. I. Milne, R.O. Ritchie and B. Karihaloo, 2003, Chapter 6.03, pp.103–161.
- [A3.3] SIMPSON, L.A., PULS, M.P., "The Effects of Stress, Temperature and Hydrogen Content on Hydride-Induced Crack Growth in Zr-2.5Nb", Metall. Trans.A, 10A, (1979), 1093–1105. 16
- [A3.4] Perryman, E.C.W., Pickering Pressure Tube Cracking Experience, Nucl. Energy, 17 (1978), pp.95-105
- [A3.5] Platanov P.A., Ryazantseva, A.V., Saenko, G.P, Knizhnikov, Y.N., Viktorof, V.F., The study of the cause of cracking in zirconium alloy fuel channel tubes, Poster paper at ASTM Zirconium in the Nuclear Industry-8th International Symposium
- [A3.6] Jonsson, A., et al. "Failure of a barrier rod in Oskarshamn" in Fuel in the '90's, International Topical Meeting on LWR Fuel Performance, Avignon, France, ANS and ENS, (1991), 371-377.
- [A3.7] Lysell, G. and Grigoriev, V., "Characteristics of axial splits in failed BWR fuel rods", 9th International Symposium on Environmental Degradation of Materials in Nuclear Power Systems – Water Reactors, AIME-TMS, (1999), 1.169-1.175.
- [A3.8] IAEA-TECDOC-1410, Delayed hydride cracking in zirconium alloys in pressure tube nuclear reactors, October 2004



APPENDIX 4 EROSION/CORROSION

CONTENTS

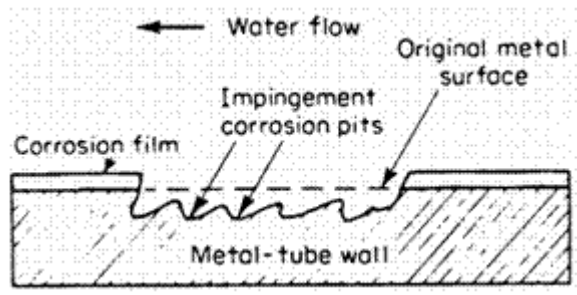
- A3.1 Physical Description of Mechanism**
- A3.2 Service Conditions / Environment**
- A3.3 Materials**
- A3.4 Susceptible Components**
- A3.5 Applicable testing standard(s) for characterising mechanism**
- A3.6 Current research programmes**
- A3.7 Knowledge gaps**
- A3.8 Useful Resource Documents**



Page intentionally left blank

A4.1 Physical Description of Mechanism

Erosion/Corrosion



Erosion-corrosion is a well-understood cause of degradation in pipes. It causes loss of thickness in pipe walls, resulting in degradation of pipe components in carbon and low alloy steel lines until they no longer operate safely. For this reason there is widespread concern that erosion-corrosion should be monitored. It has become clear that erosion-corrosion occurs when a flow of water or wet steam erodes or destroys the oxide layer that protects the surface of the pipe. This leads to the formation of new oxide and dissolution of metal. The following parameters govern the erosion-corrosion process:

- thermo-hydraulic conditions in the fluid,
- water chemistry,
- chemistry of the pipe material,
- geometry of the component,
- exposure time.

Figure A4.2 illustrates Schematic the effect of flow velocity on erosion-corrosion rate:

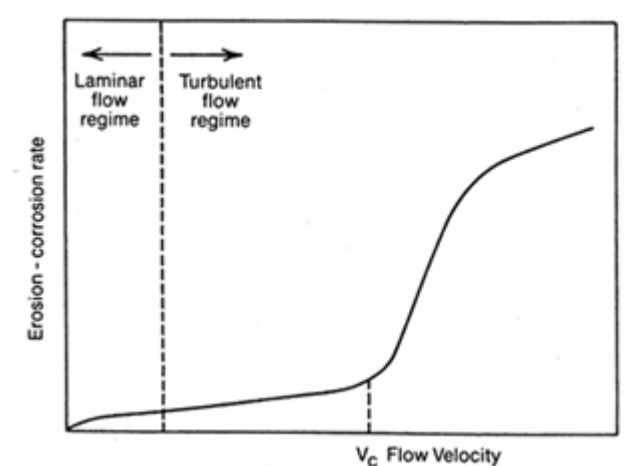


Figure A4.2 Schematic showing the effect of flow velocity on erosion-corrosion rate

Relationship between flow velocity, v , and erosion-corrosion rate, w , may be written as:

$$w = kv^a \quad \text{Eq. A4.1}$$

where 'k' and 'a' are constants that depend on the system.

The exponent 'a' varies between 0.3 (laminar flow) and 0.5 (turbulent flow) occasionally reaching > 1.0 for mass transfer and fluid shear effects. For mechanical removal of oxide films (spalling), the fluid shear stress at the surface is important, and $a > 1.0$ (may reach 2 - 4). Turbulent flow regime for $V < V_c$ is sometimes called Flow-Assisted Corrosion regime.

A4.2 Service Conditions / Environment

Erosion/Corrosion found in aqueous solutions. If fluid contains suspended solids, erosion-corrosion may be aggravated. Vulnerable equipment is that subjected to high-velocity fluid, to rapid change in direction of fluid, to excessive turbulence and when the contacting fluid has a very thin boundary layer and high mass transfer rates.



A4.3 Materials

Most metals/alloys are susceptible to erosion e.g.: Stainless steels, Carbon Steels.

Attack occurs when film cannot form because of erosion caused by suspended particles (for example), or when rate of film formation is less than rate of dissolution and transfer to bulk fluid.

A4.4 Susceptible Components

Single-phase erosion/corrosion: seen in high pressure feedwater heaters, steam generator inlets, feedwater pumps, and CANDU feeders.

Two-phase erosion/corrosion: more widespread in steam extraction piping, cross-over piping (high pressure turbine to moisture separator), the steam side of feedwater heaters, and CANDU feeders.

A4.5 Applicable Testing Standard(s) for Characterising Mechanism

G 40-02 Standard Terminology Relating to Wear and Erosion ASTM

A4.6 Current Research Programmes

Theoretical knowledge of EROSION/CORROSION mechanism

A4.7 Knowledge Gaps

Understanding of the feeder erosion/corrosion mechanism



A4.8 Useful Resource Documents

- [A4.1] INTERNATIONAL ATOMIC ENERGY AGENCY, "Nuclear power plant life management processes: Guidelines and practices for heavy water reactors", IAEA-TECDOC-1503, IAEA, Vienna (2006), ISSN 1011-4289.
- [A4.2] Cojan, M., Radu, V., Parvan, I., Lucan, D., Florescu, Gh., "Application and importance of aging management in CANDU 6 PLIM / PLEX programs", paper presented at the CNE 2004 – The 7th Regional Energy Forum – FOREN 2004 "Sustainable Energy Development and European Integration", Neptun, Romania, 13-17 June 2004.
- [A4.3] Burrill, K. A., Turner, C. W., Control of Reactor Inlet Temperature Rise in CANDU, Second International Steam Generator and Heat Transfer Conference, Toronto, 1994.
- [A4.4] Burrill, K. A., Modelling Flow – Accelerated Corrosion in CANDU, AECL – 11397, COG – 95-384, 1995.



APPENDIX 5 ASSESSEMENT ON THE EVOLUTION OF A FLAW IN A CLASS 1 ASME NUCLEAR EQUIPMENT

CONTENTS

- A5.1 Introduction**
- A5.2 Purpose and Scope**
- A5.3 Analytical Approach**
- A5.4 Analysis and Results**
 - A5.4.1 Analysis*
 - A5.4.2 Flaws*
 - A5.4.3 Stress Data*
 - A5.4.4 Stress Intensity Factory, K_I*
 - A5.4.5 Flaw Growth Calculation*
 - A5.4.6 Material Fracture Toughness*
- A5.5 Summary and Conclusions**
- A5.6 References**



Page intentionally left blank

A5.1 Introduction

This appendix addresses an evaluation of the flaws (weld indication) at PZX found during the inaugural inspection of the Cernavoda NPP#2 Pressurizer. All the indications have been evaluated based on the procedure in ASME Code Section XI. From the analysis, it has been that all the flaw is stable and grows of the flaw over the service transients is small. It is concluded that these indications are acceptable for service.

A5.2 Purpose and Scope

A 3D finite element model was generated for the lower head/heater nozzle/shell assembly and used for Stress Analysis under the Level A to D and Hydro test. Stress data obtained from analysis were used for crack growth analysis and calculation of maximum stress intensity factors for the weld indications at "PZX".

Based on the UT reports for PZX, all the indications were assessed using the acceptance standards stipulated in ASME Code Section XI (IWB-3500). For the indications exceeding the ASME Code acceptance standards, analytical evaluations were performed based on the procedure in ASME Code Section XI (IWB-3600) [A5.1]

End-of- life size of these indications were determined based on crack growth analyses. Maximum S.I Factors for these indications with end-of-service sizes were calculated and compared with ASME Code Compliance.

A5.3 Analytical Approach

Level A to D transient conditions for the pressurizer were specified in the Cernavoda U#2 NPP PHT Design Manual [A5.2]. Surface heat transfer coefficients for these transients were determined for subsequent Thermal and Structural Analyses.

A 3D finite element model was generated for the Lower Head/Heater Nozzle/Shell Assembly and is shown in Figure A5.1.

Thermal, Structural & Fatigue and Crack Growth Evaluation Analyses have been finalized using Ansys-CFX Program, [A5.3] and FlawEvo Program (an Ansys Macro), [A5.4].

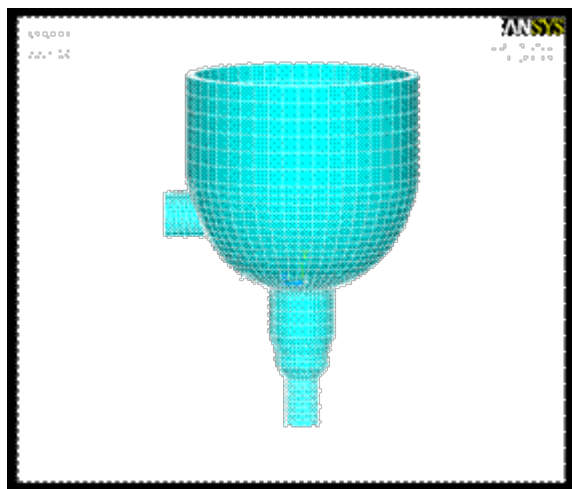


Figure A5.1 The simplified geometric model



For the Lower Head/Heater Nozzle/Shell Assembly Model, Stress Analysis was performed based on the transients conditions provided in the Design Manual [A5.2]. Thermal Transients Analysis was used to obtain temperature distributions for the model under different Level A, B, C & D Transients.

All transients and tests considered in Level A & B analysis are listed in Table A5.1. In addition to of Level A & B transients listed, hydro test (it bounds leak test) should be considered for flaw growth calculation.

Level D Condition is bounded by Level C Condition.

Table A5.1 Transients and Tests considered

Item	Name	No. cycles
1.	Heatup & Cooldown	250 Level A & B
2.	Startup & Shutdown	1000
3.	Power Manoeuvring	10000
4.	Loss of Feedwater from 100% Power	100
5.	Reactor Trip from 100% Power	500
6.	Loss of Class IV Power from 100% Power	50
7.	Loss of Regulation (Reactor Overpower)	200
8.	Turbine Trip	100
9.	Stepback	500
10.	Pressurizer Startup During Commissioning	50
11.	Emergency Over pressurization	1 Level C
12.	Crash Cooldown	15 Level C
13.	Loss of Coolant	1 Level D
14.	Steam Line Failure	1 Level D
15.	System Hydro test	20

A5.4 Analysis and Results

A5.4.1 Analysis

The analysis is carried out by creating a table from the UT inspection report that determines indications aspects ratios and compares them to the allowable parameters [A5.1]

A5.4.2 Flaws

There are 17 planar indications reported in [A5.5], as illustrated in Figure A5.2. All of the indications are in the weld material.

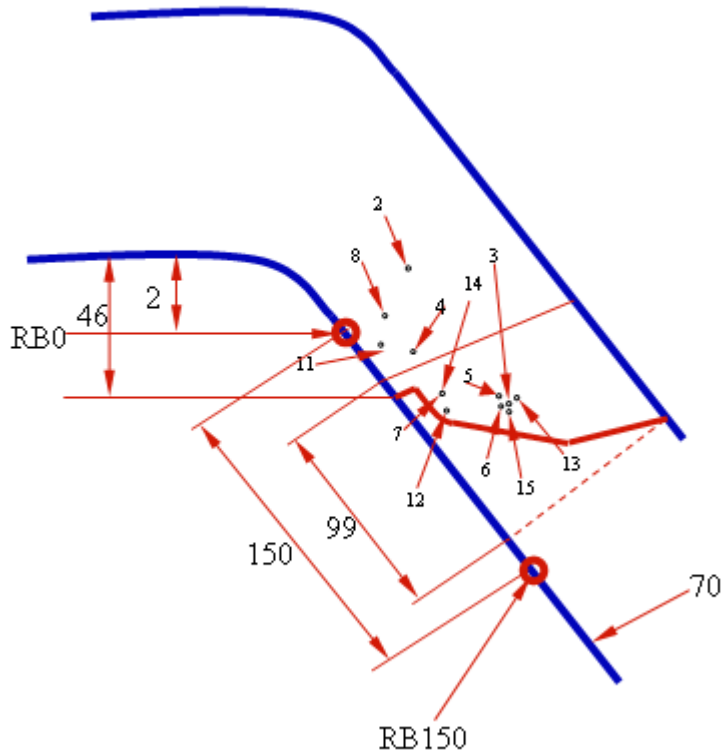


Figure A5.2 Orientation of Indications

Two of these indications have an amplitude result that exceed -6 dB, for which vertical extent data of the indications is given. The 2 indications are compared to the allowable planar flaws of Table IWB-3512 [A5.1]), and presented in Table A5.2. The second combination of indications is not acceptable.



Table A5.2

Indications Summary

Indication Number	Amp	Left end A	Right end A	Defect Length (mm)	Defect Vertical Extent (mm)	Defect Depth from OD (mm)	t (mm)	a (mm)	l (mm)	a/l	a/t %	Limit of a/t %	Comments
all flaws are subsurface flaws (Table IWB-3512-1 of [A5.2] is used)													
6	-2	63.0	57.0	6.0	1.5	19.5	74.0	0.8	6.0	0.125	1.014	2.7	4' allowable ratio of a/t is used
14	1	65.0	57.0	8.0	1.0	8.0	75.1	0.5	8.0	0.063	0.7	2.3	
Multiple flaws													
4,7,12,14	1	45	92	47.0	2.5	7.25	75.1	1.25	47.0	0.027	1.7	2.1	1.0 mm for #12 vertical extent
3,5,6,13,15	-2	56	84	28.0	4.25	20.875	74.0	2.125	28.0	0.076	2.9		1.0 mm for #13 vertical extent
Parameters for finding Mm and Mb, Figs. A-3310-1 & A-3310-2, Ref.2													
e (mm)	16.1	2a/t	0.1	2e/t	0.44	Mm	1.05	Mb	0.6				

A5.4.3 Stress Data

Structural Analyses were carried out with pressures and temperature distributions applied (see Figure A5.3).

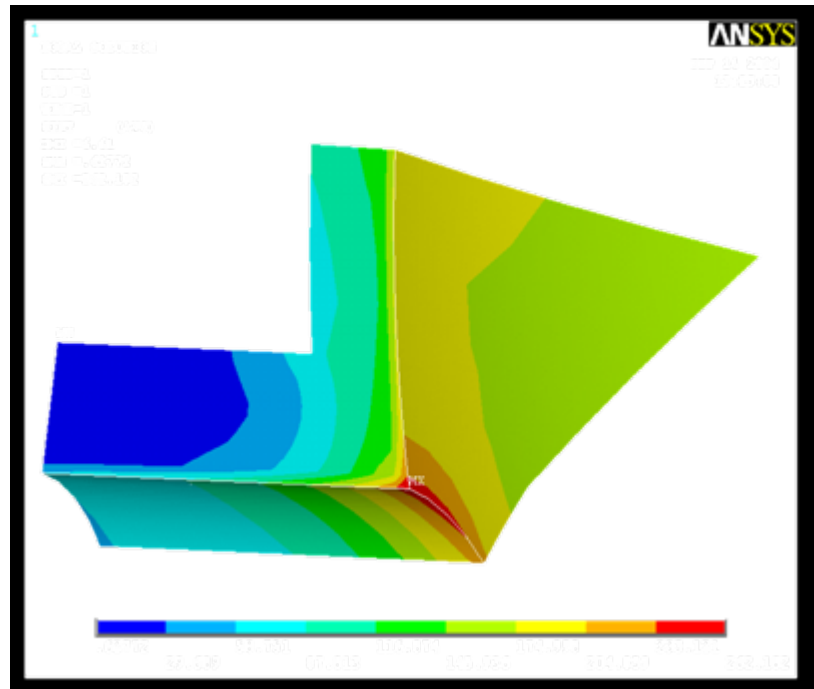


Figure A5.3 Stresses map for R4 Nozzle

Stress class lines across different weld sections were defined for the model and fatigue usage factors for these stress class lines were calculated (see Figure A5.4).

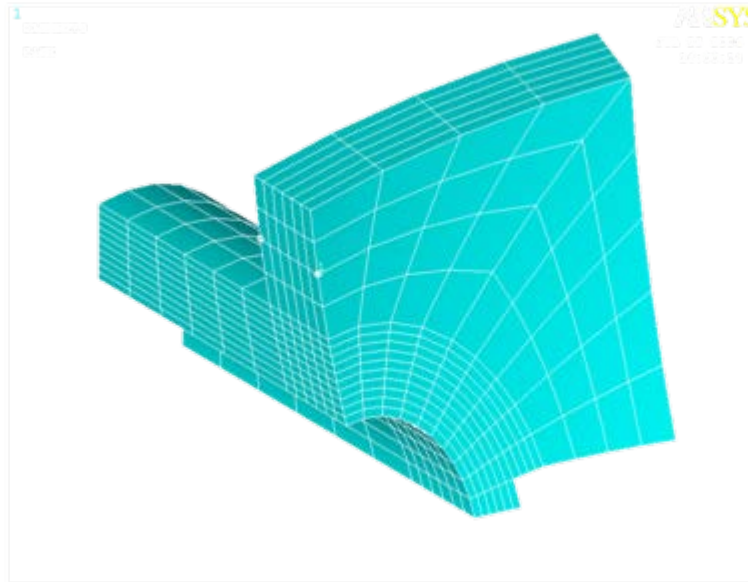


Figure A5.4 Path definition for R4 Nozzle

Stress data for the locations with the highest fatigue usage factors were summarized for subsequent assessment of the indications. Details of the analysis for the Lower Head/Heater Nozzle/Shell Assembly are documented in [A5.6]. Table A5.3 provides a summary of stresses required for analyses.

Table A5.3 Normal Conditions Stress Data(Summary)

INSIDE NODE = 14619 OUTSIDE NODE = 14722						
** MEMBRANE **						
SX	SY	SZ	SXY	SYZ	SXZ	
1.907	57.99	104.3	-12.1	9.56E-02	7.70E-02	
S1	S2	S3	SINT	SEQV		
104.3	60.49	-0.592	104.9	91.22		
** BENDING ** I=INSIDE C=CENTRE, O=OUTSIDE						
	SX	SY	SZ	SXY	SYZ	SXZ
I	-3.917	-82.61	-74.9	14.96	-0.1226	7.66E-2
C	0	0	0	0	0	0
O	3.917	82.61	74.9	-14.96	0.1226	-7.66E-2
	S1	S2	S3	SINT	SEQV	
I	-1.17	-74.9	-85.36	84.19	79.48	
C	0	0	0	0	0	
O	85.36	74.9	1.17	84.19	79.48	



A5.4.4 Stress Intensity Factor, K_I

Based on A-3200(b) in Appendix A of Section XI [A5.1]], K_I is calculated using linearised stresses. For a subsurface flaw, stress intensity factor can be calculated using Eq.(2) in A-3300, [A5.1]

A5.4.5 Flaw Growth Calculation

Flaw growth rate can be described using Eq.(1) in A-4300, [A5.1]. Results from the Flaw Growth Rate Analyses, using [A5.4] are given in the following Table A5.4.

Table A5.4 Flaw Growth Analysis for Combined Flow for Level A, B,C,D & Hydro Test. [A5.2]

Results				
Level A/B/C/D				
K_{Ia}	196.0			
K_{Ia_200F}	62.0			
Acceptance Criteria	K_I	<	K_{L_200F}	
	13.4		62.0	
Hydro Test				
K_{Ia}	66.5			
K_{Ia_100F}	21.0			
Acceptance Criteria	K_I	<	K_{L_100F}	
	11.0		21.0	
Level C				
K_{Ic}	Fig A-4200-1	200		
K_{Ic_100F}	141.40			
Acceptance Criteria	K_I	<	K_{L_100F}	
	11.0		141.4	
Conclusion:				
The combined flaw meets the req. stipulated in IWB-3600				

A5.4.6 Material Fracture Toughness

K_{Ia} and K_{Ic} given in A-4200, [A5.1] are lower bound from tests of SA-533 Gr. B/Class1,SA-508 Class 2, and SA-508 Class 3 steel provided in Figure A-4200-1, [A5.1]. $RT_{NDT} = 20^{\circ}F$, [A5.6]

A5.5 Summary and Conclusions

Table A5.5 provides a summary of the flaw assessment results.

Table A5.5 Summary of Results for Flaw Assessments

Weld	Transient	K_I (ksi*sqrt(in))	Acceptance criteria (ksi*sqrt(in))	Temperature Evaluated



PZX	Level A&B	13.43	62	200 °F(93 °C)
	Level C&D	11	141	200 °F(93 °C)
	Hydro test	12	21	158 °F(70 °C)

From the analyses, it has been shown that all the flaws are stable and growths of the flaws over the specified service cycles and transients are small. It is concluded that the indications found at these weld locations during the inaugural inspection are acceptable for service without repair with the following restrictions.

- The minimum temperature required for hydro test under a pressure of 2030 psi (14.MPa) for the Pressurizer is 158 °F(70 °C)



A5.6 References

- [A5.1] ASME Code, Section XI, Rules for Inspection of Nuclear Power Plant Components, 2001 Edition
- [A5.2] Cernavoda 2 Design Manual
- [A5.3] Ansys-CFX Program, Ver. 11.0
- [A5.4] FlawEvo Program, Versiunea 2, CITON/ACD
- [A5.5] MT Cernavoda 2 UT Report 82-MT-33324-IIUT-039, Pressurizer Weld PZ39
- [A5.6] U2- Pressurizer Stress Analysis 2-2-33324-1-1-AT1/Rev.0



APPENDIX 6 OXIDATION

CONTENTS

- A6.1 Physical Description of Mechanism**
- A6.2 Service Conditions/Environment**
- A6.3 Materials**
- A6.4 Susceptible Components**
- A6.5 Applicable Testing Standard(s) for Characterising Mechanism**
- A6.6 Governing Codes and Assessment Procedures for NPP integrity and lifetime assessment**
- A6.7 Current research Programmes**
- A6.8 Knowledge Gaps**
- A6.9 Future Research Requirements**
- A6.10 References**



Page intentionally left blank

A6.1 Physical Description of Mechanism

The films formed by corrosion of the structural materials contain a variety of oxides and hydroxides as a function of chemical composition of the materials, having different thicknesses and porosities depending on coolant oxidation conditions. In formation process of the corrosive layers on surface two mechanisms exists: one as result of physic-chemical reaction between fluid and metallic ions and other of the corrosion products deposition, the both depending on alloys nature and chemical composition of the environment.

Carbon and martensitic steels Under highly reducing ($O_2 < 0,1 \text{ ppm}$) and alkaline ($\text{pH} = 10.2 \times 10^8$) conditions and at temperatures more than 180°C , the magnetite film (Fe_3O_4) is the major corrosion product formed on carbon and martensitic steel, by Schikorr's reaction [A6.1]:



and



The magnetite solubility has an important role in formation mechanism of the oxide layers. It depends on electrochemical potential of the solution, which depends on the solution pH, the concentration of H_2 (D_2), O_2 , Cl^- and temperature [A6.2]. By analysis complementary methods was evidenced that the magnetite, formed into composition very close by stoichiometric report, ensures from beginning an adherent and protective oxide film. The protective oxide film confers of the metallic interface the resistance at oxidation and hydration, phenomena, which appear at fluid/metal, interface and generate corrosion products as different oxides, hydroxides and oxihydroxides of iron and alloying elements from steels.

The corrosion mechanism of materials in alkaline environment at high temperature consists of the formation of two overlapping layers of iron oxide compounds and was assumed to conform to the Potter and Mann model [A6.3].

Initially, an amorphous oxide film forms, but magnetite nuclei develop on this film and increase without a preferential orientation, conducting after certain time to formation of thin film with fine granulation. This inner oxide layer is a compact, continuous, adherent and fine-grained (granule dimension being $0.05 \div 2 \mu\text{m}$) oxide. In the second stage, over this internal film, which is in direct contact with the metal, the magnetite crystals develop at oxide/metal interface, simultaneous with his development at oxide/solution interface, forming a film with a bigger granulation. Thus the corroded iron that cannot precipitate as the inner layer diffuses through it as Fe^{2+} ions to the oxide-coolant interface. There, if the coolant already is saturated in dissolved iron, the emerging Fe^{2+} will tend to supersaturate the fluid boundary layer and provoke the precipitation of the outer oxide layer.

The magnetite of the outer layer forms coarser crystals, usually octahedral or tetrahedral habit with sizes of the order of a few micrometers ($0.5 \div 5 \mu\text{m}$). Therefore, the exterior oxide layer is formed by re-deposition of iron ions from solution. He is no continuous, no uniform and no adherent, but his growth is controlled by iron solubility and concentration in solution.

The interior oxide layer being microcrystalline and containing alloying elements as Cr, from the ground metal, can form complex oxides with low solubility, but the exterior oxide layer from big magnetite crystals (about $1 \mu\text{m}$) can contain Mn or Ni. The proportions of internal and exterior layers are roughly 50-50 [A6.4].

The kinetics of the formation and the growth of the magnetite protective oxide layer was considered that initially a parabolic law, but then a cubic or logarithmic law follows. But, because

the fortuitous character of the second magnetite layer, the steel corrosion in aqueous environment can be under a mixed control, thus that the kinetics of oxide film growth is of parabolic form ($y=kx^n$) and logarithmic form ($y=k \ln x-C$) in the first period, after that probably, a linear law ($y=Ax+B$) follows. The corrosion rate decreases with the growth of the oxide thickness, being in correlation with the magnetite solubility, which depends strongly on water chemistry.

Nickel alloys

In the case of nickel alloys (Incoloy-800) besides Fe oxides are formed Cr and Ni oxides, as well as complex oxides of Fe, Cr or Ni ($FeCr_2O_4$ and $NiFe_2O_4$). The exterior side of the corrosive films, formed on Incoloy-800 alloy, consists from magnetite particles deposits and of iron oxides with a tendency for increasing in the first time of nickel content and then of the chromium content. Thus, in the beginning, an exterior layer enriched in iron and nickel oxides (FeO , $FeOOH$, Fe_2O_3 , Fe_3O_4 , NiO and $NiFe_2O_4$) forms. Progressively, takes place and the oxidation of the chromium, due to oxygen diffusion in alloy bulk, which oxidizes preferably the chromium forming a thin, nonporous and homogenous oxide film, uniformly distributed on surface, being a barrier for transport of another ions at oxide/oxidizing surface. This internal oxide layer contains Cr_2O_3 and $FeCr_2O_4$.

The increase of the barrier oxide film takes place by oxygen diffusion to interior and chromium diffusion to exterior, and the increasing rate can be described by parabolic rate law:

$$\frac{dw_p}{dt} = \frac{k_p}{w_p} \quad \text{Eq. A6.1}$$

where

w_p is the metal weight used in barrier oxide film formation in mg/dm^2

k_p is the parabolic rate constant in $mg/dm^2 \cdot month$.

The growth of the barrier non porous oxide film, described by above equation, decreases with the increase of the exposure time and will begin to be prevalent the increase of the exterior oxide film richly in Ni-Fe, which contains also, quantities relatively small of Cr, Mn and Mo. While the exposure time increases, the oxidation rate depends linear of this and takes place after equation:

$$\frac{dw_1}{dt} = k_1 \quad \text{Eq. A6.2}$$

where

w_1 is the metal weight implicated in non-barrier oxide film in mg/dm^2

k_1 is the linear rate constant in $mg/dm^2 \cdot month$.

The stability of the barrier oxide film decreases with the increase of its thickness, caused either of mechanical tensions generated in oxide during of its thickening or due to transformation reaction at barrier/no barrier interface.

The oxidation varies straight with the exposure time but after long exposure times, because the thickening of the oxide film, reaches a stationary value, resulting an equilibrium between the

increase of the interior nonporous oxide layer and its transformation rate in exterior porous oxide layer. The oxidation rate tends to a constant variation with exposure time until a certain moment.

The corrosion process is dependent on a lot of material parameters (surface state, metallurgical structure due to some thermal treatments, as well as existence of some mechanical tensions), and depends by the water chemistry (pH, chemical impurities concentration). For water with pH=10.2÷10.8 and without impurities Incoloy-800 alloy corrosion is uniformly and the double-layers oxide films are protective and adherent.

A6.2 Service Conditions/Environment

Demineralised water pH=9.5 ÷ 9.7 (AVT) 260° C, 5.1 MPa (CANDU secondary circuit);

Demineralised water pH=10.2 ÷ 10.8 (LiOH) 310° C, 10.0 MPa (CANDU primary circuit).

A6.3 Materials

Carbon steel (SA 508, SA 106); Incolloy 800.

A6.4 Susceptible Components

Piping; ; SG Tubesheet; SG tubing.

A6.5 Applicable Testing Standard(s) for Characterising Mechanism

- Gravimetric analysis; Electrochemical measurements; Metallographic microscopy
- Scanning Electronic Microscopy.

A6.6 Governing Codes and Assessment Procedures for NPP Integrity and Lifetime Assessment

Internal Procedures INR

A6.7 Current Research Programmes

Corrosion of the above mentioned materials at normal parameters specific of CANDU primary and secondary circuits.

A6.8 Knowledge Gaps

- Corrosion kinetics
- Influence of pH values on the corrosion processes.

A6.9 Future Research Requirements

- Corrosion kinetics at normal parameters specific of CANDU NPP.

A6.10 References

- [A6.1] S.Velmurugan, A.L.Rufus, V.S.Sathyaseelan T.V.Padma Kumari, Nuclear Energy, 34(2), (1992).
- [A6.2] F.H. Sweeton, C.F.Jr.Baes, „ The Solubility of Magnetite and Hydrolysis of Ferrous Iron in Aqueous Solutions at Elevated Temperatures”, J. Chem. Thermodynamic, vol.2, (1995).
- [A6.3] E.C.Potter, G.M.W.Mann, "Oxidation of Mild Steel in High Temperature Aqueous Systems, „Proc.1st.Int.Cong.Metallic-Corrosion, London.
- [A6.4] N. Arbeau, H. Allsop, „Kinetics of Corrosion Product Release from Carbon Steel Corroding in High Temperature, Lithiated Water”, Corrosion NACE 54, no.6 (1998).



APPENDIX 7 THERMAL HIGH CYCLE FATIGUE IN PIPING SYSTEM TEES WITH LEAKAGE

CONTENTS

- A7.1 Physical Description of Mechanism**
- A7.2 Service Conditions/Environment**
- A7.3 Materials**
- A7.4 Susceptible Components**
- A7.5 Applicable Testing Standard(s) for Characterising Mechanism**
- A7.6 Governing Codes and Assessment Procedures for NPP integrity and lifetime assessment**
- A7.7 Current Research Programmes**
- A7.8 Knowledge Gaps**
- A7.9 Future Research Requirements**
- A7.10 Useful Resource Documents**



Page intentionally left blank

A7.1 Physical Description of Mechanism

A small cold mass flow in a Tee-branch (e.g. caused by a valve leakage) merging with a hot mass flow in the Tee-run will cause turbulent temperature mixing effects in the branch region next to the Tee-connection and in the pipe run downstream from the Tee (see Figure A7.1).

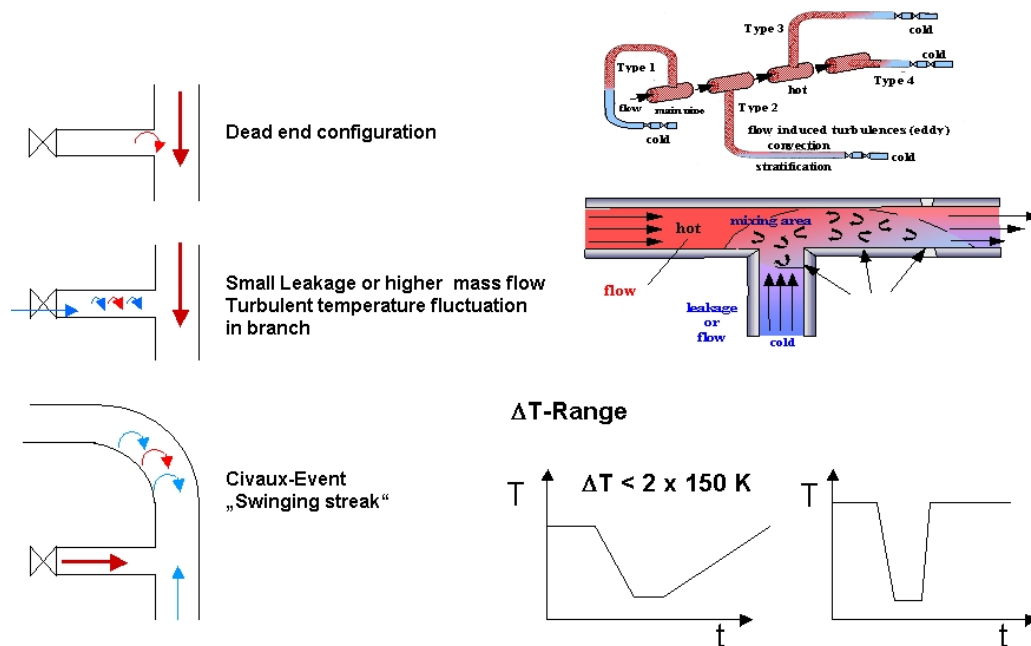


Figure A7.1 Turbulent temperature mixing in Tee-Connections

The effect is caused by differences in fluid velocity as well as in fluid density. The thermal loads occur as “down” and “up” (or “up” and “down”) thermal shock loads. The locations of the high stressed regions in the branch depend on the mass flow ratio, the diameter ratio and the position of the Tee (vertical run, horizontal run etc.). A small mass flow in the branch (valve leakage) leads to relevant temperature loads in the branch itself. With increasing branch mass flow the highly loaded locations are situated in the run region downstream from the Tee. The relevant degradation mechanism is thermal fatigue. The leading load value is the “driving temperature difference” between run and branch fluids.

A7.2 Service Conditions/Environment

- Temperature dependent on power plant system (< 350 °C)
- Temperature difference between run and branch fluids in NPP (< 250 K in normal operation)
- Mass flow ratio between run and branch fluids depending on system parameters

A7.3 Materials

Steels used for piping tees

A7.4 Susceptible Components

Piping Tees with relevant temperature differences between run and branch fluid, especially with a “dead end” and possibly valve leakage.

A7.5 Applicable Testing Standard(s) for Characterising Mechanism

- Fatigue tests (e.g. ASTM E 606) to characterise fatigue behaviour of pipe material.
- Thermal hydraulic component tests to characterise load spectra at specific conditions as “driving temperature difference” between run and branch fluids, mass flow ratio, diameter ratio and position of the Tee (vertical run, horizontal run etc.) if detailed information required.

A7.6 Governing Codes and Assessment Procedures for NPP Integrity and Lifetime Assessment

- European Procedure for Low and High Cycle Thermal Fatigue Analysis (in progress with NULIFE RA-4)
- Detection of pipe tees with potential valve leakage load on the basis of plant instrumentation systems, particularly by thermocouple installations and following proactive measures such as changing the system operation procedures or maintenance measures, e.g. stopping potential valve leakages

A7.7 Current Research Programmes

NULIFE RA-4

A7.8 Knowledge Gaps

So far there is an existing database from the THERFAT tests with a limited transferability to pipe wall thickness of any size.

The current knowledge about the real heat transfer coefficient range should be improved.

A7.9 Future Research Requirements

Additional tests at tees with increased wall thickness are recommended to improve the THERFAT-database.

Further research emphasis should be focused on fluid temperature measurements in the very thin boundary layer zone (transition from fluid to wall) to be able to determine a realistic heat transfer coefficient range more accurately.

A7.10 Useful Resource Documents

- [A7.1] Metzner K, Wilke U, Fifth Framework of the European Atomic Energy Community (EURATOM) Thermal Fatigue Evaluation of Piping System Tee-Connections (THERFAT) Final Synthesis Report, Final Issue, Revision 1, July 2007
- [A7.2] Development of a European Procedure for Assessment of High Cycle Thermal Fatigue in Light Water Reactors: Final Report of the NESCFatigue Project, Network for Evaluating Structural Components (NESCF), EUR 22763 EN, 2007
- [A7.3] European Procedure for Low and High Cycle Thermal Fatigue Analysis, C. Faidy, Draft February 2007



APPENDIX 8 PNAE G 7 002 86 (Russian Code) / IAEA-EBP-WWER-08

CONTENTS

A8.1 Introduction

A8.2 Scope

A8.3 Methodology

- A8.3.1 Sequences To Be Considered*
- A8.3.2 Acceptance Criteria*
- A8.3.3 Assumptions For PTS Analysis*
- A8.3.4 Thermal Hydraulic Analysis*
- A8.3.5 Structural Analysis*
- A8.3.6 Integrity Assessment*
- A8.3.7 Material Properties*
- A8.3.8 Corrective Actions*
- A8.3.9 Computer Codes*
- A8.3.10 Quality Assurance*

A8.4 Details of the PTS analysis

- A8.4.1 Irradiation effects to material properties*

Russian Assessment Code - PNAE G 7 002 86

VERLIFE

- A8.4.2 PTS Analysis for WWER reactors*

A8.5 Current R&D Activity

A8.6 Knowledge Gaps

A8.7 Future Research Requirements

A8.8 References



Page intentionally left blank



A8.1 Introduction

The code [A8.1] is available in Russian. It was developed for WWER type reactors and provides a method for evaluation of the integrity of the RPV during a pressurized thermal shock scenario. An IAEA guideline [A8.2] was developed based on this code. The VERLIFE code [A8.3] is a comparable but more detailed European code for WWER type reactors.

A8.2 Scope

The code aims at fracture mechanical evaluation of the RPV of WWER type reactors during a pressurised thermal shock. It includes the aspects of the thermal hydraulic analyses, mechanical and the fracture mechanical calculations, and of the neutron irradiation induced shift of ductile to brittle transition temperature of the RPV steel (material properties).

A8.3 Methodology

The guideline [A8.2] covers the following main topics:

A8.3.1 Sequences To Be Considered

- General considerations
- Initiating events groups
- Initiating events categorization

A8.3.2 Acceptance Criteria

The RPV Pressurised Thermal Shock (PTS) analysis is to demonstrate by a conservative deterministic analysis that there will be no initiation of a brittle fracture from the postulated defect during the plant design life for the whole set of anticipated transients and postulated accidents.

A8.3.3 Assumptions For Pts Analysis

- Plant data to be taken into account for PTS analyses: relevant systems pertinent to PTS, characterisation of the RPV in terms of geometry, material, weldments etc., fluence data, in-service inspection results
- Assumptions for thermal hydraulic analysis: system operation, available emergency systems, operator actions
- Assumptions for structural analysis: material properties for base material and cladding (elasticity modulus, heat conduction coefficient, thermal expansion coefficient, heat capacity etc), simplified vs. detailed mechanical analysis (FEM is recommended)

A8.3.4 Thermal Hydraulic Analysis

- Objectives: to determine downcomer temperature field, local coolant-to-wall heat transfer coefficients in the downcomer, and primary circuit pressure.
- Thermal hydraulic analysis to support transient selection (find conservative or limiting conditions for the PTS scenario)
- Sequence analysis plan (calculation of the overall progression of accidents with advanced thermal-hydraulic system codes; separate methods to account for the thermal stratification and mixing effects)
- Requirements for thermal hydraulic methods

A8.3.5 Structural Analysis

- Temperature and stress field calculations for the RPV wall based on the thermal and the pressure loading; consideration of residual stresses
- Fracture mechanics analysis (calculation of stress intensity factors based on simplified engineering equation or on FEM analysis)
- Postulation of defects and NDT requirements (surface crack, underclad crack, crack size to be postulated)

A8.3.6 Integrity Assessment

- Evaluation of results and safety factors (comparison of the calculated stress intensity factor vs. fracture toughness of the material)
- Allowable critical temperature of embrittlement
- Assessment and uncertainty of results

A8.3.7 Material Properties

- General information (phenomena contributing to aging, i.e. to the shift of the critical brittle fracture temperature)
- Determination of the initial critical brittle fracture temperature (unirradiated) by acceptance test data
- Irradiation embrittlement: Empirical formulas for the critical brittle fracture temperature in dependence on fluence, irradiation temperature and chemical composition (P, Cu)
- Fatigue and thermal aging: it is assumed that there is no shift of critical brittle fracture temperature due to thermal aging for WWER-440, in case of WWER-1000 there could be a shift; fatigue does not cause any shift of critical brittle fracture temperature

A8.3.8 Corrective Actions

Neutron flux and material properties, Loads

A8.3.9 Computer Codes

General requirements and code validation for Fluence calculations, Thermal hydraulic calculations and Structural calculations

A8.3.10 Quality Assurance

General and specific requirements

A8.4 Details of the PTS analysis

This section provides details of the PTS analysis in [A8.1], [A8.2] and [A8.3].

A8.4.1 Irradiation effects to material properties

Russian Assessment Code - PNAE G 7 002 86 [A8.1],[A8.2]

Critical brittle fracture temperature T_k is evaluated by:

$$T_k = T_{k0} + \Delta T_T + \Delta T_N + \Delta T_F = T_{k0} + \Delta T_k \quad \text{Eq. A8.1}$$

with T_{k0} - initial critical brittle fracture temperature, ΔT_T - shift in T_k due to thermal aging, ΔT_N - shift in T_k due to fatigue damage, ΔT_F - shift in T_k due to neutron irradiation. The main contribution of the shift in the cylindrical part of the vessel is caused by neutron irradiation:

$$\Delta T_k \approx \Delta T_F$$

The initial critical fracture temperature T_{k0} is determined from Charpy V-notch impact tests and tensile tests of unirradiated material:

$$T_{k0} = f(T_{DB}^{unirr}; Rp^{unirr}) \quad \text{Eq. A8.2}$$

with T_{DB}^{unirr} - Charpy transition temperature, Rp^{unirr} - yield strength of the unirradiated material. The neutron irradiation induced critical brittle fracture temperature, shift ΔT_k is determined in a procedure based on Charpy V-notch impact tests and tensile tests of irradiated material in a similar way as in an unirradiated condition:

$$\Delta T_k = T_k^{irr} - T_{k0} \quad \text{with} \quad T_k^{irr} = f(T_{DB}; Rp^{irr}) \quad \text{Eq. A8.3}$$

The following temperature dependence of the fracture toughness, K_{IC} is used for RPV PTS analyses:

$$K_{IC} = 26 + 36 \cdot \exp[0.02 \cdot (T - T_K)], \leq 200 \text{ MPa}\sqrt{\text{m}} \quad \text{Eq. A8.4}$$

This dependence corresponds to specimen thickness of 150 mm and fracture probability of $P_f = 0.05$. The prediction of ΔT_K is estimated according to:

$$\Delta T_k = A_F \cdot \sqrt[3]{\frac{F_n}{F_0}} \quad \text{Eq. A8.5}$$

with A_F - irradiation embrittlement coefficient of the RPV steel for irradiation at temperature $T(^{\circ}\text{C})$, F_n - neutron fluence in m^{-2} ($E_n > 0.5 \text{ MeV}$), $F_0 = 10^{22} \text{ m}^{-2}$.

A_F is determined from:

For WWER-440 RPV at irradiation temperature 270 $^{\circ}\text{C}$:

15Kh2MFA weld material

$$A_F = 800(C_P + 0.07 \cdot C_{Cu}) \quad \text{Eq. A8.6}$$

with C_P - phosphorous content in mass %, C_{Cu} - copper content in mass %.

- $A_F = 15$ for 15Kh2MFAA weld

For WWER-440 base metal A_F is constant:

- $A_F = 18$ for 15Kh2MFA
- $A_F = 12$ for 15Kh2MFAA

For WWER-1000 RPV materials irradiated at temperature 290 $^{\circ}\text{C}$ the A_F values are as follows:

- $A_F = 20$ for weld material
- $A_F = 29$ for 15Kh2NMFA
- $A_F = 23$ for 15Kh2NMFAA

However, recent experiment of the Kurchatov Institute have shown that the A_F value for WWER-1000 materials are not conservative for nickel content higher than 1.5 %. There is clearly a need for revision of the prediction of ΔT_k .



VERLIFE [A8.3]

For WWER reactors the “Unified Procedure for Lifetime Assessment of Components and Piping in WWER NPPs - VERLIFE” [A8.3] defines a reference temperature, RT_0 , used in integrity assessment of WWER reactors as:

$$RT_0 = T_0 + \sigma \quad \text{Eq. A8.7}$$

with T_0 - reference temperature of the irradiated material according to ASTM E1921-05 (Master curve concept). The margin σ is calculated according to:

$$\sigma = \sqrt{\sigma_1^2 + \delta T_M^2} \quad \text{Eq. A8.8}$$

with σ_1 - standard deviation according to ASTM E1921-05. δT_M considers the scatter in the materials. If this value is not available the application of the following values is suggested:

$\delta T_M = 10^\circ\text{C}$ for the base material,

$\delta T_M = 16^\circ\text{C}$ for weld metals.

The VERLIFE procedure suggests the following RT_0 indexed lower bound curve for WWER base and weld metal:

$$K_{JC}^{5\%}(T) = \text{Min}\{25.2 + 36.6 \cdot \exp[0.019 \cdot (T - RT_0)]; 200\} \text{ in } \text{MPa}\sqrt{\text{m}} \quad \text{Eq. A8.9}$$

that agrees with the standard MC for 5% fracture probability in ASTM E1921-08.

A8.4.2 PTS Analysis for WWER reactors

The initiating events and the thermal hydraulic calculations are described in [A8.2]. According to the VERLIFE code [A8.3] the K_I calculation within the PTS analyses can either be done by Finite element method (FEM) or by using analytical formulae. FEM is generally recommended. The residual stress in the weld is assumed to be:

$$\sigma_{ax}^{(res)} = \sigma_{\tan g}^{(res)} = (60 \text{ MPa}) \cdot \cos\left[\frac{2\pi x}{s}\right] \quad \text{Eq. A8.10}$$

with x – through wall thickness coordinate starting at the cladding/base material interface, s – wall thickness. Based on the thermal hydraulic calculations, the temperature and pressure in the reactor downcomer are determined and subsequently also temperature and stress fields in RPV wall are determined by FEM analyses. The fracture mechanical evaluation is based on the following postulated cracks:

- semi-elliptical sub cladding crack with $a/s=0.1$ if advanced qualified NDT is applied (generally recommended value, detailed procedure based on NDE qualification criteria for postulated crack depth is presented)
- semi-elliptical sub cladding crack with $a/W=0.25$ if qualified NDE is not applied
- 2 aspect ratios: $a/c=0.3$ and $a/c=0.7$
- 2 crack orientations: perpendicular to circumferential direction and perpendicular to the axial direction
- crack front is assumed to be located in the weldment or base material
- the cladding is assumed to be intact if its integrity is assured by qualified NDE and its material properties are known (in a new revision of the VERLIFE 2008 [A8.5] code the

crack is assumed to penetrate 1 mm into the cladding and more detailed procedure of cladding assessment is presented)

In case of FEM analyses with crack included in the mesh the K_I value is calculated via the J-integral. In case of the analytical approach the formulas in Appendix IV of [A8.3] may be used.

As an alternative to Master curve approach (Eq. A8.9), also the K_{IC} curve based on T_k for PTS scenarios may be used :

$$[K_{IC}]_3(T) = \text{Min}\{26 + 36 \cdot \exp[0.02 \cdot (T - T_k)]; 200\} \text{ in MPa}\sqrt{\text{m}} \quad \text{Eq. A8.11}$$

T is the temperature at the crack tip.

From this the maximum allowable critical temperature of embrittlement T_k is obtained:

$$T_k^a = \text{Min} \left[T - \frac{\ln \frac{K_I - 26 \text{ MPa}\sqrt{\text{m}}}{36 \text{ MPa}\sqrt{\text{m}}}}{0.02} \cdot 1\text{K} \right] \quad \text{Eq. A8.12}$$

where minimum is calculated for all pairs of K_I and T during the PTS transient. This value must be higher than end-of-life prediction of T_k .

A8.5 Current R&D Activity

Within the EU projects NURESIM/NURESP (6th / 7th FP) the thermal hydraulic models for PTS scenarios are improved. CFD models are used to describe the 3D mixing phenomena in the downcomer considering two phase flow. These activities aim at a more realistic (less conservative) evaluation of the thermal load of the RPV wall during PTS scenarios. These research activities are not related to a specific reactor type [A8.4].

A8.6 Knowledge Gaps

- Material behaviour after extended time of operation (> 30 years)
- Thermal loads of the RPV in case of two phase flow phenomena

A8.7 Future Research Requirements

- More precise description of the material degradation by neutron irradiation (Evaluation of the flux effect and late blooming phases), development of multi scale models
- Further improvement of thermal hydraulic models

A8.8 References

- [A8.1] Guide for strength analysis of the equipment and piping of nuclear power units, PNAE G 7 002 86, Energomashizdat, Moscow, 1989, in Russian.
- [A8.2] Guidelines on Pressurized Thermal Shock Analysis for WWER Power Plants ; A Publication of the Extra budgetary Programme on Safety of WWER and RBMK Nuclear Power Plants, IAEA Publication IAEA-EBP-WWER-08, Rev. 1, January 2006
- [A8.3] Unified Procedure for Lifetime Assessment of Components and Piping in WWER NPPs – VERLIFE, European Commission, Final Report, Contract N° FIKS-CT-2001-20198, September 2003.



- [A8.4] D. G. Cacuci, J. M. Aragoes, D. Bestion, P. Coddington, L. Dada, and C. Chauillac: NURESIM - A European Platform for Nuclear Reactor Simulation. FISA 2006 - Conference on EU Research and Training in Reactor Systems, 13-16 March 2006 (ftp://ftp.cordis.europa.eu/pub/fp6-euratom/docs/fisa2006_sei_nuresim_en.pdf)
- [A8.5] Unified Procedure for Lifetime Assessment of Components and Piping in WWER NPPs – VERLIFE, European Commission, Final Report, Project COVERS, March 2008



APPENDIX 9 DELAYED HYDRIDE CRACKING – RBMK-1500 NPP

CONTENTS

- A9.1 Physical Description of Mechanism**
- A9.2 Service Conditions/Environment**
- A9.3 Materials**
- A9.4 Susceptible Components**
- A9.5 Applicable Testing Standard(s) for Characterising Mechanism**
- A9.6 Governing Codes and Assessment Procedures for NPP Integrity and Lifetime Assessment**
- A9.7 Current Research Programmes**
- A9.8 Knowledge Gaps**
- A9.9 Future Research Requirements**
- A9.10 References**



Page intentionally left blank

A9.1 Physical Description of Mechanism

Zirconium and its alloys have a low absorption of heat neutrons and keeps good mechanical properties at temperatures up to 390-400°C. However, zirconium alloys can pick up hydrogen during operation as a consequence of corrosion reaction with water. Hydrogen redistributes easily at elevated temperatures migrating down a temperature or concentration gradient and up a stress gradient. Hydrogen has very limited solubility in zirconium alloys, this being less than 1 ppm at room temperature and about 80 ppm at 300°C. Whenever the solubility is exceeded a zirconium hydride phase will be precipitated and as this phase is brittle it can have an impact on the mechanical properties of the alloy. The worst embrittlement occurs when hydrides are oriented normal to the principal stress. When the terminal solid solubility is exceeded in a component such as a FC that is highly stressed for long periods of time, delayed hydride cracking (DHC) failures may occur (Figure A9.1).



Figure A9.1 Orientation of Hydrides & Formation of The Hydride Cluster Near Crack

DHC is a phenomenon where a crack can propagate in stepwise fashion as a result of hydrogen redistribution ahead of the crack tip under a stress level below the yield stress [A9.1], [A9.2]. The high mobility of hydrogen enables hydride to redistribute. If stress levels are sufficiently high the local hydrogen concentration can exceed the TSS, and the hydride platelets precipitate in the primary cracking direction.

A9.2 Service Conditions/Environment

Water inside of the fuel channel, irradiation, temperature – 300°C, pressure – 7 - 8 MPa.

A9.3 Materials

Zirconium-niobium alloy (Zr + 2.5 % Nb)

A9.4 Susceptible Components

The RBMK-1500 nuclear power plant reactor fuel channels

A9.5 Applicable Testing Standard(s) for Characterising Mechanism

- Regulations for in-service inspection of fuel channels, reactor control and protection system channels, and graphite stack of INPP, PTOed-1125-2.
- Regulations for Arrangement and Safe Operation of the Equipment and Piping of Nuclear Power Plants, PNAE G-7-008-89, Moscow, ENERGOATOMIZDAT Publishers, 1990.
- Procedures for In-Service Inspection of Fuel Channels, CPS Channels and Graphite Stack at Ignalina NPP. RBM-K15. Sb.01 D3. No 449, INPP, 1993.

- Standard Regulations for the In-Service Inspection of Fuel and CPS Channels at RBMK-1000 and RBMK-1500. 1985.

A9.6 Governing Codes and Assessment Procedures for NPP integrity and lifetime assessment

- The norms of the calculation on Strength of the equipment and pipelines of the nuclear power installations (PNAE G-7-002-86) / Gosatomenergondzor USSR.-Moskow: Energoatomizdat, 1989. (In Russian)
- Assessment of the Integrity of Structures Containing Defects. Nuclear Electric, R/H/R6 – Revision 3. – Gloucester: Nuclear Electric Ltd.,1996. – 318p.
- Guidance for application of the Leak Before Break concept at Ignalina NPP RBMK-1500 reactors. VD-E-03-98.-Vilnius, 1998.

A9.7 Current Research Programmes

Delayed hydride cracking (DHC) of zirconium alloy fuel cladding. Investigation of hydrogen induced degradation of zirconium cladding tubes (IAEA coordinated research project CRP No. T12017)

A9.8 Knowledge Gaps

Influence of Zr-2.5Nb structure and properties on the threshold stress intensity factor (K_{IH}) values for hydride crack propagation.

Influence of loading type (constant and low cyclic) on DHC and K_{IH}

A9.9 Future Research Requirements

The study of influence of Zr-2.5Nb structure, properties and loading type on the threshold stress intensity factor (K_{IH}) values for hydride crack propagation

A9.10 References

- [A9.1] Delayed hydride cracking in zirconium alloys in pressure tube nuclear reactors. Final report of coordinated research project. 1996-2002. IAEA-TECDOC-1410. October 2004, Vienna.
- [A9.2] Investigation of RBMK fuel channel aging process and determination of safe operation criteria. Final report, LEI, 2006, Kaunas. This project was supported by Lithuanian Science Foundation.



APPENDIX 10 INTERGRANULAR STRESS CORROSION CRACKING

CONTENTS

- A10.1 Physical Description of Mechanism**
- A10.2 Service Conditions/Environment**
- A10.3 Materials**
- A10.4 Susceptible Components**
- A10.5 Applicable Testing Standard(s) for Characterising Mechanism**
- A10.6 Governing Codes and Assessment Procedures for NPP Integrity and Lifetime Assessment**
- A10.7 Future Research Requirements**
- A10.8 References**



Page intentionally left blank

A10.1 Physical Description of Mechanism

Inter Granular Stress Corrosion Cracking (IGSCC) is a dominant damage mechanism in RBMK Reactor Cooling System piping [A10.1], [A10.2].

The IGSCC cracks in MCC austenitic piping of Ignalina NPP appear at the inner surface in HAZ near to weld root and grow to outside close to fusion line (Figure A10.1). The HAZ material is susceptible to IGSCC and sensitised in most cases. The sensitisation occur due to overheating during welding and is an important factor in the cracking behaviour.



Figure A10.1 IGSCC of piping welded joints heat affected zones (HAZ)

A10.2 Service Conditions/Environment

Water, temperature – 300°C, pressure – 7 – 8.5 MPa.

A10.3 Materials

Austenitic stainless steel 08X18H10T

A10.4 Susceptible Components

The RBMK-1500 nuclear power plant reactor cooling system piping components

A10.5 Applicable Testing Standard(s) for Characterising Mechanism

- Rules for Construction and Safe Operation of Equipment and Pipelines of NPP, PNAE-G-7-008-89, Gosatomenergondzor USSR, Moscow, Energoatomizdat, 1990.
- The equipment and pipelines of nuclear power installations. Welding (PNAE G-7-009-89),
- The equipment and pipelines of nuclear power installations. Welding. Rules for testing (PNAE G-7-010-89,
- Welding of the main material of the equipment and pipelines of nuclear power installations. Testing using ultrasonic method. Testing of main material (PNAE G-7-014-89)

A10.6 Governing Codes and Assessment Procedures for NPP Integrity and Lifetime Assessment

- Requirements for Assessment of Intergranular Stress Corrosion Cracking Damages in RBMK-1500 Reactors', P-2004-01



A10.7 Future Research Requirements

Leak-Before-Break analysis of austenitic piping systems welds

A10.8 References

- [A10.1] IAEA extra-budgetary programme on mitigation of intergranular stress corrosion cracking in RBMK reactors. Working group 2 on comprehensive assessment techniques. Final report, IAEA (2002).
- [A10.2] Technical Report No. 66173 "Determination of Downcomer Piping Joints Damage Reasons, Development of Technological Measures and Experimental Evaluation of Damaged Joints Manufactured of 08Ch18N10T Steel Durability After Definite Operation and Repair Period", PROMETEY, Sankt-Peterburg 1997.



APPENDIX 11 IRRADIATION INDUCED DIMENSIONAL AND MATERIAL PROPERTY CHANGES TO THE GRAPHITE

CONTENTS

- A11.1 Physical Description of Mechanism**
- A11.2 Service Conditions/Environment**
- A11.3 Materials**
- A11.4 Susceptible Components**
- A11.5 Applicable Testing Standard(s) for Characterising Mechanism**
- A11.6 Governing Codes and Assessment Procedures for NPP Integrity and Lifetime Assessment**
- A11.7 Knowledge Gaps**
- A11.8 Future Research Requirements**
- A11.9 References**



Page intentionally left blank

A11.1 Physical Description of Mechanism

During the operation of a graphite-moderated reactor, the irradiation dose causes dimensional and material property changes to the graphite (Figure A11.1).

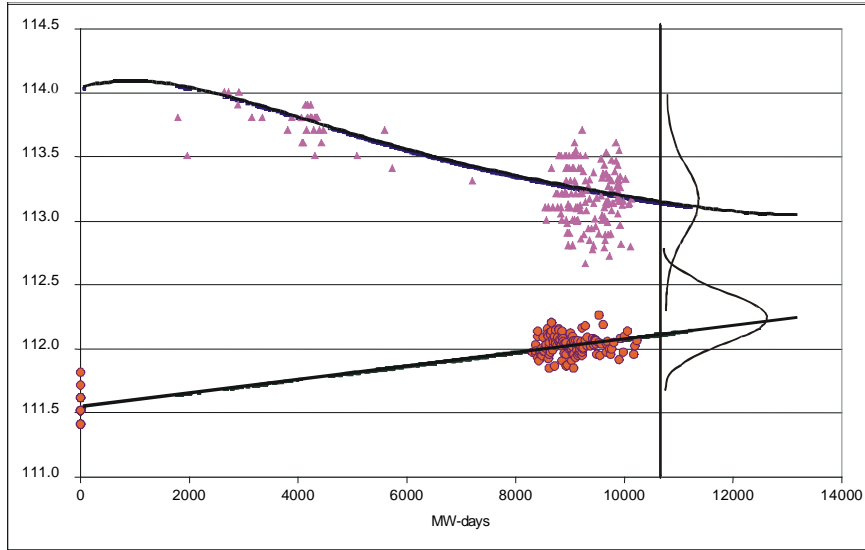


Figure A11.1 Illustration of the probabilistic gas gap closure model

During the first half of the reactor life, the graphite shrinks due to dimensional changes so that, if the process continued the gap between the graphite moderator brick and the graphite rings would be taken up. The diameter of the bore in the graphite block then reaches a minimum value (“turn-around”, see Figure A11.2) and starts to expand in the second half of reactor life [A11.1], [A11.2], [A11.3].

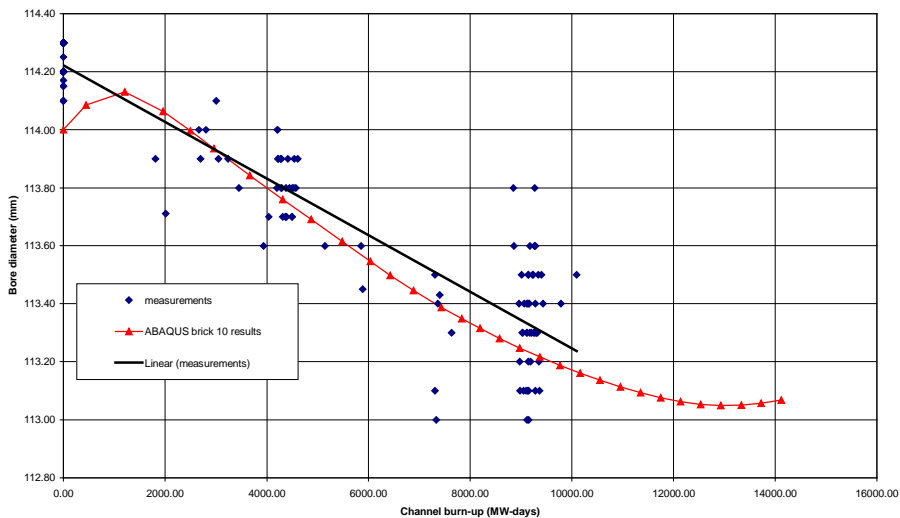


Figure A11.2 Comparison of brick calculations with measurements

This is normal graphite behaviour under irradiation. In addition, the zirconium pressure tube expands due to irradiation creep. To allow for irradiation induced graphite shrinkage and fuel channel tube expansion there is a gap between the fuel channel tube and the graphite moderator bricks. As the reactors operate this gap reduces. Operation of these reactors with a closed gas-gap is a non-design condition and continued operation of with closed gas-gaps has been shown to lead to damage to the graphite bricks and pressure tube welds. Closure of this gap has therefore been identified as a safety case issue by reactor designers and independent reviews as it could cause the pressure tube to be tightly gripped by the bricks.

A11.2 Service Conditions/Environment

Water inside of the fuel channel, irradiation, temperature - 300⁰C, pressure – 7 - 8 MPa.

The reactor cavity is filled with a helium-nitrogen mixture.

A11.3 Materials

Zirconium-niobium alloy (Zr + 2.5 % Nb)

Graphite GR-280 and GRP-2-125

A11.4 Susceptible Components

The RBMK-1500 nuclear power plant reactor fuel channels and the graphite moderator bricks

A11.5 Applicable Testing Standard(s) for Characterising Mechanism

- Regulations for Layout and Safe Operation of Components and Pipelines of Nuclear Power Plants, PN AE G-7-008-89, 1989.
- Procedures for In-Service Inspection of Fuel Channels, CPS Channels and Graphite Stack at Ignalina NPP. RBM-K15. Sb.01 D3. No 449, INPP, 1993.
- Regulations for the In-Service Inspection of Fuel, CPS Channels and Graphite Stack of Ignalina NPP, code ПТОэд-1125-2B1.
- Standard Regulations for the In-Service Inspection of Fuel and CPS Channels at
- RBMK-1000 and RBMK-1500. 1985.

A11.6 Governing Codes and Assessment Procedures for NPP integrity and Lifetime Assessment

- Standards for Strength Analysis of Typical Graphite Components and Parts of Channel-type Uranium-fuelled Graphite-moderated Reactors. RDIPE, Ref. No E230-2536, 1991.
- Technical Regulations for Operation of the INPP RBMK-1500 Reactors, code ПТОэд-0905-1.

A11.8 Knowledge Gaps

Interaction of the graphite bricks and fuel channel in case closure gap

A11.11 Future Research Requirements

The study of the interaction and contact between the graphite bricks and fuel channel in case closure gap



A11.10 References

- [A11.1] Bouganenko S.E., Baldin V.D., Rodchenkov B.S., Sinitsyn E.N., Marsden B.J., Blackburn N., Davies M.A., Introduction to the safety assessments related to RBMK graphite reactors. BNES Conference on Thermal Reactor Safety Assessment, Manchester, May 1994.
- [A11.2] Marsden B.J., Review of Russian Graphite Data and Assessment Methods for the Safety of Operation and Life Limiting Features of Nuclear Power Plant. AEA-RS-5415, GNSR(DTI)/P(92)114, December 1992.
- [A11.3] Hopkinson K.I., Marsden B.J., Dundulis G., Kopustinskas V., Liaukonis M., Augutis J., Uspuras E., Prediction of fuel channel-graphite gas-gap behaviour in RBMK reactors. Nuclear Engineering and Design, ISSN 0029-5493. - 2003. - Vol. 223. - P. 117-132.



APPENDIX 12 IRRADIATION INDUCED CHANGE OF FUEL CHANNEL LENGTH

CONTENTS

- A12.1 Physical Description of Mechanism**
- A12.2 Service Conditions/Environment**
- A12.3 Materials**
- A12.4 Susceptible Components**
- A12.5 Applicable Testing Standard(s) for Characterising Mechanism**
- A12.6 Governing Codes and Assessment Procedures for NPP Integrity and Lifetime Assessment**
- A12.7 References**



Page intentionally left blank

A12.1 Physical Description of Mechanism

During the operation the length of the PT increase a case of thermal and radiation creep (Figure A12.1). This is important in terms of the inadmissibility of reaching the limit of bellows movement [A12.1].

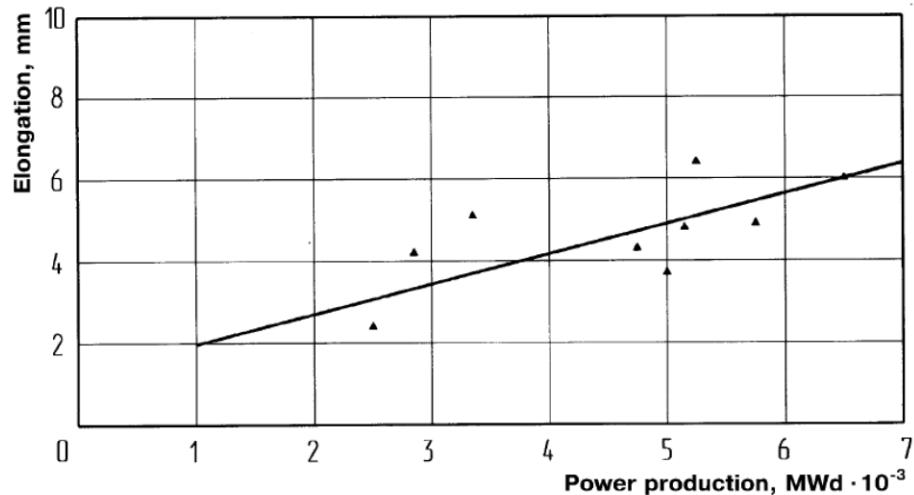


Figure A12.1 Increase in FC Lengths with Power Production at INPP-2

A12.2 Service Conditions/Environment

Water inside of the fuel channel, irradiation, temperature – 300°C, pressure – 7 - 8 MPa.

The reactor cavity is filled with a helium-nitrogen mixture.

A12.3 Materials

Zirconium-niobium alloy (Zr + 2.5 % Nb)

A12.4 Susceptible Components

The RBMK-1500 nuclear power plant reactor fuel channels

A12.5 Applicable Testing Standard(s) for Characterising Mechanism

- Regulations for the In-Service Inspection of Fuel, CPS Channels and Graphite Stack of Ignalina NPP, code ПТОэд-1125-2B1.
- Procedures for In-Service Inspection of Fuel Channels, CPS Channels and Graphite Stack at Ignalina NPP. RBM-K15. Sb.01 D3. No 449, INPP, 1993.
- Standard Regulations for the In-Service Inspection of Fuel and CPS Channels at RBMK-1000 and RBMK-1500. 1985.

A12.6 Governing Codes and Assessment Procedures for NPP integrity and Lifetime Assessment

- Technical Regulations for Operation of the INPP RBMK-1500 Reactors, code ПТОэд-0905-1.



A12.7 References

- [A12.1] Safety Analysis Report for Ignalina NPP, Task group 7 Report "Prediction of Fuel Channel Lifetime at Ignalina NPP" July, 1995.



APPENDIX 13 GUIDANCE FOR APPLICATION OF THE LEAK BEFORE BREAK CONCEPT AT IGNALINA NPP RBMK-1500 REACTORS.

CONTENTS

- A13.1 Introduction**
- A13.2 Scope**
- A13.3 Methodology**
- A13.4 Applications to lifetime assessment of degraded materials & components**
- A13.5 Associated material test standards**
- A13.6 References**



Page intentionally left blank



A13.1 Introduction

The regulatory Guidance for Application of the Leak Before Break Concept at Ignalina NPP RBMK-1500 Reactors developed by Lithuanian Nuclear Power Safety Inspectorate in 1998 is based on International IEC Standard 1250 [A13.1], IAEA-TECDOC-710 [A13.2]] and US NRC Standard Review Plan, 3.6.3 [A13.3].

The implementation of Leak-Before-Break (LBB) concept for primary circuit piping is important question for nuclear reactors safety. Especially it is important for RBMK-1500 with large number of Main Circulation Circuit piping some of that are located outside the Accident Localization System. The consequences of guillotine rupture could be tremendous and are difficult predictable. One of the means to avoid undesirable guillotine ruptures of pipes is implementation of LBB concept. The application of LBB concept criteria's and installation of leak monitoring systems is accepted by Lithuanian Nuclear Power Safety Inspectorate.

A13.2 Scope

The technical requirements, which should be fulfilled in case application of the leak before break, are described in this document. The general requirements are presented in this guidance only. This document contains the requirements for leak detection system; requirements for initial conditions in case application LBB; requirements for deterministic LBB analysis.

The basic requirement of the given document is that the flow of coolant through through-wall crack must be detected before crack will reach the critical sizes.

A13.3 Methodology

The general points for LBB analysis and application are the following:

- 1) Should be determined that is not possible fast piping degradation mechanisms due to fatigue, corrosion or erosion.
- 2) The postulated through wall crack length should be two times less then critical size calculated using most hazardous loads combination.
- 3) The postulated crack should remains stable at the most dangerous loading increased by safety factor (1.4).
- 4) The calculated leak rate through postulated crack should be enough to be detected by leak monitoring systems during 1 hour of normal operation. 10 times less then calculated leak rate should be used for analysis of leak monitoring system capability analysis.

The deterministic analysis should be performed using actual material properties data. The fracture toughness should be taken in conservative way selecting the minimal values of base metal, weld metal or heat-affected zone. The R6-method [A13.4] or other J-integral based methods shall be used for through-wall cracks evaluation.

A13.4 Applications to Lifetime Assessment of Degraded Materials & Components

The regulatory Guidance for Application of the Leak Before Break Concept are used for deterministic analysis of compliance to LBB concept of the RBMK pressure tube containing DHC cracks and austenitic pipes containing IGSCC cracks.

A13.5 Associated Material Test Standards

- Rules for Construction and Safe Operation of Equipment and Pipelines of NPP, PNAE-G-7-008-89, Gosatomenergondzor USSR, Moscow, Energoatomizdat, 1990.
- European standard 10002-1. Metallic materials. Tensile testing – Part 1. Method of test at ambient temperatures, 2001.



- European standard 10002-5. Metallic materials. Tensile testing – Part 5. Method of test at elevated temperatures, 1991.
- ASTM E1152 Standard Test Method for Determining J-R Curves. American Society for Testing and Materials, Philadelphia, U.S.A.
- ASTM E-399 Test method for plane-strain fracture toughness of metallic materials. American Society for Testing and Materials, Philadelphia, U.S.A.
- ASTM E-813 Standard test method for J_{IC} , a measure of fracture toughness. American Society for Testing and Materials, Philadelphia, U.S.A.

A13.6 References

- [A13.1] INTERNATIONAL IEC STANDARD 1250. First edition 1994-01 important for safety. Detection of leakage in coolant systems. Nuclear reactors - instrumentation and control systems.
- [A13.2] INTERNATIONAL ATOMIC ENERGY AGENCY, Applicability of the Leak Before Break Concept, IAEA-TECDOC-710, Vienna (1993).
- [A13.3] United States Nuclear Regulatory Commission, US NRC Standard Review Plan, 3.6.3 Leak Before Break Evaluation Procedures. US NRC, Washington, 1986.
- [A13.4] Assessment of the Integrity of Structures Containing Defects. British Energy Generation Ltd, R6 – Revision 4. Gloucester GL4 3RS, United Kingdom, February 2003.



APPENDIX 14 REQUIREMENTS FOR ASSESSMENT OF INTERGRANULAR STRESS CORROSION CRACKING DAMAGES IN RBMK-1500 REACTORS

CONTENTS

- A14.1 Introduction**
- A14.2 Scope**
- A14.3 Methodology**
- A14.4 Applications to Lifetime Assessment of Degraded Materials &
 Components**
- A14.5 Associated Material Test Standards**
- A14.6 References**



Page intentionally left blank



A14.1 Introduction

The Inter Granular Stress Corrosion Cracking (IGSCC) is a dominant damage mechanism in RBMK Reactor Cooling System piping. The results received in the IAEA Extra budgetary Program on Mitigation of Intergranular Stress Corrosion Cracking in RBMK Reactors [A14.1] was evaluated in the requirements for IGSCC crack evaluation.

The regulations and acceptance criteria, given in the regulatory document, describe the general principles of assessment of RBMK-1500 piping containing IGSCC cracks, give the requirements for damage tolerance analysis, requirements for inspection extent and frequency, requirements for quality assurance and documentation and describe the responsibilities of the plant.

A14.2 Scope

This document contains the Requirements for General Principles, Damage Tolerance Analysis Requirements, ISI and Quality Assurance and Documentation Requirements. The regulations include the safety factors and list of necessary documentation which should be prepared by plant operator in case if detected IGSCC defect is going to be left to further operation.

A14.3 Methodology

The procedures for evaluation of cracks consist of two parts. The first part is determination of the acceptable crack size for the component with crack, and the second part is the crack growth calculation. The acceptable flaw size provides information about the largest flaw size which component can tolerate without failure with accepted safety factors. The crack growth calculation determines how long does it take for the existing crack to reach the acceptable size. The results of these calculations (acceptable crack size and crack growth) determine the further inspection schedule of the components with crack.

The following fracture assessment methods shall be used for IGSCC crack evaluation:

- For postulated surface cracks the limit load analysis as ASME XI App. C [A14.2],
- For detected as well as postulated surface cracks the R6-method [A14.3] or other established methods, which employ the J-integral as a fracture parameter;
- For through-wall cracks the R6-method [A14.3] or other J-integral based methods.

A14.4 Applications to Lifetime Assessment of Degraded Materials & Components

The requirements include the procedures for safety assessment of RBMK-1500 piping components containing IGSCC cracks.

A14.5 Associated Material Test Standards

- Rules for Construction and Safe Operation of Equipment and Pipelines of NPP, PNAE-G-7-008-89, Gosatomenergoadzor USSR, Moscow, Energoatomizdat, 1990.
- European standard 10002-1. Metallic materials. Tensile testing – Part 1. Method of test at ambient temperatures, 2001.
- European standard 10002-5. Metallic materials. Tensile testing – Part 5. Method of test at elevated temperatures, 1991.
- ASTM E1152 Standard Test Method for Determining J-R Curves. American Society for Testing and Materials, Philadelphia, U.S.A.
- ASTM E-399 Test method for plane-strain fracture toughness of metallic materials. American Society for Testing and Materials, Philadelphia, U.S.A.



- ASTM E-813 Standard test method for J_{Ic} , a measure of fracture toughness. American Society for Testing and Materials, Philadelphia, U.S.A.

A14.6 References

- [A14.1] AEA extra-budgetary programme on mitigation of intergranular stress corrosion cracking in RBMK reactors. Working group 2 on comprehensive assessment techniques. Final report, IAEA (2002).
- [A14.2] American Society of Mechanical Engineers (ASME), Boiler and Pressure Vessel (B&PV) Code, Section XI, IWB=3640 and Appendix C "Evaluation of flaws in Austenitic Piping." Edition 1995.
- [A14.3] Assessment of the Integrity of Structures Containing Defects. British Energy Generation Ltd, R6 – Revision 4. Gloucester GL4 3RS, United Kingdom, February 2003.



APPENDIX 15 RPV CLADDING – Overview of results from EC projects

CONTENTS **Summary of relevant reports**

More details are given in ANNEX 1

A15.1 Study to generate Information on RPV Cladding Materials Data Including Aspects and Provide State-of-the-Art Report on the role of Cladding in RPV Safety Analysis

WGCS DGXI Contract B7-5340/96/000716/MAR/C2, 1996-2000

A15.2 NESC IV Project: An investigation of the transferability of Master Curve technology to shallow flaws in reactor pressure vessel applications, Final Report June 2005

A15.3 VVER Cladded Reactor Pressure Vessel Integrity Evaluation with Respect to PTS Events

Pistora, V., Brumovsky, M., Kohopaa, J., Lauerova, D., Wallin, K.: Semi-Large Scale Experiments Performed on Specimens with Underclad Cracks. SMIRT 19 Conference, Toronto, 2007.

A15.4 References

E. Keim, E. Capurro, A. Popov

Evaluation of Manufacturing and Inspection Program on RPV Cladding

Proceedings of PVP 2000, 2000 ASME PRESSURE VESSELS AND PIPING CONFERENCE, JULY 23-27, 2000, SEATTLE, WASHINGTON



APPENDIX 16 PRESSURIZED THERMAL SHOCK (PTS)

CONTENTS

- A16.1 Reactor Pressure Vessel**
 - A16.1.1 Pressurized Thermal Shock (PTS)**
- A16.2 Example of PTS Analysis**
 - A16.2.1 Computational Methods**
 - A16.2.2 Results**
- A16.3 References**



Page intentionally left blank

A16.1 Reactor Pressure Vessel

A16.1.1 Pressurised thermal shock (PTS)

PTS analysis is a part of the reactor pressure vessel (RPV) structural integrity assessment. PTS is a reactor transient that subjects the vessel to severe thermal shock starting at normal operating loading. Initial sharp cracks are typically postulated to be located at the weld seam area. see Figure A16.1. Safety margins against brittle fracture have to be justified in an appropriate manner.

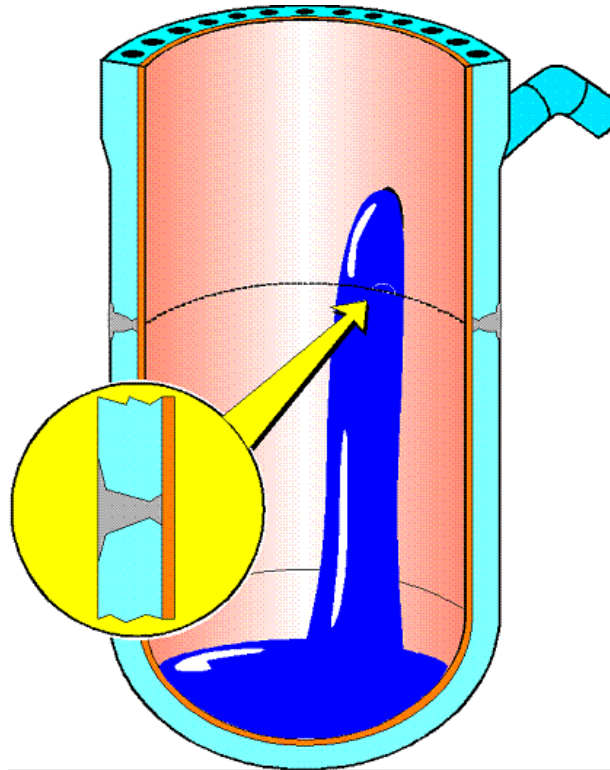


Figure A16.1. Pressurized thermal shock.

Firstly, the most significant transients are selected. Thermal hydraulic analyses are used for calculating the thermal loading transients. The fluid temperature distribution and the corresponding heat transfer coefficients are needed for the thermal conductivity analyses.

Secondly, pressure and thermal stresses through the wall are calculated in selected transient cases. Also the effect of residual stresses in the cladding, under the cladding and in the welds may be considered in stress analysis. The location, size and shape of the postulated crack is assumed based on the fabrication, NDE (non destructive evaluation), previous ISI (in-service inspection) or conventional values. Fracture mechanics analyses are applied for assessing the crack initiation. The stress intensity factor K can be used as a crack initiation criteria;

$$K_I < K_{IC}/SF, \quad \text{E. A16.1}$$

where K_I is the calculated stress intensity factor, K_{IC} is the crack initiation value, material toughness, and SF is the safety factor.

A16.2 Example of PTS Analysis

The example structure is the pressure vessel shell ring of the N4 type (1500 MWe). The inside diameter of the considered pressure vessel is 4500 mm at base metal/cladding interface. The total wall thickness is 232 mm including a 7 mm thick cladding.

The base material is a low alloy steel type SA 508 Class 3 and the stainless steel cladding is of grade 309L/308L. Thermal conductivity, specific heat, modulus of elasticity and thermal expansion coefficient for both base and cladding materials are shown in Table A16.1. The Poisson ratio was taken as 0.3 for both materials.

Table A16.1. Material properties of base and cladding materials.

T (°C)	Thermal conductivity (J/(s·m·°C))		Specific heat (J/(kg·°C))		Modulus of elasticity (MPa)		Thermal expansion coefficient (1/°C)	
	SA508	309L	SA508	309L	SA508	309L	SA508	309L
20	0,0377	0,0147	447,2	461,9	209000	197000	0,0000112	0,0000164
50	0,0386	0,0152	460,4	480,0	207500	195000	0,0000115	0,0000165
100	0,0399	0,0158	484,0	500,1	205000	191500	0,0000118	0,0000168
150	0,0405	0,0167	503,6	526,0	202000	187500	0,0000121	0,0000170
200	0,0405	0,0172	524,0	534,0	199000	184000	0,0000125	0,0000172
250	0,0402	0,0180	547,2	546,8	195500	180000	0,0000128	0,0000175
275	0,0399	0,0183	557,1	548,8	193500	178250	0,0000129	0,0000176
300	0,0395	0,0186	567,1	550,8	191500	176500	0,0000131	0,0000177
343	0,0388	0,0192	586,8	556,4	188060	172630	0,0000134	0,0000179
370	0,0383	0,0196	599,9	559,3	185700	170400	0,0000135	0,0000180

RT_{NDT} was 35°C for the base material. The fracture initiation and arrest toughness as a function of the reference temperature $T - RT_{NDT}$ is according to ASME XI /3/ (units: kpsi√in and Fahrenheit):

$$K_{Ic} = 33.2 + 20.734 \cdot e^{0.02 \cdot (T - RT_{NDT})} \quad \text{Eq. A16.2}$$

$$K_{Ia} = 26.8 + 12.445 \cdot e^{0.0145 \cdot (T - RT_{NDT})} \quad \text{Eq A16.3}$$

The stress strain curves are shown in Fig. A16.2. These curves were approximated using the given values for the yield strength.

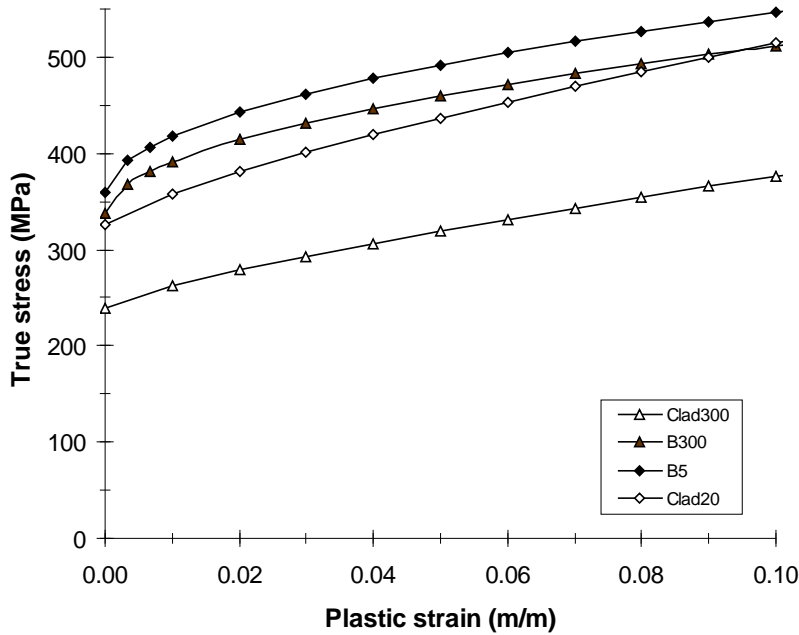


Figure A16.2 Approximated true stress versus plastic strain curves for base material and cladding material.

The crack depth used in the assessment of the cooldown and refuelling and pressure test was 56.25 mm ($\frac{1}{4}$ of the wall thickness) and length 337.5 mm. This crack size was taken from ASME XI.

An axial surface crack $15 \times 30 \text{ mm}^2$ (total depth x total length) was assumed in the category III and IV transients. The crack shape was an ellipse as is shown in Figure A16.3.

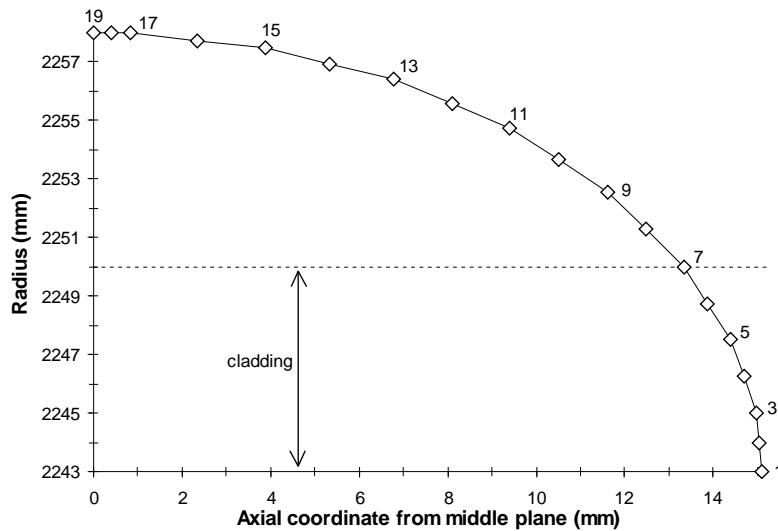


Figure A16.3 The elliptical $15 \times 30 \text{ mm}^2$ crack shape in the computation of category III and IV transients.

For the III category transient (2 inch small break) the pressure and temperature are shown in Figures A16.4 and A16.5.

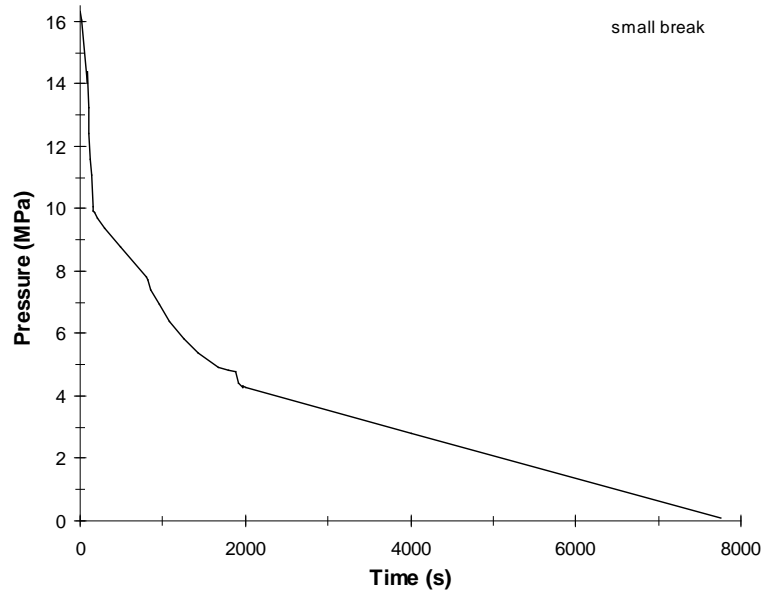


Figure A16.4 Pressure loading for category III transient (2 inch small break).

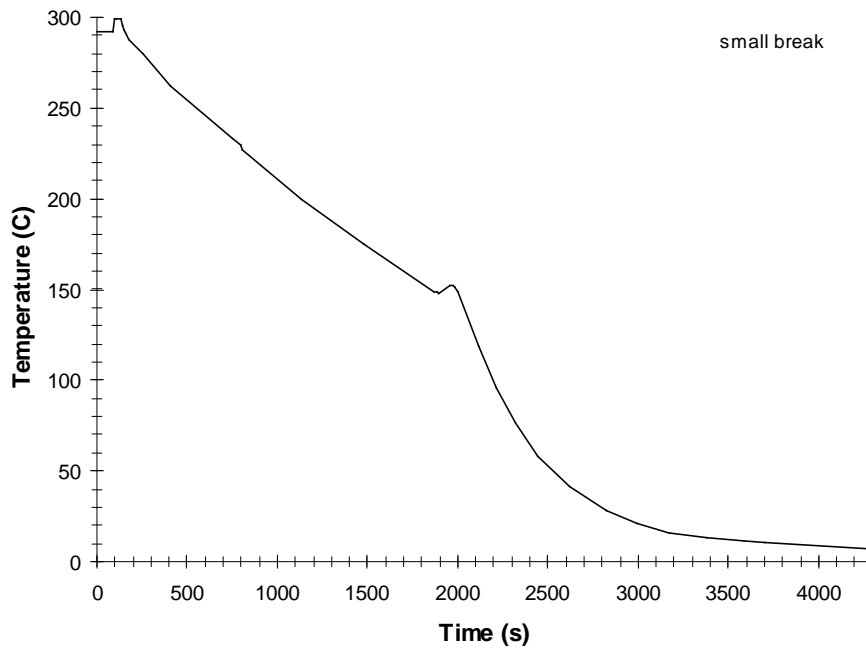


Figure A16.5 Temperature evolution for Category III transient (2 inch small break).

A16.2.1 Computational models

Abaqus 5.8 [A16.1] finite element code was used for the computation.

The stainless steel cladding was included both in the thermal and mechanical analyses. The stress free temperature was assumed to be 292°C.

All thermal analyses were performed with the axisymmetric model, which is shown in Figure A16.6. The stresses for the crack assessment utilising ASME XI formulas (cooldown & refuelling and pressure test) were produced with the axisymmetric model and a linear elastic analysis.

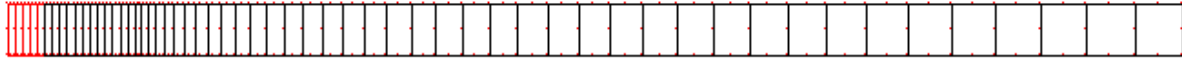


Figure A16.6 The axisymmetric finite element model

The stresses were resolved into membrane and bending components (linearisation method), as is specified in ASME XI (A-3200). The linearisation was performed using the stress at the base metal/cladding- interface (at the base metal side) and at the deepest point of the crack (in the base metal). Thus the stress distribution in the cladding was ignored in the linearisation. The stress distribution was extrapolated to the inside surface and the surface flaw equation of ASME XI (A-3310) was used for stress intensity factor calculation. The calculation procedure was performed using a FORTRAN code.

In the case of the axisymmetric model appropriate symmetry boundary conditions were modelled. Thus the axial displacement of the lower edge was fixed and the upper edge was constrained to remain as plane.

Three dimensional mechanical analyses were performed corresponding to the 2 inch small break and LOCA transients assuming thermo-elastic-plastic material behaviour and small strains and displacements. The three dimensional model of the cylinder with crack is shown in Figure A16.7. Symmetry boundary conditions were modelled in the crack plane (except crack surface), in the middle plane of the vessel length and in the 90° plane.

The crack loading was determined by the J -integral computed by the domain integration technique in the Abaqus code [16.1]. The J -integral was computed as mean value from second and third integration paths. The well known plane strain relation was used to determine the stress intensity factor K from J -integral.

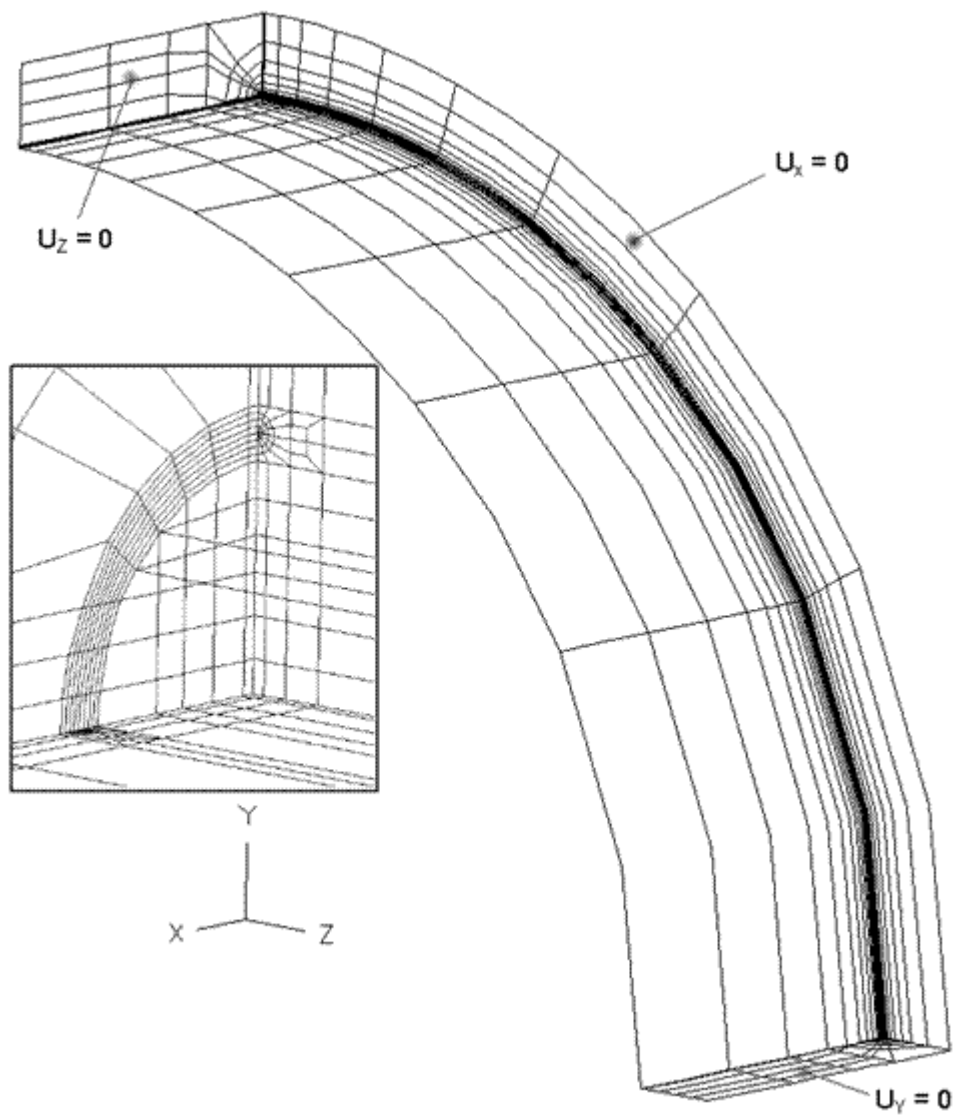


Figure A16.7 Three dimensional finite element model of the cylinder with crack. The displacement boundary conditions are shown in the figure.

A16 2.2 Results

Figures A16.8 and A16.9 show computed temperature profiles through the vessel wall in the case of LOCA and small break transient. Figures A16.10 and A16.11 compare the hoop stress distributions computed with the axisymmetric and three dimensional models. Figures A16.12 and A16.13 show the hoop stress distributions from the three dimensional model in a location far from the crack. Figure A16.14 shows the computed stress intensity factor from the analysis according to ASME XI as a function of time for cooldown and refuelling transients.

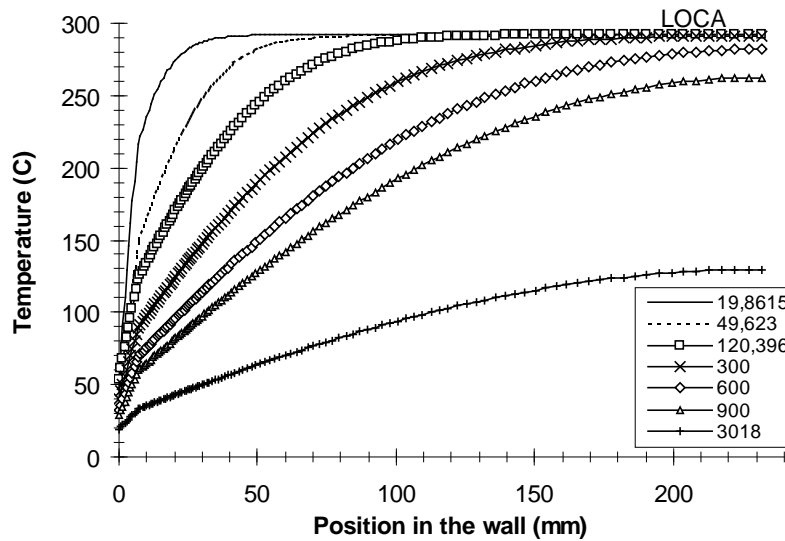


Figure A16.8 Computed temperature through the vessel wall for different time values in the case of LOCA transient.

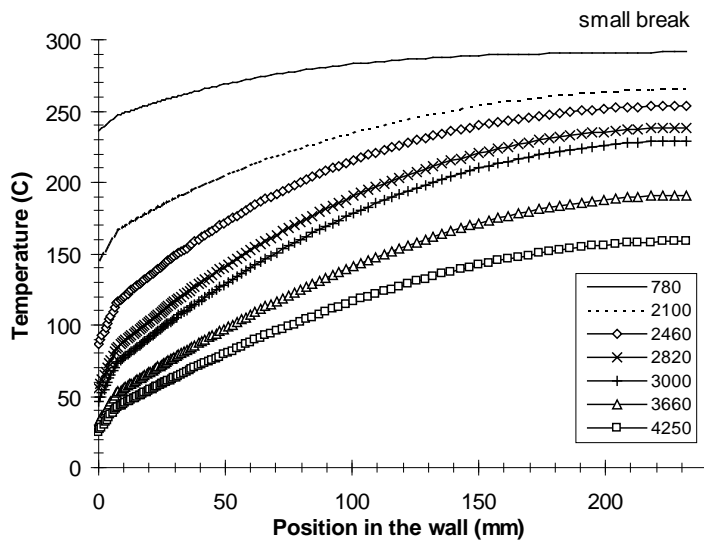


Figure A16.9 Computed temperature through the vessel wall for different time values in the case of small break transient.

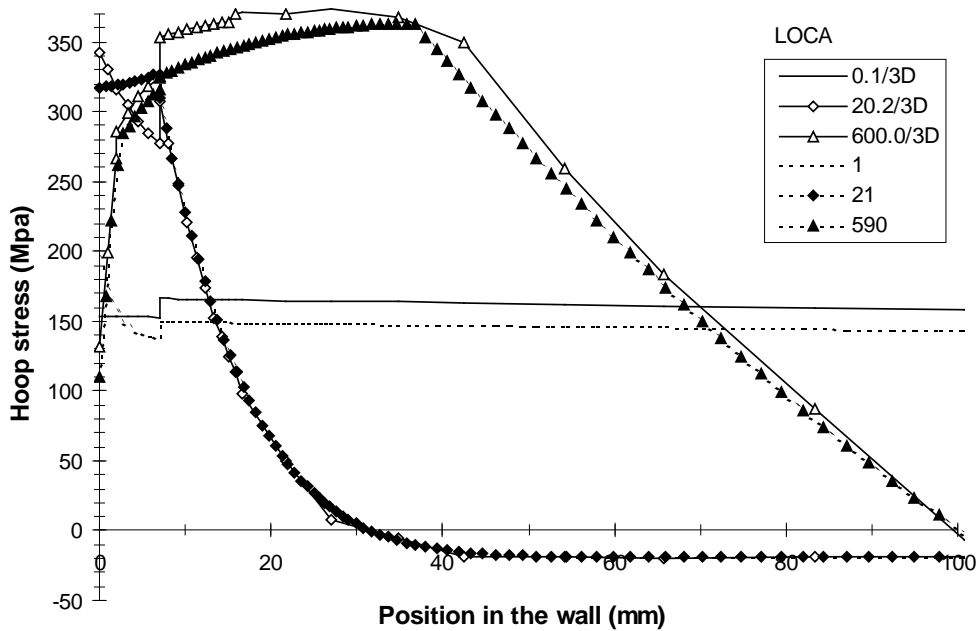


Figure A16.10 Comparison of hoop stress distribution through the wall by axisymmetric and three dimensional model (without influence of the crack) for different time values, LOCA transient.

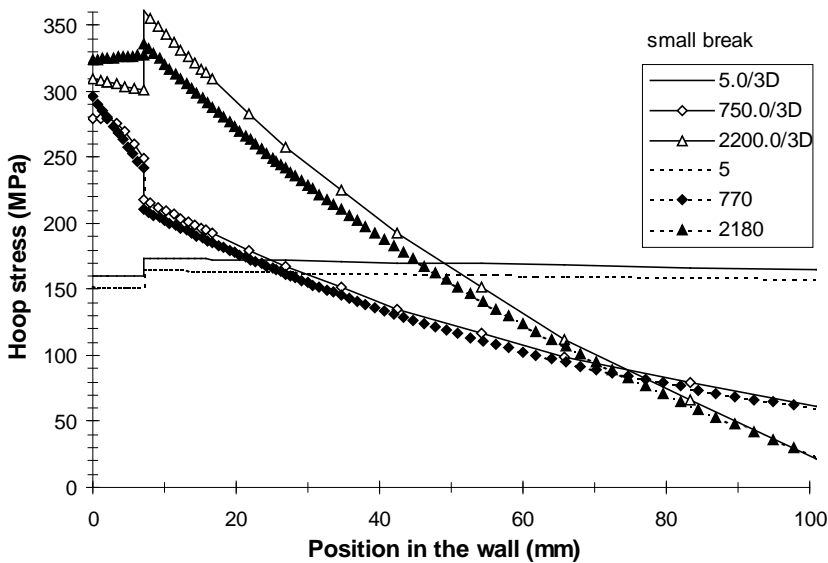


Figure A16.11 Comparison of hoop stress distribution through the wall by axisymmetric and three dimensional model (without influence of the crack) for different time values, small break transient

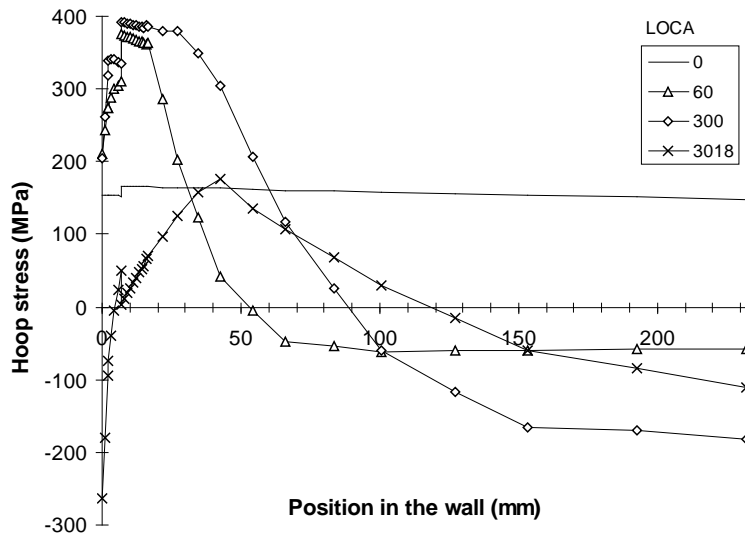


Figure A16.12 Hoop stresses computed for different time values by the three dimensional model in the case of LOCA transient far from the crack.

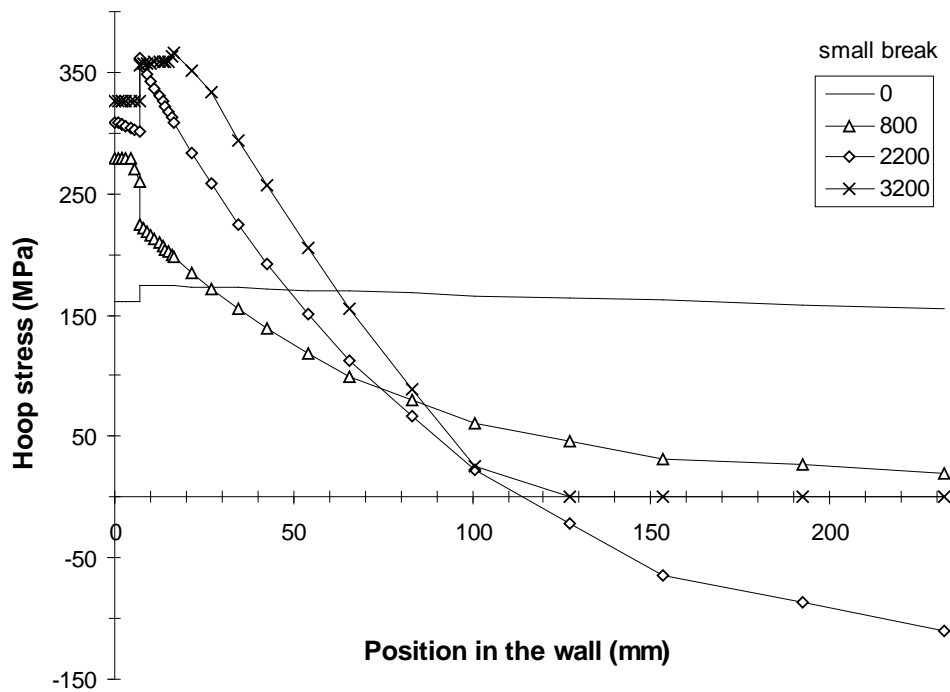


Figure A16.13 Hoop stresses computed for different time values by the three dimensional model in the case of small break transient far from the crack.

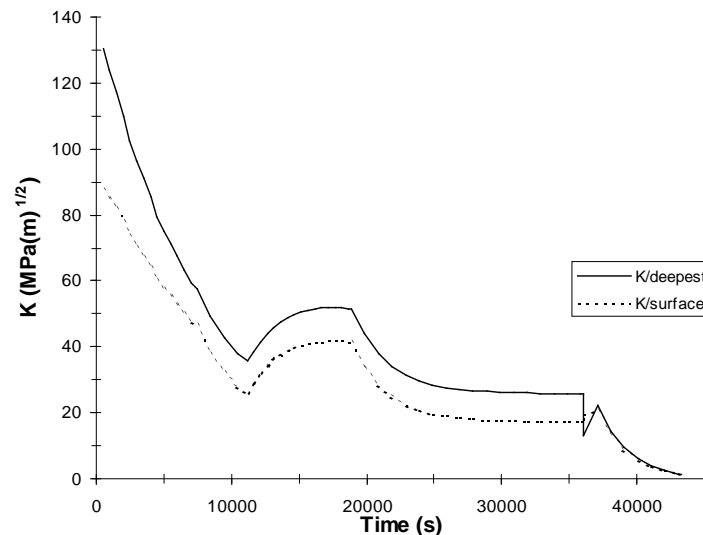


Figure A16.14 Computed stress intensity factor as function of time, cooldown and refuelling transient. Results from the analysis according to ASME XI.

The computed stress intensity factor during cooldown and refuelling transient and pressure test is shown in Figure A16.15 together with the arrest toughness curve of ASME XI [16.3]. The stress intensity factor K_I is assessed in two points: at the deepest point of the crack front and near the cladding/base material interface on the base material side. A safety factor of 2 has been applied to the stress intensity factor values caused by pressure in the case of cooldown and refuelling transient. The stress intensity factor due to pressure test has been multiplied by 1.5.

The situation in the cooldown and refuelling transient is far from critical. The crack loading due to pressure test is not acceptable despite of the safety factor 1.5. A safety factor of $\sqrt{10}$ for pressure is used in the assessment of allowable p - T limits in Finland [16.2].

The computed stress intensity factors by the three dimensional finite element model during LOCA and small break transients are shown in Figures A16.16 and A16.17 together with the initiation toughness curve of ASME XI [16.3]. The stress intensity factor K_I is assessed again in two points: at the deepest point of the crack front and near the cladding/base material interface on the base material side. The safety factor (K_{I0}/K_I) during small break transient (most critical case) is 1.3, and even in this case warm pre-stressing (WPS) occurs, Figure A16.18.

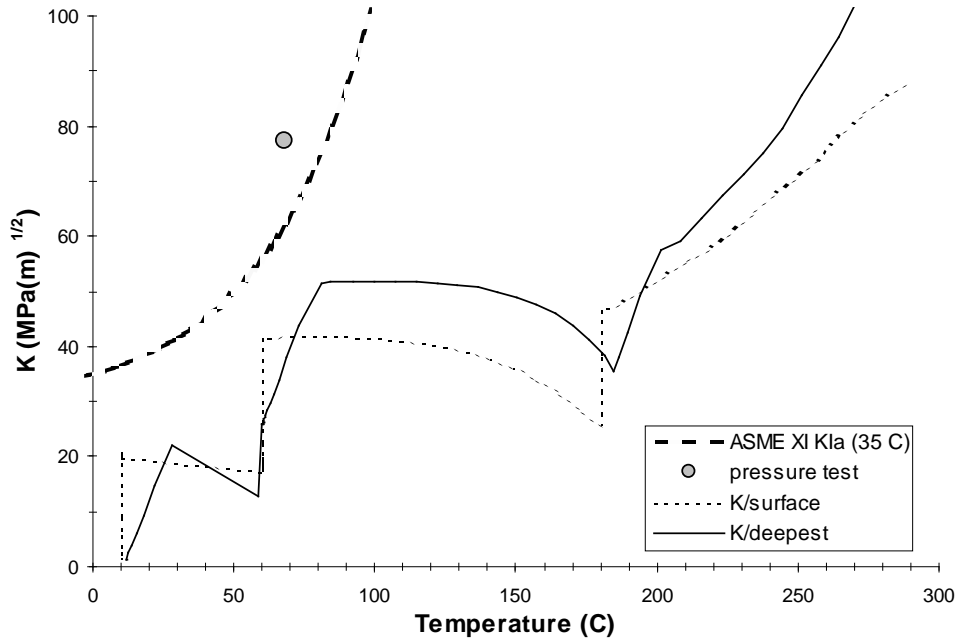


Figure A16.15 Fracture assessment by the computation according to ASME XI in the case of pressure test and cooldown and refuelling transient in the deepest point of the crack and in the base metal at the clad/base- interface. The fracture arrest toughness curve according to ASME XI [164] is shown ($RT_{NDT} = 35^\circ\text{C}$).

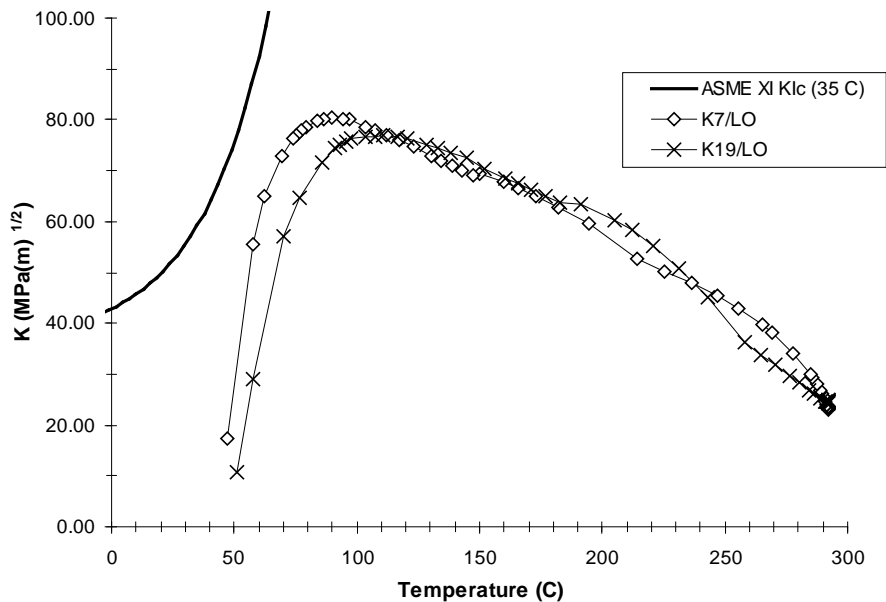


Figure A16.16 Fracture assessment (3D FE) in the deepest point of the crack (K19) and in the base metal at the clad/base- interface (K7) in the case of LOCA transient. The fracture initiation toughness curve according to ASME XI [16.4] is shown ($RT_{NDT} = 35^\circ\text{C}$)

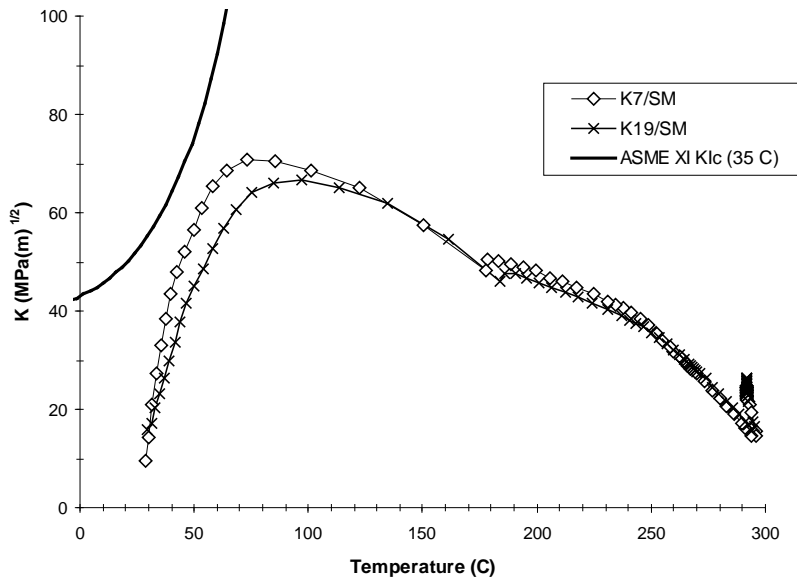


Figure A16.17 Fracture assessment (3D FE) in the deepest point of the crack (K19) and in the base metal at the clad/base- interface (K7) in the case of small break transient. The fracture initiation toughness curve according to ASME XI [164] is shown ($RT_{NDT} = 35^{\circ}\text{C}$).

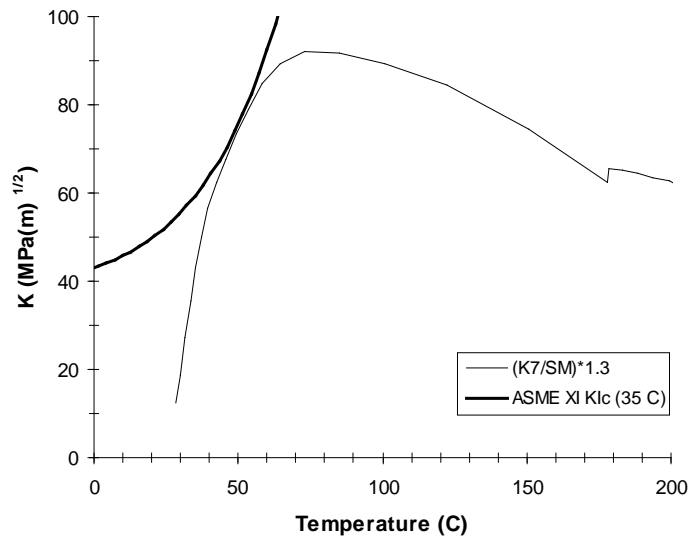


Figure A16.18 Fracture assessment (3D FE) the base metal at the clad/base- interface (K7) in the case of small break transient. The computed stress intensity factor has been multiplied by 1.3. The fracture initiation toughness curve according to ASME XI [16.4] is shown ($RT_{NDT} = 35^{\circ}\text{C}$).



A16.3 References

- [A16.1] Abaqus Theory Manual, Version 6.7, SIMULIA, Dassault Systemes, 2007.
- [A16.2] IAEA-TECDOC-1627 Pressurized Thermal Shock in Nuclear Power Plants: Good Practices for Assessment
- [A16.3] IAEA-TECDOC-1361 Assessment and management of aging of major nuclear power plant components important to safety. Primary piping in PWRs.
- [A16.4] Survey of European fast fracture procedures and requirements related to the structural integrity of the RPV's of LWR - Comparative study for harmonisation purposes. Final report of the study contract B4-3070/97/000787/MAR/C2. February 2000.TIERSDI/4NT/3133/01.



APPENDIX 17 CANDU FEEDER PIPING

CONTENTS

A17.1 Degradation Mechanisms

A17.2 Lifetime Evaluation

A17.3 References



Page intentionally left blank

A17.1 Degradation Mechanisms

CANDU 6 reactors have experienced two types of feeder degradation:

- Pipe wall thinning due to Flow Accelerated Corrosion (FAC)
- Cracking.

FAC wall thinning has been seen at most stations while cracking has only been observed in a few situations. The thinning rate of the feeder pipes has been shown to be dependent on water chemistry, particularly the pH and the electrochemical potential. The mechanistic understanding of feeder cracking is still limited. To date, inter-granular cracks have been observed on both the inner and outer surface of the first and second bends on the outlet feeder and on one repaired weld. Inner surface cracks are postulated to be caused by stress corrosion cracking. Figure A17.1 shows a schematic diagram of feeder pipe.

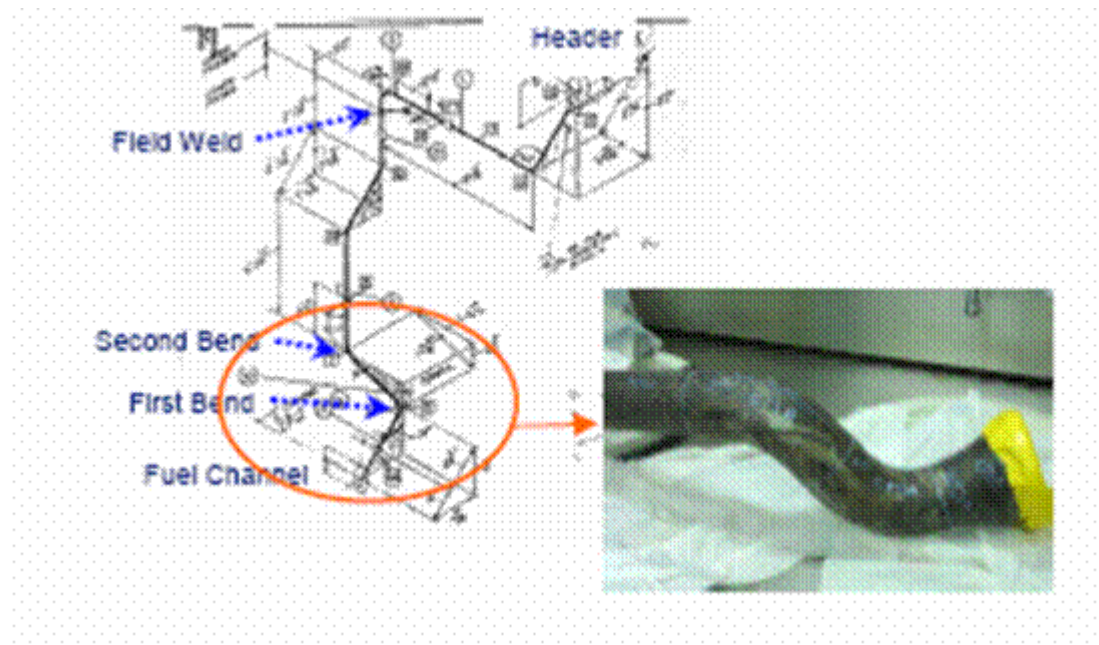


Figure A17.1 Schematic diagram of feed pipe.

Outer surface cracks are currently believed to be caused by low temperature creep cracking, assisted by hydrogen ingress due to feeder thinning. The single crack on the repaired weld is currently believed to be an interrelation of both mechanisms. It is believed that all cracks are caused by unrelieved residual stresses induced during manufacturing or welding, plus other factors such as material susceptibility and chemical environment.

Feeder Ageing Management Programs have been developed and are updated periodically to account for inspection findings and subsequent assessments. This program includes inspection plans at each planned outage and R&D plans. In addition, improved feeder inspection tools have been developed to inspect inaccessible sites. More reliable leak detection systems are also being considered. The major degradation mechanisms are presented in Table A17.1.

Table A17.1 Major Degradation Mechanisms.

Degradation Mechanisms		Location
FAC Wall Thinning	Global & Local	Bend ID
	Highly Local (blunt flaw)	Adjacent to Weld
Cracking	IGSCC	Bend ID
		Repaired Weld
	Creep Cracking	Bend OD

Feeder pipes in the Heat Transport System need to be subjected to a more rigorous assessment process, given the recent field experience where wall thinning of some portions of the feeders, and cracking of feeders at one station, has been reported. An industry methodology and feeder-specific fitness-for-service guidelines for the degradation types that have been experienced on outlet feeders are now used by all CANDU stations. Wall thickness inspection and monitoring programs are underway and mitigation strategies for older plants are under development. Most feeder pipes will meet their design life. A limited number of outlet feeder bends and/or welds may require replacement before pressure tube replacement. The techniques and procedures for feeder replacement have been developed, and have been recently used successfully at a CANDU 6 plant. The feeder repair and replacement process is now a routine procedure. Feeders on the reactor face can be replaced with little difficulty during an outage. It is clear that repair of feeders due to aging has now proven to be an effective and economical Age Management technique. Appendix 4 provides further details regarding degradation mechanisms in CANDU plant.

A17.2 Lifetime Evaluation

Material ageing management of carbon and austenitic steel pipes

It is essential to define the goals for establishing the critical elements for success in all the phases of the assessment of material degradation of carbon and austenitic pipes. These goals help staff maintain a sense of purpose and enable clear focus on areas of work. Figure A17.2 shows typical goals of the material ageing management of carbon and austenitic steel pipes.



Figure A17.2 Typical goals of the material ageing management of carbon and austenitic steel pipes in PLIM/PLEX programs.

The structural integrity of the plant is affected by corrosion degradation in percentage of 27% [A17.1]. Table A17.2 shows potential ageing mechanisms of carbon and austenitic steel pipes and resulting effects,[A17.2].

Table A17.2 Potential Ageing Mechanisms and Resulting Effects.

Ageing mechanisms ⇒ Effect on components ⇓	Irradiation	Thermal ageing	Creep	Fatigue (HCF, LCF)	Corrosion							Wear
					Corrosion fatigue	Stress corrosion cracking	Strain induced corrosion cracking	Intergranular attack	Erosion corrosion	Local corrosion attack	General corrosion	
Change of material properties	●	●	●	●								
Cracking			●	●	●	●	●	●				●
Dimensional changes	●		●									
Wall thickness									●		●	●

Figure A17.3 below. shows the flowchart of the corrosion evaluation of carbon and austenitic steel pipes.

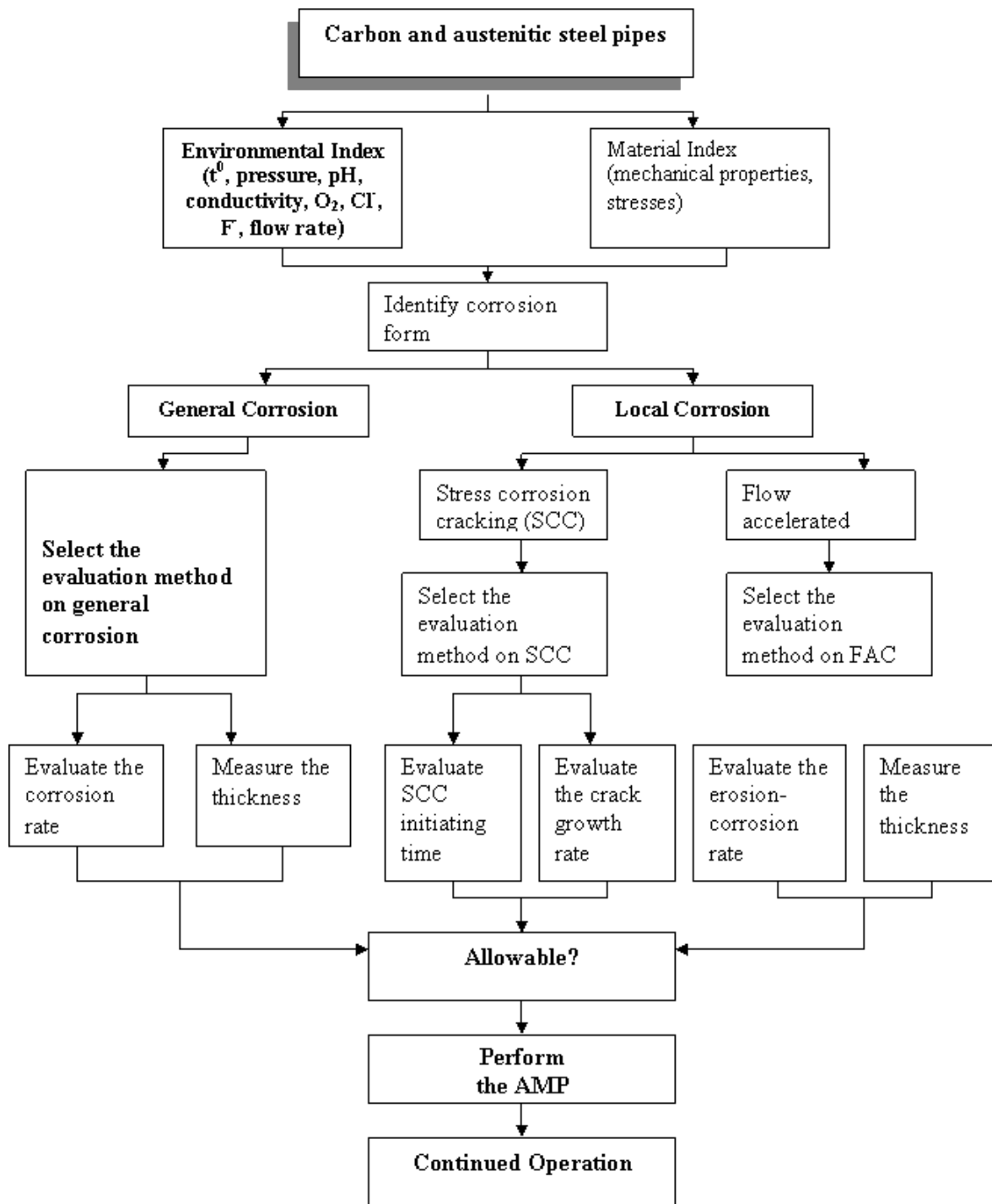


Figure A17.3 Corrosion Evaluation Process of Carbon and Austenitic Steel Pipes.



A17.3 References

- [A17.1] INTERNATIONAL ATOMIC ENERGY AGENCY, "Nuclear power plant life management processes: Guidelines and practices for heavy water reactors", IAEA-TECDOC-1503, IAEA, Vienna (2006), ISSN 1011-4289.
- [A17.2] Cojan, M., Radu, V., Parvan, I., Lucan, D., Florescu, Gh., "Application and importance of ageing management in CANDU 6 PLIM / PLEX programs", paper presented at the CNE 2004 – The 7th Regional Energy Forum – FOREN 2004 "Sustainable Energy Development and European Integration", Neptun, Romania, 13-17 June 2004.



ANNEX 1 RPV CLADDING

CONTENTS

- AN.1.1 Introduction, Materials**
- AN.1.2 Chemistry of RPV Cladding**
- AN.1.3 Defects in the Cladding**
- AN.1.4 Microstructure of the Cladding**
- AN.1.5 Mechanical Properties**
- AN.1.6 Properties and Assessment Tools for Characterizing PWR
Cladding Crack Susceptibility**
- AN.1.7 Characterization of Residual Stresses under Cladding**
- AN.1.8 Properties and Assessment Tools for Characterizing WWER
Cladding Crack Susceptibility**
- AN.1.9 Lifetime Evaluation Considering Cladding Properties**
- AN.1.10 Summary and Suggestions for Further Study**
- AN.1.11 References**



Page intentionally left blank

AN.1.1 Introduction, Materials

To prevent uniform corrosion and erosion and thus to minimize the radioactive contamination of the reactor coolant system, all ferritic parts and components wetted by the reactor coolant in service are lined with a corrosion-resistant cladding. Cr-Ni steel is the clad material used for most of these surfaces. As a rule, the RPV cladding is welded in at least two passes to ensure recrystallization of the heat affected zone in the ferritic base metal and to eliminate the potential for relaxation cracking. To neutralize the dilution with the base metal, to prevent hot cracking, and to induce resistance to inter-granular corrosion, a highly over-alloyed clad metal is used for welding the first pass of the austenitic cladding and a less over-alloyed clad metal is used for the second pass and eventually needed further passes. For the cladding of the Russian reactor pressure vessels one or two strip electrodes with the section of 0.7 x 50 mm and the distance of 10-14mm between them are used.

In this review, the existing relevant information on RPV cladding properties are summarized. The RPV cladding in Europe and Russia were mostly produced by submerged (under powder) arc strip electrode welding, while in US the submerged arc three-wire welding technology was used. Compared to US technology, the European technology provides very low penetration of the weld-deposited cladding into the base metal, low specific heat input, and very different shape of weld beads and resultant microstructure. Consequently, current US (mostly Heavy Section Steel Programme), Korean and Japanese results are collected but not included into this study.

AN.1.2 Chemistry of RPV Cladding

The base material of the WWER reactors is low-alloyed Cr-Mo-V or Cr-Mo-Ni steel. The cladding is made usually from two layers using the low penetration submerged arc strip cladding technology. The first layer is over-alloyed using Sv-07Ch25N13 electrode (containing 25%Cr and 13% Ni) weld by one pass, the second made with Sv-08Ch19N10G2B electrode usually at least by three passes [AN1.1], [AN1.2], [AN1.3].

The nominal thickness is 8^{+2}_{-0} mm, but the welding altogether is a little more, since the vessel inside is machined to have smooth surface to allow proper NDT testing.

The French RPV-s are clad with similar technology: the first layer is 309 L (24Cr – 12 Ni), and the second is 308 L (18 Cr - 10Ni) [AN1.4].

Figures AN.1.1 and AN.1.2 show some results obtained by scanning electron microscope EDX analysis of the distribution of the main alloying elements in WWER 440 cladding. The transition between the base material and the first layer of cladding is sharp, the transition between the base and austenitic material is less than 0.5 mm, and consequently this transition zone is negligible as a crack initiation layer.

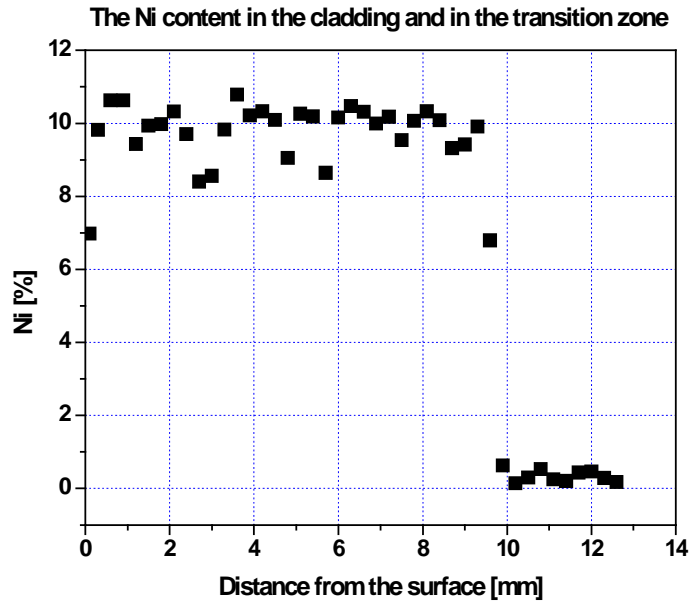


Figure AN.1.1 The distribution of Ni content in UP strip electrode cladding [AN1.1]

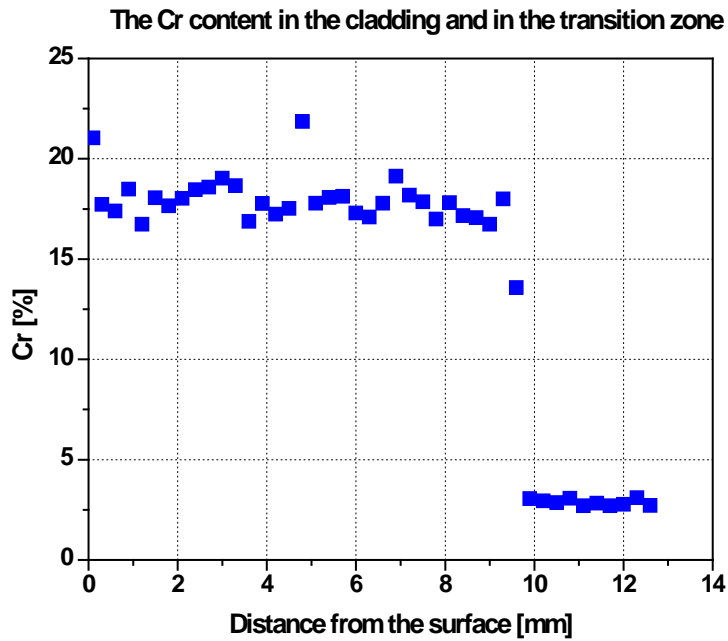


Figure AN.1.2 The distribution of Cr content in UP strip electrode cladding [AN1.1]

Typical chemical composition of the different WWER and French claddings are given in Table AN.1.1. The ferrite content of the different claddings varies between 2-7%. It can be seen that the WWER and French claddings are similar in chemical composition.

Table AN.1.1 Chemical composition of different claddings [AN1.1], [AN1.4]

Type	Layer	Composition m/m %									
		C	Si	Mn	P	S	Cr	Mo	Ni	Cu	Nb
WWER 440	1	0,056	0,86	1,16	0,015	0,004	22,8	-	13,3	0,06	-
	2	0,034	0,60	1,46	0,013	0,004	18,2	0,015	9,3	0,07	0,88
French	1	0.048	0.39	1.84	0.016	-	18.08	0.21	10.45		
	1	0.065	0.66	1.50	0.012	-	19.05	0.138	9.68		
	2	0.017	0.29	1.90	0.026	-	18.72	0.07	10.49		
	2	0.030	0.71	1.53	0.014	-	19.90	0.069	10.16		

AN.1.3 Defects in the Cladding

Careful UT testing has been performed by Forschungszentrum Rossendorf and AEKI on a test block cut from the Greifswald unit 8 WWER-440 type reactor to find the defects in the cladding. Two types of defects were discovered: porosity (gas bubbles) and joint defects (mainly remaining slag among the welding layers especially at welding over-lapping). The diameter of the gas porosity was maximum 2mm-s and the largest slag inclusion area was less than 1 cm². Figure AN.1.3 shows the defect distribution in a test block.

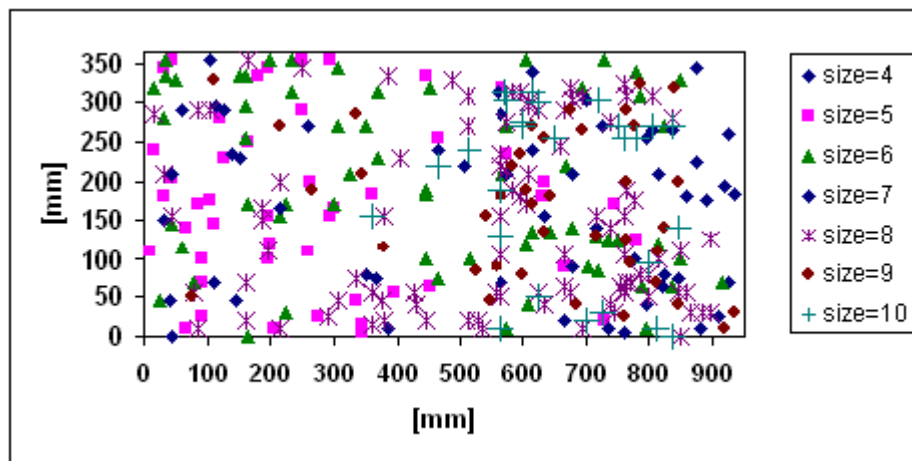


Figure AN.1.3 Defect distribution in cladding of steel block cut from Greifswald unit 8 [AN1.1]

In a small figure the defects seems to be dense, but in reality the defect density was low. To evaluate the defects size and study the grain structure of the cladding and the transition zone metallographic specimens were cut from the places where defects were found by the UT test. Figures AN.1.4, AN.1.5 and AN.1.6 show some typical defects of the cladding. No cracks were found in the tested blocks in the cladding or under the cladding [AN1.1].

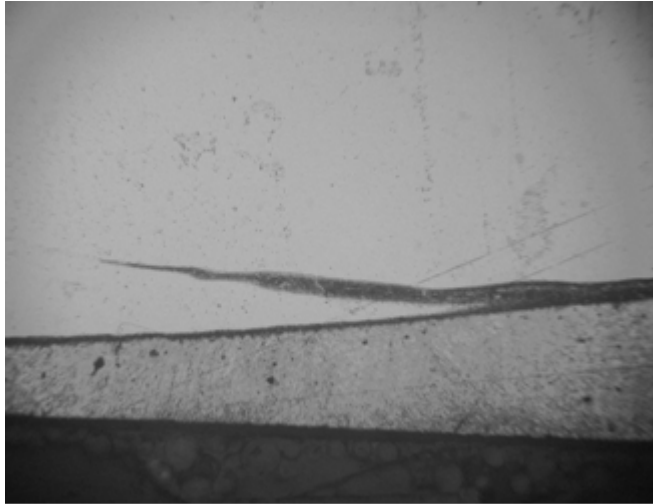


Figure AN.1.4 Typical slag inclusion between the base material and the first layer of the cladding (N=100x) [AN1.1]

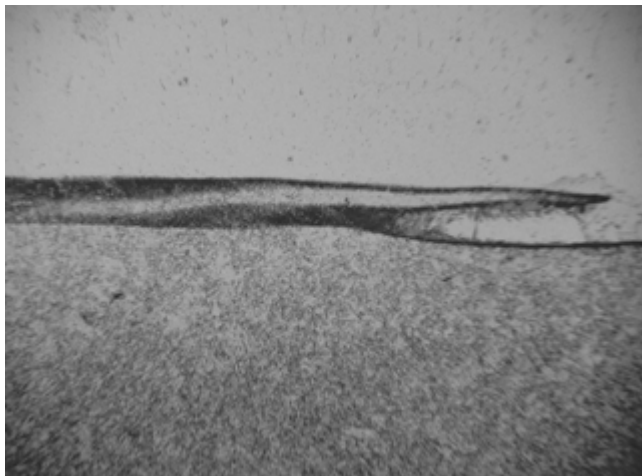


Figure AN.1.5 Lack of penetration among the base material and the first layer of the cladding (N=100) [AN1.1]



Figure AN.1.6 Small slag inclusion in the first layer of the cladding (N=100x) [AN1.1]

Most of the defects were improper penetration of the first layer cladding into the base material, or slag inclusions nearly parallel with the surface or small gas or slag bubbles in the cladding. No cracks were found in the cladding.

AN.1.4 Microstructure of the Cladding

The austenitic cladding is a welded structure, with very large grains, as illustrated in Figure AN.1.7. Sometimes the grain diameter can be greater than 1 mm, with delta ferrite net around the grain boundaries and several precipitates (mostly carbides) inside of the grains. The ferrite net and the large grains are contributing the unusual mechanical behaviour.

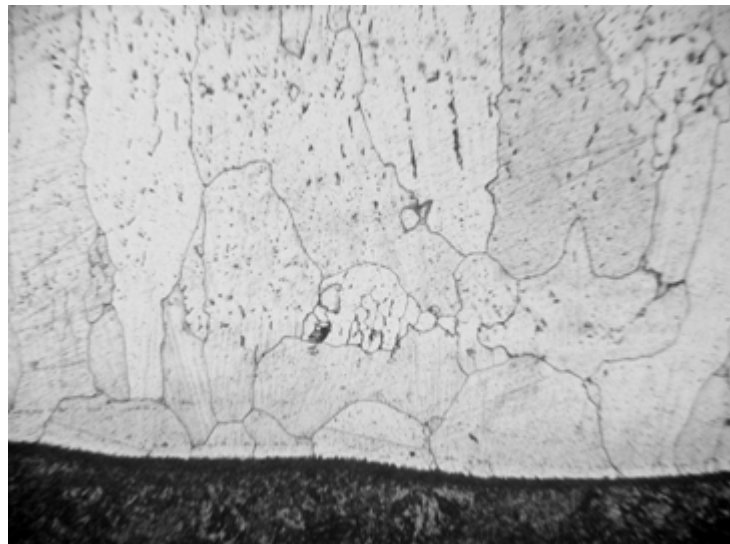


Figure AN.1.7 The grain structure of the first layer of the cladding (N=100x) [AN1.1]

AN.1.5 Mechanical Properties

Tensile properties

The behaviour of the cladding under loading is not similar to the stainless steel or to the ferrite-pearlitic low-alloyed steel. Due to the large grain sizes non-uniform deformation (necking) starts at many locations throughout the reduced gage length of the specimen, and the round specimen quickly becomes non-uniformly deformed. Figure AN.1.8 shows an irradiated cladding specimen (3 mm diameter and 15 mm long) during testing. At least two areas of necking can be seen, and several other regions of non-uniform deformation as well.

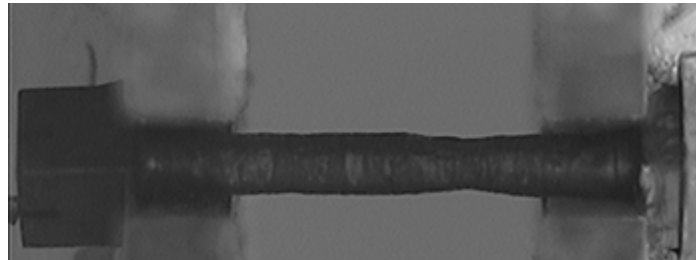


Figure AN.1.8 Tensile specimen from cladding during testing [AN1.2]

Surprisingly the tensile properties are much more affected by the testing temperature than by high fluence irradiation. Figure AN.1.9 shows tensile curves obtained on the second (surface layer) of the cladding.

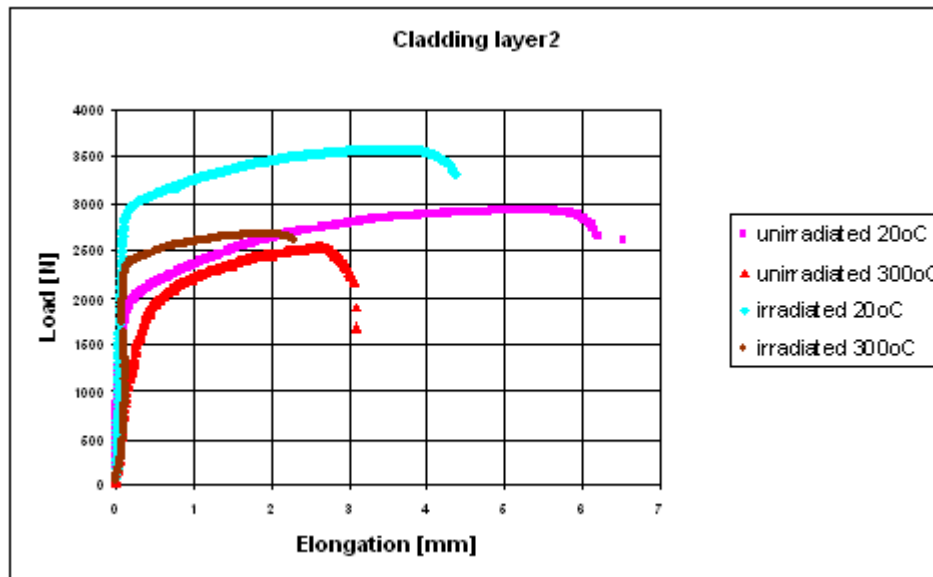


Figure AN.1.9 Tensile curves obtained on unirradiated and irradiated cladding at room and at elevated temperature [AN1.2]

■ unirradiated and tested at room temperature, ▲ unirradiated and tested at 300°C irradiated and tested at room temperature ◆ irradiated and tested at 300°C

One curve has been obtained on an unirradiated specimen at room temperature, and another one on an unirradiated specimen at 300 °C (near to reactor operating temperature). The yield strength was slightly reduced at elevated temperature testing, however, the elongation has been reduced to nearly half. Generally it is expected that elongation is increases at elevated temperatures, as in the case of ferritic or austenitic steels.

Irradiation has a much less remarkable effect on the cladding properties than the temperature. The yield and ultimate tensile strength slightly increased and the elongation was slightly reduced. Figures AN.1.10 and AN.1.11 show the combined effects of the irradiation ageing and the testing temperature on the tensile properties of the cladding [AN1.1].

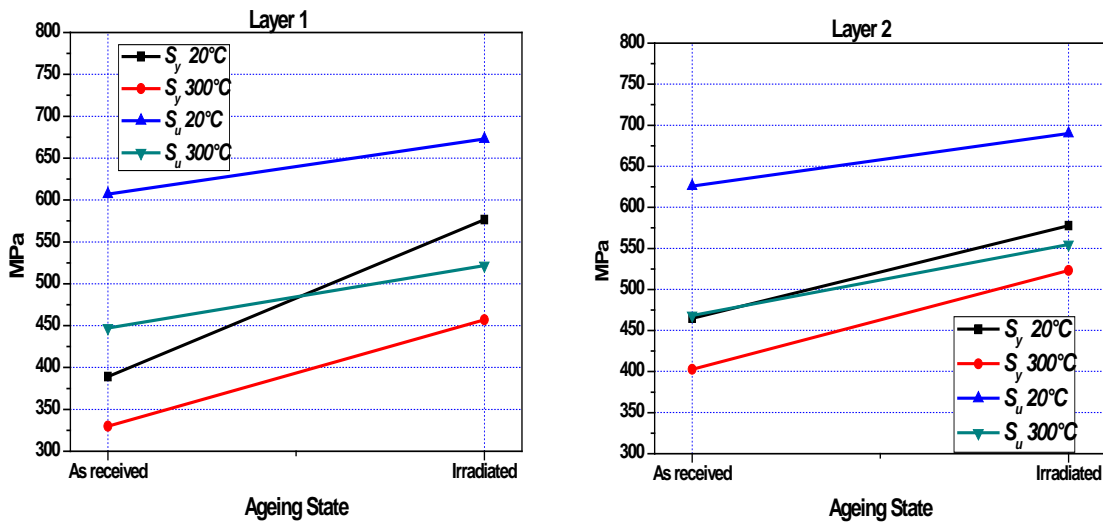


Figure AN.1.10 Effect of irradiation on the tensile properties of the different layers of WWER-440 cladding [AN1.1]

Flow curves of as received, and irradiated cladding also have been obtained [AN1.1] for elastic-plastic finite element calculation.

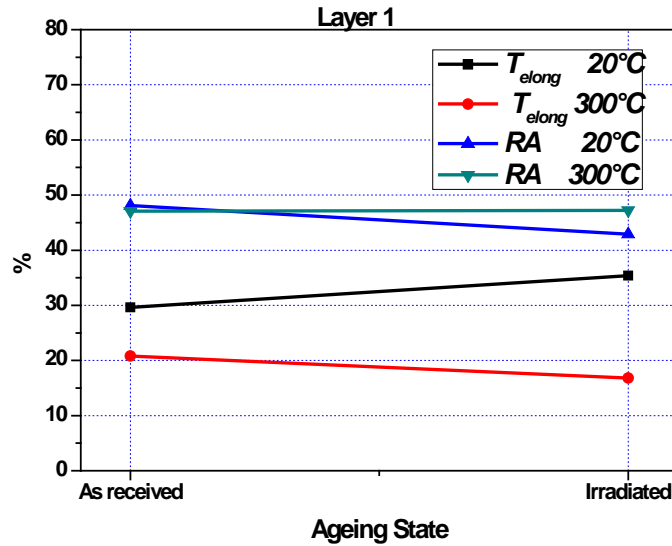


Figure AN.1.11 Effect of temperature and irradiation on the elongation and reduction of area measured on the first (over alloyed) layer of WWER-440 cladding. [AN1.1]

The early Russian literature states that the as-received cladding properties are about:

$$\sigma_{0.2} \sim 320 \text{ MPa}, \delta \sim 20\%, \psi \sim 35\%. \quad \text{Eq. 1}$$

and 10^{20} n/cm^2 neutron fluences increase the yield strength with 50-100% and reduce the ductility with 50% [AN1.2]. The French experience with 308 L type cladding shows that the ferrite content affects the irradiation hardening. Figure AN.1.12 shows the irradiation hardening of 308L type cladding as a function of the ferrite content and Figure AN.1.13 shows the effect of testing temperature on the differently aged 308L cladding. Increasing ferrite content decrease the irradiation effect, and increasing testing temperature sharply decreased the yield strength [AN1.4].

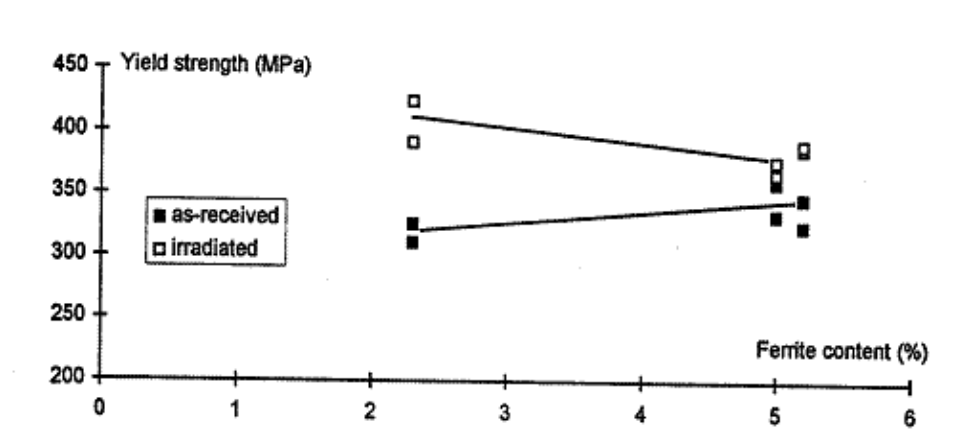


Figure AN.1.12 Irradiation hardening of 308 type cladding as a function of ferrite content [AN1.4]

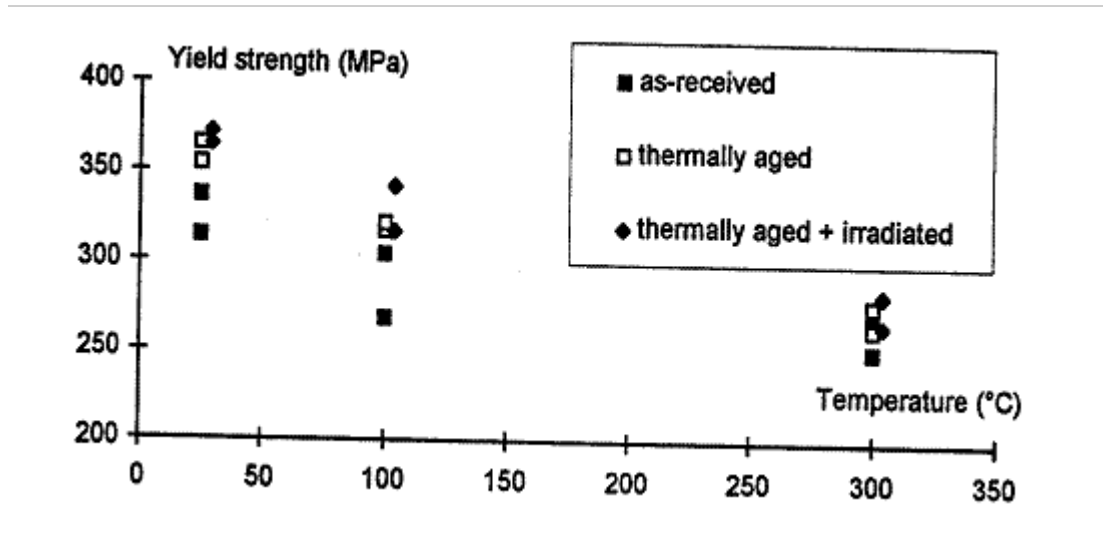


Figure AN.1.13 Effect of testing temperature on the differently aged 308 L cladding [AN1.4]

Charpy impact toughness

Charpy specimens were cut from the trepanns obtained from the Greifswald unit 8 and from the Zarnoviec reactor. One set was tested as-received, one set was thermally aged and one set was irradiated in the Budapest Research Reactor. The specimens were machined such that the notch was perpendicular to the interface of the base material and cladding, and started in the transition zone. This resulted in the notch root residing in the first layer of the cladding and crack propagation into clean cladding material during the Charpy testing. The applied thermal treatment was 3000 hours at 350°C, to modelling long term service ageing. The third set of specimens were neutron irradiated up to $0.8 \cdot 10^{22}$ n/m² E>1 MeV. The results, see Figure AN.1.14, show only a slight increase in the transition temperature, but considerable reduction in the upper shelf energy [AN1.1].

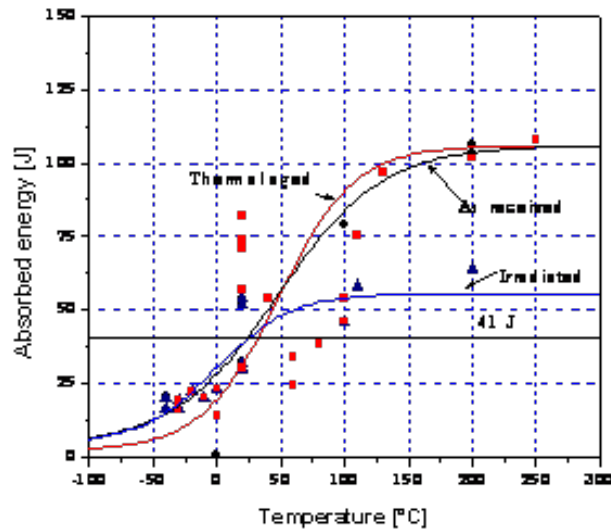


Figure AN.1.14 Decrease of the upper shelf energy of irradiated cladding [AN.1.1]

The Russian literature shows a different behaviour of the irradiated cladding [AN.1.2]. It states that the irradiation embrittlement depends on the phosphorus and copper content of the cladding. They experienced considerable increase of the Charpy transition temperature and decrease of the upper shelf energy on commercially produced WWER cladding (see Figure AN.1.15).

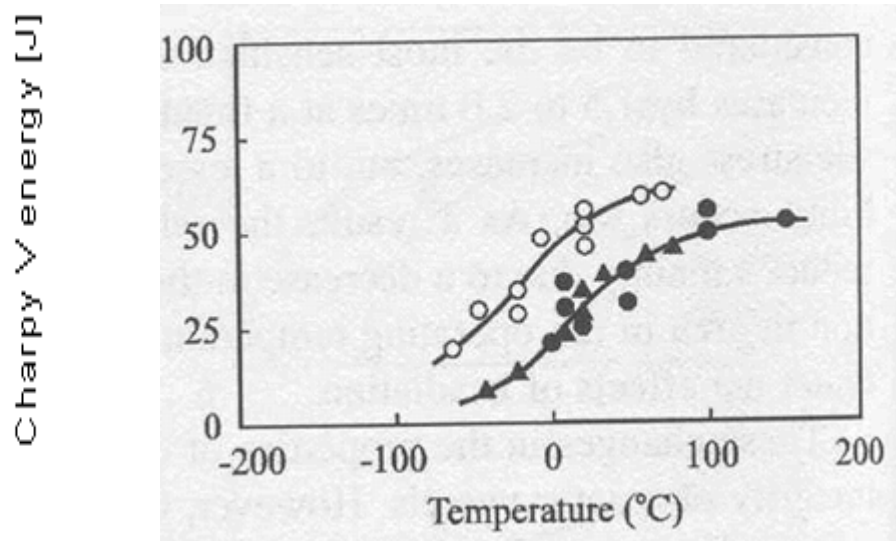


Figure AN.1.15 Effect of irradiation on the Charpy properties of WWER cladding [AN.1.2]

o = as received

● = $5.5 \cdot 10^{21} \text{ n/m}^2$ irradiation at 325 °C
 ▲ = $2.1 \cdot 10^{22} \text{ n/m}^2 \text{ E} > 0.5 \text{ MeV}$ irradiation at 265 °C [AN.1.2]

In the case of relatively high copper and phosphorus content cladding the embrittlement was increased (see Figures AN.1.16 and AN.1.17)

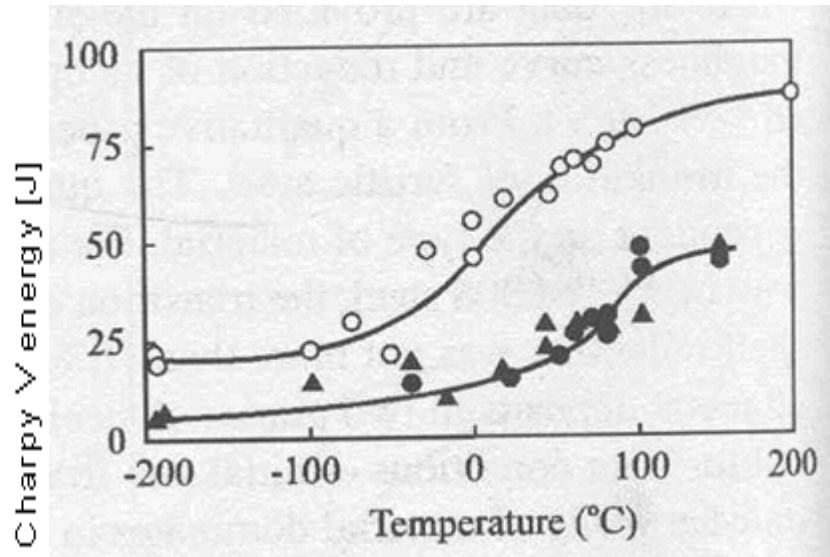


Figure AN.1.16 Effect of irradiation on the Charpy properties of WWER cladding with increased copper and phosphorus content [AN1.2]

O = as received ● = $5.5 \cdot 10^{21}$ n/m² irradiation at 325 °C ▲ = $2.1 \cdot 10^{22}$ n/m² E>0.5MeV irradiation at 265°C [AN1.2]

Further data is published in the Russian literature on the effect of sulphur and phosphorus. Relative small content of phosphorus and sulphur can strongly reduce the Charpy impact toughness of the as-received and irradiated cladding. The data also shows that the irradiation embrittlement was caused by precipitations and segregations saturating in the first stage of the irradiation and the matrix damage caused by further irradiation only slightly affects the Charpy transition curve [AN1.3].

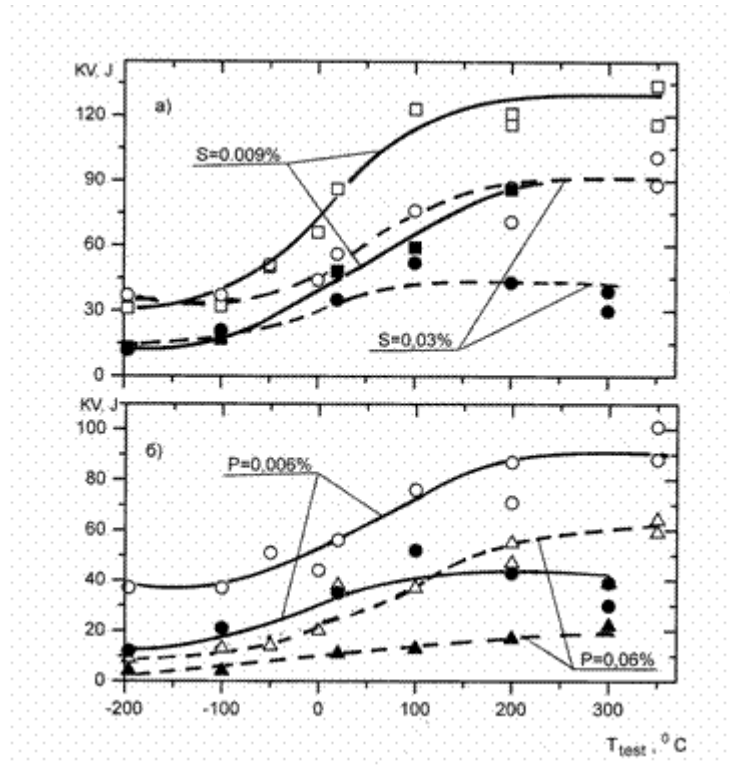


Figure AN.1.17 Influence of S and P content on temperature dependence of absorbed energy for the metal of laboratory homogeneous cladding (Sv-04Ch20N10G2B) in initial and irradiated conditions. [AN.1.2]

Tempering at $670^\circ C$, 16 hours: (o, Δ , — initial condition •, \blacktriangle ; — $F=1 \cdot 10^{20}$ neutron/cm² at $T_{irr} = 270-290^\circ C$

Different research heats were irradiated in the Osiris reactor [AN1.4]. The results show that chemical composition and ferrite content affects the irradiated properties of the cladding. One cladding was also sensitive to thermal ageing, in contradiction with the results obtained on the WWER-440 cladding (as shown in Figure AN.1.13).

Examples of Charpy impact properties for French cladding materials are presented in Figures AN.1.18 to AN.1.21.

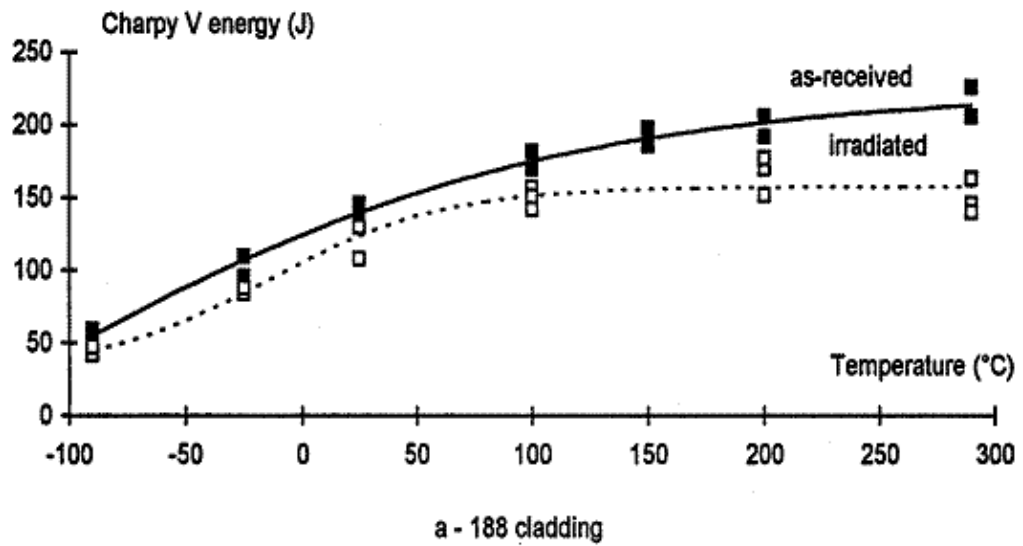


Figure AN.1.18 Charpy impact properties of French cladding type 188 in as received and after 6.5×10^{19} n/cm² (E > 1MeV) at 290 °C. The ferrite content is 2.3% [AN1.4]

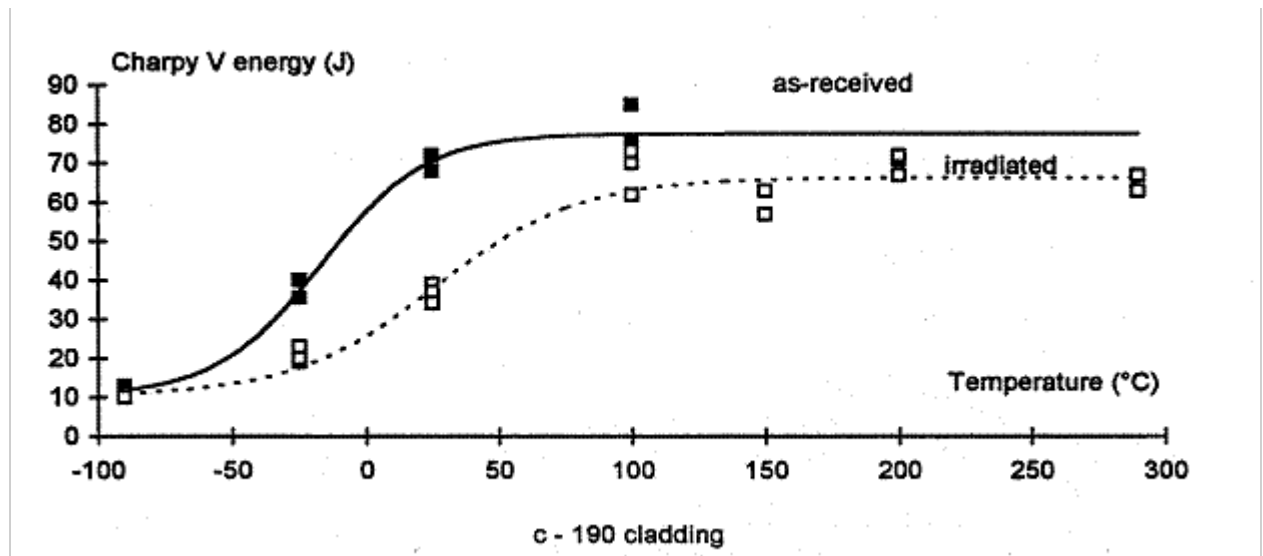


Figure AN.1.19 Charpy impact properties of French cladding type 190 in as received and after 6.5×10^{19} n/cm² (E > 1MeV) irradiation at 290°C. The ferrite content is 5.2% [AN1.4]

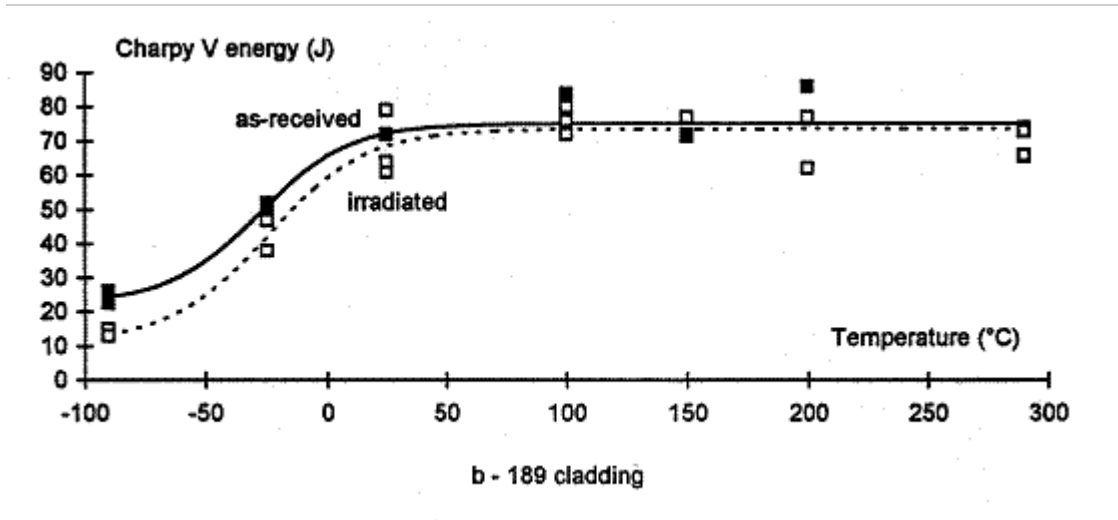


Figure AN.1.20 Charpy impact properties of French cladding type 189 cladding in as received and after $6.5 \times 10^{19} \text{ n/cm}^2$ ($E > 1 \text{ MeV}$) irradiation at 290°C . The ferrite content is 5% [AN1.4]

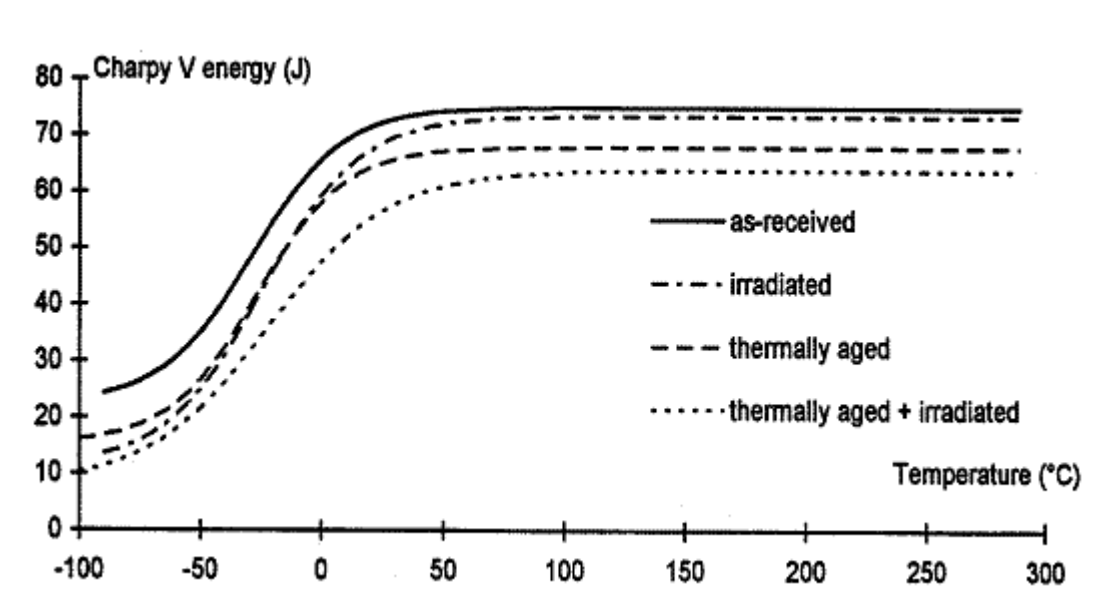


Figure AN.1.21 Charpy impact properties of French cladding type 189 cladding in as received and thermally aged, irradiated, and thermally aged and irradiated condition. Irradiation $6.5 \times 10^{19} \text{ n/cm}^2$ ($E > 1 \text{ MeV}$) at 290°C . The ferrite content is 5% [AN1.4]

Fracture toughness

Fracture toughness evaluation is difficult on RPV cladding due to its non-homogeneous behaviour. The Russian literature shows some J_{1c} results on as-received and tempered WWER cladding [AN1.4], see Figure AN.1.22.

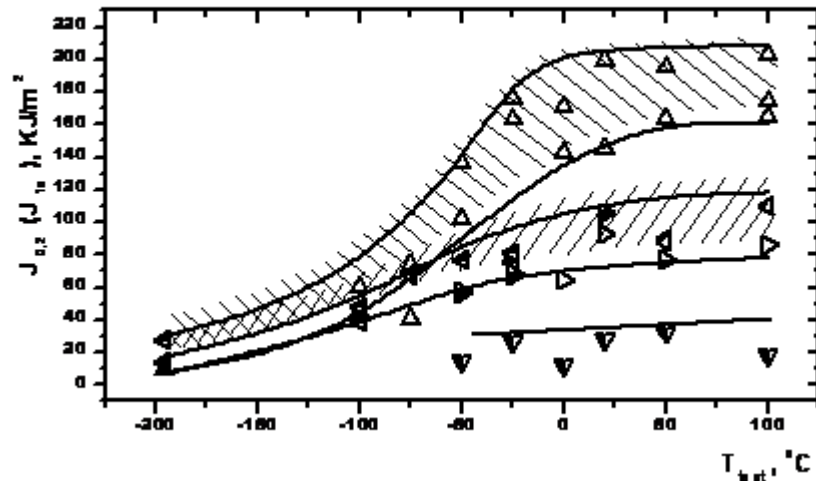


Figure AN.1.22 Temperature dependence of fracture toughness for the first (Δ) and second layer (\blacktriangleleft) of WWER as received cladding, and the same cladding after tempering at 670°C 50 hours first (\blacktriangledown) and second (\blacktriangleright) layer. [AN.1.3]

The open triangles characterize ductile fracture, the semi open ones characterize cleavage pop-in after plastic deformation and the black triangles characterize brittle fracture.

J-R curves were measured at FZR in as-received condition on cladding cut from Greifswald unit 8. NRI and VTT studied cladding properties recently in a PHARE project in the as-received and thermally treated conditions. They measured J-R curves and crack initiation and stable propagation on pre-cracked Charpy specimens with crack front embedded into the appropriate cladding layer. The results are not published yet, but are included into the VERLIFE guide as a new chapter on cladding evaluation during PTS.

AEKI irradiated a set of 10x5x55 TPB specimens from the Greifswald unit 8 cladding, but they are not tested yet.

AN.1.6 Properties and Assessment Tools for Characterizing PWR Cladding Crack Susceptibility

The mechanical properties of claddings are usually investigated by Charpy-V impact, tensile, Hardness and small punch tests. The microstructure can be investigated by Transmission Electron Microscopy (TEM) or Scanning Electron Microscopy (SEM) [AN1.6].

Residual stresses in RPV claddings are tensile stresses caused by the higher thermal expansion coefficient of the austenitic cladding compared to the ferritic base metal. Numerical and experimental investigation concerning residual stresses in RPV claddings were performed in the PHARE 2.03/97 project "Qualification of new materials for replacements/repair of original materials in WWER (440/213)" and in the FP5 project ENPOWER (Management of Nuclear Plant Operation by Optimizing Weld Repairs).

Cracks in or beneath the cladding may occur as so-called hot cracks (stress relief cracks SRC) or cold cracks (e.g. hydrogen induced cold cracks HICC). Such under-clad cracks may occur as stress relief cracks in the coarse grain area of the ferritic base metal below the cladding after a PWHT of about 600 °C or higher indicating that they are reheat cracks caused by the plastic

relaxation of residual stresses from the welding. Cold cracks differ from hot cracks arising during the PWHT because these cracks occur after welding if solidification is complete before PWHT. The formation of cold cracks can be caused by welding (residual stresses), segregations, local overstressing of the material or strain fatigue, and hydrogen. Much more dangerous than normal cold cracks are the hydrogen induced cold cracks (also referred to as “delayed” cracking) by diffusible hydrogen in the critical areas. The hydrogen induced cold cracks occur in segregated areas of the ferritic base metal.

Under-clad cracks can be detected by NDE testing with ultrasonic and magnetic crack detection or by transverse and parallel polish sections of the HAZ of claddings.

To assess the consequences of sub-clad defects regarding the structural integrity of the component it is necessary to clarify whether these defects may act as a crack starter for brittle fracture of the component or not and to determine the level of ductility in the HAZ around the crack. To obtain more representative HAZ material available for testing a special thermal simulation technique was developed at MPA Stuttgart and Siemens/KWU labs in the 70's. Usually tensile, drop-weight, Charpy-V and fracture mechanical tests are performed to determine the HAZ properties.

The under-clad cracks have some common issues concerning their safety relevance:

- The cracks are small, their extension and number is limited.
- The cracks are embedded in a ductile matrix. Therefore, no crack propagation is expected during normal operational conditions.

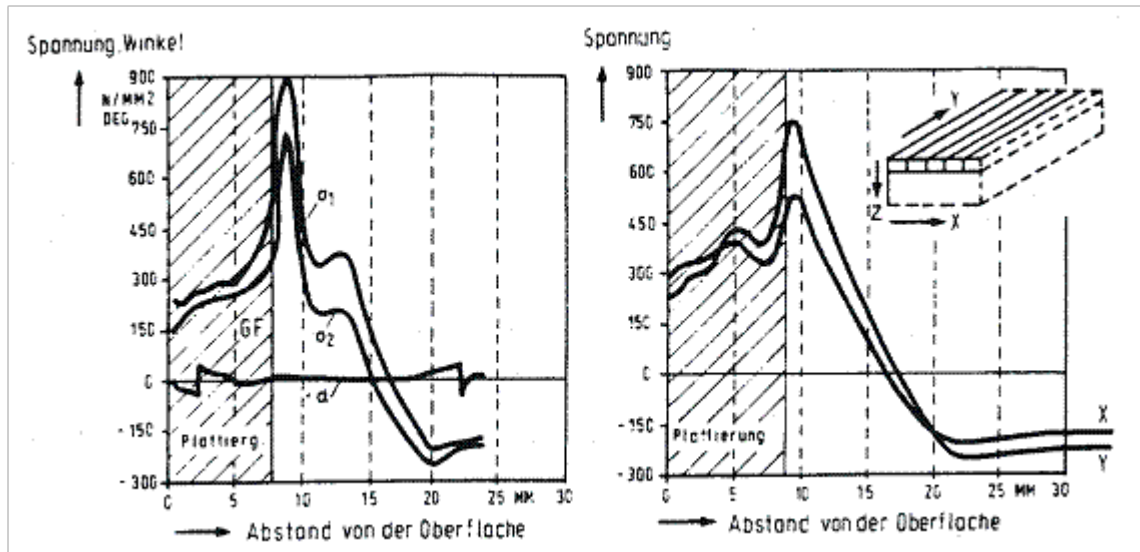
This can be confirmed by the results of RPV inspections reported in [AN1.9] where some under cladding flaw indications were detected by ultrasonic measurements as planar manufacturing flaws that were assumed as cold cracks. Some years later the measurements were repeated and no significant dimension changes were observed.

For under-clad cracks many fracture mechanic calculations were performed and experimentally confirmed in different research programmes and investigations leading to the conclusion that this kind of crack has no safety relevance for the operation of nuclear components. Nevertheless all safety relevant nuclear components including, RPVs, are subjected to a systematic NDT surveillance during their operation.

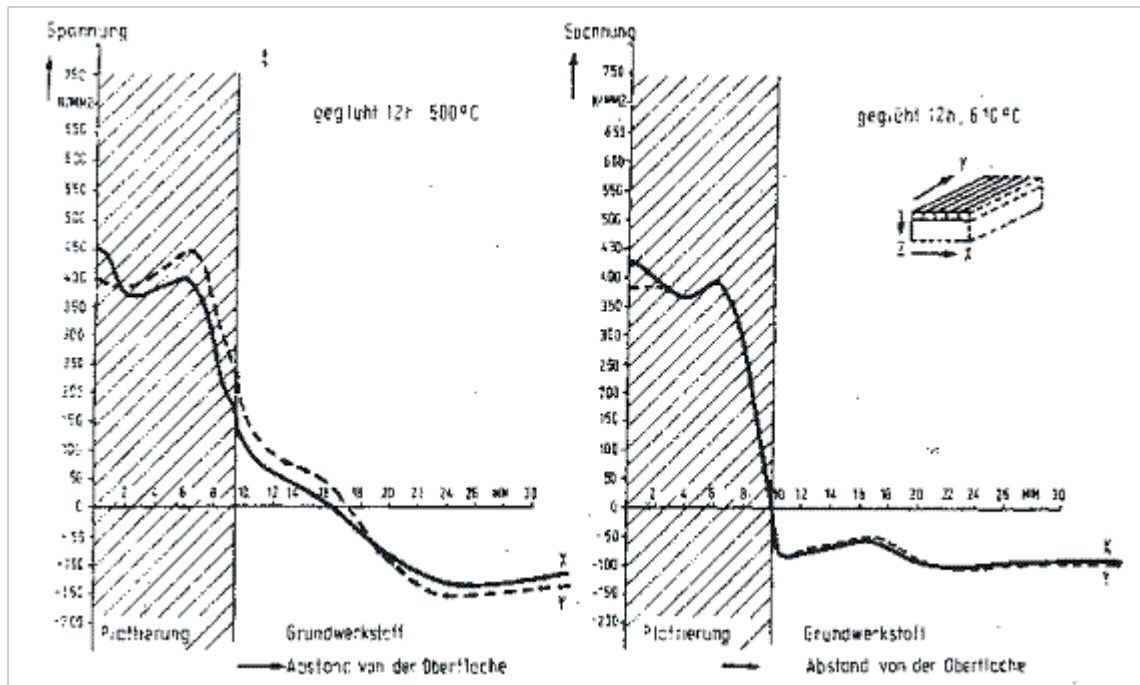
AN.1.7 Characterization of Residual Stresses under Cladding

Several investigations were performed to determine the residual stresses under the cladding. In Figure AN.1.23 the results of two experimental procedures are shown in the as welded condition and after PWHT. The stresses are highly relieved by a post weld heat treatment at about 600 °C, especially the stresses in the area of the fusion line.

As welded



Heat treated



12h, 500°C

12h, 610°C

Figure AN.1.23

Residual stresses as welded and after heat treatment

AN.1.8 Properties and Assessment Tools for Characterizing WWER Cladding Crack Susceptibility

WWER (Water-Water Energy Reactor = PWR type) reactor pressure vessels have relatively thick cladding – nominally 8 mm – made from two layers: first layer of 25/10 type welded by one pass while the second layer of 18/10/Ti typed is usually welded by three passes. The cladding in the main part of the vessels was produced by strip welding with strips 60 mm wide.

A method using incremental milling of beams has been used for the measurement and determination of residual stresses in WWER cladding. Tests were performed on specimens in the as-welded state and also after final heat treatment of the vessels, i.e. after several stress relief's and including the first hydro test in the shop. As residual stresses depend strongly on the direction of welding, beams were oriented in both directions; parallel and perpendicular to the welding direction.

The general trend of the results for all types of specimens was the same. Tensile stress in the cladding was observed to slowly increase from a level of approximately + 50 MPa on the upper cladding surface (corresponding to the inner surface of RPV) to a maximum of approximately 100 MPa in the middle of cladding thickness following by a rapid decrease close to cladding / base material (BM) interface to a compressive stress, see Figure AN.1.24. The minimum value of the stress (about -150 MPa) was reached very close to the interface. A slow linear increase of stress followed along the specimen width, with a tensile stress measured near the specimen bottom surface. The difference between the individual types is not large with the following trends: aged specimens have slightly higher tensile stress near the cladding surface than as-received specimens. Similarly, specimens with circumferential orientation have slightly higher tensile stress near the cladding surface than axially oriented specimens.

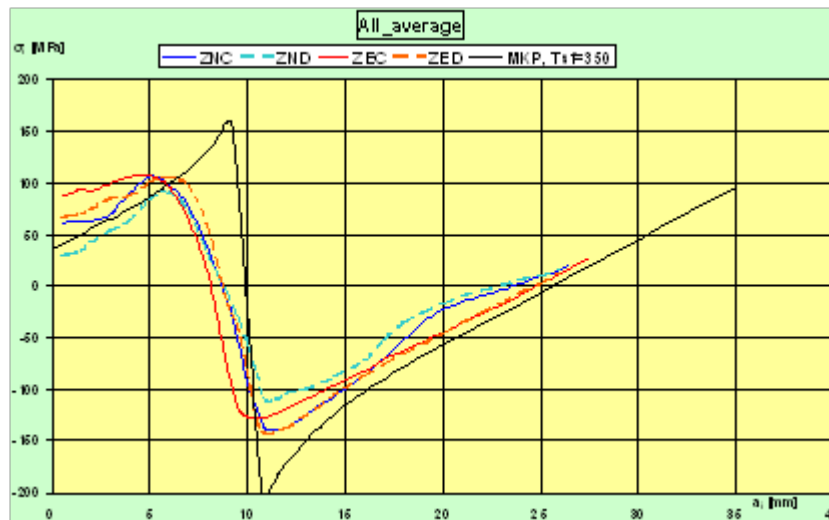


Figure AN.1.24 Distribution of residual stresses in 4 specimens

In finite element method (FEM) calculations, the measured residual stresses were treated as stresses arising due to different thermal expansion coefficients of both materials (BM and cladding) using the so-called “stress-free-temperature” approach. This approach represents a standard procedure in any calculations of stress fields in clad reactor pressure vessels that are used as inputs for fatigue damage calculations as well as calculations of the vessel resistance

against fast non-ductile failure, mainly during pressurized thermal shock events. To confirm this theory, a FEM model of the specimen was created using the COSMOS/M code.

The stress free temperature was selected as $T_{sf} = 350\text{ }^{\circ}\text{C}$. This value of stress free temperature was originally defined during large-scale test, FEM evaluations, to fit the experimental data (force-displacement curve) as well as possible. Further support for this temperature is based on the behaviour of the cladding-base material stress state during operational cycles, where cyclic loading results in elastic-plastic behaviour of the cladding, and thus the stress field is redistributed.

It can be stated that general variation of measured and calculated stresses and their magnitudes are in good agreement. The main difference is in more enhanced peaks (both tensile and compressive) close to the material interface in calculated stresses. This fact can be explained by the more gradual change of material properties in real specimen near the interface. Moreover, in formula used for calculation of residual stresses based on measured strains, there was no distinguishable difference between Young modulus for both materials.

It must be said that residual stresses in this type of bimetallic material strongly depend on the geometry. In the RPV itself, the residual stresses are different from those present in a block cut from the RPV, and these are in turn different from the residual stresses in the specimens. The thinner the specimen, the smaller the tensile stresses present in the cladding and the higher the tensile stresses in bottom specimen surface (opposite to cladding). This is due to the lower constraint, and thus higher bending, of thinner specimens. In the whole cylindrical part of RPV, practically no bending occurs and small compressive stresses are throughout the BM thickness.

Results of FEM analysis of large-scale beam specimen used for fracture tests (690x40x85 mm) loaded only by residual stress due to cladding, using the same material properties and T_{sf} as above, are presented in Figure AN.1.25. In this Figure, longitudinal and transversal stresses variations through the specimen width are presented. The results confirm the statement of the previous paragraph (higher stress in cladding, lower bending in BM).

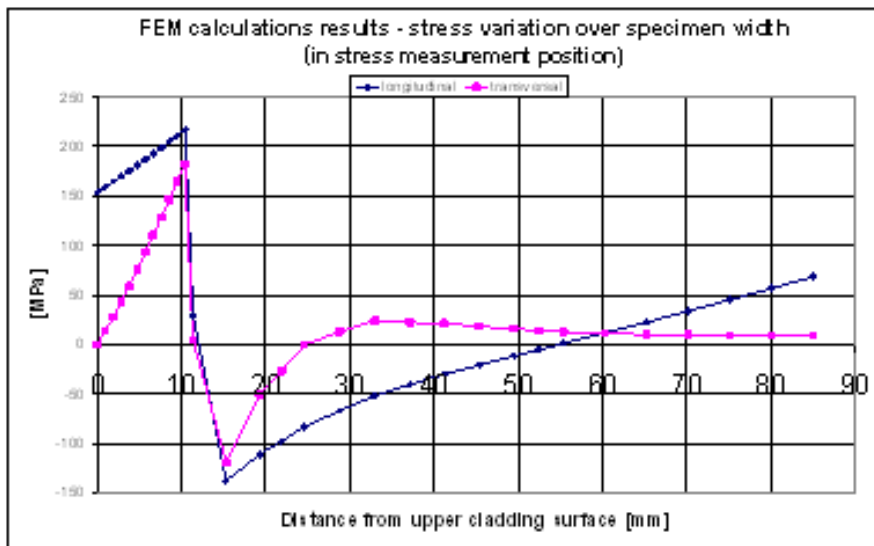


Figure AN.1.25 Calculated residual stress distribution in the test beam

AN.1.9 Lifetime Evaluation Considering Cladding Properties

License extension of NPPs requires a new safety analysis of the plant covering the extended operating life. One of the most important safety considerations is the integrity of the RPV (Reactor Pressure Vessels). The RPV material suffers several ageing-related effects during operating service: neutron (and gamma) irradiation embrittlement, thermal ageing, low cycle fatigue, thermal fatigue, and corrosion. Generally the most severe effect is irradiation and thermal embrittlement of the RPV belt near to the fuel core zone, which is often referred to as the beltline.

The life limiting components for LWR (Light Water Reactor) plants are generally the steam generators, but steam generators can be replaced, if it is economically acceptable. In terms of safety considerations, the life limiting component is the RPV, and the most important degradation mechanism is radiation embrittlement. The RPV must maintain its structural integrity during any operational or accidental event. One of the most severe hypothetical accidents is PTS (pressurized thermal shock), in which cold cooling water flows into the hot pressurized vessel along the wall of the embrittled beltline region, and operational and thermal stresses are added.

Most of the European regulatory rules and the IAEA (International Atomic Energy Agency) PTS Guide [AN1.8] require deterministic PTS analyses of the RPVs. They do not accept the probabilistic approach used in the US and in some other countries. The IAEA PTS guide for WWER-440 Reactors allows using only hypothetical under clad cracks if the cladding is ductile and free from cracks. Calculating surface cracks running through a brittle cladding into the base material is over conservative and results in short operating lifetime of the RPVs [AN1.7], [AN1.8].

The IAEA PTS guide [AN1.8] recommendation is as follows:

" For cladded vessels, cladding integrity of which is verified by redundant non-destructive testing and its mechanical properties are known, the postulated defects are underclad semi-elliptical or, if applicable, elliptical cracks with depth up to $\frac{1}{4}$ of the RPV wall thickness, and with aspect ratio a/c respectively. $2a/c$ of 0.3 and 0.7."

The European WWER users elaborated the lifetime evaluation guide "VERLIFE" [AN1.7] in the frame of FP5 (5th EU Framework project). This guide is fully or partly accepted by the national regulatory body of several EU countries and in Ukraine, Russia, and China. It recommends:

"Evaluation of emergency conditions (EC) and anticipated operating transients (AOT)

Cladded component, provided that its integrity is assured by qualified non-destructive inspection:

Assessment of effect of cladding is based on the use of its J-R curve (in the case of multi-layer cladding, J-R curve for the 1st layer). Generic J1mm values of the cladding are recommended, if no real component specific values are available.

The postulated underclad crack is conservatively defined as partially penetrating 1 mm into the cladding. The extension of the crack to the cladding is supposed with the same length as the length of original major axis of the underclad postulated crack (i.e. the major axis of the semi-ellipse remains on the interface between cladding and base or weld material).

Instead of this conservative approach for postulating the crack, a more detailed calculation of crack penetration into the cladding during the regime, based on J R curve, is allowed, if properly validated.

In this case, at least the deepest and near interface points of the postulated defect must be assessed with respect to the resistance of base or weld material against fast fracture. In this case, the integrity of cladding above the postulated defect during the whole AOT or EC regimes has to be verified. Assessment of ductile tearing for the part of the

postulated crack front lying in the cladding shall be based on J-R curve approach. J-values for all time steps of the regime shall be calculated (it is sufficient to calculate J-values only for the middle point of crack front in cladding). These J-values have to be (for all assessed time steps) smaller than the end-of-life values of J-R curve corresponding to 1 mm crack extension (i.e. J1mm values). The J1mm values are specified as follows:

- a) If no RPV specific data are available, generic values of J1mm are: 100 kJ/m² for WWER 440 RPV and 150 kJ/m² for WWER 1000 RPV.*
- b) If component specific data are available, then experimentally determined J1mm divided by safety factor 2 shall be used.*
- c) In the case of other components than WWER 440 or WWER 1000 reactor pressure vessels for which no component specific J-R data are available, surface crack as in par. 5.10.3.2 has to be postulated.*

If the condition on J is not fulfilled, surface crack has to be postulated.”

Both guides are published recently, and the use of the underclad cracks instead of surface cracks requires proper knowledge of the RPV cladding properties.

Practically most of the WWER-440 V-213 type and many other PWR reactors lifetime extension depend on the consideration of RPV cladding integrity. Since the RPV cladding was previously considered only as an anticorrosive layer the mechanical properties and the role in the RPV integrity were not properly studied.

Stress free temperature effect very much the lifetime. In the RPV annealing, the mechanical and physical properties of the base, weld and cladding materials and the pressure-temperature history (including the first hydrotest) affect the residual stresses. The different codes and guides generally recommend the operating temperature as stress-free temperature, but FM calculated values are also accepted.

AN.1.10. Summary and Suggestions for Further Study

- 1) French and WWER claddings are similar in chemical composition and welding technology
- 2) European and US cladding are produced by using different welding processes consequently the mechanical properties are different.
- 3) The RPV cladding behaviour in as received and irradiated conditions are very much different from the RPV forgings or welds
- 4) The existing literature data on the aged properties and ageing mechanisms are few, and many times they are in contradiction with each other
- 5) Further research is suggested to elaborate proper trend curves of RPV cladding for practice, and for understanding the mechanism and affecting factors of thermal and irradiation embrittlement
- 6) Further study is required to involve the cladding into the RPV stress and strain calculations, especially at PTS assessment
- 7) Further study to elaborate stress free temperature for the RPV considering the mechanical properties of the materials and load-temperature history of it also suggested.

AN.1.11. References

- [AN1.1] F. Gillemot, M. Horvath, G. Uri, T. Fekete, E. Houndeffo, B. Acosta, Debarberis, H.-W. Viehrig: "Radiation stability of WWER RPV cladding materials", International Journal of Pressure Vessels and Piping 84 (2007) 469–474
- [AN1.2] N.Alekseenko et al: "Radiation Damage of Nuclear Power Plant Pressure Vessel Steels" American Society of Nuclear Engineers ANS, Yearly meeting USA, 1997
- [AN1.3] A. Nikolaev, I. P. Kursevich, E. V. Nesterova, O.Yu. Prokoshev, V. V. Rybin: "BRITTLE FRACTURE TENDENCY OF ANTICORROSIVE CLADDING METAL ON PRESSURE VESSELS OF WATER-COOLED REACTORS" UDK 621.791.92:539.56:621.039.536.2
- [AN1.4] M. Bethmont (EDF) – P. Soulat (CEA) – B. Houssin (FRA): "Mechanical properties of reactor pressure vessel cladding. Effect of thermal ageing and irradiation" 1995.
- [AN1.5] F. Gillemot, M. Horváth, G. F. Gillemot, M. Horváth, G. Úri, H-W. Viehrig, L. Debarberis, T. Fekete, E. Houndeffo. "Behaviour of irradiated RPV: Behaviour of irradiated RPV cladding", Paper presented for AMES workshop, 6-8 February 2006, Hévíz (Hungary).
- [AN1.6] J.S. Lee, I.S. Kim, R. Kasada, A. Kimura. "Microstructural characteristics and embrittlement phenomena in neutron irradiated 309L stainless steel RPV clad", Journal of Nuclear Materials, 326 (2004) 38-46.
- [AN1.7] Unified Procedure for Lifetime Assessment of Components and Piping in WWER NPPs – VERLIFE, European Commission, Final Report, Contract N° FIKS-CT-2001-20198, September 2003. (Last updated in Prague at 1 April 2008)
- [AN1.8] Guidelines on Pressurized Thermal Shock Analysis for WWER Nuclear Power Plants (Rev. 1) IAEA-EBP-WWER No. 8 (Rev.1)2006, English, (File Size: 1447 KB). Date of Issue: 23 May 2006.
- [AN1.9] Payraudeau, K., K. Zamoum, T. Pasquiar. "Reactor Pressure Vessel of Tricastin Unit 1 Core Zone Inspection - Comparison of Non-Destructive Examination Results Among Two Core Areas Inspections Performed in 1999 and in 2003", ASME Pressure Vessels and Piping Conference, Vol. 487, July 2004, San Diego, California USA.